# Unusual Molecular Structures of Boron Halides and Carboranes – Combining Experiment and Theory.

**Iain D. Mackie**

A thesis presented for the degree of
Doctor of Philosophy in the College
of Science and Engineering at the
University of Edinburgh, 2003.

## Declaration

This thesis has not been submitted, in whole or in part, for any degree at this or any other university. The work is original and my own, carried out under the direction of Prof. D. W. H. Rankin and Dr. S. Parsons. Where this is not so credit has been duly given.

## Acknowledgements

"... noo a' ma darg is deen..." I would like to thank my supervisors, David and Simon, for their tutelage, patience and sarcasm. Thanks must also go to the EPSRC for generous funding and to Peter Timms, Jennifer Pardoe, Mark Fox, Drahomír Hnyk and Josef Holub for their help with compound synthesis and useful discussion.

To all members, past and present, of the assembly that is *ed@ed*, mainly Sarah, Blair, Lorna, Kostya, Andy, Julien, Maria, Derek and Heather, I say cheers.

For their incredible support I am forever grateful to Linda, Andy and especially Maria.

## Abstract

This thesis is concerned with the determination of the structures of the polyboron fluorides $B_4F_6CO$, $B_8F_{12}$ and $B_{10}F_{12}$ and the carboranes *closo*-2,3-$C_2B_9H_{11}$, *nido*-2,9-$C_2B_9H_{13}$ and *arachno*-6,9-$C_2B_8H_{14}$ by experiment and theoretical calculations.

The primary technique used for this research has been gas-phase electron diffraction (GED) – a powerful method for studying molecules in the gas phase, where they are free from intermolecular interactions. Whilst GED is not without its limitations, its combination with increasingly high level *ab initio* molecular orbital calculations provides more thorough structure determinations. GED, however, requires the compound of interest to possess sufficient volatility. Where this is not so it may be possible to determine experimental structure using low-temperature X-ray crystallography.

The gas-phase structure of $B(BF_2)_3CO$ has been determined by electron diffraction and high-level *ab initio* calculations. The structure compares well to the crystal phase, bonding with $C_3$ symmetry. The family of borane carbonyl compounds $B(BX_2)_3CO$ (X = F, Cl, Br and I) have all been studied by *ab initio* calculations to show the effects of halogen substitution and to gauge the effects of electron correlation and basis set. Compounds X = F, Cl and Br give calculated structures with $C_3$ symmetry, in which the boron-halogen bonds lie coplanar with the C-O bond. In the case of X = I the $BI_2$ groups are twisted by approximately 35° from being coplanar with the C-O bond, as a result of the large steric interactions between iodine atoms.

A molecule such as $B_8F_{12}$ could theoretically exhibit a plethora of chemically reasonable structures. Its structure remained a mystery for over thirty years but through the combined efforts of low-temperature X-ray crystallography, gas-phase electron diffraction and *ab initio* calculations we have determined its bonding. Its structure is unique, inconsistent both with those of electron deficient boranes such as $B_8H_{12}$ and with those of boron halides such as $B_8Cl_8$. Its structure is based upon a

folded $B_4$ central core, analogous to $B_4H_{10}$, but it is highly asymmetrical. This asymmetry is reproduced through *ab initio* calculations and is non-solvent dependent in the crystal phase. Using the bonding scheme of $B_8F_{12}$ we have calculated a possible structure for $B_8Cl_{12}$, a compound thought to be involved in the disproportionation of $B_2Cl_4$. *Ab initio* calculations have also allowed us to determine the structures of $B_8Br_{12}$, $B_8I_{12}$ and a new isomer of $B_8H_{12}$.

$B_8F_{12}$ is the first fully characterised higher boron fluoride and we can also report the second - $B_{10}F_{12}$. Its crystal structure contains a tetrahedron of boron atoms, each with a $BF_2$ substituent, similar to the known $B_4X_4$ tetrahedra but with two additional $BF_2$ bridge bonds. *Ab initio* calculations identify a very different structure. The molecule is based upon a folded $B_4$ central core as in $B_8F_{12}$, but this core is highly symmetrical in $B_{10}F_{12}$. However, calculations involving sterically larger substituents such as in $B_{10}Cl_{12}$, $B_{10}Br_{12}$ and $B_{10}I_{12}$ show molecular structures as found in crystalline $B_{10}F_{12}$.

Carboranes form a widely studied class of molecule but past structural studies have generally relied upon theoretical calculations or NMR spectroscopy whilst, due to a general inability to form single crystals, diffraction studies have been carried out on salts or derivatives of the parent cluster. To further the understanding of carborane cluster structures the compounds *closo*-2,3-$C_2B_9H_{11}$, *nido*-2,9-$C_2B_9H_{13}$ and *arachno*-6,9-$C_2B_8H_{14}$ have been experimentally characterised using gas-phase electron diffraction; they show structures comparable to known carboranes.

**Contents** *page*

# Chapter One

## Introduction

## 1.1. General Introduction

Structure determination is an important tool for the understanding of molecules and their properties. The instrumentation available at the University of Edinburgh allows the study of molecular systems in the solid and gas phase by experimental and theoretical methods. There are many techniques for the determination of molecular structures, including microwave spectroscopy, liquid crystal nuclear magnetic resonance, X-ray crystallography, and gas-phase electron diffraction.[1] In addition, quantum mechanical calculations are increasingly being used to supplement experimental methods and direct future synthetic research.[2]

Ideally, molecules should be studied in the gas phase where they are free from intermolecular interactions and the influence of packing forces that can seriously distort molecular geometries.[1] This thesis primarily concerns the use of gas-phase electron diffraction in conjunction with *ab initio* molecular orbital calculations to characterise boron halides in the gas phase. The systems of interest are unsuitable for rotational spectroscopy due to the large number and nature of atoms involved.[1] The ability to accumulate enough information to correct each rotation constant for both isotopic species of boron ($^{10}B$ and $^{11}B$) in order to define the structure accurately is limited.[1] The techniques of gas-phase electron diffraction and *ab initio* calculations also possess limitations but when they are combined, a more thorough structure determination can be attained.

One substantial drawback to the technique of gas-phase electron diffraction is the necessity for the chemical compound to have sufficient volatility.[1] In such cases it may be possible to obtain solid-phase structures using the technique of low-temperature X-ray crystallography. Whilst this too is not without disadvantages, the increasing ease with which data can be collected and refined means that such a method of structure determination is a powerful experimental tool.

## 1.2. Gas-phase Electron Diffraction

Gas-Phase Electron Diffraction (GED) is a technique that is used to study gas-phase molecular structures. It achieves this by adjustment of a theoretical model until it matches the experimental as well as possible.

### 1.2.1. Theory of Gas-phase Electron Diffraction

The technique is based on two key discoveries. In 1915, Debye stated that rigid systems of electrons, such as molecules, strongly influence the distribution of X-rays diffracted by them as a function of the scattering angle.[3] Secondly, in 1924, de Broglie found that electrons possess wave-particle duality and therefore they can be diffracted.[4] De Broglie also found that the wavelength of the electrons was dependent on their momentum, according to the relationship described in Equation 1, termed the de Broglie equation.[4]

$$\lambda = \frac{h}{p} \qquad \text{Equation 1}$$

where $\lambda$ = wavelength; $h$ = Planck's constant; $p$ = momentum.

The wavelength of the electrons depends on their energy, i.e. on the accelerating voltage used. When electrons are accelerated through approximately 40 kV, they possess a wavelength of around 0.06 Å. This value means that interatomic distances can be measured. In a series of experiments carried out by Davisson and Germer dated 1927,[5] the de Broglie hypothesis, that material particles have an associated wave, was confirmed. Diffraction of electrons by a single atom can be thought of as similar to diffraction at a single slit. The diffraction occurs at the edge of the nucleus due to the electric field gradient and the intensity falls exponentially as a function of the scattering angle.[1] Diffraction of electrons by two atoms, such as you would expect to find in a molecule, causes interference between the diffracted waves similar

to that found in the Young's slit experiments.[6] Constructive and destructive interference produce maxima and minima of scattering intensity as a function of the scattering angle. Measurement of the distance between adjacent maxima or minima determines the wavelength of the diffracted media.[6] The total scatted intensity, $I_{total}$, is usually expressed as a function of the variable $s$, instead of the scattering angle, $\theta$, where

$$s = \frac{(4\pi \sin\theta)}{\lambda} \qquad \text{Equation 2}$$

and $\lambda$ is the electron wavelength.

When the background is subtracted from the total intensity the atomic and molecular intensities, $I_{atomic}$ and $I_{molecular}$ are obtained. The background includes both inelastic scattering and other components dependent on experimental conditions. This contribution is subtracted using a smooth spline function.

The atomic scattering, $I_{atomic}$, is the sum of the contributions all the atoms make when diffracting the electron beam.[1] The atomic scattering is expressed in Equation 3.[1]

$$I_{atomic} = \sum_{i}^{N} \frac{F_i(s)^2}{s^4} \qquad \text{Equation 3}$$

where $N$ is the number of atoms in the molecule, $F_i$ is the complex atomic scattering factor for atom $i$ described in Equation 4, and $\eta_i$(s) is the phase of the electron scattering amplitude.[7]

$$F_i(s) = |F_i(s)| \exp[i\eta_i(s)] \qquad \text{Equation 4}$$

These atomic scattering factors are usually taken from existing tables such as those compiled by Ross, Hilderbrandt and Fink.[8]

The molecular scattering intensity, $I_{molecular}$, consists of contributions from non-vibrational and vibrational terms summed to include all atom pairs, as in Equation 5.[7]

$$I_{molecular}(s) = \sum_{i,j;i\neq j} \sum \exp(-0.5u_{ij}^2) \frac{F_i F_j}{s^4} \cdot \frac{\sin(s.r_{ij})}{s.r_{ij}} \qquad \text{Equation 5}$$

sum for all atom pairs $i, j$ in the molecule

vibration

molecular scattering for all atom pairs

where $r_{ij}$ is the internuclear distance of atoms $i$ and $j$ and $u_{ij}$ is the root mean square amplitude of vibration.

The overall form undertaken by the molecular scattering is of a damped sine wave where the frequency of the oscillations is a simple function of the interatomic distance, and the rate of experimental decay is determinable from the extent to which the atoms move relative to each other.

Most papers that describe molecular structures determined by GED report the original scattering intensities and molecular scattering curves. In addition to these it is common to include the so-called radial distribution curve (RDC). This is the Fourier transform of the molecular intensity function and is much simpler to understand since it does not consist of many overlapping sine waves. The RDC plots the probability of finding a distance, $r$, in the molecule, against the distance. Each peak is approximately Gaussian in shape unless several internuclear distances contribute to the same peak (see Section 1.2.4.). The amplitude of vibration of the atom pair determines the widths of the peaks, with the area related to the atomic numbers and internuclear distance concerned (see Equation 6).[1]

$$Area \propto \frac{n_{ij} Z_i Z_j}{r_{ij}} \qquad \text{Equation 6}$$

where $Z_i$ and $Z_j$ are the atomic numbers of atoms $i$ and $j$, and $n_{ij}$ is the number of times the distance $r_{ij}$ occurs in the molecule.

### 1.2.2. Gas-phase Electron Diffraction Experiment

Unlike in the field of X-ray crystallography, there exists no standardisation of experimental equipment for gas-phase electron diffraction. In the year 2000 it was reported that there were around 20 groups doing GED around the world in countries such as Germany, Hungary, Japan, Norway, Russia, the United Kingdom, and the United States of America.[9] The basic concept remains the same in each of these machines. The method of electron diffraction is based on measuring the intensity of electrons scattered from a gas jet injected into a high vacuum.[1] There are four main requirements for the diffraction experiment.

(1) A beam of electrons. In the Edinburgh apparatus[10] this is produced from a hot tungsten filament. This beam is intense with uniform energy (c.a. 1 m$\mu$A), and thus is ideal for looking at gases for which their low penetrating power does not matter. The beam of electrons is accelerated by a potential difference of 40 kV and focussed by electromagnetic lenses to generate a narrow beam (c.a. 300 m$\mu$).

(2) A diffraction chamber equipped with an inlet nozzle from which the gas to be studied is introduced. The gas is trapped on a cold surface to avoid scattering from regions other than adjacent to the nozzle.

(3) The apparatus is maintained at high vacuum, typically $10^{-6}$ Torr, so that the electron beam is diffracted only at the point where it crosses the beam of molecules emerging from the nozzle.

(4) A detector to record the diffraction pattern produced. This is done using photographic films or plates from which the intensities can be measured later. The scattering pattern consists of a series of diffuse concentric rings determined by the

interaction of the electron beam with the electric field gradients of the atomic nuclei. The scattering falls off from the diffraction centre towards higher scattering angles (roughly as the fourth power) and so the range of intensities is too large to be recorded directly on a photographic plate. A filter is thus used to screen the photographic plate. This consists of a rotating metal sector that is placed adjacent to the plate with its axis of rotation coinciding with the incoming beam.[10] The sector used in the Edinburgh apparatus is shown in Figure 1 to have an opening with an increasing width related to the fourth power of the distance from its centre. The introduction of the sector allows the exposure to be more uniform. To prevent back reflection of any undiffracted electron beam, a beam stop consisting of a metal cylinder is placed at the centre of the sector. This prevents data collection at very small scattering angles but is essential to avoid possible back scattering. Typically, data are collected at two nozzle-to-detector distances to increase the amount of structural information that can be obtained about the molecule, by widening the angular range over which the experimental data extend.

**Figure 1**. Edinburgh electron diffraction apparatus & sector

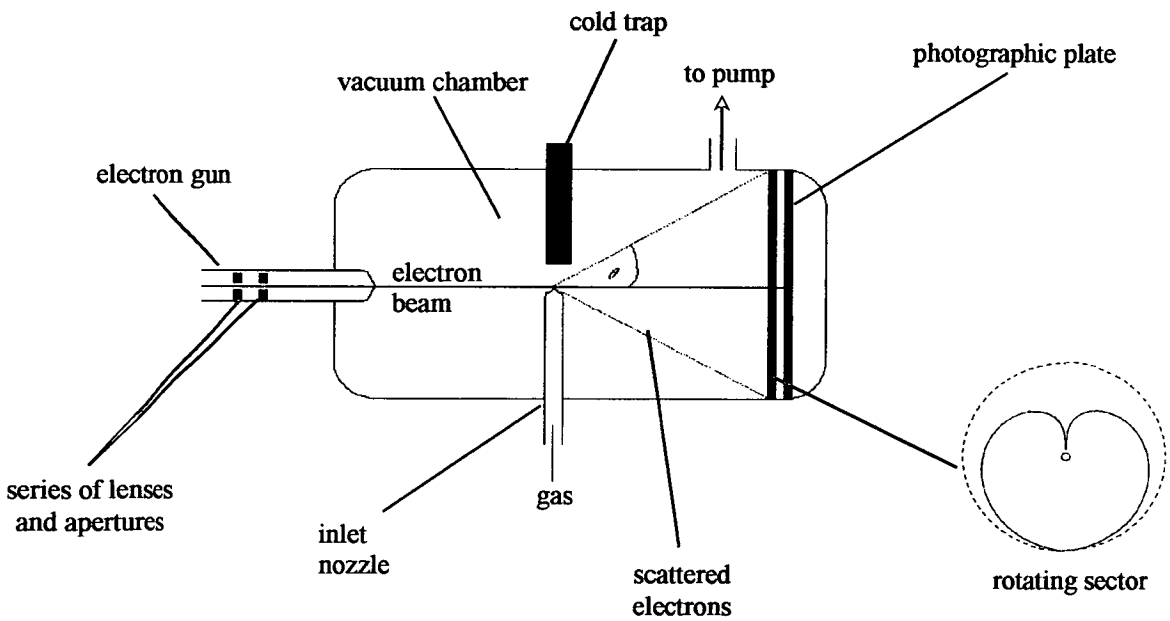

### 1.2.3. Data Analysis

The diffraction pattern consists of diffuse, concentric circles since the molecules are in a random orientation. This compares to a diffraction pattern from a single crystal that shows spots resulting from the fixed positions and orientations of the molecules. The intensities describe the diffraction pattern determined by GED as a function of the ring radius or scattering angle. The first step in analysis of data collected involves making allowances for experimental arrangements, such as the rotating sector. Calibration of the wavelength is performed prior to every experiment using benzene. Benzene is used since it contains few varying bond distances and has easy handling qualities. The recorded scattering intensities are saved as a function of the scattering angle using a microdensitometer. This is done by our collaborators at the Institute of Astronomy in Cambridge using a PDS densitometer.[11] The microdensitometer reads intensities from the whole plate and the software then determines mean intensities as a function of distance from the centre of the pattern.

The molecular structure determination is based on comparison between experimental and theoretical molecular scattering curves. This involves writing a mathematical model to describe the position of each atom in the molecule through the use of structural parameters. These parameters tend to consist of bond lengths, bond angles and torsion angles, but may also pertain to other structural features such as the distance between two planes etc. These parameters allow a set of atomic coordinates to be produced, which allow calculation of all interatomic distances, and hence the total scattering curve can be calculated. These scattering curves are then compared to the experimental curves. Earlier practice was to also take initial values for the amplitudes of vibration from similar molecules but the current routine is to utilise those calculated from *ab initio* calculations (see Section 1.4.). The amplitudes of vibration and other structural parameters are then adjusted until the best fit between the theoretical model and the experiment is obtained. This is done in a least-squares analysis procedure.[12] The goodness of fit between the model and experiment is described by the residual factor, $R_G$, which for most molecules should have a value below 10% for the model to be considered of satisfactory quality. In addition, a

difference curve is generated to highlight graphically the difference between the experimental and theoretical data. This allows any errors in the model to be more easily assigned to specific structural anomalies.

### 1.2.4. Limitations

There are many good reasons to study molecules by GED. In GED, internuclear distances are measured compared to centres of electron density in X-ray crystallography. This leads to a high level of accuracy (± 0.001 Å or better in favourable cases) compared to crystallography (± 0.003 Å) where for atoms such as hydrogen, displacement occurs towards a bonded atom.[1] However, GED is not without its limitations.

The main limitation to GED is the fact it requires the sample to be gaseous, thus limiting the range of compounds that can be studied. For a gaseous sample to be studied with conventional apparatus it must possess a vapour pressure greater than 1 Torr, otherwise the beam density does not provide sufficient diffraction intensity relative to the background.[1] Increasing the temperature of the sample too high can lead to an increase in amplitudes of vibration. It also affects the relative populations of isomers and conformers, and can also lead to sample decomposition.[1]

The GED study assumes that the composition of the gas is known. This assumption is good enough if we deal with stable compounds that have no tendency towards self-association or decomposition.[9] However, this can be dangerous since there may exist impurities in our sample or a dynamic equilibrium between monomeric and dimeric species. If there are doubts as to the vapour composition it can be determined by mass spectrometry.

Another problem arises from the small contribution made from light atoms such as hydrogen. It is therefore difficult to locate light atoms in the presence of heavy ones. Thus, positions of hydrogen atoms are invariably less well defined than those of

heavier ones, given that the area of the Radial Distribution Curve is proportional to atomic number such that a small atomic number results in a small peak.[1]

Overlapping peaks on the RDC can make structure analysis more difficult. As the peaks are approximately Gaussian in shape, if two similar peaks are almost superimposed, as would happen if two bond distances were of similar length, their sum is also Gaussian. This makes it impossible to determine the positions and amplitudes of vibration for both components separately. One possible solution is to calculate the vibrational amplitudes from spectroscopic data and then constrain these at the calculated values during the refinement procedure. However, in this case the peak positions could be reversed without affecting the overall appearance of the curve. This can be overcome using the SARACEN[13] method (see later) whereby we can calculate the separate values by high level *ab initio* calculations. When describing the molecular geometry we can utilise mean and difference values and place flexible restraints upon one or more of these values to allow completion of the structure refinement.

The shrinkage effect is a direct consequence of the fact that the atoms are not stationary in the gas phase, but are in fact vibrating.[1] The bonded and non-bonded interatomic distances measured by GED are not self-consistent as illustrated on a simplified diagram for the linear triatomic molecule $MX_2$ (Figure 2).

**Figure 2**. Schematic of bending vibration.

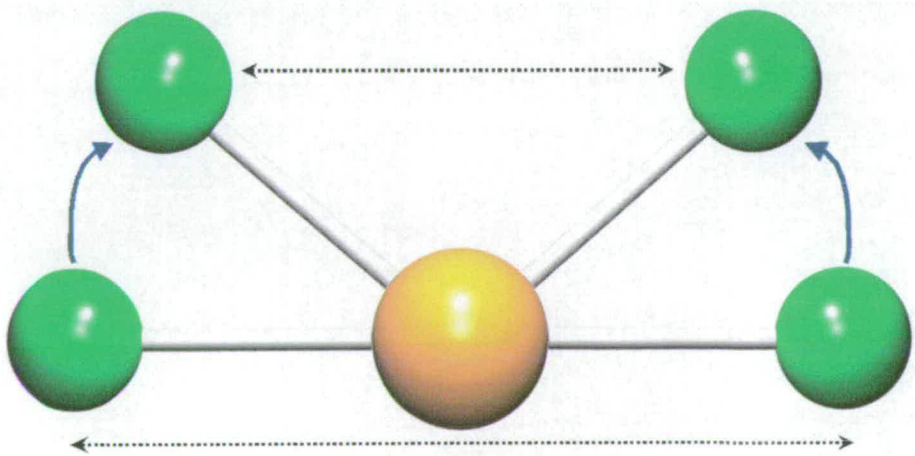

During a bending vibration, the distance between the outer pair of atoms decreases, and therefore the average X...X distance is less than twice the M-X bond length. This effect is not very large for reasonably rigid molecules such as $CO_2$, but if the bending mode has a low frequency/large amplitude, the apparent angle may be as much as 40° away from the true average angle.[1] In order to define the molecular geometry truly we need to calculate the amplitudes of vibration and incorporate shrinkage corrections such as those described by Sipachev.[14] The so-called $r_\alpha$ structure includes such corrections for perpendicular amplitudes.[14] Parameters $r_h^0$ and $r_h^1$ refer to the application of perpendicular and curvilinear corrections respectively.[14] Other important internuclear distance parameters include $r_a$, which refers to the maximum position of any peak on the RDC for the experimental temperature.[12] The $r_g$ structure corresponds to the average interatomic distance for a particular temperature.[12] $r_0$ is defined as the effective internuclear parameter which reproduces ground-state rotational constants.[12] Parameters $r_z$ and $r_e$ are defined as the distance between mean positions of atoms in the ground vibrational state and the distance between equilibrium positions respectively.[12]

## 1.3. *Ab initio* Calculations

*Ab initio* molecular orbital calculations allow the accurate prediction of many molecular properties including molecular energies and structures. Many other properties such as energies and structures of transition states, bond and reaction energies, NMR properties, etc. can also be calculated. The method involves deriving an approximate solution to the Schrödinger equation[15] (Equation 7), developed by Erwin Schrödinger in 1926, that describes molecular wavefunctions.

$$E\Psi = H\Psi \qquad \text{Equation 7}$$

where $E$ is the total molecular energy, $\psi$ is the total molecular wavefunction (describing the positions of nuclei and electrons and from which chemical properties

can be calculated), and $H$ is the Hamiltonian Operator (containing the electronic and nuclear kinetic and potential energy terms).

The Schrödinger equation may be solved exactly for the hydrogen atom given that the wavefunctions of the hydrogen atom are the familiar *s*, *p*, *d*, etc., atomic orbitals. However, for a many-electron atom or molecule, the Schrödinger equation becomes impossible to solve. The Hamiltonian operator in this situation becomes too complex to work with since it includes contributions from nuclear and electronic kinetic energies, and the potential energies of electronic repulsion, nuclear repulsion and nuclear-electronic repulsion.[16] We can however use approximations to simplify the Schrödinger equation and allow an approximate solution to be determined.

### 1.3.1. Simplifying the Hamiltonian (H) - Levels Of Theory

The Born-Oppenheimer approximation[17] is one such simplification. Nuclei are much heavier than electrons (the ratio of proton mass to electron mass equals 1826 : 1), and so, nuclear motion can be decoupled from electronic motion, i.e. the nuclei can be considered as stationary in the field of moving electrons. As a result of this, the kinetic energy of the nuclei becomes zero and the nuclear repulsion potential is a constant dependent upon the fixed position of the nuclei. The molecular wavefunction is now the only unsolvable term and to get around this, more approximations are used, the complexity of which determines the level of theory.[18]

The simplest level of theory used in this thesis is termed Hartree-Fock (Hartree, 1928; Fock, 1930)[19,20] which replaces the many-electron wavefunction with the product of one-electron wavefunctions termed a single determinant wavefunction. Hartree theory states that all electrons are moving in a static potential and are behaving like individual electrons, but at the same time they feel each other's average repulsion.[20] Fock theory takes into account Pauli's exclusion principle, which concludes that electrons with the same spin avoid each other.[20] Two electrons in the same atomic orbital are assigned spin +½ and -½ and each electron is surrounded by

a region of space that is devoid of electrons with the same spin. This leads to a reduction in the Coulomb repulsion among electrons with the same spin and thus acts on the electrons as an effective attractive potential. This energy reduction is termed the exchange energy.[18]

The result of this leads to a set of coupled differential equations, each involving one electron. Hartree-Fock (HF) calculations are often termed self-consistent, since the main task consists of an iterative self-consistency procedure to solve the Hartree-Fock equations, and hence to give the HF energy of the system (Equation 8).[2]

$$E^{HF} = E^{nuclear} + E^{core} + E^{coulomb} + E^{exchange} \qquad \text{Equation 8}$$

where $E^{nuclear}$ = Coulombic repulsion of nuclei, $E^{core}$ for both electron kinetic energy and Coulombic attraction between electrons and nuclei, $E^{Coulomb}$ accounts for the Coulombic repulsion of electrons. $E^{exchange}$ also involves electron-electron interactions, and has the effect of reducing the size of the Coulombic term.[2]

HF calculations account for approximately 99% of the experimental energy and so can be regarded as a good starting point in determining the true geometry.[16] For many molecules, such as $H_2$, $H_2O$, $C_2H_4$, $C_6H_6$ and $NH_3$, the predicted equilibrium interatomic distances and bond angles are within a few pm or degrees of experiment. Even the vibrational frequencies, derived from the curvature of the total energy as a function of nuclear separation, are found to be within about 10% of experiment.[2] However, the values of the total energies are less satisfactory. Ignoring electron correlation is a major source of error. In reality, electronic motions are correlated and the HF wavefunction results in a higher energy for the system because it has no way of correlating the orbitals, often resulting in bond distances that are too short. The missing energy is termed the correlation energy.[2]

### 1.3.2. Simplifying the Molecular Wavefunction - Basis Sets

The Molecular Wavefunction ($\psi$) describes the region of space around each nucleus for electron motion. It too can be simplified - the Born-Oppenheimer approximation used to simplify H also simplifies $\psi$ since the nuclei are stationary. The wavefunction is generated by considering the molecular orbitals as a linear combination of atomic orbitals; also known as basis functions. These basis functions collectively are the basis set, in other words, the set of atomic orbitals built around the static nuclei.[21] The most common method of approximating the size and shape of these atomic orbitals is to use Gaussian functions. Whilst at first glance the use of Gaussian functions may seem like a poor representation for atomic radial functions, this is overcome by summing multiple Gaussian functions with different components (see Figure 3). This means that the overall representation is in fact a good approximation. In addition, analytic expressions exist for calculating their integrals, thereby making them computationally efficient.[2]

**Figure 3**. Three Gaussian functions (coloured red) used to model an atomic radial function (coloured blue).

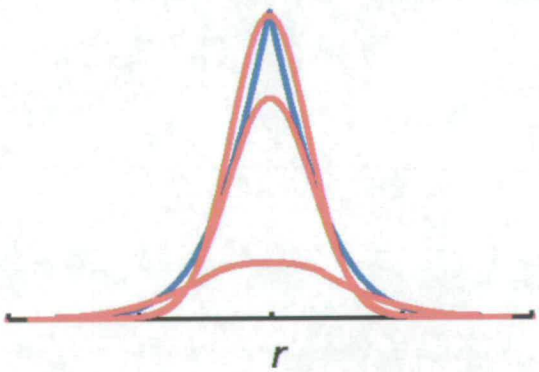


Each atom in the molecule of interest requires its own basis set, many examples of which exist. Basis sets are termed single-ξ, where one function describes each occupied atomic orbital; double-ξ in which two functions describe each occupied atomic orbital; triple-ξ, where an inner orbital is described by three Gaussians, and middle and outer orbitals are represented as single Gaussians. This work has used

split-valence basis sets, whereby the atomic orbitals are split into two parts: an inner, compact orbital and an outer, more diffuse one (see Figure 4).

**Figure 4**. Schematic showing split-valence basis set.

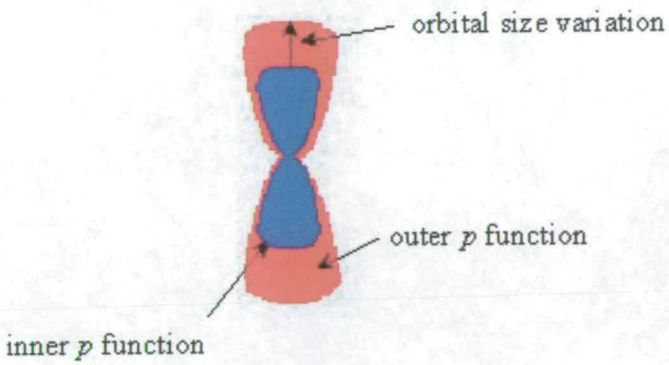


The coefficients of these two kinds of orbital can be varied independently during the construction of the molecular orbitals. Hence the size of the atomic orbital can be varied between the limits set by the inner and outer functions. In the 3-21G*[22-27] basis set the valence functions are split into one basis function with two Gaussians, and one with only one Gaussian. The core consists of three Gaussians contracted into one basis function. The core described by the 6-31G*[28-34] basis set consists of six Gaussians which are not split, with the valence orbitals described by one orbital constructed from three Gaussians and one single Gaussian function. The 6-311G*[35,36] basis set is an example of triple valence whereby the valence orbitals are split into three rather than two.

Further improvement of basis functions is achieved through the use of polarisation functions (denoted +) and diffuse functions (denoted *).[2] Polarisation functions allow orbitals to change shape by adding functions with higher angular momentum than required for the ground state description for each atom, for example, by adding a *p* function to hydrogen.

Diffuse functions provide more accurate descriptions of anions, or neutral molecules with unshared electron pairs. These functions are simply larger versions of *s* and *p* functions, thus allowing the orbitals to fill a larger region of space.

In addition, for heavy atoms (i.e. for atoms larger than Br) it is possible to use pseudopotential basis sets. Computational efficiency dictates that for such large systems pseudopotentials or effective core potentials (ECP) should be used. This involves treating only the valence electrons that are involved in bonding and replacing the core with a single function. Used in this thesis has been the lanl2dz basis set described by Hay and Wadt.[37]

### 1.3.3. Introducing Electron Correlation

Techniques exist that incorporate electron correlation effects and so can lead to improved accuracy in structure determination. The first of these to be discussed is termed Density Functional Theory (DFT). Thomas (1926) and Fermi (1928) first introduced the idea of expressing the total energy of a system as a functional of the total electron density.[38] However, it wasn't until the 1960's that what we now regard as DFT was formulated by Hohenberg and Kohn (1964) and Kohn and Sham (1965).[38]

In contrast to HF theory, DFT starts with a consideration of the entire electron system. The total energy is composed of three contributions, a kinetic energy, a Coulomb energy due to classical electrostatic interactions among all charged particles in the system, and a term called the exchange-correlation energy that describes all many-body interactions. This energy due to exchange and correlation can be conveniently approximated using the Local Density Approximation (LDA)[38] where the exchange-correlation energy is taken from the known results of the many-electron interactions in an electron system of constant density. In other words, at each point in a molecule there exists a well-defined electron density. It is then

assumed that electrons at such points experience the same interactions, as seen in a uniform gas.

The energy according to DFT can be described as Equation 9,[2] where the nuclear and Coulomb terms are as seen in HF methods, but the HF exchange energy is replaced by an exchange functional, $E^X(P)$, and a correlation functional, $E^C(P)$, is added. Both of the latter are functions of the electron density, $P$.[2]

$$E^{DFT} = E^{nuclear} + E^{core} + E^{coulomb} + E^{x}(P) + E^{c}(P) \qquad \text{Equation 9}$$

LDA models are exact for perfect metals, which have a constant electron density, but they become less accurate for systems with varying electron density. The more common approach utilised today is to introduce explicit dependence on the gradient as well as the electron density. Such procedures are termed gradient-corrected or non-local density functional models and they can be used in conjunction with hybrid functionals that are a mixture of HF and DFT exchange, along with DFT correlation. Most commonly used in this thesis is the B3LYP model. This is Becke's three-parameter hybrid exchange functional using the LYP correlation of Lee, Yang and Parr.[39]

DFT calculations are able to predict molecular properties more accurately, for a given basis set, than HF models yet are similarly computationally demanding.[2,38] For this reason, DFT calculations are deemed desirable. But DFT is not always the most reliable calculation that is available. DFT calculations are almost semi-empirical since the functionals used are tested on known systems.[2,38] Therefore for unknown systems, such as the higher boron subhalides studied in this thesis, the resultant DFT calculations cannot be determined as very accurate until they are compared to other calculations and experimentally determined structures.

Another method that has been developed to account for electron correlation is the so-called Møller-Plesset Perturbation model.[2] This involves mixing the ground state (i.e.

HF) wavefunction with excited-state wavefunctions. This entails implicit or explicit promotion of electrons from molecular orbitals that are occupied in the HF wavefunction to molecular orbitals that are unoccupied.[2] The HF wavefunction is used as the zeroth order wavefunction. This is then perturbed to add higher excitations to HF theory as a non-iterative correction, e.g. MP2 refers to the second order energy correction (see Equation 10).[2]

$$\Psi = \Psi^0 + X\Psi^1 + X^2\Psi^2 + X^3\Psi^3 + \ldots\ldots \qquad \text{Equation 10}$$

MP2 theory is able to recover roughly 80% of the correlation energy per electron pair, thus increasing the accuracy of our calculations greatly.[40] Further perturbations such as MP3 and MP4 can be carried out but this greatly increases the computational demand.[2] This is the crux of the problem for MP theory - the demand on computational facility. Whilst it is generally desirable to use the most accurate model possible, i.e. DFT in preference to HF, and MP in preference to DFT, this is not always possible. It is important to strike a balance between accuracy and efficiency.

### 1.3.4. Computational Procedure

The Schrödinger equation was solved using the Gaussian 98[41] or PQS[42] programs. The first calculation to determine an optimised molecular geometry needs to be quick and non-computationally demanding. We therefore start with a simple basis set (e.g. 3-21G*) and a simple level of theory such as HF. If the output geometry is sensible then this level of theory and basis set can be improved to increase the accuracy of our results.

A starting geometry is entered using either a *Z*-matrix (a matrix that describes the geometry and symmetry of the molecule) or Cartesian coordinates to specify the nuclear positions of the atoms. The SCF energy is then calculated and minimised.[2] This can be thought of as the calculations finding a point on the correct potential energy surface (PES) for the molecule. The forces on the atoms are then calculated -

this is the first derivative of the calculated molecular energy, allowing the location of stationary points on the PES to be found.[2] The force constants are then estimated and the geometry perturbed until the forces on the atoms are approximately equal to zero.[2] The force constants ascertain the nature of any stationary points found during the calculations, and they enable the normal modes of vibration to be determined.[2] The optimised structure can be (a) a saddle point - indicated by more than one imaginary frequency, (b) a transition state - indicated by one imaginary frequency, thus a maximum in one coordinate and a minimum in all others on the PES, and (c) a real structure, where there are no imaginary frequencies and we have reached a minimum on the PES.[2] Determination of a real structure however does not mean that we have determined the true structure, or one expected to be found by experiment. It merely means that we have located a local energy minimum - a possible structural isomer with the correct atom numeration. The correct structure will lie at the global minimum and it may take further calculation before this is determined.

## 1.4. Combining Gas-phase Electron Diffraction and Other Data

It is not rare in GED for multiple structural models to produce similar $R_G$ factors. These models may all be mathematically and chemically sensible; it can therefore be important to utilise further information to distinguish between them and also to allow the refinement of more parameters. Such additional information can be input from sources such as vibrational spectroscopy, rotational spectroscopy, liquid crystal NMR, and/or theoretical calculations. The last is generally used in the Edinburgh group since the availability and increased power of computing resources make such a method increasingly useful.

The use of theoretical calculations, generally *ab initio* and DFT methods, allows the determination, and sometimes more importantly, the comparison of molecular geometries and energies (amongst other properties). For example, in the case of a conformational mixture, the calculation of energies provides an estimate of a conformational ratio. This ratio can then be put into our theoretical model.

Molecular Mechanics and *ab initio* calculations have been used to supplement GED structure analysis since the 1970's, when Molecular Orbital Constrained Electron Diffraction (MOCED)[43] was first used. In this procedure the differences between parameter values are constrained to equal the calculated values. However, parameters that refine poorly need not be fixed. Fixing parameters is undesirable since it assumes that the calculated values are absolutely correct, and can therefore result in unrealistically low standard deviations for correlated parameters. Instead, flexible restraints can be added, whereby the parameters are allowed to vary within a specified limit. The values of these restraints are taken from *ab initio* calculations. This procedure was developed in Edinburgh and is now the standard methodology employed by the Edinburgh group. The name given to this methodology is SARACEN,[13] which is an acronym for Structure Analysis Restrained by *Ab initio* Calculations for Electron diffractioN.

*Ab initio* calculations can also be used to determine amplitudes of vibration through a theoretical force field. This can help produce the shrinkage corrections discussed in Section 1.2.4.[14] Thus we use *ab initio* calculations to construct the predicate observations necessary to complete the refinement and determine a more reliable structure than would otherwise be possible.

## 1.5. X-ray Crystallography[44]

X-ray crystallography is a widely available technique for the structure determination of molecules in the solid phase, either as single crystals or as powders. The purpose of this section is not to describe every detail of this technique, but merely to provide a (very) brief introduction to some of its principles that will help in understanding the results of this research. To that end, for a more detailed description of the technique, the reader may wish to review some of the numerous texts and journals such as Ref. 44.

The structures of crystalline solids are described by the repeated geometry within the crystal. This is known as the unit cell, where all the cells in the crystal are related to one another by displacements without rotation, reflection, or inversion. In three dimensions, the unit cell has lengths ($a$,$b$,$c$) and angles ($\alpha$,$\beta$,$\gamma$) associated with it such that angle $\alpha$ lies between $b$ and $c$. Rotation and reflection symmetries impose restrictions and special values on the unit cell parameters. On this basis, crystal systems are divided into seven types: triclinic, monoclinic, orthorhombic, tetragonal, rhombohedral, hexagonal and cubic.

Unlike single finite molecules, crystals can have other types of symmetry element in which rotation or reflection is combined with translation to give screw axes and glide planes. These operations are common because they are related to improved packing properties. Glide reflection involves the displacement of the two mirror images relative to each other by half a unit cell. Similarly, screw axes combine a simple rotation with a translation along the direction of the axis.

In a single molecule, symmetry elements all pass through one point and the combinations of these symmetry elements are known as point groups. The same cannot be said for crystal structures. In a crystal, symmetry elements do not pass through one point, but they are regularly arranged in space in accordance with the lattice translation symmetry. They are hence termed space groups, and are listed in the *International Tables for Crystallography*.[45]

### 1.5.1. Diffraction of X-rays by Crystals

The measurement of the geometry and symmetry of an X-ray scattering pattern provides information on the unit cell geometry and symmetry since X-rays have a wavelength similar to the atomic spacing in crystals (0.7 - 2.0 Å). The individual intensities of the diffraction pattern determine the positions of the atoms in the unit cell.

X-ray diffraction can be observed using two techniques – single crystal or powder diffraction. These techniques are mainly used to establish crystal and molecular structures, and powder diffraction techniques complement single crystal measurements. For diffraction by a three-dimensional lattice there are three conditions that have to be met – the *Laue* conditions, in which each allowed diffracted beam is labelled by the Miller Indices *h*, *k* and *l*. W.L. Bragg in the single Bragg equation derived an alternative description: [46]

$$n\lambda = 2d\sin\theta \qquad \text{Equation 11}$$

where $n$ = integer; $\lambda$ = wavelength(nm); $d$ = atomic spacing(nm); $\theta$ = glancing angle.

The intensities of the diffraction pattern and the arrangement of atoms in the unit cell of the crystal structure are related to each other by Fourier transformation: the diffraction pattern is the Fourier transform of the electron density and vice-versa. The two numerical values associated with each reflection in a crystal diffraction pattern are the amplitude, $|F|$, and the phase, $\phi$, of the diffracted wave. One of the central difficulties in structure determination by X-ray crystallography is referred to as the phase problem.[47] This arises from the fact that the diffraction pattern contains information only on the magnitude of the amplitude but not the phase of the diffracted wave. The phase may be 0 or $\pi$ and $F$ may be positive or negative. The phase problem can be overcome by a variety of methods; the main two techniques are Patterson synthesis and Direct methods.[47] In Patterson synthesis, instead of the structure factor $F_{hkl}$, the Fourier transform of the observed diffracted beam amplitudes $|F_0|$ gives the electron density, $p(xyz)$. The Fourier transform of the squared amplitudes $F_0^2$ with all phases set equal to zero (all waves taken in phase) produces what is called a Patterson synthesis:[47]

$$p(xyz) = V^{-1}\sum F_o(hkl)^2 \cdot \exp\left[-2\pi i(hx + ky + lz)\right] \qquad \text{Equation 12}$$

where $V$ = volume /Å$^3$; $F_o$ = observed structure amplitude; $h,k,l$ are Miller indices.

The result is a map, rather like an electron density map in that it has peaks of positive density in various positions. It is a map of vectors between pairs of atoms in the structure. If some atoms are heavy, they dominate the scattering (because their scattering factors are large) and their locations may be deduced quite readily. The sign of $F_{hkl}$ can then be calculated from the locations of the heavy atoms in the unit cell, and to a high probability the phase calculated for them will be the same as the phase for the entire unit cell. Patterson methods are useful when there are small numbers of heavy atoms or when the structure contains rigid groups.

In contrast Direct methods is based on the possibility of treating atoms in the unit cell as being virtually randomly distributed, and then using statistical techniques to compute the probabilities that the phases have a particular value,[47] i.e. to get the relations among phases. For example, if $F_1$, $F_2$ & $F_3$ are all strong and $h_1 + h_2 + h_3 = 0$; $k_1 + k_2 + k_3 = 0$; $l_1 + l_2 + l_3 = 0$ then $\phi_1 + \phi_2 + \phi_3 \approx 0$.[46]

### 1.5.2. Data Collection and Corrections

Using an area detector means that many diffracted beams are recorded simultaneously, whereas the old four-circle diffractometers recorded a single beam.[47] All symmetry-unique data should be collected if possible. Redundant or repeated measurements for each unique ($h$, $k$, $l$) are collected to improve the quality of data. The crystal is rotated about one axis and each exposure covers a small angular range, the details of which depend on the instrument. The use of an area detector results in quicker data collection due to the fact it is not necessary to bring all reflections into the horizontal plane in order to record them.[47] In addition, when used with a CCD camera, snapshots of the diffraction pattern can be taken to view its suitability before data collection.

All the crystal structures studied in this thesis were collected at low temperatures using the laser technique employed by Boese and Nussbaumer.[48] For this purpose, the diffractometer is fitted with a low-temperature attachment, which provides a

continuous stream of cooling gas at a controlled temperature.[48] The crystal can then be studied on the same instrument without interrupting the cooling process. Crystallisation is undertaken in a capillary mounted onto the goniometer head. On cooling the sample, a polycrystalline solid (with possibly a glassy intermediate) forms. This can then be converted into a single crystal by inducing a solid-liquid equilibrium in the capillary using a heat source such as a laser.[48] The position of the heat source is brought into line with the solid before being withdrawn to allow the sample to cool slowly to form a (single) crystal. The continuation of a crystal growing process in the capillary may be monitored by means of a video camera. The pictures may be taken by a computer at time intervals and compared to give an idea of the increasing size of the crystals.

Once the data have been collected, they must be reduced by applying background and various other corrections, the most important of which is the absorption correction.[47] The term data reduction is given to this process of converting electronic measurements into usable diffraction data, i.e. the conversion of intensities, $I$, to observed structure amplitudes, $F$, and correspondingly, of associated standard uncertainties, $\sigma$.[47] Background scattering is due to the experimental conditions employed. It may be composed of scattering from the goniometer head, scattering from air, fluorescence radiation from the sample or goniometer head, and cosmic radiation.[47] The removal of this background involves producing both raw intensities and estimated standard deviations in the intensities.

Further corrections are made that are associated with the geometry of the equipment. Lorentz-polarisation factors account for an increase in scattering at low angles, which causes polarisation of the beam, and are dependent on the geometry of the machine used.[47] A decay correction may also be needed for changes in the incident X-ray beam intensity or in the scattering power of the crystal during the experiment. This is less of a problem for data collected at low temperatures where there is seldom any decay, but using the area detector, the data are corrected by an examination of symmetry-equivalent peaks that were measured at the start and end of the data collection.[47]

All matter absorbs X-rays, the intensity of which varies with the size and shape of the crystal as well as the types and relative amounts of different atoms in the sample, and the wavelength of radiation used in the experiment. A proper treatment of the absorption effect ($\mu$), which largely influences the intensities of the diffracted beams, is of great importance in an accurate structure analysis.[47] Ignoring $\mu$ adds systematic error to the resulting crystal structure. The absorption of X-rays follows the Beer-Lambert Law, shown in Equation 13.[49]

$$\frac{I}{I_o} = \exp(-\mu l c) \qquad \text{Equation 13}$$

where $I_0$ is the intensity of the incident light, $I$ is the intensity after passing through the material, $l$ is the distance that the light travels through the material (the path length), $c$ is the concentration of absorbing species in the material and $\mu$ is the absorption coefficient of the absorber.

Hence, the value of $\mu$ depends only upon the atomic composition of the material and the X-ray wavelength. The empirical method employed to apply absorption corrections relies on further intensity measurements.[50] The multiscan method is of most use when there is a large redundancy in the data-set, as is usually the case for area-detector data. Equivalent intensities are analysed in terms of a multipolar spherical harmonic expansion and the method is implemented in programs such as SADABS.[51]

The final step of data reduction involves the merging and averaging of symmetry-equivalent intensity data to produce a unique, corrected and scaled set of data. This is achieved through the numerical measurement of the agreement among equivalent reflections, which are an indication of the quality of the data and the appropriateness of the applied corrections.[49]

### 1.5.3. Structure Refinement

In the final stages of the determination of a crystal structure, the parameters describing the structure (e.g. atom positions) are adjusted systematically to give the best fit between the observed intensities and those calculated from the model of the structure deduced from the diffraction pattern.[47] The process is called structure refinement and it uses the well-established least-squares method. This defines the best fit of two sets of data ($|F_o|$ and $|F_{calc}|$) to be that which minimises $\sum w(|F_o| - |F_{calc}|)^2$, where $w$ is a weighting factor.[47] The result is an approximation and therefore must be repeated many times until it converges.[47] The weights used in least-squares refinements are chosen to represent the relative influence an observation should have on the result and they typically include some term representing the statistical error of the diffraction data.[47]

The X-ray scattering power of an atom decreases as the scattering angle increases due to the finite size of the electron cloud around the nucleus.[47] The electron cloud for a vibrating atom is larger than that of a similar atom at rest and the magnitude of the vibration correlates with temperature. This displacement due to atomic vibration can be described by the isotropic displacement parameter, $U$, where the electron cloud is uniformly smeared in all directions.[47] However, the vibrational motions of bonded atoms are not isotropic, and so a significantly better fit to the data can be achieved by using more than one displacement parameter per atom in the model, allowing each atom to vibrate by different amounts in different directions.[47] This anisotropic vibration can be described by the six independent components of the tensor $U_{ij}$, which are termed the anisotropic displacement parameters,

The parameters being refined in a crystal structure determination are the atom positions ($x$, $y$ and $z$) and displacement parameters, $U$ or $U_{ij}$. One way to describe how well the model fits the observed data is to calculate discrepancy, or residual factors, defined as in Equations 14 and 15.[47]

$$R_1 = \frac{\sum |F_o - F_{calc}|}{\sum |F_o|}$$ Equation 14

$$wR_2 = \sqrt{\frac{\sum w(F_o^2 - F_{calc}^2)^2}{\sum w(F_o^2)^2}}$$ Equation 15

The $R_1$ expression is reported with refinements on $F$ and is based only on the observed data, $F_o^2 > 4\sigma(F_o^2)$. $wR_2$ is a weighted $R$ factor based upon each reflection having its own weight, $w$, where $F^2$ values are used rather than $F$ values.[47]

### 1.5.4. Limitations

Other than the phase problem discussed in Section 1.5.1., X-ray crystallography suffers from other limitations.

The main limitation to X-ray crystallography is the fact that we require a single crystal (powder diffraction is regarded as a separate technique that requires expertise). Not only does the crystal have to be single, but it also needs to be of a suitable size. There are many compounds that do not crystallise, but give glasses or twinned crystals (see later), hence limiting the number of compounds that can be studied. The emergence of low-temperature techniques, specifically the Boese and Nussbaumer method,[48] means that compounds that are gases or liquids under ambient conditions are now able to be studied, but the use of low temperatures may result in phase changes and hence not represent the true structure.

One major limitation in X-ray crystallography is the determination of hydrogen positions within a crystal structure. The diffraction experiment shows the electron density distribution, and from this determines the atomic positions, of the system. In other words, X-ray crystallography measures the distances between centres of electron density, and not internuclear distances (see Section 1.2.4.).[1] This electron

density is generally distributed symmetrically around the nucleus, but in reality there are deviations from this spherical symmetry due to chemical bonding and other valence effects. In addition, the scattering power of an atom is directly proportional to its atomic number. The effect is particularly marked for hydrogen atoms, which are consistently located too close to their bonded atoms. This problem is exacerbated when there are large scattering atoms in the unit cell that will mask further the scattering contribution of the hydrogen.[47]

Twinning can be defined as two or more crystals of the same material inter-grown so that the unit cell of the first is related to the unit cell of the second by a symmetry element.[47] It can be difficult to know that the crystal is twinned rather than just not of sufficient quality. A twinned crystal results in a diffraction pattern that is the superposition of the diffraction patterns of the two (or more) components of the crystal.[47] Patterson or direct method analysis may not yield interpretable maps, thus making structure determination more difficult. However if the twin relationship can be worked out from the diffraction pattern, then there are methods for solving and refining the structure.[47] This requires the expertise of an experienced crystallographer.

A further problem often found in X-ray crystallography is that of disorder.[47] Static disorder is the name given when groups of atoms are orientated in alternative positions at random.[47] This results in all the molecules not actually being identical, with the experiment giving us the average structure.[47] This disorder is usually included in the model as an occupancy ratio, but it is sometimes difficult to incorporate into a model which is refined, especially when some alternative atom sites lie close together or where there is multiple disorder. Static disorder results in the electron density being spread out from ideal ordered positions and hence increases interference effects and reduces diffraction intensities so that it is more difficult to model the experimental intensity accurately.[47] It is also possible for the disorder to go unnoticed and hence for an inaccurate structure to be determined.[47]

## 1.6. Aims of Ph.D.

The structures of many borane compounds are known, however those of the higher boron halides are less well known. The compounds $B_8F_{12}$ (Chapter 3), $B_{10}F_{12}$ (Chapter 5) and a selection of carboranes (Chapter 7) have been studied in this work. The compound $B(BF_2)_3CO$ has also been studied since it is a precursor to $B_8F_{12}$, thus creating interest in any structure correlation between the $B(BF_2)_3$ fragment and $B_8F_{12}$.

The techniques of GED, *ab initio* calculations and X-ray diffraction have been used to study these borane molecules to increase the knowledge of boron structures for future use.

## 1.7. References


1. E. A. V. Ebsworth, D. W. H. Rankin and S. Cradock, *Structural Methods in Inorganic Chemistry*, pp.305-315, Blackwell Scientific Publications, 1987.
2. W. J. Hehre, J. Yu, P. E. Klunzinger and L. Lou, *A Brief Guide to Molecular Mechanics and Quantum Chemical Calculations*, pp.15-21, Wavefunction Inc., 1998.
3. P. P. Debye, *Phys. Z.*, 1939, **80**, 404.
4. L. de Broglie, *Phil. Mag.*, 1924, **47**, 446 and *Ann. Phys.*, 1925, **3**, 22.
5. C. J. Davisson and L. H. Germer, *Phys. Rev.*, 1927, **30**, 705.
6. T. Young, *The Bakerian Lecture: On the theory of light and colours. Philosophical Transactions*, 1802, **92**, 12. (Summarised in www.eiu.edu/~mediasrv/davis/chapter_20/ch20_2.htm)
7. I. Hargittai and M. Hargittai, *Stereochemical Applications of Gas-phase Electron Diffraction, Part A: The Electron Diffraction Technique*, pp.17-20, VCH, 1988.
8. A. W. Ross, M. Fink and R. L. Hilderbrandt, in *International Tables for X-ray Crystallography*, (A. J. C. Wilson, Ed.), Vol. C, p.245, Kluwer Academic, 1992.
9. J. R. Durig, *Vibrational Spectra and Structure, Equilibrium Structural Parameters*, p.85, Elsevier, 2000.
10. C. M. Huntley, G. S. Laurenson and D. W. H. Rankin, *J. Chem. Soc., Dalton Trans.*, 1980, 954.
11. J. R. Lewis, P. T. Brain and D. W. H. Rankin, *Spectrum*, 1997, **15**, 7.
12. I. Hargittai and M. Hargittai, *Stereochemical Applications of Gas-phase Electron Diffraction, Part A: The Electron Diffraction Technique*, pp.30-33, VCH, 1988.
13. A.J. Blake, P. T. Brain, H. McNab, J. Miller, C. A. Morrison, S. Parsons, D.W.H Rankin, H. E. Robertson and B. A. Smart, *J. Phys. Chem.*, 1996, **100**, 12280; P. T. Brain, C. A. Morrison, S. Parsons and D. W. H. Rankin, *J. Chem. Soc., Dalton Trans.*, 1996, 4589.
14. V. A. Sipachev, *J. Mol. Struct. (Theochem)*, 1985, **121**, 143.
15. E. Schrödinger, *Letters on Wave Mechanics* ed. K. Przibram, Vision, London, 1967.

16. F. Jensen, *Introduction to Computational Chemistry*, pp.3, 59, John Wiley and Sons, 1999.
17. M. Born and J. R. Oppenheimer, *Ann. Phys.*, 1927, **84**, 457.
18. W. J. Hehre, L. Radom, P. Schleyer and J. A. Pople, *Ab initio Molecular Orbital Theory*, p.71, John Wiley & Sons, 1986.
19. D. R. Hartree, *Proc. Camb. Phil. Soc.*, 1928, **24**, 89.
20. V. Fock, *Z. Physik*, 1930, **61**, 126 and *Z. Physik*, 1930, **62**, 795.
21. E. R. Davidson and D. Feller, *Chem. Rev.*, 1986, **86**, 681.
22. J. S. Binkley, J. A. Pople and W. J. Hehre, *J. Am. Chem. Soc.*, 1980, **102**, 939.
23. M. S. Gordon, J. S. Binkley, J. A. Pople, W. J. Pietro and W. J. Hehre, *J. Am. Chem. Soc.*, 1982, **104**, 2797.
24. W. J. Pietro, M. M. Francl, W. J. Hehre, D. J. Defrees, J. A. Pople and J. S. Binkley, *J. Am. Chem. Soc.*, 1982, **104**, 5039.
25. K. D. Dobbs and W. J. Hehre, *J. Comp. Chem.*, 1986, **7**, 359.
26. K. D. Dobbs and W. J. Hehre, *J. Comp. Chem.*, 1987, **8**, 861.
27. K. D. Dobbs and W. J. Hehre, *J. Comp. Chem.*, 1987, **8**, 880.
28. R. Ditchfield and W. J. Hehre, J. A. Pople, *J. Chem. Phys.*, 1971, **54**, 724.
29. W. J. Hehre, R. Ditchfield and J. A. Pople, *J. Chem. Phys.*, 1972, **56**, 2257.
30. P. C. Hariharan and J. A. Pople, *Mol. Phys.*, 1974, **27**, 209.
31. M. S. Gordon, *Chem. Phys. Lett.*, 1980, **76**, 163.
32. P. C. Hariharan and J. A. Pople, *Theo. Chim. Acta.*, 1973, **28**, 213.
33. R. C. Binning Jr. and L. A. Curtiss, *J. Comp. Chem.*, 1990, **11**, 1206.
34. G. A. Petersson, A. Bennett, T. G. Tensfeldt, M. A. Al-Laham, W. A. Shirley and J. Mantazaris, *J. Chem. Phys.*, 1988, **89**, 2193.
35. A. D. McLean and G. S. Chandler, *J. Chem. Phys.*, 1980, **72**, 5639.
36. R. Krishnan, J. S. Binkley, R. Seeger and J. A. Pople, *J. Chem. Phys.*, 1980, **72**, 650.
37. P. J. Hay and W. R. Wadt, *J. Chem. Phys.*, 1985, **82**, 270; *J. Chem. Phys.*, 1985, **82**, 284 and *J. Chem. Phys.*, 1985, **82**, 299.
38. B. I. Dunlap, *Density Functional Methods in Chemistry*, pp.49–60, Springer-Verlag, 1991.
39. R. Neumann, R. H. Nobes and N. C. Handy, *Mol. Phys.*, 1996, **87**, 1.

40. M. Head-Gordon, *J. Phys. Chem.*, 1996, **100**, 13213.
41. Gaussian 98, Revision A.7, M. J. Frisch, G. W. Trucks, H. B. Schlegel, G. E. Scuseria, M. A. Robb, J. R. Cheeseman, V. G. Zakrzewski, J. A. Montgomery, R. E. Stratmann Jr, J. C. Burant, S. Dapprich, J. M. Millam, A. D. Daniels, K. N. Kudin, M. C. Strain, O. Farkas, J. Tomasi, V. Barone, M. Cossi, R. Cammi, B. Mennucci, C. Pomelli, C. Adamo, S. Clifford, J. Ochterski, G. A. Petersson, P. Y. Ayala, Q. Cui, K. Morokuma, D. K. Malick, A. D. Rabuck, K. Raghavachari, J. B. Foresman, J. Cioslowski, J. V. Ortiz, A. G. Baboul, B. B. Stefanov, G. Liu, A. Liashenko, P. Piskorz, I. Komaromi, R. Gomperts, R. L. Martin, D. J. Fox, T. Keith, M. A. Al-Laham, C. Y. Peng, A. Nanayakkara, C. Gonzalez, M. Challacombe, P. M. W. Gill, B. Johnson, W. Chen, M. W. Wong, J. L. Andres, C. Gonzalez, M. Head-Gordon, E. S. Replogle and J. A. Pople, Gaussian, Inc., Pittsburgh PA, 1998.
42. PQS *Ab initio* Program Package version 2.4, Parallel Quantum Solutions, Fayetteville, Arkansas, 2001.
43. V. J. Klimkowski, J. D. Ewbank, C. Van Alsenoy, J. N. Scarsdale and L. Schäfer, *J. Am. Chem. Soc.*, 1982, **104**, 1476.
44. J.-J. Rousseau, *Basic Crystallography*, John Wiley and Sons, 1999.
45. *International Tables for Crystallography*, Volume A, Fourth Edition, IUCr, 1996.
46. C. Hammond, *The Basics of Crystallography and Diffraction Second Edition*, pp. 160-165, OUP, 2001.
47. W. Clegg, *Crystal Structure Determination*, pp.35-45, OUP, 1998.
48. R. Boese and M. Nussbaumer, in *Correlations, Transformations and Interactions in Organic Crystal Chemistry, IUCr Crystallographic Symposia, Vol. 7 (Eds.: D. W. Jones and A. Katrusiak)*, pp.20-37, Oxford, 1994.
49. P. W. Atkins, *Physical Chemistry, Sixth Edition*, p.458, OUP, 1998.
50. R.H. Blessing, *Acta Cryst., Sect. A*, 1995, **51**, 33.
51. SADABS: Area-Detector Absorption Correction; Siemens Industrial Automation Inc., 1996.

# Chapter Two

## The Molecular Structures of Borane Carbonyl Compounds $B(BX_2)_3CO$ (X = F, Cl, Br and I) studied by Gas-phase Electron Diffraction and Theoretical Calculations

## 2.1. Introduction

The compound $B(BF_2)_3CO$ is of particular interest due to its formation in the decomposition of the higher boron fluoride $B_8F_{12}$ in the presence of CO.[1,2] The compound $B_8F_{12}$ is discussed in Chapter 3.

$B(BF_2)_3CO$ was first prepared by Timms in 1967[1,2] but its crystal structure was not known until it was recently published by Jefferey *et al.*, along with that of its chlorine analogue.[3] The bonding of CO to elements, such as boron, without accessible *d* electrons is receiving attention as a result of interest in non-classical metal carbonyls.[4] These non-classical metal carbonyls exhibit reduced metal-to-CO $\pi$ back-bonding compared to more classical species.[4-6]

Work in this chapter investigates the gas-phase structure of $B(BF_2)_3CO$ by both gas-phase electron diffraction and *ab initio* theoretical calculations. This is then compared by theoretical calculations to its halogen analogues $B(BX_2)_3CO$ (X = F, Cl, Br and I) in order to investigate substituent effects. Calculations on the family of compounds $B(BX_2)_3$ (X = F, Cl, Br and I) show how the coordination of CO affects the orientation of $BX_2$ groups and give the dimensions of the parent borane molecules.

As this is a study of boron halides, the compounds $B_2X_4$ are investigated to determine the effects of halogen substitution and to gauge the effects of electron correlation on more simple structures than those of the carbonyl compounds. These can then be compared to experimentally determined structures.[7-9]

## 2.2. Experimental

### 2.2.1. Compound Synthesis

The compound $B(BF_2)_3CO$ was prepared by J. A. J. Pardoe using literature methods.[1,2] This involved the warming of a BF condensate to room temperature.[1,2] The samples provided were used for GED without further purification.

### 2.2.2. Gas-phase Electron Diffraction (GED) Study of $B(BF_2)_3CO$

Data for $B(BF_2)_3CO$ were collected at two different camera distances (128.7 and 285.6 mm) using the Edinburgh apparatus,[10] with a sample temperature of 273 K and the nozzle temperature held at 298 K. Data were recorded photographically on Kodak Electron Image films, which were converted into digital form using a PDS densitometer at the Institute of Astronomy in Cambridge with a scanning program described elsewhere.[11] The weighting points for the off-diagonal weight matrices, correlation parameters and scale factors for the two camera distances are given in Table 1, together with the electron wavelengths, which were determined from the scattering patterns of benzene vapour.[11] The data reduction and analysis were performed using standard programs,[12] employing the scattering factors of Ross *et al.*[13]

**Table 1**. GED data analysis parameters for $B(BF_2)_3CO$.

| | | |
|---|---|---|
| Camera distance /mm | 128.27 | 285.58 |
| $\Delta s$ /nm$^{-1}$ | 4 | 2 |
| $s_{min}$ /nm$^{-1}$ | 80 | 20 |
| $sw_1$ /nm$^{-1}$ | 100 | 40 |
| $sw_2$ /nm$^{-1}$ | 272 | 110 |
| $s_{max}$ /nm$^{-1}$ | 320 | 130 |
| Correlation parameter | -0.2054 | 0.4415 |
| Scale factor, $k^a$ | 0.757(16) | 0.739(9) |
| Electron wavelength /pm | 0.06016 | 0.06015 |

[a] Figures in parenthesis are the estimated standard deviations.

On the basis of the *ab initio* calculations described, electron diffraction refinements[14] were carried out for $B(BF_2)_3CO$ using a model with $C_3$ symmetry and assuming each of the B-$BF_2$ groups to be planar. The structure was refined using nine geometrical parameters as shown in Table 2. Parameters $p_1$ and $p_2$ define the C-O and C-B bond distances respectively. The B-B bond length is defined by $p_3$. Mean and difference values were used for B-F distances ($p_4$ and $p_5$) where the B-F bonds eclipsing B-C-O are longer than the other B-F bonds by $p_5$. The C-B-B angles were defined by $p_6$. Mean and difference B-B-F angles ($p_7$ and $p_8$) were used because the structure calculated *ab initio* (see section 2.3.2) indicated a significant difference. The angles involving the F atoms closest to the C-O bond were larger than those with the F atoms furthest away. The torsional angle representing C-B-B-F is defined as $p_9$. The structure of $B(BF_2)_3CO$ obtained in the GED refinement is shown in Figure 1.

**Figure 1**. Molecular framework for $B(BF_2)_3CO$

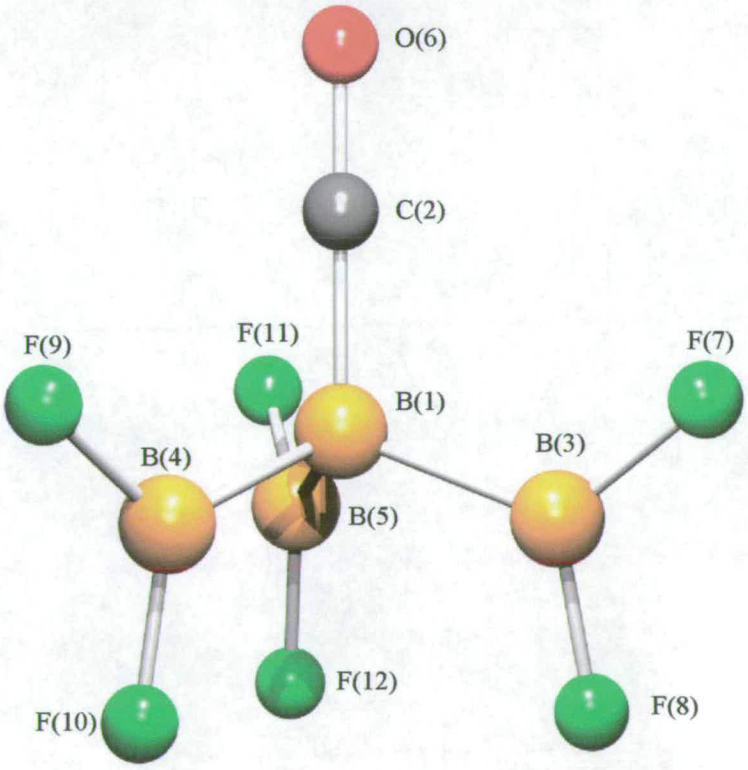

### 2.2.3. *Ab initio* and DFT Calculations

All calculations were performed using the Gaussian 98 computer program.[15] Series of calculations were carried out for all compounds to determine the effects of basis set and electron correlation on the optimised structures. The basis set used was dependent upon the halogen substituents. Two starting geometries were used: first, conformer A, where the $BX_2$ groups lie coplanar with the C-O bond, and secondly conformer B, where the $BX_2$ groups are twisted 90° away from the coplanar arrangement. Calculations on conformer A, for X = F and Br, were performed using a Dec Alpha 1000 4/200 workstation. Calculations for X = Cl and I were carried out using resources of the U.K. Computational Chemistry Facility, on a DEC 8400 superscalar cluster equipped with 10 fast processors, 6 GB of memory and 150 GB disk. Calculations were performed using HF, [16] MP2[17] and DFT[18] methods. For X = F and Cl, calculations were performed at the HF level of theory using the 3-21G*[19] and 6-31G*[20] basis sets; at the MP2 level using 6-31G* and 6-311G*[21] basis sets; and at the B3LYP[22] level using 6-31G* and 6-31+G* basis sets,[23] and a calculation using the 6-31G* basis set on the boron, oxygen and carbon atoms with the 6-31+G* basis set on the halogen atoms. For X = Br, HF calculations were carried out using the 3-21G* and 6-31G* basis sets in addition to a calculation utilising a 6-31G* basis set on the boron, oxygen and carbon atoms and CEP-4G[24] basis set on the bromine atoms. At the B3LYP level of theory, calculations were run using the 6-31G* and 6-31+G* basis sets, and with 6-31G* on the boron, oxygen and carbon atoms but with the 6-31+G* basis set on the bromine atoms. MP2 calculations were performed using 6-31G* and 6-311G* basis sets. For X = I, calculations were performed at HF level using a 3-21G* basis set on all atoms. Calculations were also carried out with 6-31G*, 6-311G* or 6-311+G* basis sets on the B, C and O atoms, coupled with a lanl2dz[25] basis set on the I atoms. MP2 calculations using 6-31G* and 6-311G* basis sets on the B, C and O atoms coupled with a lanl2dz basis set on the I atoms were also performed.

Calculations on conformer B at the HF level using 3-21G* and 6-31G* basis sets were performed for X = F, Cl and Br. The calculations for the iodide were performed

at the HF level using first the 3-21G* basis set, and then using the 6-31G* basis set on the B, C and O atoms with the lanl2dz basis set on the I atoms.

Calculations were performed on the family of compounds $B_2X_4$ (X = F, Cl, Br, I) to determine the effects of halogen substitution and to gauge the effects of electron correlation on a simpler structure to that of the carbonyl compounds. Calculations up to HF/6-31G*, MP2/6-311G* and B3LYP/6-311+G* levels were carried out for all X. In the case of X = I, the lanl2dz basis set was used on the I atoms.

Calculations were performed on the family of compounds $B(BX_2)_3$ (X = F, Cl, Br, I) to determine how the coordination of CO affects the orientation of $BX_2$ groups and the dimensions of the parent borane molecules. Calculations at the MP2/6-311G* level were carried out for all X. In the case of X = I, the lanl2dz basis set was used on the I atoms.

Frequency calculations allowed the nature of any stationary points to be determined, confirming the structure as either a local minimum, transition-state or higher order stationary point on the potential-energy surface. For $B(BF_2)_3CO$, the force field described by Cartesian force constants at the HF/6-31G* level was transformed into one described by a set of symmetry coordinates using the program ASYM40[26] to provide rectilinear vibrational corrections for use in the GED refinement.

## 2.3. Results

### 2.3.1. GED Refinement of $B(BF_2)_3CO$

Two approaches were used during the refinement of the structure of $B(BF_2)_3CO$. First, the C-B-B-F torsion was fixed at 0° and the other parameters were allowed to refine. The torsion was then subsequently refined subject to restraint, using the SARACEN[27] method. Allowing the C-B-B-F torsion to deviate from 0° reduced the $R_G$ factor from 0.080 to 0.077. Using a scaled harmonic *ab initio* force field to obtain

approximations to vibrational amplitudes subsequently reduced the $R_G$ factor further to give a final value of 0.047. The resultant values for the parameters determined from the least-squares refinement along with their comparison with *ab initio* values calculated at the MP2/6-311G* level and the average crystal structure[3] are all listed in Table 2.

Some parameters and amplitudes were subject to flexible restraints (Table 3). The least-squares correlation matrix for the structural refinement is listed in Table 4. The success of the final refinement can be assessed on the basis of the molecular scattering curves (Figure 2) and the radial distribution curve (Figure 3).

**Table 2.** Geometrical parameters ($r_a$ structure) for $B(BF_2)_3CO$ ($r$/pm, angles in °).

| | Parameter | GED | MP2/6-311G* | Crystal[a] |
|---|---|---|---|---|
| $p_1$ | $r$OC | 115.8(3) | 114.1 | 111.7 |
| $p_2$ | $r$CB | 150.2(5) | 150.6 | 152.2 |
| $p_3$ | $r$BB | 169.4(3) | 169.2 | 168.3 |
| $p_4$ | $r$BF$_m$[b] | 133.0(1) | 132.8 | 131.2 |
| $p_5$ | $r$BF$_d$[b] | 1.5(1) | 0.9 | 1.5 |
| $p_6$ | ∠CBB | 108.3(2) | 110.0 | 109.6 |
| $p_7$ | ∠BBF$_m$[b] | 122.2(6) | 121.7 | 123.0 |
| $p_8$ | ∠BBF$_d$[b] | 2.6(1) | 2.0 | 4.1 |
| $p_9$ | ϕCBBF | 2.02(24) | 0.0 | - |

[a] Average crystal structure. [b] m = mean, d = difference.

**Table 3.** Flexible restraints for $B(BF_2)_3CO$.

| Parameter | Value/pm or ° | Uncertainty/pm or ° |
|---|---|---|
| $p_8$ | 2.60 | 0.25 |
| $p_9$ | 2.02 | 0.20 |
| $u_2$ | 4.1 | 0.4 |
| $u_4$ | 33.5 | 2.9 |
| $u_5$ | 29.6 | 2.3 |
| $u_7$ | 31.3 | 2.6 |
| $u_9$ | 21.2 | 3.1 |
| $u_{14}$ | 11.7 | 0.8 |

**Table 4**. Least-squares correlation matrix (x100) for GED structure refinement of $B(BF_2)_3CO$.[a]

| | $p_2$ | $p_5$ | $u_5$ | $u_6$ | $u_9$ | $u_{10}$ | $u_{12}$ | $u_{15}$ | $k_1$[b] |
|---|---|---|---|---|---|---|---|---|---|
| $p_2$ | | 61 | | | | | | | 52 |
| $p_4$ | -50 | | -62 | | -50 | | | | |
| $p_6$ | | 64 | | | | | | | |
| $p_8$ | | | | | 66 | | 66 | | |
| $u_1$ | | | | | | | | | 67 |
| $u_2$ | | | | | | 66 | | 51 | 61 |
| $u_4$ | | | 58 | 71 | | | | | |
| $u_7$ | | | | | -62 | | | | |
| $u_{12}$ | | | | | 67 | | | | |
| $u_{22}$ | 60 | | | | | | | | |
| $u_{23}$ | | | | | | | | 55 | |

[a] Only elements with absolute values >50% are shown.
[b] Scale factor.

**Figure 2**. Experimental and final weighted difference (experimental - theoretical) molecular scattering intensities for $B(BF_2)_3CO$.

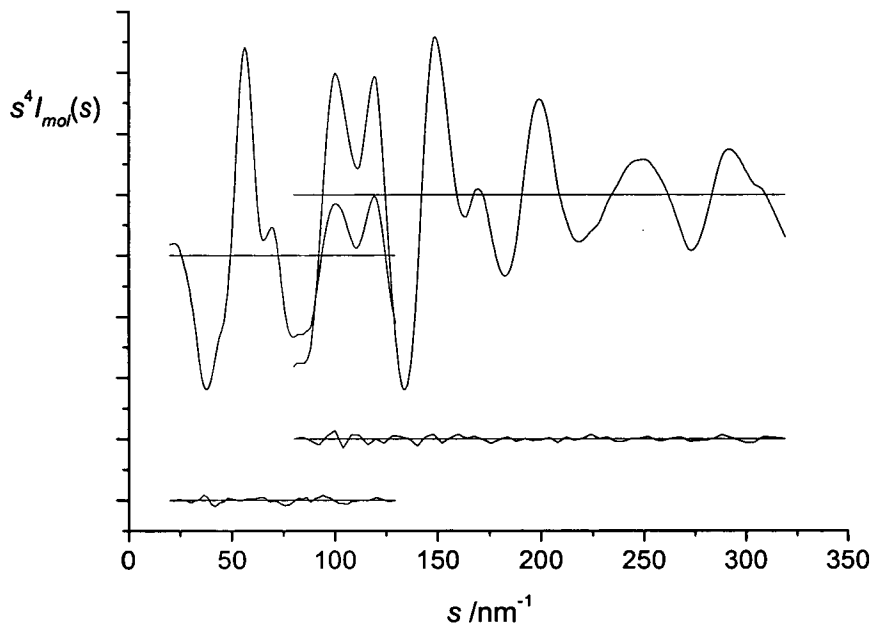

**Figure 3**. Experimental and difference (experimental - theoretical) radial distribution curves, $P(r)/r$ for $B(BF_2)_3CO$. Before Fourier inversion the data were multiplied by $s.\exp(-0.00002s^2)/(Z_B-f_B)/(Z_F-f_F)$.

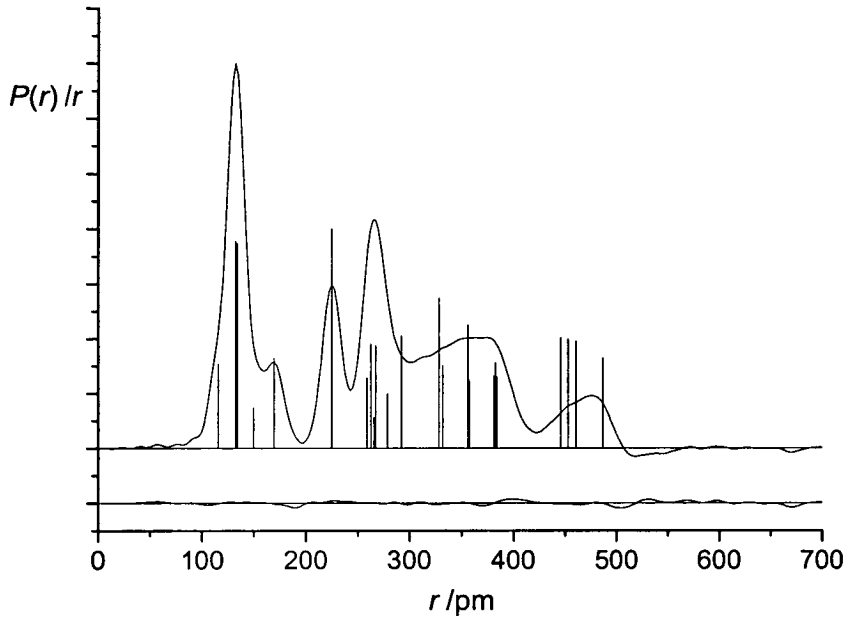


Of the nine geometrical parameters, seven refined without the application of restraints. Parameters $p_8$ ($\angle BBF_d$) and $p_9$ ($\phi CBBF$) were restrained using the SARACEN[27] method, where each restraint has a value and an uncertainty derived from *ab initio* calculations, and so the refined parameters are the best fit to all available information, both experimental and theoretical. Direct amplitude restraints for $u_2$[F(8)-B(3)], $u_4$[F(10)...F(8)], $u_5$[F(7)...O(6)], $u_7$[F(9)...F(8)], $u_9$[F(9)...F(7)] and $u_{14}$[F(8)...C(2)] were found to be necessary to avoid obtaining unrealistic values in the least-squares refinement. Final bond distances and amplitudes of vibration are listed in Table 5.

**Table 5.** Bond distances ($r_a$/pm) and amplitudes of vibration ($u$/pm) obtained in the GED refinement of $B(BF_2)_3CO$.[a]

| $u$ | Atom pair | $r_a$ | Amplitude |
|---|---|---|---|
| 1 | F(8)...F(7) | 225.1(2) | 6.5(2) |
| 2 | F(8)-B(3) | 132.3(6) | 4.1(2) |
| 3 | F(7)-B(3) | 133.7(7) | 4.5 (tied to $u_2$) |
| 4 | F(10)...F(8) | 328.7(14) | 33.5(12) |
| 5 | F(7)...O(6) | 355.9(7) | 29.6(16) |
| 6 | F(7)...C(2) | 292.1(5) | 17.0(13) |
| 7 | F(9)...F(8) | 445.9(10) | 31.3(15) |
| 8 | F(10)...F(7) | 452.9(10) | 28.1 (tied to $u_7$) |
| 9 | F(9)...F(7) | 460.7(10) | 21.2 (19) |
| 10 | F(8)...B(1) | 263.1(5) | 8.2(3) |
| 11 | F(7)...B(1) | 267.6(7) | 7.6 (tied to $u_{10}$) |
| 12 | F(8)...O(6) | 486.7(8) | 14.4(9) |
| 13 | B(3)-B(1) | 169.4(3) | 6.5(3) |
| 14 | F(8)...C(2) | 382.8(7) | 11.7(3) |
| 15 | O(6)-C(2) | 115.8(3) | 4.2(4) |
| 16 | F(8)...B(4) | 328.5(8) | 18.8 (tied to $u_4$) |
| 17 | F(8)...B(5) | 331.9(8) | 18.8 (tied to $u_4$) |
| 18 | F(7)...B(5) | 381.0(8) | 19.6 (tied to $u_{14}$) |
| 19 | F(7)...B(4) | 383.8(8) | 19.6 (tied to $u_{14}$) |
| 20 | B(3)...C(2) | 259.3(4) | 9.8 (tied to $u_{10}$) |
| 21 | O(6)...B(3) | 357.4(5) | 12.7 (tied to $u_5$) |
| 22 | B(4)...B(3) | 278.6(6) | 11.9(18) |
| 23 | C(2)-B(1) | 150.2(5) | 1.1(22) |
| 24 | O(6)...B(1) | 266.0(5) | 6.2 (tied to $u_{10}$) |

[a] Estimated standard deviations, derived from the least-squares refinement, are given in parentheses.

### 2.3.2. *Ab initio* and DFT Calculations

For all cases of X, conformer B returns imaginary frequencies, indicating that these structures represent saddle points or maxima, and that the calculations have failed to reach energy minima on the potential energy surfaces. For conformer A, energy minima were found for all levels of calculation performed for X = F and Cl (see Tables 6 and 7). For X = Br (Table 8), one imaginary frequency was returned at HF/3-21G*, indicating a transition state. However, when the level of calculation was increased to HF/6-31G*, no imaginary frequency was found, indicating a real structure and confirming $C_{3v}$ symmetry.

The results of the calculations performed when X = I (Table 9) differ in that three imaginary frequencies were found for conformer A. When the size of basis set was increased a transition state was reached, in which one $BI_2$ group lay as in conformer B and the other two $BI_2$ groups lay as in conformer A. The mode corresponding to one imaginary frequency was the torsional motion of the perpendicularly positioned $BI_2$ group, so further calculations were performed in which the C-B-B-I angle torsion was allowed to deviate from 0°. The C-B-B-I starting torsion was changed from 0° to 30° whilst maintaining $C_3$ symmetry to allow a greater distance between iodine atoms and calculations at HF level were performed. The structure optimised to give a minimum when the twist had a value of approximately 35° (see Figure 4). The basis sets used were 3-21G* on all atoms, and 6-31G*, 6-311G* or 6-311+G* on the B, C and O atoms with lanl2dz on the I atoms. Calculations at the B3LYP level using a 6-31G*, 6-311G* or 6-311+G* basis set on the B, C and O atoms were performed with the lanl2dz basis set on the I atoms.

**Figure 4**. Molecular framework for $B(BI_2)_3CO$.

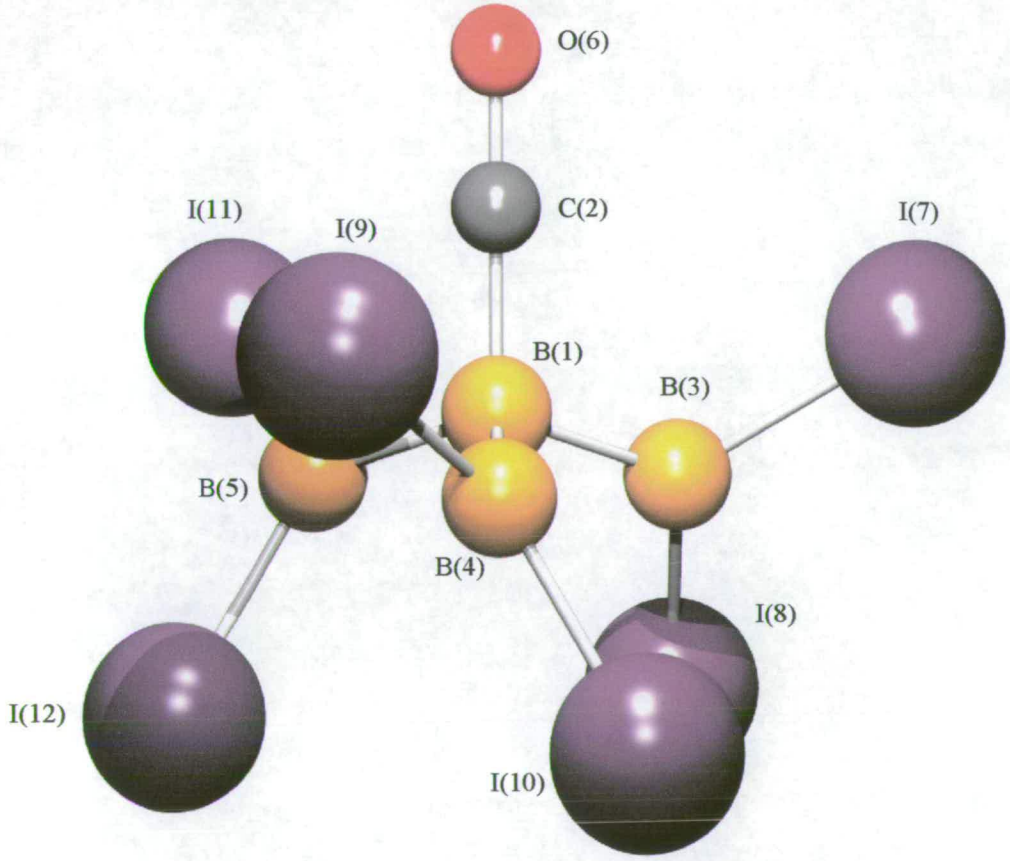

**Table 6**. Geometric parameters for $B(BF_2)_3CO$ ($r_e$/pm, angles in °).

| Geometric parameter | Level of theory / Basis set | | | | | | |
|---|---|---|---|---|---|---|---|
| | HF | | MP2 | | B3LYP | | |
| | 3-21G* | 6-31G* | 6-31G* | 6-311G* | 6-31G* | GEN[a] | 6-31+G* |
| *r*OC | 112.3 | 110.8 | 115.2 | 114.1 | 114.2 | 113.7 | 114.0 |
| *r*CB | 154.4 | 156.9 | 150.2 | 150.6 | 149.7 | 150.7 | 150.6 |
| *r*BB | 168.6 | 171.5 | 169.1 | 169.2 | 170.3 | 170.8 | 171.1 |
| $rBF_m$[b] | 134.5 | 131.5 | 133.5 | 132.8 | 132.7 | 133.3 | 133.2 |
| $rBF_d$[b] | 0.8 | 1.1 | 0.9 | 0.9 | 0.7 | 0.0 | 1.0 |
| ∠CBB | 110.3 | 108.1 | 110.2 | 110.0 | 110.4 | 109.2 | 109.4 |
| $\angle BBF_m$[b] | 122.6 | 122.0 | 121.7 | 121.7 | 121.7 | 121.9 | 121.9 |
| $\angle BBF_d$[b] | 2.2 | 1.7 | 2.5 | 2.0 | 2.9 | 1.4 | 1.7 |
| ∠FBF | 114.9 | 116.0 | 116.6 | 116.6 | 116.6 | 116.1 | 116.2 |
| ϕCBBF | 0.0 | 0.0 | 0.0 | 0.0 | 0.0 | 0.0 | 0.0 |
| Energy[c] | -804.1550 | -808.4922 | -810.1211 | -810.5703 | -812.1559 | -812.1956 | -812.2082 |

[a] 6-31G* on B, C, O atoms and 6-31+G* on F atoms.

[b] m = mean, d = difference.

[c] absolute energy in Hartrees.

**Table 7**. Geometric parameters for $B(BCl_2)_3CO$ ($r_e$/pm, angles in °).

| Geometric parameter | Level of theory / Basis set | | | | | | |
|---|---|---|---|---|---|---|---|
| | HF | | MP2 | | B3LYP | | |
| | 3-21G* | 6-31G* | 6-31G* | 6-311G* | 6-31G* | GEN[a] | 6-31+G* |
| *r*OC | 112.1 | 110.5 | 115.1 | 114.0 | 113.8 | 113.9 | 113.9 |
| *r*CB | 159.0 | 160.7 | 151.6 | 151.6 | 152.1 | 152.1 | 152.1 |
| *r*BB | 171.7 | 173.2 | 170.1 | 169.9 | 172.2 | 172.2 | 172.3 |
| $rBCl_m$[b] | 176.6 | 176.4 | 174.9 | 175.1 | 176.7 | 176.6 | 176.7 |
| $rBCl_d$[b] | 3.0 | 2.5 | 2.8 | 2.1 | 2.3 | 1.1 | 2.2 |
| ∠CBB | 107.4 | 106.3 | 107.6 | 107.6 | 107.3 | 107.3 | 107.3 |
| $\angle BBCl_m$[b] | 121.5 | 121.9 | 121.4 | 121.2 | 121.7 | 121.7 | 121.7 |
| $\angle BBCl_d$[b] | 2.2 | 0.9 | 0.5 | 0.6 | 0.6 | 0.6 | 0.4 |
| ∠ClBCl | 117.1 | 116.3 | 117.3 | 117.5 | 116.6 | 116.6 | 116.5 |
| ϕCBBCl | 0.0 | 0.0 | 0.0 | 0.0 | 0.0 | 0.0 | 0.0 |
| Energy[c] | -2954.9296 | -2968.6159 | -2970.0236 | -2970.8036 | -2974.1672 | -2974.1538 | -2974.1794 |

[a] 6-31G* on B, C, O atoms and 6-31+G* on Cl atoms.

[b] m = mean, d = difference.

[c] absolute energy in Hartrees.

**Table 8**. Geometric parameters for $B(BBr_2)_3CO$ ($r_e$/pm, angles in °).

| Geometric parameter | Level of theory / Basis set | | | | | | | |
|---|---|---|---|---|---|---|---|---|
| | HF | | | MP2 | | B3LYP | | |
| | 3-21G* | 6-31G* | CEP[a] | 6-31G* | 6-311G* | 6-31G* | GEN[b] | 6-31+G* |
| *r*OC | 112.2 | 110.5 | 110.5 | 115.0 | 114.0 | 113.8 | 113.8 | 113.9 |
| *r*CB | 158.6 | 161.3 | 161.8 | 152.1 | 152.4 | 152.4 | 152.9 | 152.7 |
| *r*BB | 170.9 | 172.8 | 173.9 | 169.9 | 170.5 | 171.7 | 172.4 | 172.0 |
| $rBBr_m$[c] | 190.8 | 191.8 | 193.0 | 190.9 | 191.6 | 191.5 | 192.6 | 192.1 |
| $rBBr_d$[c] | 3.1 | 2.9 | 3.1 | 2.9 | 2.7 | 2.6 | 2.7 | 2.3 |
| ∠CBB | 107.5 | 106.8 | 105.7 | 108.2 | 106.9 | 107.7 | 106.6 | 106.7 |
| $\angle BBBr_m$[c] | 120.9 | 121.4 | 122.2 | 121.0 | 121.5 | 121.2 | 122.0 | 121.8 |
| $\angle BBBr_d$[c] | 2.6 | 0.6 | 2.1 | 1.0 | 2.3 | 0.3 | 1.8 | 1.3 |
| ∠BrBBr | 118.3 | 117.1 | 115.6 | 118.0 | 116.9 | 117.6 | 116.1 | 116.5 |
| ϕCBBBr | 0.0 | 0.0 | 0.0 | 0.0 | 0.1 | 0.0 | 0.0 | 0.0 |
| Energy[d] | -15572.1615 | -15631.0522 | -290.5230 | -15632.3546 | -15647.3655 | -15643.2085 | -15528.0605 | -15641.3349 |

[a] 6-31G* on B, C, O atoms and CEP-4G on Br atoms.
[b] 6-31G* on B, C, O atoms and 6-31+G* on Br atoms.
[c] m = mean, d = difference.
[d] absolute energy in Hartrees.

**Table 9**. Geometric parameters for $B(BI_2)_3CO$ ($r_e$/pm, angles in °).

| Geometric parameter | Level of theory / Basis set | | | | | | | | |
|---|---|---|---|---|---|---|---|---|---|
| | HF | | | | MP2 | | B3LYP | | |
| | 3-21G* | 6-31G*[a] | 6-311G*[b] | 6-311+G*[c] | 6-31G*[a] | 6-311G*[b] | 6-31G*[a] | 6-311G*[b] | 6-311+G*[c] |
| $r$OC | 112.2 | 110.6 | 109.8 | 107.8 | 115.6 | 114.5 | 114.1 | 113.2 | 113.2 |
| $r$CB | 158.1 | 160.2 | 159.6 | 159.5 | 150.6 | 150.3 | 151.6 | 151.0 | 150.9 |
| $r$BB | 172.7 | 174.3 | 174.1 | 174.2 | 171.1 | 171.1 | 173.2 | 172.8 | 172.8 |
| $r\mathrm{BI_m}$[d] | 217.5 | 216.4 | 215.8 | 215.8 | 214.2 | 121.3 | 215.6 | 215.1 | 215.2 |
| $r\mathrm{BI_d}$[d] | 2.3 | 2.4 | 2.3 | 2.3 | 1.7 | 1.5 | 2.0 | 1.9 | 1.8 |
| ∠CBB | 107.2 | 106.0 | 106.1 | 106.1 | 107.4 | 107.6 | 106.4 | 106.6 | 106.7 |
| $\angle\mathrm{BBI_m}$[d] | 121.4 | 121.8 | 121.8 | 121.8 | 121.1 | 120.8 | 121.7 | 121.6 | 121.6 |
| $\angle\mathrm{BBI_d}$[d] | 3.2 | 2.1 | 2.2 | 2.2 | 1.2 | 1.5 | 1.5 | 1.5 | 1.4 |
| ∠IBI | 117.1 | 116.4 | 116.4 | 116.4 | 117.7 | 118.2 | 116.7 | 116.7 | 116.7 |
| ϕCBBI | 32.0 | 33.8 | 34.3 | 34.1 | 36.4 | 38.1 | 33.6 | 34.6 | 34.8 |
| Energy[e] | -41537.8816 | -278.5559 | -278.6132 | -278.6176 | -279.4728 | -279.5947 | -281.1885 | -281.2437 | -281.2490 |

[a] 6-31G* on B, C, O atoms and lanl2dz on I atoms.
[b] 6-311G* on B, C, O atoms and lanl2dz on I atoms.
[c] 6-311+G* on B, C, O atoms and lanl2dz on I atoms.
[d] m = mean, d = difference.
[e] absolute energy in Hartrees.

Geometry changes for $B(BF_2)_3CO$ were found as a result of the inclusion of electron correlation and from increasing the size of the basis set. Increasing the size of the basis set from 3-21G* to 6-31G* at the HF level, from 6-31G* to 6-311G* at the MP2 level, and from 6-31G* to 6-31+G* at the B3LYP level resulted in decreased C-O bond lengths (by 1.5 pm, 1.1 pm and 0.2 pm at the HF, MP2 and DFT levels respectively). Increased C-B bond distances resulted from the same increase in basis set size (by 2.6 pm at HF, 0.4 pm at MP2 and 1.1 pm at the DFT level). These differences are more sensitive to increased levels of theory, which include electron correlation effects. Of particular interest are the increased differences found for the three B-F bonds lying closest to the C-O bond compared to the three furthest away. This occurs when the basis set size is increased. For example, at the HF level the difference between the B-F bond distances for the substituent closest to the C-O bond and for the substituent furthest away ($r$BF$_d$) increased from 0.8 pm (3-21G* basis set) to 1.1 pm when the 6-31G* basis set was used. This led to the conclusion that this effect should be modelled in the gas-phase electron diffraction refinement.

The C-B-B angle lies close to the classic $sp^3$ hybrid angle of 109.5°, but the F-B-F angle deviates significantly from 120° (116.6°) as the fluorine atoms closest to the C-O bond position themselves as far away as possible from this region of high electron density. This also results in large differences between B-B-F angles of up to 3°.

For X = Cl, increasing the level of theory from HF to MP2 and DFT resulted in a dramatic decrease in the length of the C-B bond, by around 9 pm in both cases. Increasing the size of the basis set used had little effect on this distance, so the change can be attributed to electron correlation effects. The C-O bond increased in length by approximately 5 pm as the level of theory increased from HF/6-31G* to MP2/6-31G*, but increasing the basis set to 6-311G* resulted in a decreased bond length compared to that found at MP2/6-31G* (115.1 pm compared to 114.0 pm). The crystal structure for $B(BCl_2)_3CO$ has been reported,[3] and shows a very similar structural motif to that determined by these *ab initio* calculations. However, several differences occur in the parameter values. For example, the C-O bond in the solid phase (109.1 pm)[3] is much shorter than that determined by *ab initio* calculations at

MP2/6-311G* (114.0 pm). This is in part due to the underestimation of the inter-nuclear distance in the crystal by X-ray diffraction, which yields distances between centres of electron density. In contrast the C-B bond has a greater value in the crystal structure[3] (154.4 pm compared to 151.6 pm at MP2/6-311G*). In the solid phase[3] there was no difference between B-Cl bond lengths, but at MP2/6-311G* the difference was 2.1 pm.

For X = Br, DFT calculations produced structures with longer C-O bond distances and shorter C-B bond distances compared to calculations at the HF level. The size of the basis set had little effect on these parameters. $B(BBr_2)_3CO$ has parameter values that more closely match those for $B(BCl_2)_3CO$ than the values found for $B(BF_2)_3CO$.

For X = I, minima were found with all computational methods when $BI_2$ groups were twisted approximately 35° away from the positions in which they were coplanar with the C-O bond. This allows the iodine atoms to achieve greater separation from each other. For the optimised structure of conformer A, the distance of separation between atoms I(9)...I(12) equals 421.7 pm (HF/6-311G*). When the $BI_2$ groups are twisted by 34.8°, as at B3LYP/6-311+G*, the separation distance increases to 444.5 pm, thus reducing the amount of steric hindrance between substituent iodines. At the HF level the value of the C-B-B-I torsion angle increased as the size of basis set on the B, C and O atoms was increased from 3-21G* and 6-31G* to 6-311G* (32.0°, 33.8° and 34.3° respectively). The same level of theory saw the C-O bond length decrease from 112.2 pm using a 3-21G* basis set to 107.8 pm using a 6-311+G* basis set. The inclusion of electron correlation led to an increase in the length of the C-O bond, from 107.8 pm at HF/6-311+G* to 113.2 pm at B3LYP/6-311+G*. The C-B bond length decreased by approximately 9 pm when the level of theory was increased from HF (159.5 pm) to DFT (150.9 pm) using the 6-311+G* basis set on the B, C and O atoms and the lanl2dz basis set on the I atoms. Increasing the size of the basis set at the DFT level mirrored the effect found at the HF level, where the C-B-B-I torsion increased when the basis set was increased from 6-31G* to 6-311G* (33.6° increasing to 34.6°). Values for the other parameters were not significantly affected by increasing the basis set from 6-31G* to 6-311G* and 6-311+G*.

The molecules with general formula $B_2X_4$ (X = F, Cl, Br and I) all optimised with staggered conformations, except for $B_2F_4$, at levels from HF/6-311G* upwards. The conformations determined in high-level *ab initio* calculations are in agreement with the gas-phase electron diffraction studies of $B_2F_4$,[7] $B_2Cl_4$[8] and $B_2Br_4$.[9] The calculated geometrical parameters are listed in Tables 10 - 13. In the cases of X = F, Cl and Br, the calculated values are in close agreement to those determined in the gas-phase diffraction studies.[7-9] The calculated distances and angles are within 1pm and 1° of the experimental gas-phase structures[7-9] respectively at MP2/6-311G* level. Halogens have a negative inductive effect since they pull the bonding pair of electrons away from the respective boron atoms.[28] The B-B bond distances in $B_2X_4$ decrease as X is changed from F to I. The B-B bond in the fluoro compound is 5.2 pm longer than the iodo compound at the MP2/6-311G* level.

The family of compounds with general formula $B(BX_2)_3$ (X = F, Cl, Br and I) all optimised with the X atoms lying above and below the plane of the $BB_3$ group. This includes the iodo analogue. Addition of CO to this molecule results in twisting of the $BI_2$ groups by 38.1°. The calculated geometric parameters are listed in Tables 14-17.

The $B(BX_2)_3$ compounds contain planar $B_4$ skeletons, in contrast to the carbonyl compounds. In the parent $B(BX_2)_3$ compounds there is no difference between B-X distances within each molecule since they are related by symmetry and are unaffected by CO electron density as in the carbonyl.

Jeffery *et al.*[3] have reported CO stretching frequencies of 2176 and 2162 $cm^{-1}$ in the IR spectra of $B(BF_2)_3CO$ and $B(BCl_2)_3CO$ respectively. These experimental values compare to calculated values of 2211 $cm^{-1}$ [for $B(BF_2)_3CO$ at B3LYP/6-31+G*] and 2218 $cm^{-1}$ [for $B(BCl_2)_3CO$ at B3LYP/6-31G*]. *Ab initio* calculations at the MP2/6-311G* level show these compounds to have C-O bond distances only 1 pm apart. In comparison the well studied borane(3) carbonyl is reported to possess a CO stretching frequency of 2171 $cm^{-1}$ corresponding to a bond length of 114.8 pm.[29-31]

**Table 10**. Geometric parameters for $B_2F_4$ ($r_e$/pm, angles in °).

| Geometric parameter | Level of theory / Basis set | | | | | | |
|---|---|---|---|---|---|---|---|
| | HF | | MP2 | | B3LYP | | |
| | 3-21G* | 6-31G* | 6-31G* | 6-311G* | 6-31G* | 6-311G* | 6-311+G* |
| *r*BB | 168.8 | 172.8 | 172.1 | 172.0 | 172.2 | 171.6 | 171.8 |
| *r*BF | 133.9 | 131.0 | 132.9 | 132.2 | 132.3 | 132.2 | 132.3 |
| ∠FBF | 115.5 | 116.9 | 117.5 | 117.6 | 117.2 | 117.1 | 117.1 |
| ∠FBB | 122.6 | 121.6 | 121.2 | 121.2 | 121.4 | 121.5 | 121.5 |
| ϕFBBF | 90 | 90 | 0 | 0 | 0 | 0 | 0 |
| Energy[a] | -444.9748 | -447.3669 | -448.1921 | -448.4525 | -449.2934 | -449.4303 | -449.4444 |

[a] absolute energy in Hartrees.

**Table 11**. Geometric parameters for $B_2Cl_4$ ($r_e$/pm, angles in °).

| Geometric parameter | Level of theory / Basis set | | | | | | |
|---|---|---|---|---|---|---|---|
| | HF | | MP2 | | B3LYP | | |
| | 3-21G* | 6-31G* | 6-31G* | 6-311G* | 6-31G* | 6-311G* | 6-311+G* |
| *r*BB | 168.9 | 170.9 | 169.1 | 169.1 | 169.3 | 168.6 | 168.5 |
| *r*BCl | 175.3 | 175.2 | 174.0 | 174.2 | 175.9 | 175.6 | 175.7 |
| ∠ClBCl | 120.3 | 119.6 | 119.8 | 120.0 | 119.5 | 119.4 | 119.3 |
| ∠ClBB | 119.9 | 120.2 | 120.1 | 120.0 | 120.2 | 120.3 | 120.327 |
| ϕClBBCl | 90 | 90 | 90 | 90 | 90 | 90 | 90 |
| Energy[a] | -1878.8425 | -1887.4585 | -1888.1306 | -1888.2806 | -1890.6458 | -1890.7696 | -1890.7750 |

[a] absolute energy in Hartrees.

**Table 12**. Geometric parameters for $B_2Br_4$ ($r_e$/pm, angles in °).

| Geometric parameter | Level of theory / Basis set | | | | | | |
|---|---|---|---|---|---|---|---|
| | HF | | MP2 | | B3LYP | | |
| | 3-21G* | 6-31G* | 6-31G* | 6-311G* | 6-31G* | 6-311G* | 6-311+G* |
| *r*BB | 166.8 | 169.5 | 167.9 | 168.1 | 167.6 | 167.3 | 167.3 |
| *r*BBr | 189.5 | 190.5 | 190.0 | 190.4 | 190.7 | 191.9 | 192.0 |
| ∠BrBBr | 121.8 | 120.8 | 121.3 | 121.1 | 120.6 | 120.9 | 120.2 |
| ∠BrBB | 119.1 | 119.6 | 119.4 | 119.4 | 119.7 | 119.9 | 119.9 |
| ϕBrBBBr | 90 | 90 | 90 | 90 | 90 | 90 | 90 |
| Energy[a] | -10290.3293 | -10329.0792 | -10329.0791 | -10338.9937 | -10336.6690 | -10346.4329 | -10346.4349 |

[a] absolute energy in Hartrees.

**Table 13**. Geometric parameters for $B_2I_4$ ($r_e$/pm, angles in °).

| Geometric parameter | Level of theory / Basis set | | | | | | |
|---|---|---|---|---|---|---|---|
| | HF | | MP2 | | B3LYP | | |
| | 3-21G* | 6-31G*[a] | 6-31G*[a] | 6-311G*[b] | 6-31G*[a] | 6-311G*[b] | 6-311+G*[c] |
| *r*BB | 166.7 | 168.6 | 166.6 | 166.4 | 166.6 | 165.7 | 165.7 |
| *r*BI | 215.5 | 214.4 | 212.6 | 210.9 | 214.1 | 213.7 | 213.7 |
| ∠IBI | 121.9 | 121.3 | 122.2 | 122.8 | 121.2 | 121.4 | 121.4 |
| ∠IBB | 119.0 | 119.3 | 118.9 | 118.6 | 119.4 | 119.3 | 119.3 |
| ϕIBBI | 90 | 90 | 90 | 90 | 90 | 90 | 90 |
| Energy[d] | -27600.8214 | -94.0953 | -94.4391 | -94.4762 | -95.3395 | -95.3507 | -95.3522 |

[a] 6-31G* on B, C, O atoms and lanl2dz on I atoms.
[b] 6-311G* on B, C, O atoms and lanl2dz on I atoms.
[c] 6-311+G* on B, C, O atoms and lanl2dz on I atoms.
[e] absolute energy in Hartrees.

**Table 14**. Geometric parameters for $B(BF_2)_3$ ($r_e$/pm, angles in °).

| Geometric parameter | Level of theory / Basis set | | | | | | | |
|---|---|---|---|---|---|---|---|---|
| | HF | | MP2 | | B3LYP | | | |
| | 3-21G* | 6-31G* | 6-31G* | 6-311G* | 6-31G* | GEN[a] | 6-31+G* | 6-311G* |
| *r*BB | 168.3 | 170.6 | 168.8 | 168.7 | 168.5 | 168.6 | 168.7 | 167.7 |
| *r*BF | 134.2 | 131.2 | 133.3 | 132.6 | 132.7 | 133.2 | 133.1 | 132.6 |
| ∠BBB | 120 | 120 | 120 | 120 | 120 | 120 | 120 | 120 |
| ∠FBF | 115.3 | 116.986 | 117.6 | 117.7 | 117.4 | 117.4 | 117.4 | 117.3 |
| ∠BBF | 122.3 | 121.507 | 121.2 | 121.2 | 121.3 | 121.3 | 121.3 | 121.4 |
| ϕBBBF | 90 | 90 | 90 | 90 | 90 | 90 | 90 | 90 |
| Energy[b] | -692.0045 | -695.7255 | -697.0302 | -697.4262 | -698.7818 | -698.8271 | -698.8351 | -698.9914 |

[a] 6-31G* on B, 6-31+G* on F.
[b] absolute energy in Hartrees.

**Table 15**. Geometric parameters for $B(BCl_2)_3$ ($r_e$/pm, angles in °).

| Geometric parameter | Level of theory / Basis set | | | | | | | |
|---|---|---|---|---|---|---|---|---|
| | HF | | MP2 | | B3LYP | | | |
| | 3-21G* | 6-31G* | 6-31G* | 6-311G* | 6-31G* | GEN[a] | 6-31+G* | 6-311G* |
| *r*BB | 167.6 | 169.3 | 166.2 | 166.1 | 166.8 | 166.9 | 166.9 | 166.1 |
| *r*BCl | 175.6 | 175.5 | 174.2 | 174.3 | 176.1 | 176.0 | 176.1 | 175.8 |
| ∠BBB | 120 | 120 | 120 | 120 | 120 | 120 | 120 | 120 |
| ∠ClBCl | 120.6 | 119.6 | 120.9 | 121.1 | 120.2 | 120.1 | 120.0 | 120.2 |
| ∠BBCl | 119.7 | 120.2 | 119.5 | 119.4 | 119.9 | 119.9 | 120.0 | 119.9 |
| ϕBBBCl | 90 | 90 | 90 | 90 | 90 | 90 | 90 | 90 |
| Energy[b] | -2842.8084 | -2855.8669 | -2856.9491 | -2857.1829 | -2860.8166 | -2860.8048 | -2860.8260 | -2861.0064 |

[a] 6-31G* on B, 6-31+G* on Cl.
[b] absolute energy in Hartrees.

**Table 16**. Geometric parameters for $B(BBr_2)_3$ ($r_e$/pm, angles in °).

| Geometric parameter | Level of theory / Basis set | | | | | | |
|---|---|---|---|---|---|---|---|
| | HF | | | MP2 | | B3LYP | |
| | 3-21G* | 6-31G* | CEP-4G[a] | 6-311G* | 6-31G* | GEN[b] | 6-31+G* |
| *r*BB | 166.1 | 168.1 | 168.9 | 165.6 | 165.4 | 166.2 | 165.5 |
| *r*BBr | 189.8 | 190.7 | 191.7 | 190.5 | 190.8 | 191.6 | 191.0 |
| ∠BBB | 120 | 120 | 120 | 120 | 120 | 120 | 120 |
| ∠BrBBr | 122.5 | 121.3 | 120.1 | 122.3 | 122.3 | 121.1 | 121.6 |
| ∠BBBr | 118.7 | 119.3 | 119.9 | 118.8 | 118.8 | 119.4 | 119.2 |
| ϕBBBBr | 90 | 90 | 90 | 90 | 90 | 90 | 90 |
| Energy[c] | -15460.0405 | -15518.3003 | -177.7823 | -15534.2435 | -15529.8547 | -15528.0605 | -15529.9833 |

[a] 6-31G* on B, CEP-4G on Br.

[b] 6-31G* on B, 6-31+G* on Br.

[c] absolute energy in Hartrees.

**Table 17**. Geometric parameters for $B(BI_2)_3$ ($r_e$/pm, angles in °).

| Geometric parameter | Level of theory / Basis set | | | | | | |
|---|---|---|---|---|---|---|---|
| | HF | | MP2 | B3LYP | | | |
| | 3-21G* | 6-31G*[a] | 6-311G*[b] | 6-31G*[a] | 6-311G*[b] | 6-311+G*[c] | 6-311G*[b] |
| *r*BB | 166.7 | 168.5 | 164.5 | 165.9 | 165.2 | 165.2 | 164.9 |
| *r*BI | 215.6 | 214.8 | 210.8 | 214.1 | 213.7 | 213.7 | 212.8 |
| ∠BBB | 120 | 120 | 120 | 120 | 120 | 120 | 120 |
| ∠IBI | 121.8 | 120.4 | 123.8 | 121.2 | 121.4 | 121.4 | 121.9 |
| ∠BBI | 119.1 | 119.8 | 118.1 | 119.4 | 119.3 | 119.3 | 119.0 |
| ϕBBBI | 90 | 90 | 90 | 90 | 90 | 90 | 90 |
| Energy[d] | -41425.7791 | -165.8228 | -166.4841 | -167.8587 | -167.8798 | -167.8831 | -167.9878 |

[a] 6-31G* on B, lanl2dz on I.
[b] 6-311G* on B, lanl2dz on I.
[c] 6-311+G* on B, lanl2dz on I.
[d] absolute energy in Hartrees.

## 2.4. Discussion

Comparison of the B-B bonds in the four carbonyl molecules shows that there is a small increase in the length of these bonds as the halogen becomes heavier. The effect of electronegative substituents is to make the atom to which they are attached more positive.[28] In $X_2BBX_2$ the B atoms are positive, and so repel one another, to the greatest extent when X = F. In $B(BX_2)_3CO$, the central B will not be made positive in this way, so there will be a somewhat greater attractive force for X = F. A comparison of the gas-phase structures of $B_2F_4$,[7] $B_2Cl_4$[8] and $B_2Br_4$[9] shows that the B-B bond length in the fluoro compound is 1.8 and 3.1 pm longer than in the chloro and bromo analogues respectively. In $B(BX_2)_3CO$, the B-B bonds for X = Cl are 0.6 pm longer than for X = F at MP2/6-311G* and 1.3 pm longer at the B3LYP/6-31+G* level. The distance in the bromo compound is about the same as in the chloro compound, and there is a further slight lengthening in the iodo compound. For $B(BX_2)_3$, as X is changed from F to I, the B-B bond distances decrease steadily such that when X = F, *r*BB equals 168.7 pm and when X = I, *r*BB equals 164.5 pm. This is opposite to the trend found in the carbonyl compounds. The difference between B-B bond distances in $B(BX_2)_3$ and $B(BX_2)_3CO$ equals 0.5, 3.8, 4.9 and 6.6 pm for X = F, Cl, Br and I respectively, at the MP2/6-311G* level.

The calculated C-B-B angle is greatest in the fluoro compound, at 110.0° (MP2/6-311G* level), whereas the angles are smaller, but similar, in the other compounds (107.6, 108.2 and 107.6° for X = Cl, Br and I, respectively). This results in the central boron atom of the fluoro molecule being more regularly tetrahedral than those in the chloro, bromo and iodo analogues.

The starting parameters for the $r_a$ refinement were taken from the theoretical geometry optimised at the MP2/6-31G* level. The $r_\alpha$ structure was not refined because the curvilinear vibrational corrections (i.e. parallel and perpendicular correction terms) are known to be unreliable for molecules with many low-lying vibrational modes. The gas-phase structure exhibits pronounced lengthening of the B-F bonds closest to the B-C-O fragment compared to those furthest away. This

effect is also seen by *ab initio* calculations and in the crystal structure.[3] The C-O bond in the gas phase is more than 4 pm longer than when the compound is in the solid phase.[3] This could be because X-ray crystallography measures centres of electron density whereas gas-phase electron diffraction measures inter-nuclear distances. The C-O bond is shorter in the calculated structure (114.1 pm) than found experimentally in the gas phase (115.8 pm). The experimental value is an $r_a$ distance and the $r_e$ distance, equivalent to the computed parameter, would be almost exactly the same. The computed distance is 2.4 pm longer than the value found in the solid phase.[3] This could be due to vibrational effects whereby the average position of the O is too close to the C. The C-B bond length in the gas-phase structure is similar to that found by calculation but is 2.1 pm shorter than that determined for the solid-phase structure.[3] In other words the C is shifted towards B on the C-O axis when in the gas phase. Compare these values to those recorded for the crystal structure of 1,12-$B_{12}H_{10}(CO)_2$,[32] where CO groups are oppositely attached to apical borons of a icosahedron, which contains C-O bond lengths of 111.9(2) pm.

The C-B-B angles found by X-ray crystallography, gas-phase electron diffraction and *ab initio* calculations are close to the classic $sp^3$ hybrid angle (109.6°, 108.7° and 110.0° respectively). The need for fluorines F(7), F(9) and F(11) to distance themselves from the region of high electron density (B-C-O) is more pronounced in the solid-phase structure. This is shown by the value of $p_8$, which measures the difference between angles B(1)-B(3)-F(7) and B(1)-B(3)-F(8), and the corresponding angles for B(4) and B(5). The difference in the solid state is 4.1° compared to 2.6° in the gas phase and 2.0° in the calculated structure.

$B(BF_2)_3CO$ is an analogue of $BH_3CO$ with $BF_2$ replacing hydrogen. Bauer[29] found, by GED, that borane carbonyl contains a B-C bond of 159.0 pm, which compares to the value of 150.2 pm determined by GED for $B(BF_2)_3CO$. The B-C bond length in borane carbonyl is much longer in comparison to the calculated values, at MP2/6-311G*, of $B(BX_2)_3CO$ (X = F, Cl, Br and I) which contain bond distances of 150.6, 151.6, 152.4 and 150.3 pm respectively. The B-C bond lengths in 1,12-$B_{12}H_{10}(CO)_2$[32] equal 154.3(2) pm.

## 2.5. References


1. P. L. Timms, *J. Am. Chem. Soc.*, 1967, **89**, 1629.
2. R. W. Kirk, D. L. Smith, W. Airey and P. L. Timms, *J. Chem. Soc., Dalton Trans.*, 1972, 1392.
3. J. C. Jeffery, N. C. Norman, J. A. J. Pardoe and P. L. Timms, *Chem. Commun.*, 2000, 2367.
4. A. J. Lupinetti, G. Frenking and S. H. Strauss, *Angew. Chem., Int. Ed.*, 1998, **37**, 2113.
5. A.J. Bridgeman, *J. Chem. Soc., Dalton Trans.*, 1997, 1323.
6. A. Terheiden, E. Bernhardt, H. Willner and F. Aubke, *Angew. Chem., Int. Ed.*, 2002, **41**, 799.
7. D. D. Danielson, J. V. Patton and K. Hedberg, *J. Am. Chem. Soc.*, 1977, 6484.
8. R. R. Ryan and K. Hedberg, *J. Chem. Phys.*, 1969, **50**, 4986.
9. D. D. Danielson and K. Hedberg, *J. Am. Chem. Soc.*, 1979, **101**, 3199.
10. C. M. Huntley, G. S. Laurenson and D. W. H. Rankin, *J. Chem. Soc., Dalton Trans.*, 1980, 954.
11. J. R. Lewis, P. T. Brain and D. W. H. Rankin, *Spectrum*, 1997, **15**, 7.
12. S. Cradock, J. Koprowski and D. W. H. Rankin, *J. Mol. Struct.*, 1981, **77**, 113.
13. A. W. Ross, M. Fink and R. Hilderbrandt, *International Tables for Crystallography*, Ed. A. J. C. Wilson, Kluwer Academic Publishers, Dordrecht, Boston and London, 1992; Vol. C, p.245.
14. A. S. F. Boyd, G. S. Laurenson and D. W. H. Rankin, *J. Mol. Struct.*, 1981, **71**, 217.
15. Gaussian 98, Revision A.7, M. J. Frisch, G. W. Trucks, H. B. Schlegel, G. E. Scuseria, M. A. Robb, J. R. Cheeseman, V. G. Zakrzewski, J. A. Montgomery, R. E. Stratmann Jr, J. C. Burant, S. Dapprich, J. M. Millam, A. D. Daniels, K. N. Kudin, M. C. Strain, O. Farkas, J. Tomasi, V. Barone, M. Cossi, R. Cammi, B. Mennucci, C. Pomelli, C. Adamo, S. Clifford, J. Ochterski, G. A. Petersson, P. Y. Ayala, Q. Cui, K. Morokuma, D. K. Malick, A. D. Rabuck, K. Raghavachari, J. B. Foresman, J. Cioslowski, J. V. Ortiz, A. G. Baboul, B. B. Stefanov, G. Liu, A. Liashenko, P. Piskorz, I. Komaromi, R. Gomperts, R. L. Martin, D. J. Fox, T.

Keith, M. A. Al-Laham, C. Y. Peng, A. Nanayakkara, C. Gonzalez, M. Challacombe, P. M. W. Gill, B. Johnson, W. Chen, M. W. Wong, J. L. Andres, C. Gonzalez, M. Head-Gordon, E. S. Replogle and J. A. Pople, Gaussian, Inc., Pittsburgh PA, 1998.

16. W. J. Hehre, L. Radom, P. v. R. Schleyer and J. A. Pople, *Ab initio Molecular Orbital Theory*, J . Wiley & Sons, 1986, p.71; D. R. Hartree, *Proc. Camb. Phil. Soc.*, 1928, **24**, 89; V. Fock, *Z. Physik*, 1930, **61**, 126 and *Z. Physik*, 1930, **62**, 795.
17. C. Møller and M. S. Plesset, *Phys. Rev.*, 1934, **46**, 618; P. Hohenburg, W. Kohn, *Phys. Rev.*, 1964, **B136**, 864.
18. P. J. Knowles, K. Somasundram, N. C. Handy and K. Hirao, *Chem. Phys. Lett.*, 1993, **211**, 272; W. Kohn, L. J. Sham, *Phys. Rev.*, 1965, **A140**, 1133.
19. J. S. Binkley, J. A. Pople and W. J. Hehre, *J. Am. Chem. Soc.*, 1980, **102**, 939; M. S. Gordon, J. S. Binkley, J. A. Pople, W. J. Pietro and W. J. Hehre, *J. Am. Chem. Soc.*, 1982, **104**, 2797; W. J. Pietro, M. M. Francl, W. J. Hehre, D. J. Defrees, J. A. Pople and J. S. Binkley, *J. Am. Chem. Soc.*, 1982, **104**, 5039.
20. W. J. Hehre, R. Ditchfield and J. A. Pople, *J. Chem. Phys.*, 1972, **56**, 2257; P. C. Hariharan and J. A. Pople, *Mol. Phys.*, 1974, **27**, 209; M. S. Gordon, *Chem. Phys. Lett.*, 1980, **76**, 163.
21. A. D. McLean and G. S. Chandler, *J. Chem. Phys.*, 1980, **72**, 5639; R. Krishnan, J. S. Binkley, R. Seeger and J. A. Pople, *J. Chem. Phys.*, 1980, **72**, 650.
22. A. D. Becke, *Phys. Rev.*, 1988, **A38**, 3098; A. D. Becke, *J. Chem. Phys.*, 1993, **98**, 5648; J. P. Perdew, *Phys. Rev.*, 1986, **B33**, 8822; L. A. Curtiss, K. Raghavachari, G. W. Trucks and J. A. Pople, *J. Chem. Phys.*, 1991, **94**, 7221.
23. K. Raghavachari and G. W. Trucks, *J. Chem. Phys.*, 1989, **91**, 1062.
24. W. Stevens, H. Basch and J. Krauss, *J. Chem. Phys.*, 1984, **81**, 6026; W. J. Stevens, M. Krauss, H. Basch and P. G. Jasien, *Can. J. Chem.*, 1992, **70**, 612; T. R. Cundari and W. J. Stevens, *J. Chem. Phys.*, 1993, **98**, 5555.
25. T. H. Dunning Jr. and P. J. Hay, *Modern Theoretical Chemistry*, Vol. 3, Ed. H. F. Schaefer III, Plenum, 1976, p.1; P. J. Hay and W. R. Wadt, *J. Chem. Phys.*, 1985, **82**, pp.270, 284 and 299.
26. L. Hedberg and I. M. Mills, ASYM40 version 4.1, *J. Mol. Spec.*, 1998, **160**, 117.

27. A.J. Blake, P. T. Brain, H. McNab, J. Miller, C. A. Morrison, S. Parsons, D.W.H Rankin, H. E. Robertson and B. A. Smart, *J. Phys. Chem.*, 1996, **100**, 12280; P. T. Brain, C. A. Morrison, S. Parsons and D. W. H. Rankin, *J. Chem. Soc., Dalton Trans.*, 1996, 4589.
28. D. F. Shriver, P. W. Atkins and C. H. Langford, *Inorganic Chemistry 2nd Edition*, Oxford University Press, 1994, pp.43-46.
29. S. H. Bauer, *J. Am. Chem. Soc.*, 1937, **59**, 1804.
30. A. Skancke and J. F. Liebman, *J. Phys. Chem.*, 1994, **98**, 13215.
31. R. S. Mulliken and W. C. Ermler, *Polyatomic Molecules: The Results of Ab initio Calculations*, Academic Press, New York, 1981.
32. M. A. Fox, J. A. K. Howard, J. M. Maloney and K. Wade, *Chem. Commun.*, 1998, 2487.

# Chapter Three

The Molecular Structure of the Higher Boron Fluoride $B_8F_{12}$ studied by X-ray Crystallography, Gas-phase Electron Diffraction and Theoretical Calculations

## 3.1. Introduction

To a structural chemist borane complexes are fascinating, since simple valence bond theory cannot account for their bonding.[1] Whilst the structural prediction of boranes is assisted through skeletal electron counting methods such as those described by Wade,[2] polyboron halides do not conform to such rules.[3-5] Much is known about the structure of polyboron chlorides, bromides and iodides and of cluster compounds of other Group 13 elements derived from their monohalides.[6-9] However, with the exception of $B_2F_4$,[10] experimental structures of the polyboron fluorides are unknown.

The electron deficiency of boranes, allied to the facilitation of electron donation via $p\pi$-$\pi$ bonding from halides,[3-5] means that a plethora of possible structures is feasible for a compound such as the higher boron fluoride $B_8F_{12}$. The relative stability of $B_8F_{12}$ arises from this possibility of multi-centre bonding to improve electron distribution. The structure of $B_8F_{12}$ has been sought since it was first synthesised in 1967,[9] and there has been no report of a theoretically predicted structure since the molecule was first postulated to adopt a borane-like structure, $B_2(BF_2)_6$, in 1972.[11] The work in this chapter investigates the molecular structure of $B_8F_{12}$ through the use of X-ray crystallography, gas-phase electron diffraction and theoretical calculations.

## 3.2. Experimental

### 3.2.1. Compound Synthesis

J. A. J. Pardoe (University of Bristol) prepared the compound $B_8F_{12}$ using literature methods.[9,11] This involved the low-temperature decomposition of $(BF_2)_2BF$ that is made by condensing gaseous BF with the vapor of $B_2F_4$ at 77 K. [9,11] The samples provided were used for X-ray crystallography and GED without further purification.

### 3.2.2. X-ray Crystallography

Two samples of $B_8F_{12}$ were sealed in glass capillaries and crystals grown at low temperatures (120 and 150 K respectively) on a diffractometer by using the laser technique employed by Boese and Nussbaumer.[12] The first of these samples transpired to be $B_8F_{12}.½BF_3$ containing distinct $B_8F_{12}$ and $BF_3$ molecules.

### 3.2.3. *Ab initio* and DFT Calculations

All calculations were performed using the Gaussian 98 computer program[13] and the resources of the U.K. Computational Chemistry Facility, on a DEC 8400 superscalar cluster equipped with 10 fast processors, 6 GB of memory and 150 GB disk. Series of calculations were carried out starting with the crystal coordinates of $B_8F_{12}$ to determine the effects of basis set and electron correlation on the optimised structures. Calculations were performed using HF[14] (3-21G*[15] and 6-31G*[16] basis sets), MP2[17] (6-31G* basis set) and DFT[18] (6-31G* and 6-31+G*[19] basis sets using the B3LYP functional) methods. Calculations were also carried out on a similar structure with $C_{2v}$ symmetry, in which the central four boron core distances were constrained by symmetry to be equal.

Two previously determined theoretical structures of $B_8F_{12}$ were revisited,[20] using HF (3-21G* and 6-31G* basis sets), MP2 (6-31G* basis set) and DFT (6-31G* and 6-311G*[21] basis sets) methods. These systems consist of two $B_4F_6$ molecules bonded through weak B...F interactions. In the first of these systems, the central boron atom of each $B_4F_6$ molecule bonds to a terminal $F_2B$ group on the adjacent $B_4F_6$ molecule to form a six-membered ring. The two $B_4F_6$ molecules are joined through B...F interactions, 256 pm long. The second system differs from the first by the fact that an eight-membered ring is formed with B...F interactions of 179 pm. This involves B of $BF_2$ groups instead of the central B as in the first case. For pictorial representations of these systems see section 3.3.2. pp 75-77, Figures 3 and 4.

Frequency calculations allowed the nature of any stationary points to be determined, confirming each structure as either a local minimum, transition-state or higher order stationary point on the potential-energy surface. The force field described by Cartesian force constants at the HF/6-31G* level was transformed into one described by a set of symmetry coordinates using the program ASYM40[22] to provide vibrational corrections for use in the GED refinement.

### 3.2.4. Gas-phase Electron Diffraction (GED)

Data for $B_8F_{12}$ were collected at two different camera distances (128.05 and 285.34 mm) using the Edinburgh apparatus,[23] with a sample temperature of 262 K and the nozzle temperature held at 298 K. Data were recorded photographically on Kodak Electron Image films, and were converted into digital form using a PDS densitometer at the Institute of Astronomy in Cambridge with a scanning program described elsewhere.[24] The weighting points for the off-diagonal weight matrices, correlation parameters and scale factors for the two camera distances are given in Table 1, together with the electron wavelengths, which were determined from the scattering patterns of benzene vapour.[24] The data reduction and analysis were performed using standard programs,[25] employing the scattering factors of Ross *et al.*[26]

**Table 1**. GED data analysis parameters for $B_8F_{12}$.

| Camera distance /mm | 128.05 | 285.34 |
|---|---|---|
| $\Delta s$ /nm$^{-1}$ | 4 | 2 |
| $s_{min}$ /nm$^{-1}$ | 96 | 20 |
| $sw_1$ /nm$^{-1}$ | 116 | 40 |
| $sw_2$ /nm$^{-1}$ | 288 | 116 |
| $s_{max}$ /nm$^{-1}$ | 300 | 126 |
| Correlation parameter | 0.3340 | -0.2248 |
| Scale factor, $k$ | 0.7064 | 0.5793 |
| Electron wavelength /pm | 0.0602 | 0.0602 |

On the basis of *ab initio* calculations, electron diffraction refinements[27] were carried out for $B_8F_{12}$ using a model that assumed each of the B-$BF_2$ groups to be planar. The structure was refined using twenty-one geometrical parameters. Parameters $p_1$ and $p_2$ define the central and undistorted ring B-B bond distances respectively. The B-F bond distances found in the bridging $BF_2$ groups are defined by $p_3$. The B-B and B-F bond distances of the four terminal $BF_2$ groups are described by $p_4$ and $p_5$. The *endo* and *exo* angles made between the mid-point of the central B-B bond and the bridging $BF_2$ groups are defined by $p_6$ and $p_7$. The mean B-B-F angle was included ($p_8$) and the four B-B-B-B angles for the terminal B-$BF_2$ groups are described by $p_9$ [for B(8)], $p_{10}$ [for B(7)], $p_{11}$ [for B(6)] and $p_{12}$ [for B(5)]. The torsional motions made by the bridging $BF_2$ groups in relation to the mid-point of the central B(2)-B(4) bond and the opposite bridging B are defined by $p_{13}$ [for B(3)$F_2$] and $p_{14}$ [for B(1)$F_2$]. Parameters $p_{15}$ - $p_{18}$ define the B-B-B-F torsions for the terminal $BF_2$ groups with B(8), B(7), B(6) and B(5) respectively. The out-of-plane movement of B(6)$F_2$ from the co-plane made by B(5), B(2), B(4), B(7) and B(8) is defined by $p_{19}$. The fold angle made by the central butterfly is defined by $p_{20}$. Finally, the distortion of the ring away from the calculated symmetrical structure is described by a distortion coordinate ($p_{21}$) such that the bond lengths B(1)-B(2), B(1)-B(4), B(2)-B(3) and B(3)-B(4) are equal to $p_2$-0.1168$p_{21}$, $p_2$-0.0207$p_{21}$, $p_2$-0.0610$p_{21}$ and $p_2$+0.2000$p_{21}$ respectively. These numbers were derived from the MP2/6-31G* calculation carried out on the crystal coordinates of $B_8F_{12}$ (see section 3.2.3). See Figure 1 for the general molecular structure and atom numbering of $B_8F_{12}$.

## 3.3. Results

### 3.3.1. X-ray Crystallography

There are four crystallographically independent molecules in pure $B_8F_{12}$, and two in the structure of $B_8F_{12}.½BF_3$. However, the structures of all six of these molecules are essentially the same, as shown in Figure 1.

**Figure 1**. Molecular framework for $B_8F_{12}$.

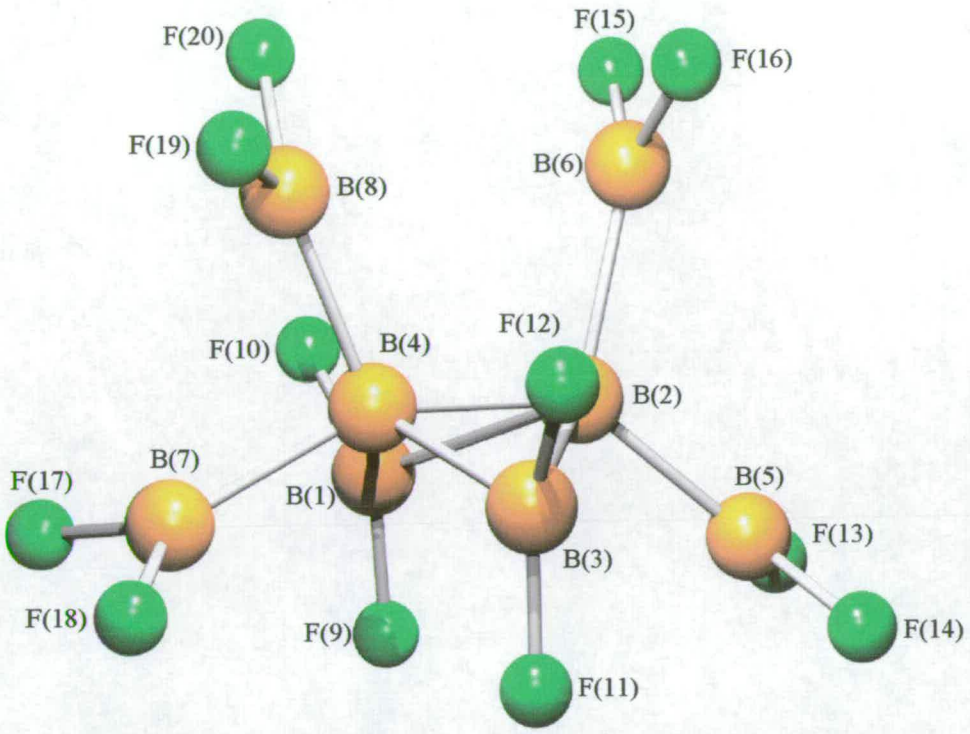


The crystal structure of pure $B_8F_{12}$ was solved by direct methods and refined using the Crystals program[28] to give an $R$ factor of 2.93% and $R_w = 3.38\%$. The compound crystallised in the monoclinic space group $P2/c$ with four molecules in the asymmetric unit. A full list of the crystal data, and data collection and structure solution parameters is shown in Table 2. Tables of fractional coordinates, atomic displacement parameters, bond lengths and angles are given in Appendix A.

**Table 2**. Crystal data for $B_8F_{12}$.

| | |
|---|---|
| (a) Crystal data | |
| Formula | $B_8F_{12}$ $(B_{32}F_{48})$ |
| Formula weight | 1257.86 |
| Temperature | 120 K |
| Wavelength | 0.71073 Å |
| Crystal system | Monoclinic |
| Space group | $P2/c$ |
| Unit cell dimensions | $a = 24.577(3)$ Å, $\alpha = 90°$ |
| | $b = 7.3341(8)$ Å, $\beta = 106.708(2)°$ |
| | $c = 24.493(3)$ Å, $\gamma = 90°$ |

| | |
|---|---|
| Volume, $Z$ | 4401.1(9) $Å^3$, 16 |
| Density (calc.) | 1.898 $Mg/m^3$ |
| Absorption coefficient | 0.244 $mm^{-1}$ |
| $F(000)$ | 2370 |
| | |
| (b) Data collection | |
| Crystal size | 0.30 x 0.30 x 1.0 mm |
| Crystal description | yellow cylinder |
| $\theta$ range | 1.64 to 28.82° |
| Limiting indices | $-31 \leq h \leq 31$, $-9 \leq k \leq 9$, $-34 \leq l \leq 33$ |
| Reflections collected | 37918 |
| Unique data | 8274 |
| Observed data [$I > 2\sigma(I)$] | 7462 [$R_{int} = 0.020$] |
| Scan type | $\omega$ multi-scan |
| Absorption correction | $T_{min} = 0.93$, $T_{max} = 0.93$ |
| | |
| (c) Solution and Refinement | |
| Solution | direct [Crystals] |
| Refinement method | full-matrix least-squares on $F$ |
| Data/restraints/parameters | 7462 / 0 / 721 |
| Goodness-of-fit on $F$ | 1.074 |
| Final $R$ indices | $R_1 = 2.983$, $wR_2 = 3.344$ |
| Max shift | 0.0013 |
| Weighting scheme | Chebychev,[28] 3 polynomials 1.37, 1.08, 1.07 |

The four $B_8F_{12}$ molecules in the asymmetric unit are all approximately identical with the same asymmetry. The B-B bonds range from 165.9 to 215.6 pm. The smallest B-B distance corresponds to the spinal bond of the butterfly (165.9 - 167.4 pm) and the terminal B-B bonds have distances lying in the range 170.5 - 173.4 pm. All B-F bonds have lengths in the region of 130.0 to 133.4 pm, with the greater distances corresponding to bonds in bridging $BF_2$ groups.

The core B(4)[$\mu$-$BF_2$]$_2$B(2) unit of $B_8F_{12}$ is non-planar, with an average angle between the B(1)-B(2)-B(4) and B(2)-B(3)-B(4) planes of 123.1° (range 121.6 - 125.7°). The core is markedly asymmetric, with the four B-B bridge bonds varying in length in all six crystallographically independent molecules. The range of these B-B bonds is 179 to 216 pm in the sequence B(1)-B(2) < B(2)-B(3) < B(1)-B(4) << B(3)-B(4).

The solid-phase structure of a crystal containing $B_8F_{12}$ and $BF_3$ was solved by direct methods and refined using the Crystals program.[28] The compound crystallised in the triclinic $P\bar{1}$ space group at 120 K. The structure refinement gave an $R$ factor of 3.89% and weighted $R$ factor of 3.51%. The weighting scheme was achieved using Chebychev polynomials with five parameters.[28] Two approximately identical molecules of $B_8F_{12}$ crystallised for every one $BF_3$ in the asymmetric unit. A full list of crystal data, and data collection and structure refinement parameters is given in Table 3. Tables of fractional coordinates, atomic displacement parameters, bond lengths and angles are given in Appendix A.

**Table 3**. Crystal data for $B_8F_{12}.½BF_3$.

| | |
|---|---|
| (a) Crystal data | |
| Formula | $(B_8F_{12})_2.BF_3$ $(B_{17}F_{27})$ |
| Formula weight | 696.73 |
| Temperature | 120 K |
| Wavelength | 0.71073 Å |
| Crystal system | Triclinic |
| Space group | $P\bar{1}$ |
| Unit cell dimensions | $a$ = 7.321(3) Å, $\alpha$ = 69.364(6)° |
| | $b$ = 13.176(5) Å, $\beta$ = 79.511(6)° |
| | $c$ = 13.529(6) Å, $\gamma$ = 81.299(6)° |
| Volume, $Z$ | 1195.5(9) Å$^3$, 2 |
| Density (calc.) | 1.935 Mg/m$^3$ |
| Absorption coefficient | 0.251 mm$^{-1}$ |
| $F$(000) | 656 |
| | |
| (b) Data collection | |
| Crystal size | 0.34 x 0.34 x 1.0 mm |
| Crystal description | colourless cylinder |
| $\theta$ range | 1.62 to 29.02° |
| Limiting indices | $-9 \le h \le 9$, $-17 \le k \le 17$, $-18 \le l \le 18$ |
| Reflections collected | 11053 |
| Unique data | 5715 |
| Obs. data [ $I > 2\sigma(I)$] | 3354 [$R_{int}$ = 0.0389] |
| Scan type | $\omega$ multi-scan |
| Absorption correction | $T_{min}$ = 0.615, $T_{max}$ = 0.928 |
| | |
| (c) Solution and Refinement | |
| Solution | direct [Crystals] |
| Refinement method | full-matrix least-squares on $F$ |

| | |
|---|---|
| Data/restraints/parameters | 3354 / 0 / 397 |
| Goodness-of-fit on *F* | 1.0728 |
| Final *R* indices | $R_1 = 3.890$, $wR_2 = 3.510$ |
| max shift | 0.0005 |
| Weighting scheme | Chebychev,[28] 5 polynomials |
| | 0.175, -2.06, -0.402, -1.01, -0.214 |

The two $B_8F_{12}$ molecules show the same asymmetry as seen for pure $B_8F_{12}$ with similar bond distances. One of the four core B-B bonds [B(3)-B(4)] is much longer than the others, with an average value of 207.1 pm compared to 185.8 pm for the two molecules of $B_8F_{12}$ in $B_8F_{12}.½BF_3$. This difference would be even greater if it were not for the B(1)-B(4) distance in residue 1 which is 3.5 pm shorter than the corresponding distance in residue 2 [186.9(4) compared to 190.4(4) pm]. Distance B(3)-B(4) has the greatest value with both values over 205.0 pm. This is also seen in the crystal of pure $B_8F_{12}$. The short B(2)-B(4) bond averages to 166.5 pm - over 40 pm shorter than the average B(3)-B(4) bond length. All B-F bonds lie in the range 129.0 to 133.4 pm, with the largest values seen in the terminal $BF_2$ groups.

Selected bond distances and angles for the six molecules are listed in Tables 4 and 5.

For the pure compound, all $BF_2$ groups have angles close to 120°, with the F-B-F angle (115 - 118°) less than the two corresponding B-B-F angles (121 - 122°). Borons B(2) and B(4) have approximately tetrahedral angles with their terminal $BF_2$ groups and the bridging borons but angles between terminal [B(5), B(6), B(7), and B(8)] and bridging borons [B(1), B(3)] depend on the relative position of each boron. These angles have a very wide range of values, those containing B(5) and B(7) lying from 81° - 101° [B(1)-B(2)-B(5), B(3)-B(2)-B(5), B(1)-B(4)-B(7), B(3)-B(4)-B(7)], and those containing B(6) and B(8) ranging between 116 - 147° [B(1)-B(2)-B(6), B(3)-B(2)-B(6), B(1)-B(4)-B(8), B(3)-B(4)-B(8)]. The angles for the $B_8F_{12}$ molecules in $B_8F_{12}.½BF_3$ are similar to those seen for the four molecules in pure $B_8F_{12}$ (see Table 5).

**Table 4**. B-B bond lengths (pm) for pure $B_8F_{12}$ and $B_8F_{12}.½BF_3$ crystal structures.

| Molecule Residue | $B_8F_{12}$ 1 | $B_8F_{12}$ 2 | $B_8F_{12}$ 3 | $B_8F_{12}$ 4 | $B_8F_{12}.½BF_3$ 1 | $B_8F_{12}.½BF_3$ 2 | Average |
|---|---|---|---|---|---|---|---|
| B(1)-B(2) | 179.2 | 177.1 | 180.6 | 177.0 | 181.6 | 180.2 | 180.1 |
| B(1)-B(4) | 190.0 | 196.1 | 190.3 | 196.8 | 186.9 | 190.4 | 190.2 |
| B(2)-B(3) | 185.8 | 182.9 | 187.3 | 183.0 | 188.2 | 187.3 | 186.8 |
| B(2)-B(4) | 165.9 | 167.1 | 166.8 | 167.4 | 166.1 | 166.9 | 166.6 |
| B(2)-B(5) | 173.4 | 175.1 | 174.9 | 174.8 | 174.7 | 174.1 | 174.4 |
| B(2)-B(6) | 170.5 | 171.0 | 171.8 | 171.3 | 172.0 | 172.1 | 171.7 |
| B(3)-B(4) | 210.9 | 213.4 | 208.5 | 215.6 | 205.0 | 209.3 | 208.8 |
| B(4)-B(7) | 173.4 | 173.3 | 173.2 | 173.1 | 174.9 | 174.3 | 174.1 |
| B(4)-B(8) | 171.0 | 171.0 | 170.9 | 171.7 | 172.7 | 172.1 | 172.0 |

**Table 5**. Average bond angles (°) for pure $B_8F_{12}$ and $B_8F_{12}.½BF_3$ crystal structures.

| | | | |
|---|---|---|---|
| B(1)-B(2)-B(3) | 111.5 | F(11)-B(3)-F(12) | 120.0 |
| B(1)-B(2)-B(4) | 66.8 | F(9)-B(1)-F(10) | 117.9 |
| B(1)-B(2)-B(5) | 81.1 | F(13)-B(5)-F(14) | 117.6 |
| B(1)-B(2)-B(6) | 130.1 | F(15)-B(5)-F(16) | 115.8 |
| B(1)-B(4)-B(7) | 84.2 | F(17)-B(7)-F(18) | 118.5 |
| B(1)-B(4)-B(8) | 144.4 | F(19)-B(8)-F(20) | 117.0 |
| B(2)-B(1)-B(4) | 53.3 | B(2)-B(3)-F(11) | 116.9 |
| B(2)-B(4)-B(1) | 59.9 | B(2)-B(3)-F(12) | 120.7 |
| B(2)-B(4)-B(7) | 137.4 | B(2)-B(1)-F(9) | 118.4 |
| B(2)-B(4)-B(8) | 114.2 | B(2)-B(1)-F(10) | 119.6 |
| B(3)-B(2)-B(4) | 72.7 | B(4)-B(1)-F(9) | 115.4 |
| B(3)-B(2)-B(5) | 101.8 | B(4)-B(1)-F(10) | 115.1 |
| B(3)-B(2)-B(6) | 114.7 | B(2)-B(5)-F(13) | 120.4 |
| B(4)-B(2)-B(5) | 141.3 | B(2)-B(5)-F(14) | 121.3 |
| B(4)-B(2)-B(6) | 111.8 | B(2)-B(6)-F(15) | 121.9 |
| B(5)-B(2)-B(6) | 105.3 | B(2)-B(6)-F(16) | 122.2 |
| B(7)-B(4)-B(8) | 108.1 | B(4)-B(7)-F(17) | 120.0 |
| | | B(4)-B(7)-F(18) | 121.1 |
| | | B(4)-B(8)-F(19) | 122.2 |
| | | B(4)-B(8)-F(20) | 120.8 |

The crystal structure of $B_8F_{12}$ gives rise to an extensive network of inter- and intramolecular contacts between boron [B(3)] and fluorine (see Figure 2). These contacts serve to stabilise the molecular structure.

**Figure 2**. Intermolecular contacts found in (a) $B_8F_{12}.½BF_3$, (b) pure $B_8F_{12}$.

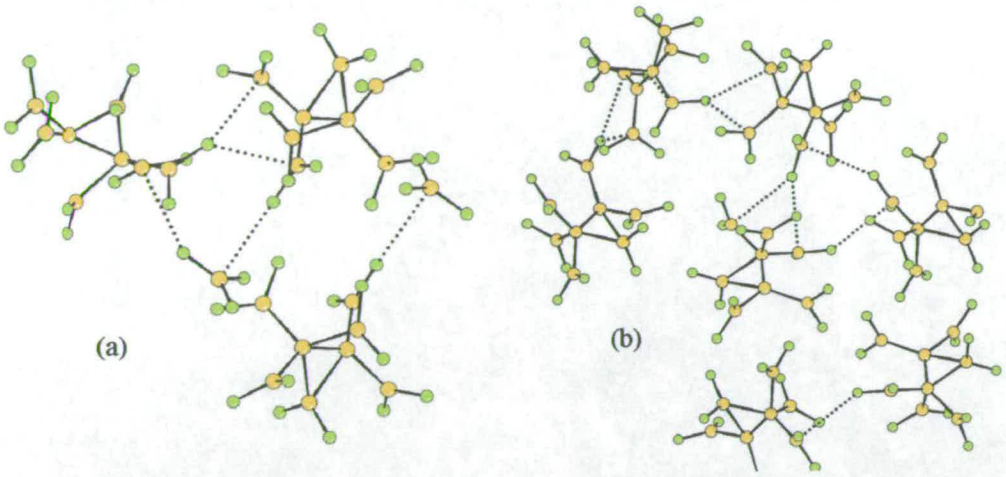


$B_8F_{12}$ possesses a long bifurcated, intramolecular interaction between F(9) and the boron atoms B(5) and B(7) in two of the terminal $BF_2$ groups (see Figure 1). This serves to pull the B(1) atom out of the plane of B(3), B(2) and B(4) [observed ranges 260.3 - 267.5 pm for B(5)...F(9) and 262.0 - 269.3 pm for B(7)...F(9)]. These interactions also affect the B(1)-F(9) bond, which, at an average of 133.5 pm, is longer than other such bonds in the molecule. Furthermore, the atoms B(2), B(4), B(5), B(7) and B(8) are coplanar, but B(6) is displaced from this plane by an average of 0.43(7)° to accommodate an interaction between B(8) and F(15). The longest B...F interaction (273.3 - 294.2 pm) is formed between B(3) and F(13). This contact may be responsible for the lengthening of the B(3)-B(4) bond.

### 3.3.2. *Ab initio* and DFT Calculations

*Ab initio* calculations run starting with the crystal coordinates optimise to give an energy minimum structure similar to that seen in the solid phase (Figure 1). The remarkable asymmetry seen in the crystal is also evident by calculation at all levels of theory, including those that incorporate electron correlation effects. The extent of this asymmetry is dependent upon the level of theory used, with the MP2/6-31G* calculation showing less asymmetry than is found at HF and B3LYP[29] levels. The level of asymmetry seen in the central boron fragment is described in Table 6.

**Table 6**. Calculated ($r_e$) B-B bond lengths (pm) for $B_8F_{12}$, optimised starting with the crystal coordinates.

| Geometric parameter | Level of theory / Basis set | | | | | | | |
|---|---|---|---|---|---|---|---|---|
| | HF | | MP2 | | B3LYP | | | |
| | 3-21G* | 6-31G* | 6-31G* | 6-31+G* | 6-31G* | GEN[a] | 6-311G* | 6-311+G** |
| B(1)-B(2) | 171.4 | 174.3 | 175.5 | 176.2 | 176.0 | 176.6 | 175.9 | 176.0 |
| B(1)-B(4) | 212.4 | 196.7 | 185.1 | 186.6 | 188.1 | 188.4 | 188.7 | 189.6 |
| B(2)-B(3) | 170.8 | 175.6 | 181.1 | 181.9 | 178.9 | 178.7 | 177.8 | 178.1 |
| B(2)-B(4) | 179.7 | 174.7 | 163.5 | 164.3 | 165.7 | 167.1 | 166.3 | 166.8 |
| B(2)-B(5) | 172.7 | 178.1 | 171.9 | 172.9 | 172.9 | 174.3 | 173.4 | 173.9 |
| B(2)-B(6) | 167.3 | 172.4 | 169.8 | 170.8 | 170.8 | 171.9 | 170.8 | 171.3 |
| B(3)-B(4) | 228.0 | 242.6 | 207.2 | 210.0 | 216.9 | 224.0 | 223.4 | 226.0 |
| B(4)-B(7) | 168.9 | 172.8 | 171.5 | 172.2 | 171.1 | 171.7 | 171.0 | 171.4 |
| B(4)-B(8) | 169.8 | 171.8 | 170.4 | 171.0 | 170.5 | 170.9 | 170.2 | 170.5 |
| Energy[b] | -1384.0331 | -1391.4318 | -1394.1239 | -1394.2183 | -1397.5985 | -1397.6661 | -1398.0061 | -1398.0345 |

[a] 6-31G* on B, 6-31+G* on F.

[b] absolute energy in Hartrees.

Calculations on the $C_{2v}$ structure with a non-planar $B_4$ unit and constrained B-B core distances (where the B-B core bonds are constrained to be equal, but their value is not constrained) failed to produce a system with lower energy than that found for the asymmetric crystal coordinates (Table 7). This system is not a potential energy minimum and is 8.40 kJ $mol^{-1}$ higher in energy (at the MP2/6-31G* level) than the optimised crystal coordinates.

The asymmetry seen in the solid phase is also evident in the calculations described thus far. We can therefore be confident that this apparent structural anomaly cannot be attributed to crystal packing forces and that this asymmetry is an inherent structural property of this molecule. One possible explanation for the asymmetry seen in the central boron ring could be the presence of short intramolecular B...F contacts between bridging $BF_2$ groups and terminal $BF_2$ groups. The shortest contact in the optimised crystal coordinates, at the MP2/6-31G* level, is similar to that observed in the solid phase [calculated 257.2 and 258.8 pm for B(5)...F(9) and B(7)...F(9) respectively]. This could explain the relative energy of the system compared to the transition state structure, which has relatively longer contacts of 267.8 and 266.1 pm for B(5)...F(9) and B(7)...F(9) at the MP2/6-311G* level.

Vast geometry changes for the optimised crystal coordinates were found as a result of the inclusion of electron correlation and from increasing the size of the basis set (Table 6). Increasing the size of the basis set, from 3-21G* to 6-31G* at the HF level, and from 6-31G* to 6-311G* at the B3LYP level, resulted in an increase in the B(3)-B(4) bond distance, by 14.6 and 7.1 pm at the HF and DFT levels respectively. The inclusion of electron correlation decreases the same bond length from 242.6 pm at the HF/6-31G* level to 216.9 pm at the B3LYP/6-31G* level and 207.2 pm at the MP2/6-31G* level. The values at the MP2 level more closely resemble the average crystal structure.

**Table 7**. Calculated ($r_e$) B-B bond lengths (pm) for $B_8F_{12}$ constrained to $C_{2v}$ symmetry.

| Geometric parameter | Level of theory / Basis set | | | | | |
|---|---|---|---|---|---|---|
| | HF | | MP2 | | B3LYP | |
| | 3-21G* | 6-31G* | 6-31G* | 6-311G* | 6-31G* | 6-311G* |
| B(1)-B(2)[a] | 189.6 | 192.7 | 186.6 | 187.2 | 188.2 | 188.9 |
| B(2)-B(4) | 167.1 | 168.1 | 163.3 | 163.2 | 164.6 | 164.6 |
| B(2)-B(5) | 171.3 | 173.6 | 171.5 | 171.9 | 171.6 | 171.4 |
| B(2)-B(6) | 169.4 | 172.6 | 170.6 | 170.7 | 171.2 | 170.9 |
| B(4)-B(7) | 171.3 | 173.6 | 171.4 | 171.6 | 171.4 | 171.3 |
| B(4)-B(8) | 169.4 | 172.6 | 170.0 | 170.1 | 170.6 | 170.4 |
| Energy[b] | -1384.0237 | -1391.4299 | -1394.1207 | -1394.9123 | -1397.5951 | -1398.0017 |

[a] B(1)-B(2) = B(1)-B(4) = B(2)-B(3) = B(3)-B(4).

[b] absolute energy in Hartrees.

Calculations at the HF level give a much longer B(2)-B(4) bond than the calculations that include electron correlation. A comparison using the 6-31G* basis set shows this bond at the HF level to be 9.0 and 11.2 pm longer than at the B3LYP and MP2 levels respectively. With a sufficiently large basis set (6-31G*), the terminal B-B bonds involving atoms B(5) and B(7) are longer than their counterparts B(6) and B(8). The differences between B(2)-B(5) and B(2)-B(6), and B(4)-B(7) and B(4)-B(8) are 5.7 and 1.0 pm (at the HF level); 2.1 and 0.6 pm (at the B3LYP level); and 2.1 and 1.1 pm (at the MP2 level).

Constraining the core B-B bond distances to be equal reduces the differences between levels of theory. The bond distance B(2)-B(4) is 168.1 pm at the HF/6-31G* compared to the values 164.6 and 163.3 pm at the B3LYP/6-31G* and MP2/6-31G* levels.

Calculations on the first dimer system returned an energy minimum structure as shown in Figure 3. This system is established from two $B(BF_2)_3$ molecules bonded through long-range B...F interactions 298.8 pm in length (at the MP2/6-31+G* level) to produce an eight-membered ring. Selected bond distances are shown in Table 8.

**Figure 3**. $B_8F_{12}$ dimer structure (energy minimum).

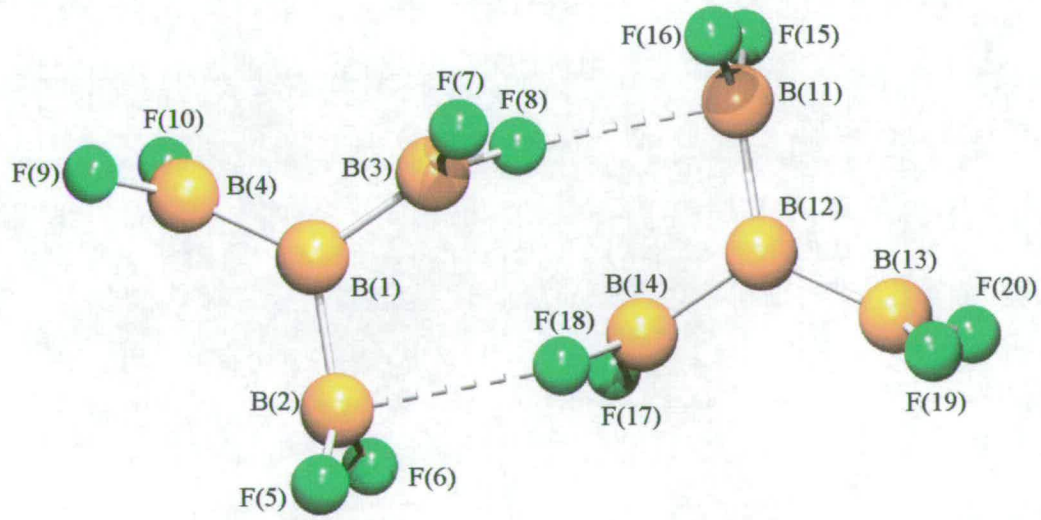

**Table 8**. Calculated ($r_e$) bond lengths (pm) for $B_8F_{12}$ energy minimum dimer.

| Geometric parameter | Level of theory / Basis set | | | | | |
|---|---|---|---|---|---|---|
| | HF | | MP2 | | B3LYP | |
| | 3-21G* | 6-31G* | 6-31G* | 6-31+G* | 6-31G* | 6-311G* |
| B(1)-B(2) | 168.7 | 170.9 | 169.1 | 169.3 | 168.7 | 168.0 |
| B(1)-B(3) | 167.4 | 170.3 | 168.3 | 168.7 | 168.1 | 167.4 |
| B(1)-B(4) | 167.8 | 170.6 | 168.6 | 169.0 | 168.2 | 167.7 |
| B(11)-B(12) | 167.7 | 170.9 | 169.1 | 169.3 | 168.7 | 168.0 |
| B(12)-B(13) | 168.8 | 170.6 | 168.6 | 169.0 | 168.2 | 167.7 |
| B(12)-B(14) | 167.4 | 170.3 | 168.3 | 168.7 | 168.1 | 167.4 |
| B(2)…F(18) | 255.7 | 306.7 | 281.1 | 298.8 | 294.3 | 307.2 |
| B(11)…F(8) | 255.6 | 306.7 | 281.0 | 298.8 | 294.2 | 307.9 |
| Energy[a] | -1384.0387 | -1391.4588 | -1394.0748 | -1394.1831 | -1397.5734 | -1397.9894 |

[a] absolute energy in Hartrees.

Changes in the level of theory and basis set do not have a huge effect on the B-B bond distances in the system. The same cannot be said for the distance between the two monomeric species. Table 8 shows that increasing the basis set (from 3-21G* to 6-31G* at the HF level, from 6-31G* to 6-31+G* at the MP2 level, and from 6-31G* to 6-311G* at the B3LYP level) results in an increased separation distance between the $B(BF_2)_3$ molecules. This increase equals 51.1 pm at the HF level, 17.8 pm at the MP2 level, and 13.7 pm at the DFT level. Using the 6-31G* basis set, the MP2 level of theory indicates the strongest B...F interaction with a distance of 281.1 pm, some 25.7 pm shorter than at the HF level, and 13.2 pm shorter than the DFT level calculation with the same basis set.

Calculations on the second dimer system returned a transition state structure as shown in Figure 4. The two $B(BF_2)_3$ molecules in this system are arranged to form a six-membered ring that includes two B...F interactions equalling 200.9 pm at the MP2/6-31+G* level of theory, thus representing a huge difference (97.9 pm) compared to the B...F interaction for the energy minimum dimer. This B...F interaction is dependent upon the level of theory and size of basis set used. Selected bond distances are shown in Table 9.

**Figure 4**. $B_8F_{12}$ dimer structure (transition state).

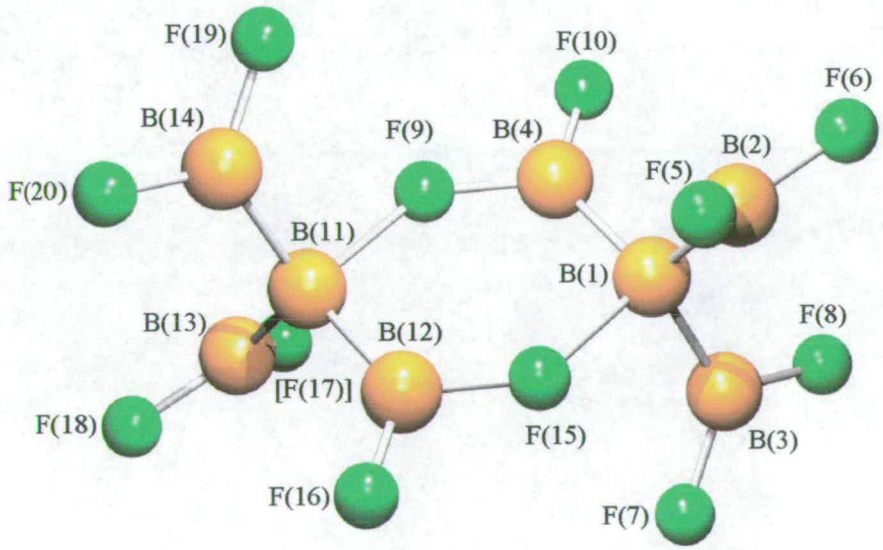

**Table 9**. Calculated ($r_e$) bond lengths (pm) for $B_8F_{12}$ transition state dimer.

| Geometric parameter | Level of theory / Basis set | | | | | |
|---|---|---|---|---|---|---|
| | HF | | MP2 | | B3LYP | |
| | 3-21G* | 6-31G* | 6-31G* | 6-31+G* | 6-31G* | 6-311G* |
| B(1)-B(2) | 168.3 | 170.7 | 168.8 | 169.3 | 168.8 | 168.2 |
| B(1)-B(3) | 168.3 | 170.7 | 168.6 | 169.1 | 168.8 | 168.2 |
| B(1)-B(4) | 167.2 | 170.3 | 167.5 | 168.3 | 166.4 | 166.9 |
| B(11)-B(12) | 167.2 | 170.3 | 167.5 | 168.3 | 166.4 | 166.9 |
| B(11)-B(13) | 168.3 | 170.7 | 168.6 | 169.1 | 168.8 | 168.2 |
| B(11)-B(14) | 168.3 | 170.7 | 168.8 | 169.3 | 168.8 | 168.2 |
| B(11)...F(9) | 178.0 | 254.2 | 186.0 | 200.9 | 183.6 | 215.3 |
| B(1)...F(15) | 178.9 | 254.0 | 186.0 | 200.6 | 183.6 | 215.3 |
| Energy[a] | -1384.0773 | -1391.4651 | -1394.0945 | -1394.1947 | -1397.5811 | -1397.9949 |

[a] absolute energy in Hartrees.

As Table 9 indicates, increasing the size of basis set (from 3-21G* to 6-31G* at the HF level, from 6-31G* to 6-31+G* at the MP2 level, and from 6-31G* to 6-311G* at the B3LYP level) results in an increase in the separation distance. This increase equals 76.2 pm at the HF level, 14.9 pm at the MP2 level, and 31.7 pm at the DFT level. The greatest of these increases represents one of the largest basis set effects we have ever seen.

The *ab initio* and DFT calculations carried out on these $B_8F_{12}$ systems highlight the unusual and varied bonding that a compound such as $B_8F_{12}$ can adopt. The ability or inability to synthesise these varied systems underlines the importance of experimental data to corroborate theoretical calculations. The comparison of absolute energies calculated by *ab initio* and DFT methods gives an indication of which systems are more likely to exist experimentally, in that a lower energy denotes a more stable system. A comparison of the calculated energies of the systems discussed in this section (see Table 10) shows that at the HF level the second dimer system is the lowest in energy, indicative of the most stable structure that $B_8F_{12}$ can adopt.

**Table 10**. Absolute energies (Hartrees) for calculated $B_8F_{12}$ systems.

| System | Level of theory / Basis set | | |
|---|---|---|---|
| | HF | MP2 | B3LYP |
| | 6-31G* | 6-31G* | 6-31G* |
| **1** | -1391.4318 | -1394.1239 | -1397.5985 |
| **2** | -1391.4299 | -1394.1207 | -1397.5951 |
| **3** | -1391.4588 | -1394.0748 | -1397.5734 |
| **4** | -1391.4651 | -1394.0945 | -1397.5811 |

**1** = optimised crystal coordinates, **2** = constrained $C_{2v}$ structure,
**3** = energy minimum dimer system, **4** = transition state dimer system.

Using the key in Table 10, the sequence for molecular stability at the HF/6-31G* level is **4** > **3** (+ 16.54 kJmol$^{-1}$) >> **1** (+ 87.44 kJmol$^{-1}$) > **2** (+ 92.43 kJmol$^{-1}$). The sequences found at the MP2/6-31G* level [**1** > **2** (+ 8.40 kJmol$^{-1}$) >> **4** (+ 77.20 kJmol$^{-1}$) >> **3** (+ 128.92 kJmol$^{-1}$)] and B3LYP/6-31G* level [**1** > **2** (+ 8.93 kJmol$^{-1}$)

>> **4** (+ 45.69 kJmol$^{-1}$) >> **3** (+ 65.91 kJmol$^{-1}$)] indicate that the inclusion of electron correlation when calculating the structure of $B_8F_{12}$ is crucial.

### 3.3.3. Gas-phase Electron Diffraction (GED)

The model used for the GED refinement of $B_8F_{12}$ was based upon the geometry calculated from the optimised crystal coordinates. The unusual asymmetry determined in the solid phase and by high level *ab initio* calculations was confirmed to also be present in the experimental gas-phase structure by the comparison of two models. The first assumed local symmetry in the boron core, whilst the second model included a distortion coordinate ($p_{21}$). The symmetric model resulted in an $R_G$ factor of 0.068, compared to 0.044 for the asymmetric model using a scaled harmonic *ab initio* force field to obtain approximations to vibrational amplitudes. The resultant values for the parameters determined from the least-squares refinement are listed in Table 11.

Of the twenty-one geometrical parameters, eleven refined without the application of restraints. The parameters which required restraints were the B-B-B angles ($p_{10}$ and $p_{12}$), the torsional angles ($p_{13}$ - $p_{19}$) and the distortion coordinate ($p_{21}$). The details of the uncertainties associated with these restraints are included in Table 11. Some amplitudes were subject to flexible restraints, the details of which are recorded in Appendix A. These were restrained using the SARACEN method,[30] where each restraint has a value and an uncertainty derived from *ab initio* calculations, so that the refined parameters are the best fit to all available information. The least-squares correlation matrix for the structural refinement is listed in Table 12. The success of the final refinement can be assessed on the basis of the molecular scattering curves (Figure 5) and the radial distribution curve (Figure 6). Final bond distances and amplitudes of vibration are listed in Appendix A.

**Table 11**. Geometrical parameters ($r_a$ structure) for $B_8F_{12}$ ($r$/pm, angles in °).

| Parameter[a] | | Value | Uncertainty |
|---|---|---|---|
| $p_1$ | $r$[B(2)B(4)] | 164.2(19) | |
| $p_2$ | $r$BB(ring) | 195.5(12) | |
| $p_3$ | $r$[B(1)F(1)] | 127.0(5) | |
| $p_4$ | $r$[B(2)B(5)] | 174.9(5) | |
| $p_5$ | $r$[B(5)F(5)] | 133.4(2) | |
| $p_6$ | ∠[mB(1)F(*endo*)] | 114.1(15) | |
| $p_7$ | ∠[mB(1)F(*exo*)] | 113.4(11) | |
| $p_8$ | ∠[B(2)B(5)F(5)] | 122.9(2) | |
| $p_9$ | ∠[B(2)B(4)B(8)] | 103.3(15) | |
| $p_{10}$ | ∠[B(2)B(4)B(7)] | 141.7(20) | 14.0 |
| $p_{11}$ | ∠[B(4)B(2)B(6)] | 114.3(16) | |
| $p_{12}$ | ∠[B(4)B(2)B(5)] | 153.8(19) | 15.0 |
| $p_{13}$ | ϕ[F(3)B(3)mF(4)] | -10.3(11) | 1.0 |
| $p_{14}$ | ϕ[F(1)B(1)mF(2)] | 1.1(16) | 1.5 |
| $p_{15}$ | ϕ[B(2)B(4)B(8)F(11)] | 5.4(11) | 1.0 |
| $p_{16}$ | ϕ[B(2)B(4)B(7)F(9)] | 7.8(11) | 1.0 |
| $p_{17}$ | ϕ[B(2)B(4)B(6)F(7)] | -24.7(24) | 2.5 |
| $p_{18}$ | ϕ[B(2)B(4)B(5)F(5)] | 10.2(11) | 1.0 |
| $p_{19}$ | ϕ[B(6)B(2)B(4)B(8)] | 7.8(16) | 2.0 |
| $p_{20}$ | tilt | 20.7(11) | |
| $p_{21}$ | distort | 0.99(2) | 0.02 |

[a] For definition of parameters see Section 3.2.4.
m = mid-point between B(2)-B(4); for atom numbering see Figure 1.

**Table 12**. Least-squares correlation matrix (x100) for GED structure refinement of $B_8F_{12}$.[a]

| | $p_5$ | $p_8$ | $p_9$ | $p_{19}$ | $u_3$ | $u_{13}$ |
|---|---|---|---|---|---|---|
| $p_3$ | -85 | -56 | | | | |
| $p_5$ | | 65 | | | | |
| $p_6$ | | -51 | | | | |
| $p_8$ | 65 | | | | | |
| $p_{10}$ | | | | 63 | | |
| $p_{11}$ | | | -52 | | | |
| $p_{12}$ | | | 60 | | | |
| $u_2$ | | | | | | -84 |
| $u_6$ | | | | | -84 | |
| $u_{23}$ | | | | 50 | | |
| $k_1$[b] | 51 | | | | | |
| $k_2$[b] | | | | | -59 | 61 |

[a] Only elements with absolute values >50% are shown.
[b] Scale factor.

**Figure 5**. Experimental and final weighted difference (experimental - theoretical) molecular scattering intensities for $B_8F_{12}$.

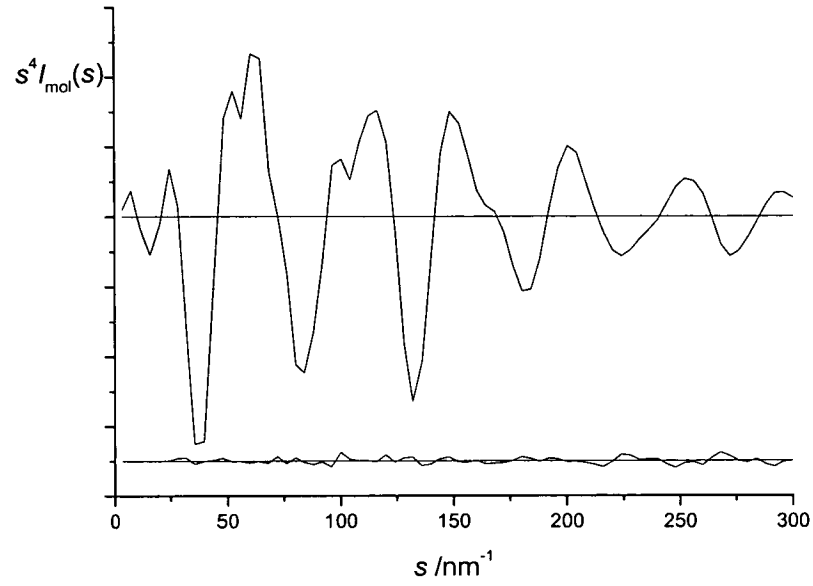


**Figure 6**. Experimental and final weighted difference (experimental - theoretical) radial distribution curves, $P(r)/r$ for $B_8F_{12}$. Before Fourier inversion the data were multiplied by $s.\exp(-0.00002s^2)/(Z_B-f_B)/(Z_F-f_F)$.

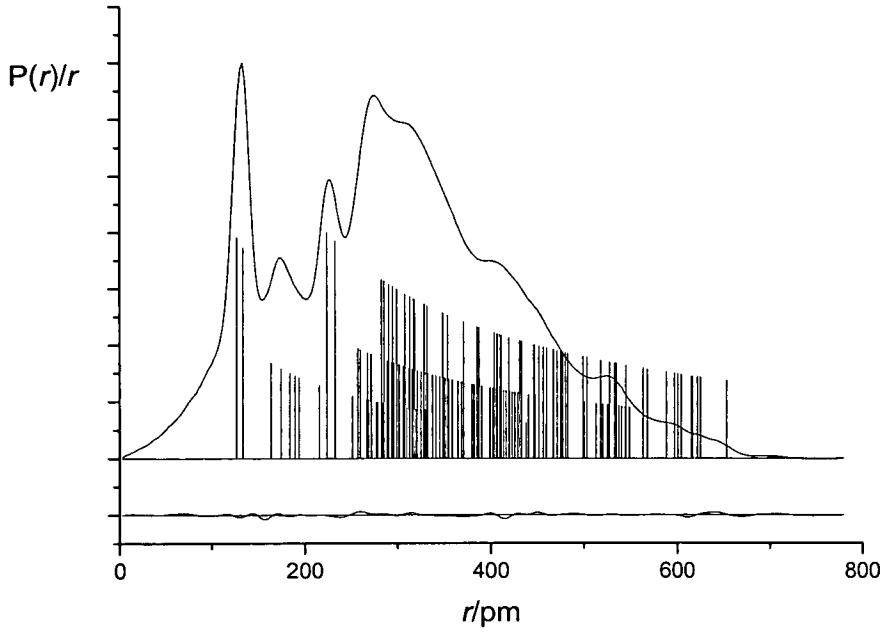

## 3.4. Discussion

The structure of the compound $B_8F_{12}$ had remained a mystery for thirty years until we determined the structure using low-melting point X-ray crystallography, *ab initio* calculations and gas-phase electron diffraction. It has a most unusual structure, inconsistent both with those of electron deficient boranes, such as $B_8H_{12}$,[31] and with those of boron halides, such as $B_8Cl_8$.[32] Not only is it based upon a $B_4$ central core, analogous to $B_4H_{10}$,[33] but this is also highly asymmetrical in both the solid and gas phase. It has bridge bonds and a short central B-B bond, i.e. it combines all the structural elements once considered for diborane.[34] However, $BF_2$ is not just an isolobal replacement for H. The two groups seem very similar in compounds such as the borane carbonyl analogue $(BF_2)_3BCO$ (Chapter 2), with two-centre two-electron B-B bonds. In situations of greater electron deficiency $BF_2$ can be more versatile than H, for it can interact with $\sigma$ and $\pi$ orbitals and provide one electron for $\sigma$-framework bonding and additional electron density through $\pi$ back-bonding from its fluorine atoms.[3-5]

Intermolecular contacts are far from unusual in borane compounds. For example, B...F contacts exist in the crystal structure of $BF_3$ with an average distance of 269.0 pm, by which the boron atoms achieve a total coordination of five fluorine atoms with nearly trigonal bipyramidal geometry.[35] This may go some way to explain the molecular stability in the crystal phase of $B_8F_{12}$, but this does not explain the asymmetry that is also observed, in the absence of long-range order, by *ab initio* calculations and gas-phase electron diffraction data (see Table 13). Indeed, a calculated symmetrical $C_{2v}$ structure pertains to a transition state that is 8.40 kJ $mol^{-1}$ higher in energy than the optimised crystal coordinates. It therefore begs the question: "What is the cause of this asymmetry?"

One possible reason for this asymmetry is the occurrence of hyperconjugated interactions between boron and fluorine that serve to provide molecular stability.[36] The B(5)...F(9) and B(7)...F(9) interactions in the GED determined structure are at distances of 301.7 and 295.8 pm respectively. These are longer than the contacts

determined by X-ray crystallography (260.3 - 267.5 pm and 262.0 - 269.3 pm respectively) and *ab initio* calculations (257.2 and 258.8 pm respectively at the MP2/6-31G* level).

The weaker contacts found by GED are reflected in the longer B-B core bonds, which suggest increased electron deficiency for this region compared to the solid phase (see Table 13). The B(3)-B(4) bond length in the gas phase equals 215.4 pm, which is 8.2 pm longer than in the calculated gas-phase structure and 6.6 pm longer than in the experimental solid-phase structure. The differences in the other core bond lengths between the GED and crystal structures equal +3.8 pm [B(1)-B(2)], +3.2 pm [(B(1)-B(4)], +2.6 pm [B(2)-B(3)], and -2.4 pm [B(2)-B(4)].

**Table 13**. B-B bond distances (pm) in $B_8F_{12}$.

| | GED | MP2/6-31G* | Average crystal |
|---|---|---|---|
| B(1)-B(2) | 183.9(21) | 175.5 | 180.1 |
| B(1)-B(4) | 193.4(21) | 185.1 | 190.2 |
| B(2)-B(3) | 189.4(21) | 181.1 | 186.8 |
| B(2)-B(4) | 164.2(33) | 163.5 | 166.6 |
| B(2)-B(5) | 174.9(9) | 171.9 | 174.4 |
| B(2)-B(6) | 174.9(9) | 169.8 | 171.7 |
| B(3)-B(4) | 215.4(24) | 207.2 | 208.8 |
| B(4)-B(7) | 174.9(9) | 171.5 | 174.1 |
| B(4)-B(8) | 174.9(9) | 170.4 | 172.0 |

In the gas-phase structure of $(BF_2)_3BCO$, F...F intramolecular contacts range from 227.2 to 460.5 pm. In the calculated (MP2/6-31G*) structure of $B_8F_{12}$, forty-two different F...F interactions exist that fall into this range.

Valence bond calculations carried out on $B_8F_{12}$ indicate that the structure lies closer to being made up of $B_5$ and $B_3$ fragments than to two $B_4$ fragments, which would be expected. Calculations on the two $B(BF_2)_3$ dimer structures show that these systems are higher in energy than the optimised crystal coordinates. However, reaction with CO yields $(BF_2)_3BCO$,[9] the structure of which has been studied in Chapter 2.

The structure of $B_8F_{12}$ was first hypothesised by Kirk and Timms in 1972 to be related to that of diborane.[11] This is a simplified description of the true structure, but we have shown that $B_8F_{12}$ and diborane share a common bonding scheme, with $BF_2$ groups in the place of hydrogen. The bridged molecular structure of diborane was established through the separate work of Stitt[37] and Price.[38] The crystal structure of diborane contains a B-B bond distance of 177.6(1) pm.[34] The equivalent distance in $B_8F_{12}$ [B(1)...B(3)] equals 298.6 pm in the crystalline phase!

$B_8F_{12}$ also shows structural similarities to tetraborane ($B_4H_{10}$).[33,39] The core B(2)[$\mu$-$BF_2$]$_2$B(4) unit of $B_8F_{12}$ is non-planar, as is the equivalent B($\mu$-$BH_2$)$_2$B unit of tetraborane. The crystal structure of $B_4H_{10}$ contains a central B-B bond equalling 175.0 pm in the study by Nordman and Lipscomb,[33] and 171.7(4) pm in the more recent study by Brain *et al.*[39] This compares to the average central B-B distance of 166.6 pm in crystalline $B_8F_{12}$ (see Table 13). The gas-phase study by Brain *et al.*[39] showed this bond to be 173.7(5) pm long, compared to the experimental gas-phase distance of 164.2(2) pm in $B_8F_{12}$. The bridging B-B bonds in the crystal structure of $B_4H_{10}$ are 184.5(2) pm in the Nordman and Lipscomb study[33] and 185.2(1) pm in the Brain *et al.* study.[39] In the gas phase these bond lengths equal 186.6(2) pm. The relatively long distances of these bridging bonds in $B_8F_{12}$ (see Table 12) indicate that there are fewer electrons available than in the classic three-centre two-electron bridges of diborane and tetraborane. $B_8F_{12}$ seems to rely on the short, central, two-centre two-electron B(2)-B(4) bond, with additional coordination to these atoms, for its stability.

However, the description of the structure of $B_8F_{12}$ as related to diborane and tetraborane is misleading since it fails to account for the amazing asymmetry found in the boron core, or the twisting of $BF_2$ groups to accommodate hyperconjugation. The structure of $B_8F_{12}$ is unique; it has only been through the combined efforts of low-temperature crystallography, *ab initio* calculations and GED that we have finally been able to solve the thirty-year mystery.

## 3.5. References


1. D. F. Shriver, P. W. Atkins and C. H. Langford, *Inorganic Chemistry 2nd Edition*, Oxford University Press, 1995.
2. K. Wade, *Adv. Inorg. Radiochem.*, 1976, **18**, 1.
3. A. K. Holliday and A. G. Massey, *J. Inorg. Nucl. Chem.*, 1961, **18**, 108.
4. A. G. Massey, *Adv. Inorg. Chem and Radiochem.*, 1983, **26**, 1.
5. J. A. Morrison, *Chem. Rev.* 1991, **91**, 35.
6. C. Dohmeier, D. Loos and H. Schnöckel, *Angew. Chem. Int. Ed.*, 1996, **35**, 129.
7. A. Rodig and G. Lintl, *Angew. Chem. Int. Ed.*, 2000, **39**, 2952.
8. A. Schnepf and H. Schnöckel, *Angew. Chem. Int. Ed.*, 2001, **40**, 712.
9. P. L. Timms, *J. Am. Chem. Soc.*, 1967, **89**, 1629.
10. L. Trefonas and W. N. Lipscomb, *J. Chem. Phys.*, 1958, **28**, 54.
11. R. W. Kirk, D. L. Smith, W. Airey and P. L. Timms, *J. Chem. Soc., Dalton Trans.*, 1972, 1392.
12. R. Boese and M. Nussbaumer, in *Correlations, Transformations and Interactions in Organic Crystal Chemistry, IUCr Crystallographic Symposia, Vol. 7 (Eds.: D. W. Jones and A. Katrusiak)*, pp.20-37, Oxford, 1994.
13. Gaussian 98, Revision A.7, M. J. Frisch, G. W. Trucks, H. B. Schlegel, G. E. Scuseria, M. A. Robb, J. R. Cheeseman, V. G. Zakrzewski, J. A. Montgomery, R. E. Stratmann Jr, J. C. Burant, S. Dapprich, J. M. Millam, A. D. Daniels, K. N. Kudin, M. C. Strain, O. Farkas, J. Tomasi, V. Barone, M. Cossi, R. Cammi, B. Mennucci, C. Pomelli, C. Adamo, S. Clifford, J. Ochterski, G. A. Petersson, P. Y. Ayala, Q. Cui, K. Morokuma, D. K. Malick, A. D. Rabuck, K. Raghavachari, J. B. Foresman, J. Cioslowski, J. V. Ortiz, A. G. Baboul, B. B. Stefanov, G. Liu, A. Liashenko, P. Piskorz, I. Komaromi, R. Gomperts, R. L. Martin, D. J. Fox, T. Keith, M. A. Al-Laham, C. Y. Peng, A. Nanayakkara, C. Gonzalez, M. Challacombe, P. M. W. Gill, B. Johnson, W. Chen, M. W. Wong, J. L. Andres, C. Gonzalez, M. Head-Gordon, E. S. Replogle and J. A. Pople, Gaussian, Inc., Pittsburgh PA, 1998.
14. W. J. Hehre, L. Radom, P. v. R. Schleyer and J. A. Pople, *Ab initio Molecular Orbital Theory*, J . Wiley & Sons, 1986, p.71; D. R. Hartree, *Proc. Camb. Phil.*

*Soc.*, 1928, **24**, 89; V. Fock, *Z. Physik*, 1930, **61**, 126 and *Z. Physik*, 1930, **62**, 795.

15. J. S. Binkley, J. A. Pople and W. J. Hehre, *J. Am. Chem. Soc.*, 1980, **102**, 939; M. S. Gordon, J. S. Binkley, J. A. Pople, W. J. Pietro and W. J. Hehre, *J. Am. Chem. Soc.*, 1982, **104**, 2797; W. J. Pietro, M. M. Francl, W. J. Hehre, D. J. Defrees, J. A. Pople and J. S. Binkley, *J. Am. Chem. Soc.*, 1982, **104**, 5039.
16. W. J. Hehre, R. Ditchfield and J. A. Pople, *J. Chem. Phys.*, 1972, **56**, 2257; P. C. Hariharan and J. A. Pople, *Mol. Phys.*, 1974, **27**, 209; M. S. Gordon, *Chem. Phys. Lett.*, 1980, **76**, 163.
17. C. Møller and M. S. Plesset, *Phys. Rev.*, 1934, **46**, 618; P. Hohenburg, W. Kohn, *Phys. Rev.*, 1964, **B136**, 864.
18. P. J. Knowles, K. Somasundram, N. C. Handy and K. Hirao, *Chem. Phys. Lett.*, 1993, **211**, 272; W. Kohn and L. J. Sham, *Phys. Rev.*,1965, **A140**, 1133.
19. W. J. Hehre, R. Ditchfield and J. A. Pople, *J. Chem. Phys.*, 1972, **56**, 2257; P. C. Hariharan and J. A. Pople, *Mol. Phys.*, 1974, **27**, 209; M. S. Gordon, *Chem. Phys. Lett.*, 1980, **76**, 163.
20. P. Truscott, University of Edinburgh BSc(Hons) project report, 2000.
21. A. D. McLean and G. S. Chandler, *J. Chem. Phys.*, 1980, **72**, 5639; R. Krishnan, J. S. Binkley, R. Seeger and J. A. Pople, *J. Chem. Phys.*, 1980, **72**, 650.
22. L. Hedberg and I. M. Mills, ASYM40 version 4.1, *J. Mol. Spec.*, 1998, **160**, 117.
23. C. M. Huntley, G. S. Laurenson and D. W. H. Rankin, *J. Chem. Soc., Dalton Trans.*, 1980, 954.
24. J. R. Lewis, P. T. Brain and D. W. H. Rankin, *Spectrum*, 1997, **15**, 7.
25. S. Cradock, J. Koprowski and D. W. H. Rankin, *J. Mol. Struct.*, 1981, **77**, 113.
26. A. W. Ross, M. Fink and R. Hilderbrandt, *International Tables for Crystallography*, Ed. A. J. C. Wilson, Kluwer Academic Publishers, Dordrecht, Boston and London, 1992; Vol. C, p.245.
27. A. S. F. Boyd, G. S. Laurenson and D. W. H. Rankin, *J. Mol. Struct.*, 1981, **71**, 217.
28. D. J. Watkin, C. K. Prout, J. R. Carruthers, P. W. Betteridge and R. I. Cooper, CRYSTALS issue 11, Chemical Crystallography Lab., University of Oxford.

29. A. D. Becke, *Phys. Rev.*, 1988, **A38**, 3098; A. D. Becke, *J. Chem. Phys.*, 1993, **98**, 5648; J. P. Perdew, *Phys. Rev.*, 1986, **B33**, 8822; L. A. Curtiss, K. Raghavachari, G. W. Trucks and J. A. Pople, *J. Chem. Phys.*, 1991, **94**, 7221.
30. A. J. Blake, P. T. Brain, H. McNab, J. Miller, C. A. Morrison, S. Parsons, D.W.H Rankin, H. E. Robertson and B. A. Smart, *J. Phys. Chem.*, 1996, **100**, 12280; P. T. Brain, C. A. Morrison, S. Parsons and D. W. H. Rankin, *J. Chem. Soc., Dalton Trans.*, 1996, 4589.
31. R. E. Enrione, F. P. de Boer and W. N. Lipscomb, *J. Am. Chem. Soc.*, 1964, **86**, 1451.
32. S. L. Emery and J. A. Morrison, *J. Am. Chem. Soc.*, 1982, **104**, 6790.
33. C. E. Nordman and W. N. Lipscomb, *J. Chem. Phys.*, 1953, **21**, 1856.
34. H. W. Smith and W. N. Lipscomb, *J. Chem. Phys.*, 1965, **43**, 1060.
35. D. Mootz and M. Steffen, *Z. Anorg. Chem.*, 1981, **483**, 171.
36. J. C. Cramer, *J. Molec. Struct. (Theochem)*, 1996, **370**, 135.
37. F. Stitt, *J. Chem. Phys.*, 1940, **8**, 981; F. Stitt, *J. Chem. Phys.*, 1941, **9**, 780.
38. W. C. Price, *J. Chem. Phys.*, 1947, **15**, 614; W. C. Price, *J. Chem. Phys.*, 1948, **16**, 614.
39. P. T. Brain, C. A. Morrison, S. Parsons and D. W. H. Rankin, *J. Chem. Soc. Dalton Trans.*, 1996, 4589-4596.

# Chapter Four

The Molecular Structures of the Polyboron Compounds $B_8X_{12}$ (X = Cl, Br, I and H) studied by Theoretical Calculations

## 4.1. Introduction

The determination of the structure of $B_8F_{12}$ by low-temperature crystallography, *ab initio* calculations and gas-phase electron diffraction (Chapter 3) has produced a new and unique geometry for polyboron halide compounds. Theoretical calculations are a useful tool to focus the direction of synthetic research. Work in this chapter investigates the molecular structures of the compounds $B_8X_{12}$ (X = Cl, Br and I), which have not as yet been synthesised.

The number of polyboron chlorides, bromides and iodides with known structures is far greater than for the polyboron fluorides.[1-4] Large cluster subchlorides, subbromides and subiodides are common, with examples including $B_nCl_n$ ($n$ = 8 - 12),[5-8] $B_nBr_n$ ($n$ = 7 - 10)[7-12] and $B_nI_n$ ($n$ = 8 and 9).[7,8,13] The known structures of these subhalides significantly differ from the fluoride structures discussed in Chapter 3. In general, polyboron chlorides form polyhedral cage systems as opposed to the borane-like structure seen for $B_8F_{12}$. This could be attributable to the fact that no B*n*X*n* systems exist for X = F, but may also be because although both F and Cl donate electrons to the B atom by $p\pi$-$\pi$ bonding; F is more electronegative than Cl and therefore the electrons in the B $p_z$ orbital may be less able to delocalise over a boron cage from a BF group than from a BCl group.[1]

The very low thermal stability of $B_8F_{12}$ means that the synthesis of compounds such as $B_8Cl_{12}$ may prove difficult given that $B_2F_4$ is so much more stable than $B_2Cl_4$.[1] However, it has been postulated that $B_8Cl_{12}$ may be involved in the disproportionation of $B_2Cl_4$.[2] The calculation of the structures of $B_8X_{12}$ (X = Cl, Br and I) will provide synthetic chemists with some insight as to possible synthetic reaction schemes.

The crystal structure of $B_8H_{12}$ has been known since 1964.[14] It shows a very different structure to that seen for $B_8F_{12}$, complying with Wade's rules to give a *nido* structure of $C_s$ symmetry. The substitution of F by H in the experimental structure of $B_8F_{12}$

will determine if another isomer of $B_8H_{12}$ exists and how this compares in energy to the optimised crystal coordinates of the known structure.

## 4.2. Experimental

### 4.2.1. *Ab initio* and DFT Calculations

All calculations were performed using the Gaussian 98 computer program[15] and resources of the U.K. Computational Facility, on a DEC 8400 superscalar cluster equipped with 10 fast processors, 6 GB of memory and 150 GB disk. Calculations were carried out using HF,[16] MP2[17] and DFT[18] methods and a series of basis sets to gauge the effects of electron correlation and basis set on each structure.

Calculations were performed on the compounds $B_8X_{12}$ (X = Cl, Br, I and H), substituting each of the fluorine atoms in $B_8F_{12}$ by X to show the effects of halogen substitution and to compare the resultant structures to the known crystal structure of $B_8H_{12}$.[14,19] For the molecules $B_8X_{12}$ (X = Cl, Br and I), three systems were studied:

1. Based on the experimentally determined structure of $B_8F_{12}$, substituting Cl, Br or I respectively for F (denoted system **1**).

2. A dimer structure consisting of two $B_4X_6$ molecules forming an eight-membered ring through B...X interactions (denoted system **2**).

3. A dimer structure including six-membered rings, in which the central atom of each $B_4X_6$ molecule weakly bonds to a terminal $X_2B$ group on the adjacent $B_4X_6$ molecule (denoted system **3**).

Calculations on $B_8Cl_{12}$, $B_8Br_{12}$ and $B_8I_{12}$ were carried out at the HF/3-21G*,[20] HF/6-31G*,[21] MP2/6-31G*, B3LYP/6-31G* and B3LYP/6-311G*[22] levels. Additional calculations were performed for $B_8Cl_{12}$ (**1**) at the B3LYP level using the 6-31+G*[23]

and 6-311+G* basis sets. For the iodo analogue the lanl2dz[24] basis set was used on the I atoms.

Calculations were performed on the compound $B_8H_{12}$, replacing each of the fluorine atoms in $B_8F_{12}$ by H (**1**), to compare the resultant structure with the optimised structure of the known crystalline $B_8H_{12}$ (**4**).These calculations were carried out at the HF and MP2 levels with the 6-31G* basis set, and at the B3LYP level using the 6-31G*, 6-311G* and 6-311+G* basis sets.

Frequency calculations allowed the nature of any stationary points to be determined, confirming the structure as a local minimum, transition-state or higher order stationary point on the potential energy surface.

## 4.3. Results

### 4.3.1. *Ab initio* and DFT Calculations

#### 4.3.1.1. $B_8Cl_{12}$

Calculations on $B_8Cl_{12}$ (**1**) converged to give an energy minimum (see Figure 1) at all levels of theory and basis set. As Table 1 reveals, this system shows many structural similarities to that determined for $B_8F_{12}$ (see Chapter 3).

Geometry changes for $B_8Cl_{12}$ (**1**) were found as a result of using different levels of theory (see Table 1). Calculations at the HF and B3LYP levels result in geometries that are more closely matched than the MP2 geometry. Using the 6-31G* basis set, the B(2)-B(4) bond equals 168.4 pm at the MP2 level of theory. This compares to values of 189.6 and 189.4 pm at the HF and DFT levels using the same basis set. In other words, at the MP2 level, there exists more electron density in this region of the molecule compared to the HF and DFT calculated structures. In order to compensate for this vastly increased electron deficiency the HF and DFT structures attempt to

locate electron density from other sources within the molecule. This is highlighted by the relatively short B(1)-B(5) distances at these levels compared to the MP2 level (8.0 and 10.2 pm shorter at the HF and DFT levels respectively).

**Figure 1**. Molecular framework for $B_8Cl_{12}$ (**1**). B(3)-B(4) is found in $B_8F_{12}$ (see Chapter 3) but is much longer here.

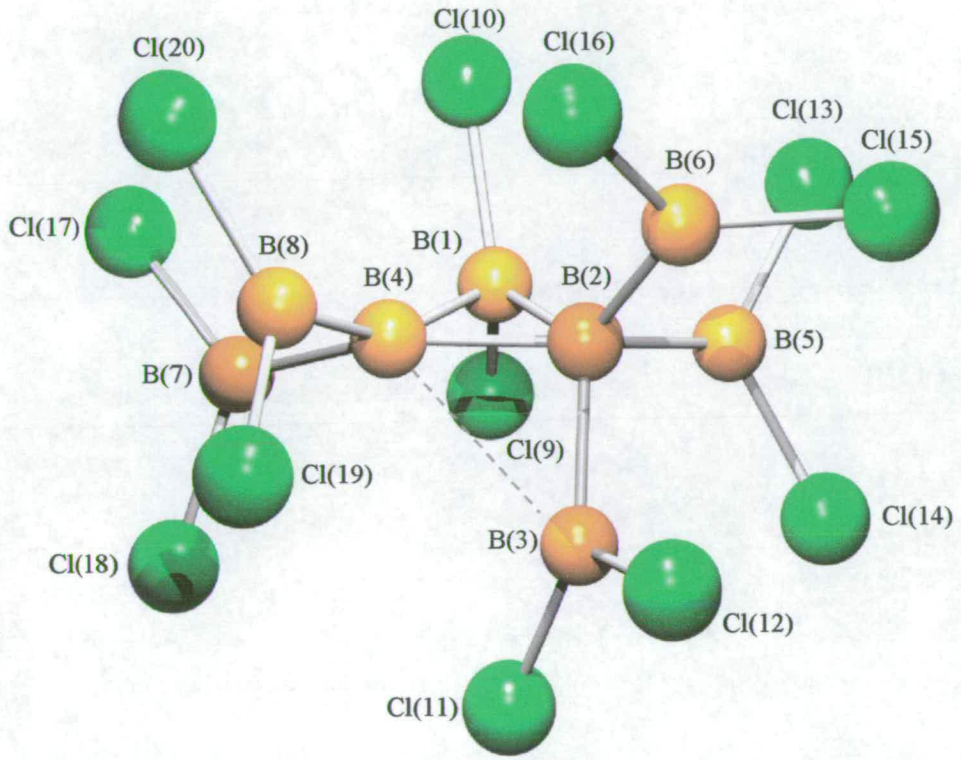

**Table 1**. Calculated ($r_e$) B-B bond lengths (pm) for $B_8Cl_{12}$ (**1**).

| Geometric parameter | Level of theory / Basis set | | | | | | |
|---|---|---|---|---|---|---|---|
| | HF | | MP2 | B3LYP | | | |
| | 3-21G* | 6-31G* | 6-31G* | 6-31G* | 6-31+G* | 6-311G* | 6-311+G* |
| B(1)-B(2) | 183.1 | 176.7 | 176.2 | 173.1 | 173.1 | 172.6 | 172.8 |
| B(1)-B(4) | 214.5 | 186.0 | 176.9 | 175.9 | 176.1 | 175.7 | 175.8 |
| B(1)-B(5) | 243.0 | 207.1 | 215.1 | 204.9 | 204.9 | 205.8 | 205.7 |
| B(2)-B(3) | 177.9 | 176.6 | 175.8 | 174.5 | 174.5 | 173.9 | 173.9 |
| B(2)-B(4) | 178.4 | 189.6 | 168.4 | 189.4 | 189.8 | 190.0 | 189.8 |
| B(2)-B(5) | 177.8 | 196.3 | 178.1 | 176.7 | 181.1 | 180.8 | 180.7 |
| B(2)-B(6) | 174.4 | 175.2 | 172.8 | 177.3 | 177.3 | 176.7 | 176.7 |
| B(3)-B(4) | 240.8 | 279.3 | 242.5 | 296.3 | 296.7 | 296.4 | 296.1 |
| B(4)-B(7) | 171.8 | 174.3 | 173.2 | 172.3 | 172.3 | 171.9 | 171.8 |
| B(4)-B(8) | 171.0 | 172.2 | 169.7 | 171.0 | 171.1 | 170.5 | 170.5 |
| Energy[a] | -5685.5398 | -5711.6444 | -5713.9213 | -5721.5963 | -5721.6128 | -5721.9785 | -5721.9928 |

[a] absolute energy in Hartrees.

As expected, the 3-21G* basis set proved to be a poor representation in the determination of the molecular structure of $B_8Cl_{12}$ (**1**). Increasing the size of the basis set from 3-21G* to 6-31G* at the HF level changes the molecular geometry drastically. B-B bonds B(1)-B(2), B(1)-B(4) and B(1)-B(5) are over-estimated by 6.4, 28.5 and 32.9 pm using the 3-21G* instead of the 6-31G* basis set. In contrast, B-B bonds B(2)-B(4), B(2)-B(5) and B(3)-B(4) are under-estimated using the 3-21G* basis set by 11.2, 18.5 and 38.5 pm respectively. These differences are not so marked when the 6-31G* basis set is increased to 6-311G* at the B3LYP level. The introduction of diffuse functions has little effect on the molecular geometry.

$B_8Cl_{12}$ (**1**) [Figure 1] is similar to $B_8F_{12}$ (Chapter 3, Figure 1), but with the long B-B bond [B(3)-B(4)] lengthened a great deal more so that the $B(3)Cl_2$ is effectively another terminal group (the fifth). The interaction B(3)-B(4) can be as long as 296.7 pm (at the B3LYP/6-31+G* level), which is 54.2 pm longer than its value at the MP2/6-31G* level calculation. The bridging bonds utilising B(4) with B(1) and B(3) are longer than those involving B(2), as seen for $B_8F_{12}$. This is especially true at the HF level of theory, but for calculations at the MP2 and DFT levels it is only B(3)-B(4) that is of noticeably increased length. At the MP2 and DFT levels $B_8Cl_{12}$ (**1**) has an unusual deltahedral arrangement in which three of the core bonds [B(1)-B(2), B(1)-B(4) and B(2)-B(3)] have very similar lengths.

Calculations on the $(B_4Cl_6)_2$ dimers (**2**) and (**3**) optimise to give energy minima (see Figures 2 and 3) at all levels of theory and basis set. For dimer **2** the accepter atom is a central boron compared to an outer boron in dimer **3**. Selected bond distances for these systems are listed in Tables 2 and 3.

**Figure 2**. Molecular framework for $B_4X_6$ dimer (**2**) [X = Cl, Br and I].

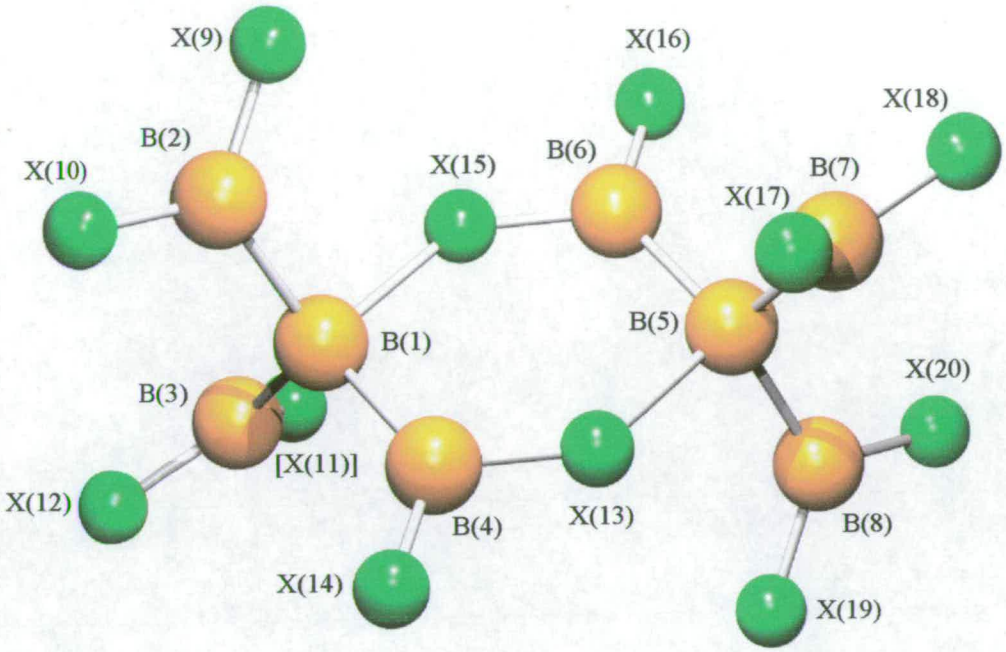


**Figure 3**. Molecular framework for $B_4X_6$ dimer (**3**) [X = Cl, Br and I].

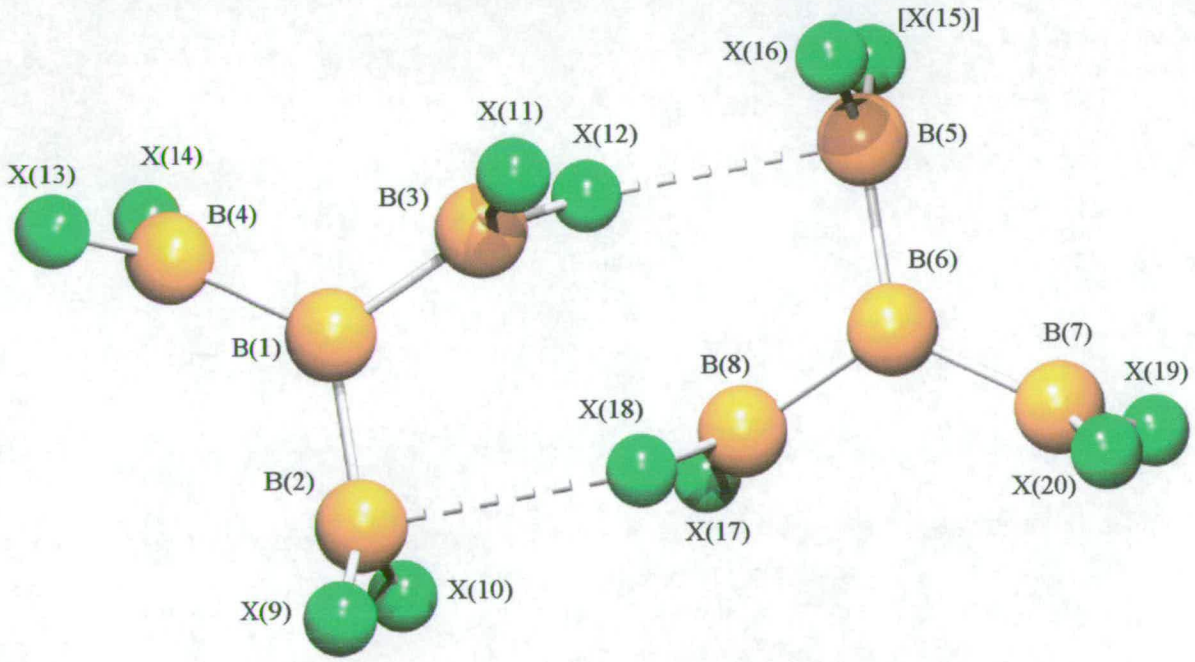

**Table 2**. Calculated ($r_e$) bond lengths (pm) for $B_4Cl_6$ dimer **2**.

| Geometric parameter | Level of theory / Basis set | | | | |
|---|---|---|---|---|---|
| | HF | | MP2 | B3LYP | |
| | 3-21G* | 6-31G* | 6-31G* | 6-31G* | 6-311G* |
| B(1)-B(2) | 167.6 | 169.3 | 166.2 | 166.8 | 166.1 |
| B(1)...Cl(15) | 507.5 | 560.6 | 463.8 | 537.0 | 496.7 |
| B(5)...Cl(13) | 497.4 | 560.0 | 463.8 | 536.0 | 495.2 |
| Energy[a] | -5685.6172 | -5711.7340 | -5713.9013 | -5721.6332 | -5722.0123 |

[a] absolute energy in Hartrees.

**Table 3**. Calculated ($r_e$) bond lengths (pm) for $B_4Cl_6$ dimer **3**.

| Geometric parameter | Level of theory / Basis set | | | | |
|---|---|---|---|---|---|
| | HF | | MP2 | B3LYP | |
| | 3-21G* | 6-31G* | 6-31G* | 6-31G* | 6-311G* |
| B(1)-B(2) | 167.7 | 169.4 | 166.0 | 166.8 | 166.2 |
| B(1)-B(3) | 167.5 | 169.3 | 166.3 | 166.8 | 166.1 |
| B(2)...Cl(18) | 397.9 | 464.9 | 354.5 | 573.8 | 608.2 |
| B(5)...Cl(12) | 391.3 | 462.6 | 731.8 | 606.8 | 864.6 |
| Energy[a] | -5685.6183 | -5711.7344 | -5713.9044 | -5721.6332 | -5722.0127 |

[a] absolute energy in Hartrees.

The B-B bond distances in $B_4Cl_6$ dimer **2** are largest when the HF level of theory is used with the 6-31G* basis set. The B-B bonds at this level of calculation are 3.1 pm longer than when electron correlation is incorporated using the MP2 level of theory and the equivalent basis set. At this level, the B-B bonds are 0.6 pm shorter than when the B3LYP level of theory is used with the 6-31G* basis set, and the difference between MP2/6-31G* and B3LYP/6-311G* equals only 0.1 pm for the B-B bond lengths. However, the distance between the monomeric species [B(1)...Cl(15)] is largely dependent upon both the size of basis set and the level of theory used. Such separation distances range from 463.8 pm (MP2/6-31G*) to 560.6 pm (HF/6-31G*), thus reflecting a huge difference between non-correlated methods and those that incorporate electronic correlation effects. The difference between the B3LYP/6-31G* and MP2/6-31G* calculated values is 72.2 pm, but when the size of the basis set is increased at the B3LYP level from 6-31G* to 6-311G*, the difference decreases to 31.4 pm. Increasing the size of the basis set at the B3LYP level (from 6-31G* to 6-311G*) thus results in a significant decrease in the monomer separation distance. This is the opposite trend to the one found when the basis set at the HF level is increased from 3-21G* to 6-31G*. In this case the separation distance increases by 53.1 pm.

The intramolecular geometry of each monomer in the dimers of type **3** is very similar to that found in the type **2** dimers, but the intermolecular geometry between each $B(BCl_2)_3$ species is very incongruent. Whilst in $B_4Cl_6$ dimer **2** the separation between the monomers is symmetric to formulate an eight-membered ring, within $B_4Cl_6$ dimer **3** there exists great asymmetry. This is especially true when correlated methods are employed. For example, the smallest separation distance between the monomers [B(2)...Cl(18)] at the MP2/6-31G* level equals 354.5 pm, but the equivalent interaction (*i.e.* one that would complete a ring formation) is 377.3 pm longer. The differences between these distances at other levels of calculation equal 6.6, 2.3, 33.0 and 256.4 pm at the HF/3-21G*, HF/6-31G*, B3LYP/6-31G* and B3LYP/6-311G* levels respectively.

#### 4.3.1.2. $B_8Br_{12}$

Calculations on $B_8Br_{12}$ (**1**) optimise to give an energy minimum (see Figure 4) at all levels of theory and basis set. The structure of $B_8Br_{12}$ (**1**) is based on a butterfly formed through the interaction of B(1), B(2), B(4) and B(5) with a Br bridging B(1)-B(4). In addition, there are four terminal $BBr_2$ groups on B(2) and B(4) with two on each of them. The geometry of $B_8Br_{12}$ (**1**) depends on both the basis set and the level of theory used, resulting in the parameter values in Table 4.

**Figure 4**. Molecular framework for $B_8Br_{12}$ (**1**).

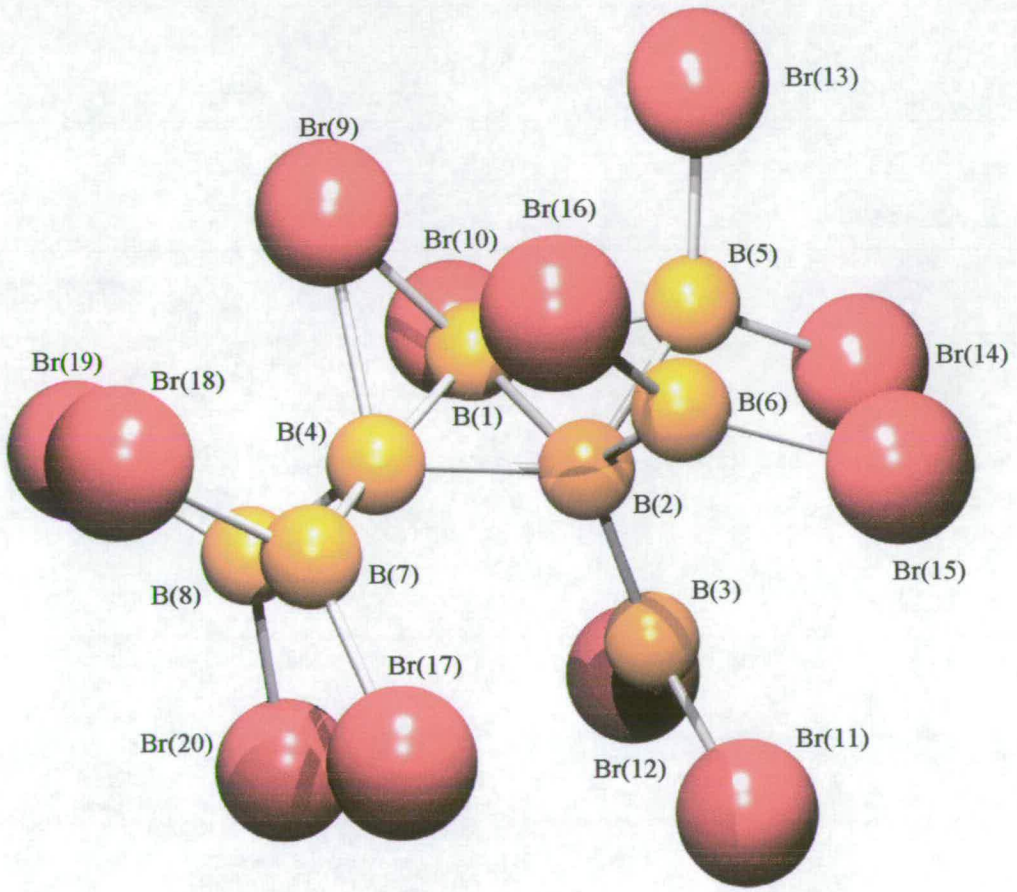


The length of the bond B(1)-B(5) is not affected by increasing the basis set from 3-21G* to 6-31G* at the HF level of theory. However, when the size of the basis set is increased from 6-31G* to 6-311G* at the B3LYP level, this bond length increases by 62.7 pm, representing a huge change. This value is only 0.2 pm shorter than the

distance determined at the MP2/6-31G* level. At the same time as this bond is increasing, the B(2)-B(5) bond is following the opposite trend. The value of B(2)-B(5) at the B3LYP/6-31G* level is 36.6 and 40.3 pm longer than the distances found at the B3LYP/6-31G* and MP2/6-31G* levels, respectively.

**Table 4**. Calculated ($r_e$) B-B bond lengths (pm) for $B_8Br_{12}$ (**1**).

| Geometric parameter | Level of theory / Basis set | | | | |
|---|---|---|---|---|---|
| | HF | | MP2 | B3LYP | |
| | 3-21G* | 6-31G* | 6-31G* | 6-31G* | 6-311G* |
| B(1)-B(2) | 187.8 | 195.4 | 172.0 | 162.8 | 173.8 |
| B(1)-B(4) | 178.2 | 180.0 | 172.6 | 166.3 | 176.9 |
| B(1)-B(5) | 174.0 | 174.6 | 201.6 | 138.7 | 201.4 |
| B(2)-B(3) | 171.6 | 174.4 | 172.9 | 179.9 | 174.9 |
| B(2)-B(4) | 184.4 | 182.3 | 180.3 | 182.2 | 184.5 |
| B(2)-B(5) | 254.0 | 267.4 | 173.6 | 213.9 | 177.3 |
| B(2)-B(6) | 170.2 | 173.3 | 178.0 | 186.4 | 196.2 |
| B(3)-B(4) | 310.6 | 309.5 | 295.8 | 305.3 | 302.7 |
| B(4)-B(7) | 171.2 | 174.3 | 170.0 | 170.4 | 171.6 |
| B(4)-B(8) | 172.1 | 174.7 | 170.8 | 166.5 | 173.0 |
| B(5)-B(6) | 312.6 | 323.7 | 221.8 | 328.3 | 246.0 |
| Energy[a] | -30920.0445 | -31036.5465 | -31038.6373 | -31059.7144 | -31088.9415 |

[a] absolute energy in Hartrees.

The asymmetric deltahedron evident in the F and Cl analogues discussed thus far is also evident in $B_8Br_{12}$ (**1**), but the extent of the asymmetry exhibited forces the central boron atoms to seek electron density from other sources. They achieve this through the formation of an additional deltahedron with B(5), which in $B_8F_{12}$ belongs to a terminal $BF_2$ group. B(3)-B(4) is the shortest non-bonded interaction at the MP2 level of theory (by 9.5 pm compared to the B3LYP level using the equivalent basis set which gives a distance of 305.3 pm). This interaction can be described as very weak at best. Atom B(4) acquires electron density through a bridging contact with Br(9). These asymmetric bridges between B(4), Br(9) and B(1) range from 206.1 - 226.8 pm and are shortest at the MP2/6-31G* level when they are 206.1 and 212.0 pm for the B(1)-Br(9) and B(4)-Br(9) interactions respectively.

Calculations on $(B_4Br_6)_2$ dimers of type **2** and **3** optimise to give energy minima (see Figures 2 and 3) at all levels of theory and basis set. Selected bond distances for these systems are listed in Tables 5 and 6.

The B-B bond distances in dimer **2** range from 168.6 pm (HF/6-31G*) to 164.9 pm (MP2/6-31G*). The formation of a weakly bonded ring results from the interactions B(1)...Br(15) and B(5)...Br(13). These interactions are incredibly weak and become increasingly weak when correlated methods are employed. For example, the interaction between B(1) and Br(15) at the HF/6-31G* level is 4.6, 216.0 and 273.3 pm shorter than the values determined at the B3LYP/6-31G*, B3LYP/6-311G* and MP2/6-31G* levels respectively. These represent huge discrepancies between the various levels of theory.

The B-B bond distances in dimer **3** are similar to those determined for dimer **2**. However the separation between monomers is very different for the two dimeric species. For example, the distance between B(2) and Br(18) in dimer **3** is 77.4 pm shorter than the interaction between B(5) and Br(13) in dimer **2** at the MP2/6-31G* level. The interactions between $B(BBr_2)_3$ monomers in dimer **3** vary according to the level of theory and size of basis set employed. Increasing the basis set from 3-21G* to 6-31G* at the HF level and from 6-31G* to 6-311G* at the B3LYP level results in increasing the separation between monomers. For example, the distance B(5)...Br(12) increases by 171.8 and 166.6 pm at the HF and B3LYP levels respectively. Further to this, comparison of the calculated values when the 6-31G* basis set is used shows that when the level of theory is increased from HF to MP2 and B3LYP levels, the same interaction is increased by 321.6 and 221.0 pm respectively.

**Table 5**. Calculated ($r_e$) bond lengths (pm) for $B_4Br_6$ dimer **2**.

| Geometric parameter | Level of theory / Basis set | | | | |
|---|---|---|---|---|---|
| | HF | | MP2 | B3LYP | |
| | 3-21G* | 6-31G* | 6-31G* | 6-31G* | 6-311G* |
| *r*BB | 166.2 | 168.6 | 164.9 | 165.9 | 165.7 |
| B(1)...Br(15) | 445.9 | 622.7 | 896.0 | 627.3 | 838.7 |
| B(5)...Br(13) | 445.9 | 622.9 | 905.8 | 627.1 | 839.1 |
| Energy[a] | -30920.0856 | -31062.5523 | -31036.5947 | -31085.0240 | -31089.0059 |

[a] absolute energy in Hartrees.

**Table 6**. Calculated ($r_e$) bond lengths (pm) for $B_4Br_6$ dimer **3**.

| Geometric parameter | Level of theory / Basis set | | | | |
|---|---|---|---|---|---|
| | HF | | MP2 | B3LYP | |
| | 3-21G* | 6-31G* | 6-31G* | 6-31G* | 6-311G* |
| B(1)-B(2)[a] | 166.3 | 168.6 | 165.1 | 165.9 | 165.7 |
| B(1)-B(3)[b] | 165.9 | 168.5 | 165.1 | 165.9 | 165.7 |
| B(2)...Br(18) | 344.1 | 526.0 | 828.4 | 755.2 | 894.0 |
| B(5)...Br(12) | 344.7 | 516.5 | 838.1 | 737.5 | 904.1 |
| Energy[c] | -30920.0914 | -31062.5525 | -31036.5971 | -31085.0241 | -31089.0059 |

[a] B(1)-B(2) = B(1)-B(4) = B(5)-B(6) = B(5)-B(7).

[b] B(1)-B(3) = B(6)-B(8).

[c] absolute energy in Hartrees.

#### 4.3.1.3. $B_8I_{12}$

Calculations on $B_8I_{12}$ (**1**) optimise to give an energy minimum (see Figure 5) at all levels of theory and basis set, resulting in parameter values as recorded in Table 7.

**Figure 5**. Molecular framework for $B_8I_{12}$ (**1**).

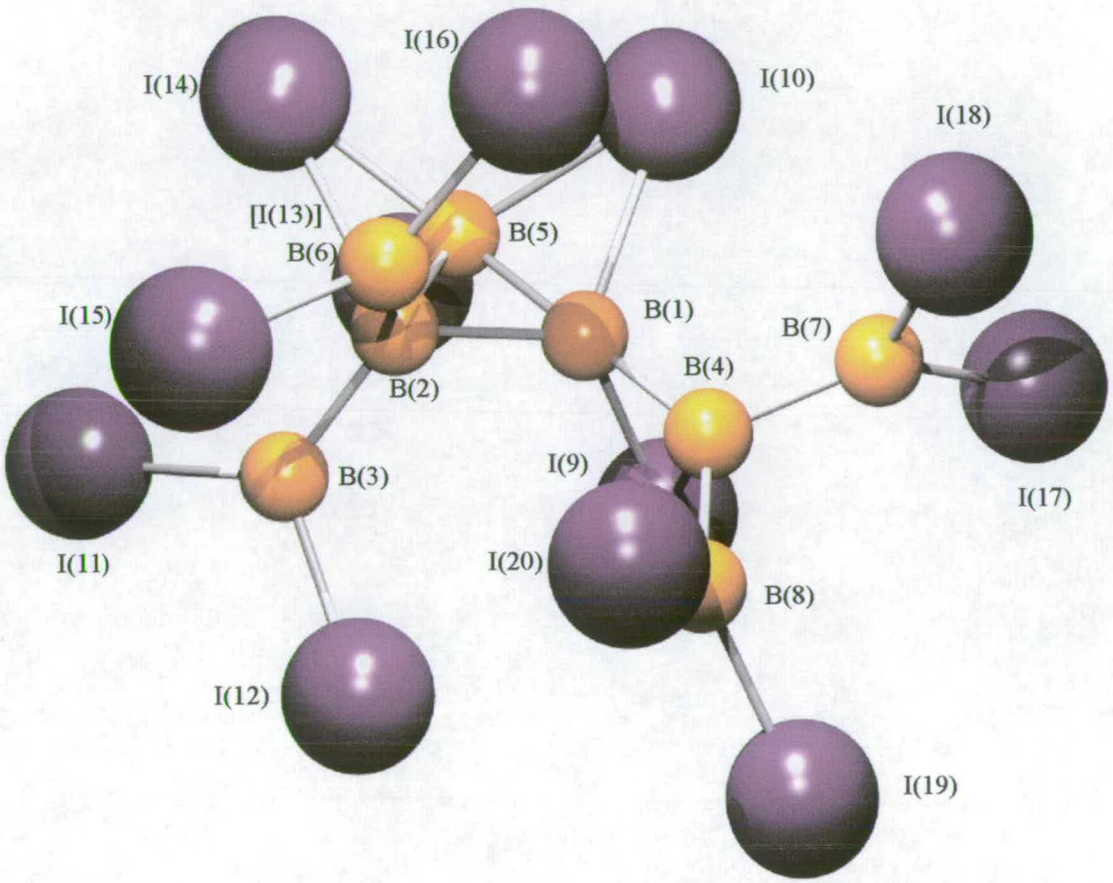


The structure of $B_8I_{12}$ (**1**) corresponds to a more open framework structure than currently known iodo-boranes which adopt cage-like structures. This could be due to steric effects of the large iodine atoms. $B_8I_{12}$ incorporates a B(1)-B(2)-B(5) deltahedron with two $BI_2$ groups [$B(3)I_2$ and $B(6)I_2$]. There are also three B-I-B bridges, two of which are situated on the B(1)-B(5)-B(2) bridge.

**Table 7**. Calculated ($r_e$) B-B bond lengths (pm) for $B_8I_{12}$ (**1**).

| Geometric parameter | Level of theory / Basis set | | | | |
|---|---|---|---|---|---|
| | HF | | MP2 | B3LYP | |
| | 3-21G* | 6-31G*[a] | 6-31G*[a] | 6-31G*[a] | 6-311G*[b] |
| B(1)-B(2) | 175.7 | 211.5 | 186.0 | 194.6 | 198.6 |
| B(1)-B(4) | 179.1 | 172.5 | 168.4 | 169.9 | 169.0 |
| B(1)-B(5) | 185.0 | 195.1 | 180.5 | 186.8 | 186.1 |
| B(2)-B(3) | 173.6 | 173.8 | 171.8 | 172.5 | 172.5 |
| B(2)-B(4) | 254.3 | 325.4 | 304.6 | 308.2 | 313.6 |
| B(2)-B(5) | 237.5 | 199.0 | 187.4 | 198.0 | 194.2 |
| B(2)-B(6) | 171.7 | 173.5 | 170.7 | 172.0 | 171.4 |
| B(3)-B(4) | 357.1 | 356.3 | 355.2 | 357.8 | 358.8 |
| B(4)-B(7) | 172.9 | 172.6 | 170.4 | 171.0 | 170.4 |
| B(4)-B(8) | 170.4 | 171.8 | 168.5 | 169.4 | 169.0 |
| B(5)-B(6) | 340.7 | 334.4 | 325.5 | 330.9 | 329.6 |
| Energy[c] | -82851.4417 | -331.5089 | -332.8351 | -335.6233 | -335.6648 |

[a] 6-31G* on B atoms and lanl2dz on I atoms.
[b] 6-311G* on B atoms and lanl2dz on I atoms.
[c] absolute energy in Hartrees.

The central B(1)-B(2) bond, which forms the base of the only boron deltahedron in this molecule, is greatly affected by the level of theory and basis set used. Increasing the basis set (from 3-21G* to 6-31G* at the HF level and from 6-31G* to 6-311G* at the B3LYP level) results in an increased B(1)-B(2) bond distance by 35.8 and 4.0 pm respectively. The inclusion of electron correlation effects at the MP2 level results in a distance that is 25.5 pm shorter than at the HF level using the equivalent basis set. This value is also 12.6 pm shorter than the distance determined using the B3LYP level of theory with the 6-311G* basis set.

Calculations on the weak $B_4I_6$ dimers **2** and **3** optimise to give energy minima (see Figures 2 and 3) at all levels of theory and basis set. Selected bond distances for these systems are listed in Tables 8 and 9.

As with the chloro and bromo analogues, the $B(BI_2)_3$ species in **2** and **3** are geometrically similar. The major cause of difference between forms **2** and **3**, as in $B_8Cl_{12}$ and $B_8Br_{12}$, is due to the relative orientation of the monomers. In both **2** and **3**

the shortest interaction occurs at the MP2/6-31G* level. The B(1)...I(15) interaction in **2** at the MP2/6-31G* level (using the lanl2dz basis set on the I atoms) is 110.6, 98.0 and 111.3 pm shorter than at the HF/6-31G*, B3LYP/6-31G* and B3LYP/6-311G* levels respectively (all using the lanl2dz basis set for the I atoms). For **3** the B(2)...I(18) distance at the MP2 level, with 6-31G* on the B atoms and lanl2dz on the I atoms, is 168.7, 246.8 and 248.7 pm shorter than the values calculated at HF/6-31G*, B3LYP/6-31G* and B3LYP/6-311G* levels respectively (with the lanl2dz basis set used for the I atoms).

**Table 8**. Calculated ($r_e$) bond lengths (pm) $B_4I_6$ dimer **2**.

| Geometric parameter | Level of theory / Basis set | | | | |
|---|---|---|---|---|---|
| | HF | | MP2 | B3LYP | |
| | 3-21G* | 6-31G*[a] | 6-31G*[a] | 6-31G*[a] | 6-311G*[b] |
| *r*B-B | 166.6 | 168.5 | 164.8 | 165.9 | 165.2 |
| B(1)...I(15) | 594.0 | 631.8 | 521.2 | 619.2 | 632.5 |
| B(5)...I(13) | 594.0 | 631.9 | 521.1 | 619.1 | 632.5 |
| Energy[c] | -82851.5595 | -331.6464 | -332.8577 | -335.7178 | -335.7599 |

[a] 6-31G* on B atoms and lanl2dz on I atoms.
[b] 6-311G* on B atoms and lanl2dz on I atoms.
[c] absolute energy in Hartrees.

**Table 9**. Calculated ($r_e$) bond lengths (pm) for $B_4I_6$ dimer **3**.

| Geometric parameter | Level of theory / Basis set | | | | |
|---|---|---|---|---|---|
| | HF | | MP2 | B3LYP | |
| | 3-21G* | 6-31G*[a] | 6-31G*[a] | 6-31G*[a] | 6-311G*[b] |
| B(1)-B(2)[c] | 166.7 | 168.6 | 164.7 | 165.9 | 165.2 |
| B(1)-B(3)[d] | 166.7 | 168.6 | 164.9 | 165.9 | 165.2 |
| B(2)...I(18) | 482.1 | 556.7 | 388.0 | 634.8 | 636.7 |
| B(5)...I(12) | 482.1 | 556.7 | 388.1 | 634.8 | 636.7 |
| Energy[e] | -82951.5594 | -331.6460 | -332.8605 | -335.7173 | -335.7596 |

[a] 6-31G* on B atoms and lanl2dz on I atoms.
[b] 6-311G* on B atoms and lanl2dz on I atoms.
[c] B(1)-B(2) = B(1)-B(4) = B(5)-B(6) = B(6)-B(7).
[d] B(1)-B(3) = B(6)-B(8).
[e] absolute energy in Hartrees.

### 4.3.1.4. Relative energies of the structures

If an optimised structure represents an energy minimum this does not necessarily imply that the global minimum has been determined. Molecules such as boranes and boron halides, in particular, can adopt unusual and varied structures (see Figures 1 - 5). The *ab initio* and DFT calculations discussed show that multiple energy minima can exist on a potential energy surface. They also highlight the vast differences in structure that different levels of theory can produce. Not only is there a need for the inclusion of electron correlation when calculating the structures of higher boron halides, but caution should be taken when employing DFT functionals, such as B3LYP, which are empirical in nature. This can be dangerous since few experimentally determined structures exist for higher boron halides, relative to more common organic compounds for example. Comparison of the relative energies calculated for each $B_8X_{12}$ (X = Cl, Br and I) [see Table 10] shows that the level of theory employed is critical in determining the stability of the bonding scheme.

**Table 10**. Relative energies (kJ $mol^{-1}$) for calculated $B_8X_{12}$ (X = Cl, Br and I) systems.

| System | | Level of theory / Basis set | | |
|---|---|---|---|---|
| | | HF 6-31G* | MP2 6-31G* | B3LYP 6-311G* |
| $B_8Cl_{12}$ | **1** | + 236.3 | 0.0 | + 96.9 |
| | **2** | + 1.0 | + 52.5 | + 1.0 |
| | **3** | 0.0 | + 44.4 | 0.0 |
| $B_8Br_{12}$ | **1** | + 68285.6 | 0.0 | + 169.1 |
| | **2** | + 0.5 | + 5634.4 | 0.0 |
| | **3** | 0.0 | + 5357.1 | 0.0 |
| $B_8I_{12}$ [a,b] | **1** | + 361.0 | + 66.7 | + 249.7 |
| | **2** | 0.0 | + 7.3 | 0.0 |
| | **3** | + 1.0 | 0.0 | + 0.8 |

[a] 6-31G* on B atoms and lanl2dz on I atoms.
[b] 6-311G* on B atoms and lanl2dz on I atoms.

For $B_8Cl_{12}$ the sequence for molecular stability at the HF/6-31G* and B3LYP/6-311G* levels is **3** > **2** (+ 1.0 and + 1.0 kJ $mol^{-1}$ respectively) > **1** (+ 235 and + 95.9

kJmol$^{-1}$ respectively). However, at the MP2/6-31G* level the sequence changes to **1** > **3** (+ 44.4 kJ mol$^{-1}$) > **2** (+ 8.1 kJ mol$^{-1}$).

For $B_8Br_{12}$ the sequence for molecular stability at the HF/6-31G* level is **3** > **2** (+ 0.5 kJ mol$^{-1}$) > **1** (+ 68285 kJ mol$^{-1}$). The enormity of this value makes it rather unbelievable since it is much more than all of the bond energies together. At the B3LYP/6-311G* level the sequence is **3** = **2** > **1** (+ 169 kJ mol$^{-1}$) compared to the sequence at the MP2/6-31G* level which is **1** > **3** (+ 5357 kJ mol$^{-1}$) > **2** (+ 6.3 kJ mol$^{-1}$).

For $B_8I_{12}$ the trend of molecular stability at the HF/6-31G* is **2** > **3** (+ 1.0 kJ mol$^{-1}$) > **1** (+ 360 kJmol$^{-1}$). This is also the trend found at the B3LYP/6-311G* level, with the relative energy differences between **2** and **3**, and **3** and **1** equalling + 0.8 kJ mol$^{-1}$ and + 249 kJ mol$^{-1}$ respectively. The energy difference between **2** and **3** at the MP2/6-31G* level becomes + 7.3 kJ mol$^{-1}$ with **3** 59.4 kJ mol$^{-1}$ lower in energy than structure **1**.

#### 4.3.1.5. $B_8H_{12}$

Calculations on $B_8H_{12}$ (**1**) and $B_8H_{12}$ (**4**) optimise to give energy minima (see Figures 6 and 7) at all levels of theory and basis set, resulting in parameter values as recorded in Tables 11 and 12.

The structure of **1** contains a distorted square pyramidal arrangement of borons, with one terminal $BH_2$ on the apical B(5) and another on the base. Additional electron density is supplied through a bridged $BH_2$ on the pyramid base. Three terminal hydrogens and three bridge hydrogens on the base borons complete the structure. It can be regarded as being derived from $B_5H_9$ with one apical H, one basal terminal H and one bridging H replaced by $BH_2$ groups.

**Figure 6**. Molecular framework for $B_8H_{12}$ (**1**).

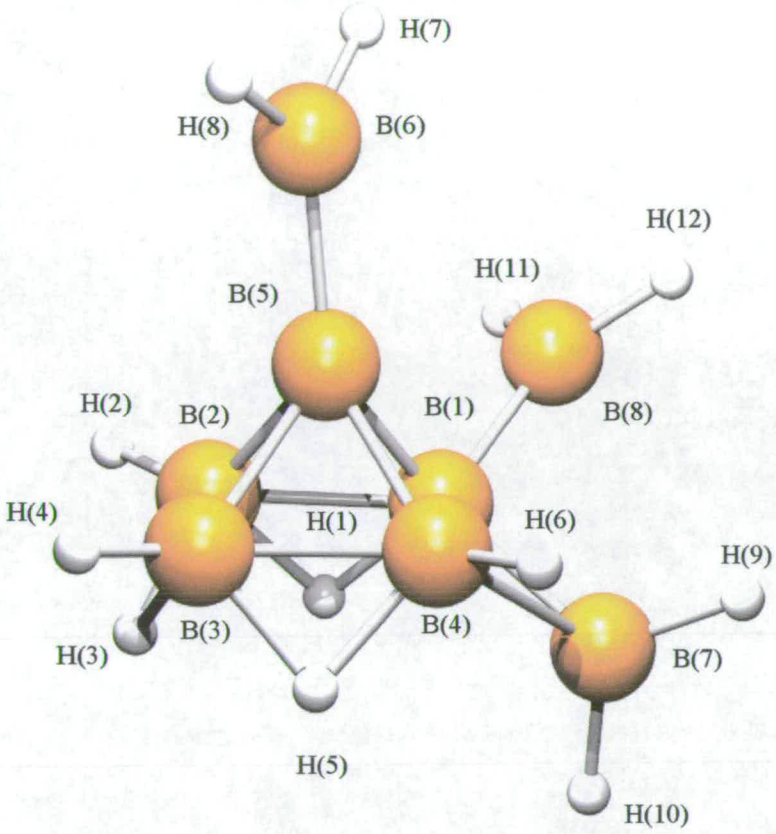


**Table 11**. Calculated ($r_e$) bond lengths (pm) for $B_8H_{12}$ (**1**).

| Geometric parameter | Level of theory / Basis set | | | | |
|---|---|---|---|---|---|
| | HF | MP2 | B3LYP | | |
| | 6-31G* | 6-31G* | 6-31G* | 6-311G* | 6-311+G* |
| B(1)-B(2) | 187.8 | 180.4 | 183.7 | 184.0 | 184.0 |
| B(1)-B(4) | 177.5 | 173.6 | 174.2 | 174.1 | 174.1 |
| B(1)-B(5) | 174.4 | 168.0 | 171.6 | 171.7 | 171.7 |
| B(1)-B(7) | 173.0 | 165.8 | 169.0 | 168.6 | 168.6 |
| B(1)-B(8) | 169.2 | 166.5 | 166.9 | 166.4 | 166.4 |
| B(2)-B(3) | 179.8 | 178.0 | 178.9 | 178.8 | 178.8 |
| B(2)-B(5) | 173.6 | 173.2 | 173.3 | 173.2 | 173.2 |
| B(3)-B(4) | 178.2 | 176.2 | 178.0 | 178.2 | 178.1 |
| B(3)-B(5) | 175.0 | 173.3 | 174.8 | 174.9 | 174.9 |
| B(4)-B(5) | 167.2 | 172.3 | 170.3 | 170.1 | 170.1 |
| B(4)-B(7) | 216.0 | 208.9 | 205.3 | 205.8 | 205.9 |
| B(5)-B(6) | 169.0 | 167.8 | 166.8 | 166.1 | 166.1 |
| Energy[a] | -204.3059 | -205.0110 | -205.9540 | -205.9822 | -205.9827 |

[a] absolute energy in Hartrees.

The pyramidal base is distorted from a square arrangement at all levels of theory and basis set. The order of the B-B bond distances that make up the base is B(1)-B(2) > B(2)-B(3) > B(3)-B(4) > B(1)-B(4). This is true for all levels of theory and basis set used. For example, at the MP2/6-31G* level, these bonds range from 173.6 pm [B(1)-B(4)] to 180.4 pm [B(1)-B(2)] compared to 174.1 – 184.0 pm at the B3LYP/6-311+G* level.

The $BH_2$ bridge in **1** is asymmetric in nature. The difference in length between bonds B(1)-B(7) and B(4)-B(7) is 43.0, 43.1 and 37.3 pm at the HF/6-31G*, MP2/6-31G* and B3LYP/6-311+G* levels respectively.

The structure of **1** differs significantly from the geometry obtained in the crystal phase, **4** (see Figure 7), which produces a structure that adheres to Wade's rules to produce a *nido* structure with $C_s$ symmetry. Pawley[19] improved upon the original crystal parameter values determined by Enrione *et al.*[14] to give the B-B bond distances recorded in Table 12.

**Figure 7**. Molecular framework for $B_8H_{12}$ (**4**).

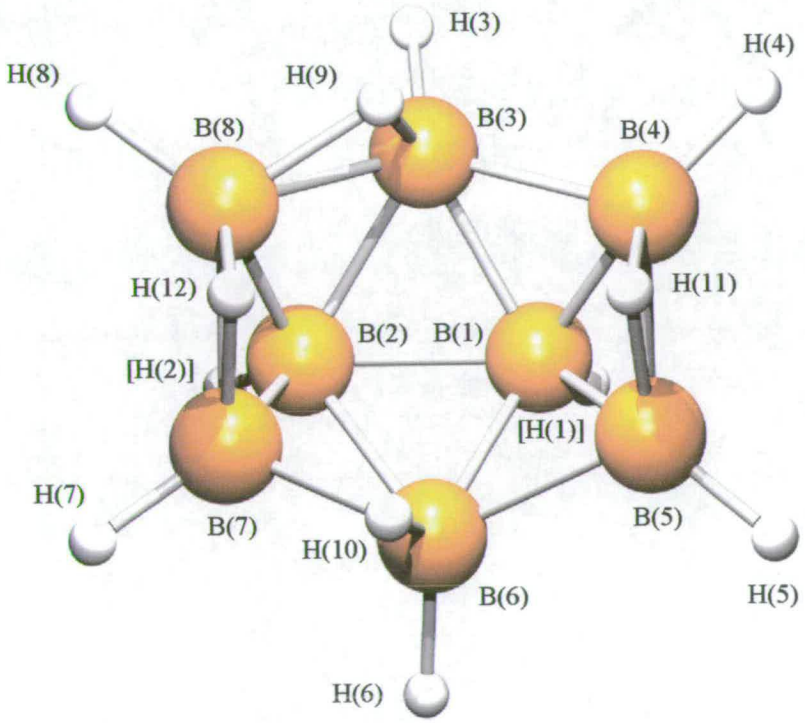

All calculations replicate the crystal structure to within relatively close agreement, even when electron correlation is not accounted for, using HF methods. However, the B(4)-B(5) bond – the shortest B-B bond in the molecule – does not agree so well with the crystal structure. Each calculation underestimates this bond by at least 3.1 pm (MP2/6-31G*) and by as much as 3.6 pm at the B3LYP/6-311+G* level. It should be noted, however, that such calculations do not model any crystal packing effects that may exist in the solid phase.

The calculations that most closely agree with the crystal coordinates are those optimised at the B3LYP level. Calculations using the 6-31G*, 6-311G* and 6-311+G* basis sets at this level contain only one bond [B(4)-B(5)] that lies more than 2 pm from the crystal structure value. At the MP2/6-31G* level two further bonds [B(3)-B(5) and B(6)-B(8)] also beyond this range of agreement. At the HF/6-31G* level the bond lengths B(2)-B(6), B(3)-B(4), B(4)-B(5) and B(7)-B(8) are more than 2 pm from the values in the crystal.

**Table 12**. B-B bond lengths (pm) for $B_8H_{12}$ (**4**).

| Geometric parameter | Level of theory / Basis set | | | | | Average crystal[19] |
|---|---|---|---|---|---|---|
| | HF | MP2 | | B3LYP | | |
| | 6-31G* | 6-31G* | 6-31G* | 6-311G* | 6-311+G* | |
| B(1)-B(2) | 183.7 | 182.5 | 182.9 | 182.8 | 182.8 | 184.2 |
| B(1)-B(3) | 179.9 | 177.9 | 178.8 | 178.6 | 178.6 | 179.4 |
| B(1)-B(4) | 171.4 | 170.6 | 170.8 | 170.6 | 170.6 | 171.1 |
| B(1)-B(5) | 171.4 | 170.6 | 170.8 | 170.6 | 170.6 | 170.9 |
| B(1)-B(6) | 179.9 | 177.9 | 178.8 | 178.7 | 178.6 | 179.7 |
| B(2)-B(3) | 183.5 | 180.7 | 182.1 | 182.1 | 182.1 | 181.8 |
| B(2)-B(6) | 183.5 | 180.7 | 182.1 | 182.1 | 182.1 | 181.2 |
| B(2)-B(7) | 173.9 | 172.0 | 172.6 | 172.4 | 172.4 | 172.2 |
| B(2)-B(8) | 173.9 | 172.0 | 172.6 | 172.4 | 172.4 | 172.7 |
| B(3)-B(4) | 185.0 | 182.5 | 183.3 | 183.3 | 183.3 | 181.7 |
| B(3)-B(8) | 181.1 | 178.2 | 179.6 | 179.6 | 179.6 | 181.0 |
| B(4)-B(5) | 164.9 | 165.1 | 164.9 | 164.7 | 164.6 | 168.2 |
| B(5)-B(6) | 185.0 | 182.5 | 183.3 | 183.3 | 183.3 | 183.3 |
| B(6)-B(7) | 181.1 | 178.2 | 179.6 | 179.6 | 179.6 | 180.4 |
| B(7)-B(8) | 175.9 | 173.5 | 174.6 | 174.4 | 174.4 | 172.2 |
| Energy[a] | -204.3611 | -205.1205 | -206.0427 | -206.0685 | -206.0691 | |

[a] absolute energy in Hartrees.

## 4.4. Discussion

The crystal structure of $B_8H_{12}$ has been known for almost four decades.[14] Work described in Chapter 3 shows that the structure of the fluoro analogue is incredibly different. The substituent $BX_2$ (X = F, Cl and Br) is able to mimic H in molecules with two-centre two-electron B-B bonds, such as in $B(BX_2)_3CO$ (X = F, Cl and Br) [see Chapter 2]. However, in molecules with greater electron deficiency, halogens are able to utilise $p\pi$-$\pi$ bonding to produce very different structures. For $B_8Cl_{12}$ and $B_8Br_{12}$, their molecular geometries utilise multicentre bonding as is the case with the experimentally determined $B_8F_{12}$. However for $B_8I_{12}$, this is not the case since calculations show this molecule to adopt a dimer structure (see Figure 3). This is perhaps not so surprising given the large steric properties of iodine such as those exhibited in $B(BI_2)_3CO$ [see Chapter 2].

It has been postulated that $B_8Cl_{12}$ is involved in the disproportionation of $B_2Cl_4$.[2] The third step in this reaction is believed to be the dimerisation of $B(BCl_2)_3$ to form $B_8Cl_{12}$.[2] It is at this stage that the boron atoms bond together by means of multicentred orbitals.[2] This compares to the calculations, which show that, at the HF and B3LYP levels, no three-centre two-electron bonding occurs. At these levels $B_8Cl_{12}$ exists as a very weakly bound dimer which is energetically stable with respect to the $B(BCl_2)_3$ monomer. However, at the MP2/6-31G* level, $B_8Cl_{12}$ adopts multicentre bonding.

The structure of the most stable form of $B_8Cl_{12}$ resembles that of $B_8F_{12}$ at the MP2/6-31G* level of calculation. The short central B(2)-B(4) bond in $B_8F_{12}$ is evident in $B_8Cl_{12}$ (1) at this level. The calculated B(2)-B(4) distance in $B_8Cl_{12}$ (1) is 4.9 pm longer at the MP2/6-31G* level than the equivalent distance in $B_8F_{12}$. But, whereas in $B_8F_{12}$ this bond remains relatively short at all levels of theory and basis set, in $B_8Cl_{12}$ (1) this bond increases vastly in length when HF and DFT methods are employed, equalling 189.8 pm using the larger basis set 6-311+G* to incorporate diffuse functions.

The B(3)-B(4) bond distance in $B_8Cl_{12}$ (**1**) is 242.5 pm at the MP2/6-31G* level of theory. This value lies close to the value found for $B_8F_{12}$ at the HF/6-31G* level, but is 35.3 pm longer when comparing the two compounds at the MP2/6-31G* level. The large distance between B(3) and B(4), especially at the DFT level, suggests that there is only a weak interaction between these two atoms. The short distance between B(1) and B(5) found at the DFT level (205.7 pm at the B3LYP/6-311+G* calculation) suggests that the molecule uses this interaction to compensate for the loss of electron density from the B(3)-B(4) bond. The formation of the deltahedron outlined by B(1)-B(4)-B(2)-B(5) stabilises the molecule by providing electron density through bridging interactions. The length of B(1)-B(5) at the MP2/6-31G* level (215.1 pm) is on average 9.2 pm longer than that found at HF and DFT levels. This is because the molecule is less reliant upon this bond for stability due to the shorter B(3)-B(4) distance at the MP2/6-31G* level.

The structure of $B_8Br_{12}$ (**1**) is quite different to that of $B_8F_{12}$. Comparison of the B(1)-B(2), B(1)-B(4) and B(2)-B(4) bonds in each molecule, at the MP2/6-31G* level, shows that for $B_8Br_{12}$ a more regular deltahedron is present. Bonds B(1)-B(2) and B(1)-B(4) only differ by 0.6 pm in $B_8Br_{12}$ but by 9.6 pm in $B_8F_{12}$. The most notable difference is observed for the B(2)-B(4) bond, which is 16.8 pm longer in the bromo compound than in the fluoro. $B_8Br_{12}$ relies upon different boron atoms to improve its electron distribution than does $B_8F_{12}$. In $B_8F_{12}$ the terminal $BF_2$ groups seem more capable of providing electrons to stabilise the boron framework. In contrast, $B_8Br_{12}$ depends upon bridging bromine atoms.

The most curious result determined for the molecular structure of $B_8Br_{12}$ (**1**) is the length of the B(1)-B(5) bond, particularly at the B3LYP/6-31G* level. At this level this bond is only 138.7 pm in order to allow the formation of a bromine bridge between atoms B(1) and B(5). It is perhaps therefore no surprise that when the B3LYP functional is used, $B_8Br_{12}$ prefers to adopt a dimeric structure such as those shown in Figures 2 and 3. Yet, when the size of the basis set is increased to 6-311G*, this same bond increases to 201.4 pm, which is only 0.2 pm shorter than the value determined by MP2 methods.

Unlike the fluoro, chloro and bromo members of the family $B_8X_{12}$, $B_8I_{12}$ adopts a dimer structure at all levels of theory and basis set. Iodine is able to donate electrons to boron; evidence for such is shown in the structures of the large boron subiodides $B_8I_8$ and $B_9I_9$.[7,8,13] However in both of these cases there exists a boron to iodine ratio of 1 : 1. For $B_8I_{12}$ there are four more iodines than borons. The increased steric bulk of the halogen therefore overrides the ability to form boron polyhedra. $B_8I_{12}$ prefers instead to form a weakly bound dimer with the $B(BI_2)_3$ molecules 388.0 pm apart (MP2/6-31G* with lanl2dz on the I atoms).

The structure of $B_8H_{12}$ (**1**) is 287.5 kJ $mol^{-1}$ higher in energy than the optimised crystal coordinates at the MP2/6-31G* level. Whilst in theory this isomer could also be synthesised – it is an energy minimum on the PES – the very high energy difference means that finding the correct preparation route is very unlikely. The geometry of $B_8H_{12}$ (**1**) is interesting due to its similarities to the well studied pentaborane(9)[25-28] and dihaloboryl pentaborane derivatives $BX_2B_5H_8$ (X = F, Cl and Br).[29] The structure of $B_5H_9$ was first determined in 1952 through separate studies by X-ray crystallography and GED.[25,26] It has subsequently been revisited by GED and X-ray crystallography.[27,28] All four studies established a square pyramidal arrangement of borons with $C_{4v}$ symmetry. A similar motif has also been found for $B_8H_{12}$ (**1**), albeit with a distorted pyramid.

In the gas-phase structure of $B_5H_9$ the B-B bonds that constitute the pyramidal base are 181.1(4) pm long.[27] This compares to the average crystal structure, which has B(base)-B(base) bonds of 179.5(25) pm.[28] In contrast, $B_8H_{12}$ (**1**) has average basal boron-boron bond lengths of 177.0 pm (MP2/6-31G*) and 178.7 pm (B3LYP/6-311+G*). The average base-apex distance in $B_5H_9$ is 169.4(4) pm (by GED)[27] and 170.0(28) pm (by X-ray crystallography)[28] compared to 171.7 and 172.5 pm at the MP2/6-31G* and B3LYP/6-311+G* levels for $B_8H_{12}$ (**1**).

*Ab initio* calculations and solution structures, when NMR data are available (IGLO), are powerful tools in estimating gas-phase structures. Calculations on $B_8X_{12}$ (X = Cl,

Br and I) have provided synthetic chemists with insight to possible structural organisation and thus provided indications of possible strategies for their synthesis.

## 4.5. References


1. A. G. Massey, *Adv. Inorg. Chem. and Radiochem.*, 1983, **26**, 1.
2. J. A. Morrison, *Chem. Rev.* 1991, **91**, 35.
3. A. K. Holliday and A. G. Massey, *J. Inorg. Nucl. Chem.*, 1961, **18**, 108.
4. D. Saulys and J. A. Morrison, *Inorg. Chem.*, 1980, **19**, 3057.
5. T. Davan and J. A. Morrison, *Inorg. Chem.*, 1986, **25**, 2366.
6. S. L. Emery and J. A. Morrison, *J. Am. Chem. Soc.*, 1982, **104**, 6790.
7. W. Hönle, Y. Grin, A. Burkhardt, U. Wedig, M. Schultheiss and H. G. von Schnering, *J. Solid State Chem.*, 1997, 59.
8. H. Binder, R. Kellner, K. Vaas, M. Hein, F. Baumann, M. Wanner, R. Winter, W. Kaim, W. Hönle, Y. Grin, U. Wedig, M. Schultheiss, R. K. Kremer, H. G. von Schnering, O. Groeger and G. Engelhardt, *Z. Anorg. Allg. Chem.*, 1999, **625**, 1059.
9. M. S. Reason and A. G. Massey, *J. Inorg. Nucl. Chem.*, 1975, **37**, 1593.
10. N. A. Kutz and J. A. Morrison, *Inorg. Chem.*, 1980, **19**, 3295.
11. A. J. Markwell, A. G. Massey and P. J. Portal, *Polyhedron*, 1982, **1**, 134.
12. J. Kane and A. G. Massey, *J. Inorg. Nucl. Chem.*, 1971, **33**, 1195.
13. A. G. Massey and P. J. Portal, *Polyhedron*, 1982, **1**, 319.
14. R. E. Enrione, F. P. de Boer and W. N. Lipscomb, *J. Am. Chem. Soc.*, 1964, **86**, 1451.
15. Gaussian 98, Revision A.7, M. J. Frisch, G. W. Trucks, H. B. Schlegel, G. E. Scuseria, M. A. Robb, J. R. Cheeseman, V. G. Zakrzewski, J. A. Montgomery, R. E. Stratmann Jr, J. C. Burant, S. Dapprich, J. M. Millam, A. D. Daniels, K. N. Kudin, M. C. Strain, O. Farkas, J. Tomasi, V. Barone, M. Cossi, R. Cammi, B. Mennucci, C. Pomelli, C. Adamo, S. Clifford, J. Ochterski, G. A. Petersson, P. Y. Ayala, Q. Cui, K. Morokuma, D. K. Malick, A. D. Rabuck, K. Raghavachari, J. B. Foresman, J. Cioslowski, J. V. Ortiz, A. G. Baboul, B. B. Stefanov, G. Liu, A. Liashenko, P. Piskorz, I. Komaromi, R. Gomperts, R. L. Martin, D. J. Fox, T. Keith, M. A. Al-Laham, C. Y. Peng, A. Nanayakkara, C. Gonzalez, M. Challacombe, P. M. W. Gill, B. Johnson, W. Chen, M. W. Wong, J. L. Andres,

C. Gonzalez, M. Head-Gordon, E. S. Replogle and J. A. Pople, Gaussian, Inc., Pittsburgh PA, 1998.

16. W. J. Hehre, L. Radom, P. v. R. Schleyer and J. A. Pople, *Ab initio Molecular Orbital Theory*, J . Wiley & Sons, 1986, p.71; D. R. Hartree, *Proc. Camb. Phil. Soc.*, 1928, **24**, 89; V. Fock, *Z. Physik*, 1930, **61**, 126 and *Z. Physik*, 1930, **62**, 795.
17. C. Møller and M. S. Plesset, *Phys. Rev.*, 1934, **46**, 618; P. Hohenburg, W. Kohn, *Phys. Rev.*, 1964, **B136**, 864.
18. P. J. Knowles, K. Somasundram, N. C. Handy and K. Hirao, *Chem. Phys. Lett.*, 1993, **211**, 272; W. Kohn, L. J. Sham, *Phys. Rev.*,1965, **A140**, 1133.
19. G. S. Pawley, *Acta Cryst.*, 1966, **20**, 631.
20. J. S. Binkley, J. A. Pople and W. J. Hehre, *J. Am. Chem. Soc.*, 1980, **102**, 939; M. S. Gordon, J. S. Binkley, J. A. Pople, W. J. Pietro and W. J. Hehre, *J. Am. Chem. Soc.*, 1982, **104**, 2797; W. J. Pietro, M. M. Francl, W. J. Hehre, D. J. Defrees, J. A. Pople and J. S. Binkley, *J. Am. Chem. Soc.*, 1982, **104**, 5039.
21. W. J. Hehre, R. Ditchfield and J. A. Pople, *J. Chem. Phys.*, 1972, **56**, 2257; P. C. Hariharan and J. A. Pople, *Mol. Phys.*, 1974, **27**, 209; M. S. Gordon, *Chem. Phys. Lett.*, 1980, **76**, 163.
22. A. D. McLean and G. S. Chandler, *J. Chem. Phys.*, 1980, **72**, 5639; R. Krishnan, J. S. Binkley, R. Seeger and J. A. Pople, *J. Chem. Phys.*, 1980, **72**, 650.
23. K. Raghavachari and G. W. Trucks, *J. Chem. Phys.*, 1989, **91**, 1062.
24. T. H. Dunning Jr. and P. J. Hay, *Modern Theoretical Chemistry*, Vol. 3, Ed. H. F. Schaefer III, Plenum, 1976, p.1; P. J. Hay and W. R. Wadt, *J. Chem. Phys.*, 1985, **82**, pp. 270, 284 and 299.
25. W. J. Dulmage and W. N. Lipscomb, *Acta Cryst.*, 1952, **5**, 260.
26. K. Hedberg, M. E. Jones, V. Schomaker, *Proc. Natl. Acad. Sci. U.S.A.*, 1952, **38**, 679.
27. R. Greatrex, N. N. Greenwood, D. W. H. Rankin and H. E. Robertson, *Polyhedron*, 1987, **6**, 1849.
28. C. E. Nordman, *J. Mol. Struct.*, 1999, **485**, 299.
29. D. A. Saulys and J. A. Morrison, *Inorg. Chem.*, 1990, **29**, 4174.

# Chapter Five

The Molecular Structures of $B_{10}X_{12}$ (X = F, Cl, Br, I and H) studied by X-ray Crystallography and Theoretical Calculations

## 5.1. Introduction

Knowledge of the chemistry of polyboron halides has been growing for about fifty years since the original discovery of $B_4Cl_4$ by Schlesinger.[1] However, with the exception of $B_2F_4$[2] and the recently determined $B_8F_{12}$ (Chapter 3), experimental structures of the polyboron fluorides are unknown. Timms has synthesised a further four boron fluorides that have molecular weights greater than that of $B_8F_{12}$.[3] These are formed as by-products in the production of $B_2F_4$ and $B_3F_5$, or from the decomposition of simpler boron fluorides.[3] The mass spectrum of a mixture of these boron fluorides contains peaks due to the ions $B_8F_6^+$, $B_9F_9^+$, $B_{10}F_{12}^+$, $B_9F_5^+$, $B_{10}F_8^+$, $B_{11}F_{11}^+$ and $B_{12}F_{14}^+$.[3] The most volatile of these species, $B_{10}F_{12}$, is the focus of research for this chapter through the investigation of its structure using X-ray crystallography and theoretical calculations.

Many halogenated borane clusters exist. Research of the available databases provides details of structures pertaining to compounds such as the boron trihalides and diboron tetrahalides in addition to larger species such as $B_nCl_n$ ($n$ = 4, 8, 9, 10, 11 and 12), $B_nBr_n$ ($n$ = 7, 8, 9 and 10) and $B_9I_9$.[3-14] However, the reader will note that such large species belong to the monohalide classification and possess *closo* structures. The structure determination of $B_{10}F_{12}$ has provided the focus for the study of a new class of boron subhalide, $B_{10}X_{12}$ (X = Cl, Br, I and H) using theoretical calculations.

## 5.2. Experimental

### 5.2.1. Compound Synthesis

J. A. J. Pardoe (University of Bristol) prepared the compound $B_{10}F_{12}$ from BF vapour using literature methods.[15] The samples provided were used for X-ray crystallography without further purification.

### 5.2.2. X-ray Crystallography

A sample of $B_{10}F_{12}$ was sealed in a glass capillary and a single crystal was grown at low temperature (200 K) on a diffractometer by using the laser technique employed by Boese and Nussbaumer.[16]

### 5.2.3. *Ab initio* and DFT Calculations

All calculations were performed using the Gaussian 98 computer program[17] using resources of the U.K. Computational Chemistry Facility, on a DEC 8400 superscalar cluster equipped with 10 fast processors, 6 GB of memory and 150 GB disk. Series of calculations were carried out starting with the crystal coordinates of $B_{10}F_{12}$ to determine the effects of basis set and electron correlation on the optimised structures. Calculations were performed using HF[18] (3-21G*[19] and 6-31G*[20] basis sets), MP2[21] (6-31G* basis set) and DFT[22] (6-31G*, 6-311G*[23] and 6-311+G* basis sets using the B3LYP[24] functional) methods.

Using the crystal structure of $B_{10}F_{12}$ as a general bonding scheme, the fluorine atoms were replaced by Cl, Br, I and H to determine substituent effects. Calculations for X = Cl, Br and I were performed using HF (3-21G* and 6-31G* basis sets), MP2 (6-31G* basis set) and DFT (6-31G* and 6-311G* basis sets using the B3LYP functional) methods. In the case of X = I, the lanl2dz[25] basis set was used on the I atoms in calculations above HF/3-21G* level. Calculations on $B_{10}H_{12}$ were performed using HF (3-21G* and 6-31G* basis sets), MP2 (6-31G* and 6-311G* basis sets) and DFT (6-31G*, 6-311G* and 6-311+G* basis sets using the B3LYP functional) methods.

Frequency calculations allowed the nature of each stationary point to be determined, confirming the structure as either a local minimum, transition-state or higher order stationary point on the potential-energy surface.

## 5.3. Results

### 5.3.1. X-ray Crystallography

The crystal structure of $B_{10}F_{12}$ (Figure 1) has crystallographic $S_4$ symmetry and is based on a central tetrahedron of boron atoms [B(2)-B(3)-B(4)-B(7)] each with a $BF_2$ substituent similar to the known $B_4X_4$ tetrahedra[7] but with $BF_2$ bridge bonds across B(2)-B(4) and B(3)-B(7).

The structure of $B_{10}F_{12}$ was solved by direct methods and refined against $F$, with anisotropic displacement parameters on all atoms and a Chebychev 3-term polynomial weighting scheme.[26] The final $R$ factor was 2.19% and $R_w$ = 2.52%. A full list of the crystal data and information concerning data collection and structure solution are shown in Table 1. Tables of fractional coordinates and atomic displacement parameters are given in Appendix B. The refined bond distances and angles are given in Tables 2 and 3.

**Figure 1**. Molecular framework for crystal structure of $B_{10}F_{12}$.

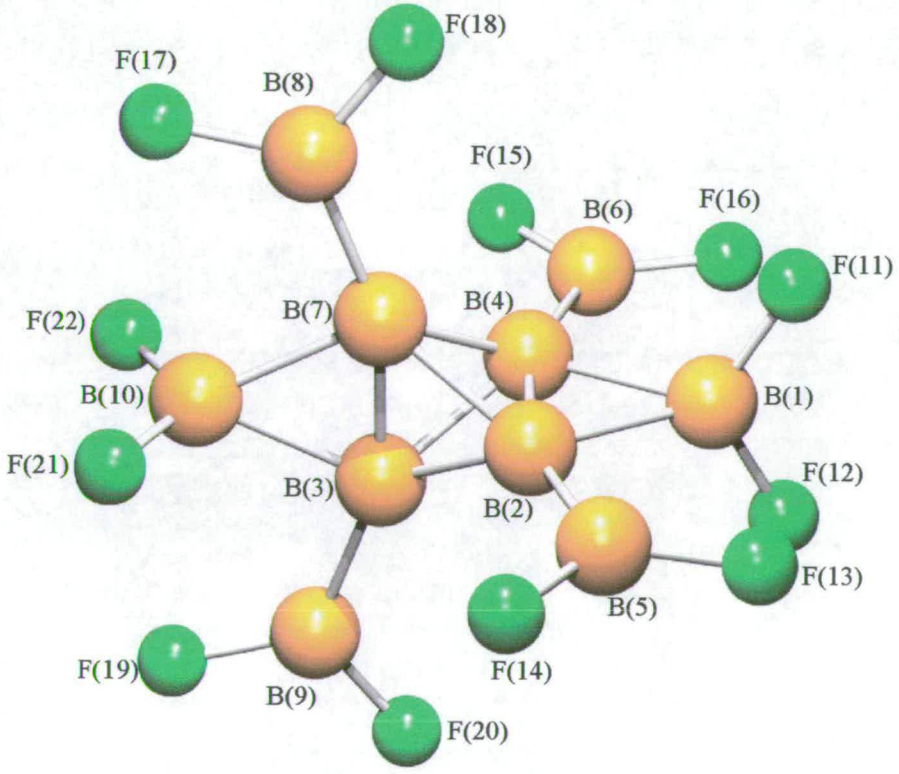

**Table 1**. Crystal data for $B_{10}F_{12}$.

| | |
|---|---|
| (a) Crystal data | |
| Formula | $B_{10}F_{12}$ |
| Formula weight | 336.08 |
| Temperature | 150 K |
| Wavelength | 0.71073 Å |
| Crystal system | Tetragonal |
| Space group | $I4_1/a$ |
| Unit cell dimensions | $a = 6.4118(8)$ Å, $\alpha = 90°$ |
| | $b = 6.4118(8)$ Å, $\beta = 90°$ |
| | $c = 25.551(5)$ Å, $\gamma = 90°$ |
| Volume, Z | 1132.6 $Å^{-3}$, 4 |
| Density (calc.) | 1.971 g $cm^{-3}$ |
| Absorption coefficient | 0.242 $mm^{-1}$ |
| F(000) | 632.583 |
| | |
| (b) Data collection | |
| Crystal size | 0.36 x 0.36 x 1.00 |
| Crystal description | colourless cylinder |
| θ range | 3 to 29° |
| Limiting indices | $-8 \leq h \leq 5$, $-8 \leq k \leq 8$, $-33 \leq l \leq 36$ |
| Reflections collected | 3613 |
| Unique data | 728 |
| Observed data [ $I > 2\sigma(I)$ ] | 685 |
| Scan type | multi-scan using Sadabs ($0.762 < T < 1$) |
| Absorption correction | $T_{min} = 0.92$, $T_{max} = 0.92$ |
| | |
| (c) Solution and Refinement | |
| Solution | direct |
| Refinement method | full-matrix least-squares on $F$ |
| Data/restraints/parameters | 3613 / 0 / 52 |
| Goodness-of-fit on $F$ | 1.0287 |
| Final $R$ indices | $R_1 = 2.19$, $wR_2 = 2.52$ |
| Max. shift | 0.014863 |
| Weighting scheme | Chebychev, 3 polynomials 0.428, 0.374, 0.203 |

**Table 2**. Bond lengths (pm) for $B_{10}F_{12}$ crystal structure.[a]

| | | | | | |
|---|---|---|---|---|---|
| B(1)-B(2) | 180.6 | B(3)-B(10) | 180.7 | B(6)-F(5) | 131.9 |
| B(1)-B(4) | 180.6 | B(4)-B(6) | 170.4 | B(6)-F(6) | 130.5 |
| B(2)-B(3) | 175.8 | B(4)-B(7) | 175.9 | B(8)-F(7) | 130.6 |
| B(2)-B(4) | 160.5 | B(7)-B(8) | 170.3 | B(8)-F(8) | 131.8 |
| B(2)-B(5) | 170.3 | B(7)-B(10) | 180.7 | B(9)-F(9) | 130.5 |
| B(2)-B(7) | 175.9 | B(1)-F(1) | 132.7 | B(9)-F(10) | 131.9 |
| B(3)-B(4) | 175.8 | B(1)-F(2) | 132.7 | B(10)-F(11) | 132.7 |
| B(3)-B(7) | 160.5 | B(5)-F(3) | 130.5 | B(10)-F(12) | 132.7 |
| B(3)-B(9) | 170.4 | B(5)-F(4) | 131.9 | | |

[a] Atom numbering shown in Figure 1.

**Table 3**. B-B bond angles (°) for $B_{10}F_{12}$ crystal structure.[a]

| | | | |
|---|---|---|---|
| B(1)-B(2)-B(3) | 118.8 | B(2)-B(1)-B(6) | 92.8 |
| B(1)-B(2)-B(4) | 63.6 | B(2)-B(3)-B(7) | 62.9 |
| B(1)-B(2)-B(5) | 96.8 | B(2)-B(3)-B(9) | 135.3 |
| B(1)-B(2)-B(7) | 118.8 | B(2)-B(3)-B(10) | 118.8 |
| B(1)-B(4)-B(3) | 118.8 | B(2)-B(4)-B(6) | 160.2 |
| B(1)-B(4)-B(6) | 96.8 | B(2)-B(7)-B(8) | 131.3 |
| B(1)-B(4)-B(7) | 118.7 | B(2)-B(7)-B(10) | 118.7 |
| B(3)-B(2)-B(4) | 62.8 | B(4)-B(1)-B(5) | 92.8 |
| B(3)-B(2)-B(5) | 131.3 | B(4)-B(2)-B(5) | 160.2 |
| B(3)-B(4)-B(6) | 135.3 | B(4)-B(2)-B(7) | 62.8 |
| B(3)-B(7)-B(8) | 160.2 | B(4)-B(3)-B(7) | 62.9 |
| B(3)-B(10)-B(8) | 92.8 | B(4)-B(3)-B(9) | 131.2 |
| B(5)-B(1)-B(6) | 132.9 | B(4)-B(3)-B(10) | 118.8 |
| B(5)-B(2)-B(7) | 135.3 | B(4)-B(7)-B(8) | 135.3 |
| B(6)-B(4)-B(7) | 131.2 | B(4)-B(7)-B(10) | 118.7 |
| B(7)-B(3)-B(9) | 160.2 | B(8)-B(7)-B(10) | 96.8 |
| B(7)-B(3)-B(10) | 63.6 | B(8)-B(10)-B(9) | 132.9 |
| B(7)-B(10)-B(9) | 92.8 | B(9)-B(3)-B(10) | 96.8 |
| | | | |
| B(2)-B(1)-F(1) | 119.8 | B(2)-B(5)-F(3) | 122.9 |
| B(4)-B(1)-F(1) | 116.1 | B(2)-B(5)-F(4) | 119.7 |
| B(2)-B(1)-F(2) | 116.0 | B(4)-B(6)-F(5) | 119.6 |
| B(4)-B(1)-F(2) | 119.7 | B(4)-B(6)-F(6) | 122.9 |
| B(7)-B(8)-F(7) | 122.9 | B(3)-B(9)-F(9) | 122.9 |
| B(7)-B(8)-F(8) | 119.7 | B(3)-B(9)-F(10) | 119.7 |
| B(3)-B(10)-F(11) | 119.8 | F(1)-B(1)-F(2) | 117.0 |
| B(7)-B(10)-F(11) | 116.1 | F(3)-B(5)-F(4) | 117.3 |
| B(3)-B(10)-F(12) | 116.0 | F(5)-B(6)-F(6) | 117.3 |
| B(7)-B(10)-F(12) | 119.7 | F(7)-B(8)-F(8) | 117.3 |
| F(11)-B(10)-F(12) | 117.0 | F(9)-B(9)-F(10) | 117.3 |

[a] Atom numbering shown in Figure 1.

### 5.3.2. *Ab initio* and DFT calculations

Calculations carried out starting with the crystal coordinates of $B_{10}F_{12}$ return an imaginary frequency at HF/3-21G*, which indicates that this structure is a transition state on the potential energy surface. This imaginary frequency ($7.2i$ $cm^{-1}$) represents a scissors motion of the four terminal $BF_2$ groups [$B(5)F_2$, $B(6)F_2$, $B(8)F_2$ and $B(9)F_2$], which in turn results in the deformation of the central tetrahedron [B(2), B(3), B(4) and B(7)]. However, the structure optimises to an energy minimum using a larger basis set (6-31G*) and higher levels of theory (see Figure 2). The structure changes to one that more closely resembles the structure seen for $B_8F_{12}$ (see Chapter 3). The molecule is based upon a folded $B_4$ central core, as in $B_8F_{12}$, but this core is highly symmetrical in $B_{10}F_{12}$. There are no bridging $BF_2$ groups in $B_{10}F_{12}$, but instead these are replaced with $B(BF_2)_2$ groups. The long bridging B-B bonds in the crystal structure are replaced with much shorter terminal B-B bonds. For example, B(1)-B(2) in the crystal phase represents a bridging bond (180.6 pm) compared to non-bridging bonds by calculation – equalling 165.1 and 167.7 pm at the MP2/6-31G* and B3LYP/6-311+G* levels respectively. The optimised geometric parameters are listed in Table 4.

**Figure 2**. Molecular framework for calculated structure of $B_{10}F_{12}$.

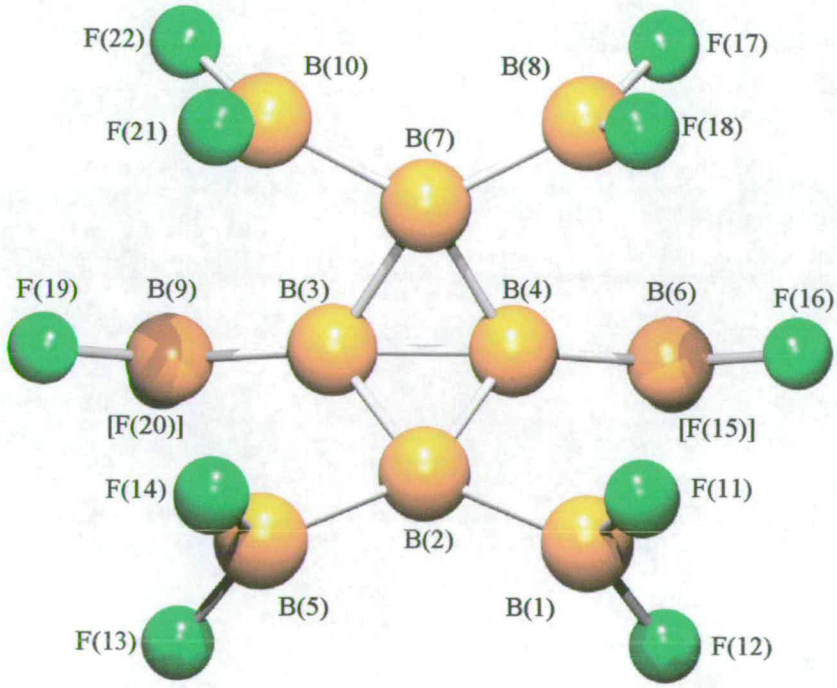

**Table 4**. Calculated ($r_e$) B-B bond lengths (pm) for $B_{10}F_{12}$ optimised crystal coordinates.

| Geometric parameter | Level of theory / Basis set | | | | | |
|---|---|---|---|---|---|---|
| | HF | | MP2 | B3LYP | | |
| | 3-21G* | 6-31G* | 6-31G* | 6-31G* | 6-311G* | 6-311+G* |
| B(1)-B(2) | 181.9 | 169.8 | 167.8 | 167.8 | 167.5 | 167.7 |
| B(1)-B(4) | 181.9 | 254.8 | 237.3 | 244.3 | 246.4 | 248.9 |
| B(2)-B(3) | 174.3 | 172.1 | 165.1 | 166.8 | 166.7 | 167.1 |
| B(2)-B(4) | 159.7 | 172.1 | 165.1 | 166.8 | 166.7 | 167.1 |
| B(2)-B(5) | 169.1 | 169.8 | 167.8 | 167.8 | 167.5 | 167.7 |
| B(2)-B(7) | 174.4 | 254.4 | 233.9 | 240.8 | 239.0 | 240.0 |
| B(3)-B(4) | 174.4 | 156.5 | 166.2 | 163.3 | 163.2 | 163.1 |
| B(3)-B(7) | 159.7 | 172.0 | 165.1 | 166.8 | 166.7 | 167.1 |
| B(3)-B(9) | 169.1 | 171.1 | 169.2 | 169.3 | 168.7 | 168.9 |
| B(4)-B(6) | 169.1 | 171.1 | 169.2 | 169.3 | 168.7 | 168.9 |
| B(4)-B(7) | 174.3 | 172.0 | 165.1 | 166.8 | 166.7 | 167.1 |
| B(7)-B(8) | 169.1 | 169.8 | 167.8 | 167.8 | 167.5 | 167.7 |
| B(7)-B(10) | 181.9 | 169.8 | 167.8 | 167.8 | 167.5 | 167.7 |
| B(3)-B(10) | 181.9 | 254.8 | 237.3 | 244.3 | 246.4 | 248.9 |
| Energy[a] | -1433.0772 | -1440.8108 | -1443.6564 | -1447.3164 | -1447.7371 | -1447.7699 |

[a] absolute energy in Hartrees.

The short central B(3)-B(4) bond in the optimised structure of $B_{10}F_{12}$ (at levels greater than HF/3-21G*) increases in length with the inclusion of electron correlation. Its length at the B3LYP/6-311+G* and MP2/6-31G* levels is 6.6 and 9.7 pm greater respectively than at the HF/6-31G* level. The opposite trend is found for the bridging B-B bonds. At the HF/6-31G* level these bonds are 5.0 pm longer than the B3LYP/6-311+G* and 5.9 pm longer than the MP2/6-31G* value. This same trend is exhibited for the terminal B-B bonds, with the lengths at the B3LYP/6-311+G* and MP2/6-31G* levels 2.1, 2.2 and 2.0, 1.9 pm shorter than the equivalent bonds at the HF/6-31G* level.

For no cases of X were imaginary frequencies returned, indicating that these structures represent minima on the potential energy surface at all levels of theory used (see Tables 5-7). The two structural motifs determined for $B_{10}F_{12}$ (see Figures 1 and 2) are also found for $B_{10}X_{12}$ (X = Cl, Br and I). For X = Cl, Br and I, the determined structure depends upon the level of calculation used. At the HF level of theory, the structure is equivalent to that which is found by calculation for X = F. For X = Cl and I, this structure is also adopted using DFT methods with the B3LYP functional. However when the MP2 level of theory is utilised each molecule of $B_{10}X_{12}$ (X = Cl, Br and I) reverts to that which is found in the solid phase of $B_{10}F_{12}$. This is also true for X = Br using DFT methods.

Geometry changes for $B_{10}Cl_{12}$ were found as a result of the inclusion of electron correlation and of increasing the size of the basis set (see Table 5). Increasing the size of the basis set from 3-21G* to 6-31G* at the HF level resulted in decreased bridging B-B bond distances (by 2.3 pm). Longer terminal B-B bond lengths resulted from the same increase in basis set (by 1.5 pm and 2.5 pm for B(1)-B(2) and B(3)-B(9) respectively). The calculated geometric parameters at the DFT level using the 6-31G* basis set are in close agreement with those determined using the 6-311G* basis set. This increase in basis set resulted in slight decreases of B-B bond length, the largest change occurring for B(3)-B(9) [0.8 pm].

**Table 5**. Calculated ($r_e$) B-B bond lengths (pm) for $B_{10}Cl_{12}$ (pm).

| Geometric parameter | Level of theory / Basis set | | | | |
|---|---|---|---|---|---|
| | HF | | B3LYP | | MP2 |
| | 3-21G* | 6-31G* | 6-31G* | 6-311G* | 6-31G* |
| B(1)-B(2) | 167.9 | 169.4 | 167.3 | 167.0 | 167.9 |
| B(1)-B(4) | 264.4 | 263.4 | 254.4 | 254.3 | 177.8 |
| B(2)-B(3) | 176.0 | 173.7 | 168.3 | 168.2 | 159.5 |
| B(2)-B(4) | 176.0 | 173.8 | 168.3 | 168.2 | 170.0 |
| B(2)-B(5) | 167.9 | 169.4 | 167.3 | 167.0 | 177.8 |
| B(2)-B(7) | 253.4 | 258.4 | 244.5 | 244.8 | 180.2 |
| B(3)-B(4) | 156.1 | 156.3 | 163.4 | 162.9 | 180.2 |
| B(3)-B(7) | 176.0 | 173.8 | 168.3 | 168.2 | 170.0 |
| B(3)-B(9) | 168.9 | 171.4 | 169.4 | 168.6 | 167.9 |
| B(3)-B(10) | 264.4 | 263.4 | 254.4 | 254.3 | 177.8 |
| B(4)-B(6) | 168.9 | 171.4 | 169.4 | 168.6 | 167.9 |
| B(4)-B(7) | 176.0 | 173.8 | 168.3 | 168.2 | 159.5 |
| B(7)-B(8) | 167.9 | 169.4 | 167.3 | 167.0 | 177.8 |
| B(7)-B(10) | 167.9 | 169.4 | 167.3 | 167.0 | 167.9 |
| Energy[a] | -5734.6683 | -5761.0612 | -5771.3474 | -5771.7339 | -5763.5014 |

[a] absolute energy in Hartrees.

**Table 6**. Calculated ($r_e$) B-B bond lengths (pm) for $B_{10}Br_{12}$ (pm).

| Geometric parameter | Level of theory / Basis set | | | | |
|---|---|---|---|---|---|
| | HF | | B3LYP | | MP2 |
| | 3-21G* | 6-31G* | 6-31G* | 6-311G* | 6-31G* |
| B(1)-B(2) | 166.1 | 167.9 | 171.5 | 171.2 | 172.4 |
| B(1)-B(4) | 261.3 | 262.4 | 186.9 | 194.0 | 180.1 |
| B(2)-B(3) | 174.3 | 173.5 | 166.1 | 166.8 | 165.7 |
| B(2)-B(4) | 174.3 | 173.5 | 162.5 | 165.0 | 160.0 |
| B(2)-B(5) | 166.1 | 167.9 | 165.3 | 166.3 | 165.4 |
| B(2)-B(7) | 247.7 | 253.9 | 216.1 | 231.1 | 195.9 |
| B(3)-B(4) | 156.1 | 155.9 | 172.9 | 172.1 | 179.2 |
| B(3)-B(7) | 174.3 | 173.5 | 162.5 | 165.0 | 160.0 |
| B(3)-B(9) | 167.5 | 170.3 | 168.8 | 170.4 | 167.3 |
| B(3)-B(10) | 261.3 | 262.4 | 186.9 | 194.0 | 180.2 |
| B(4)-B(6) | 167.5 | 170.3 | 168.8 | 170.4 | 167.3 |
| B(4)-B(7) | 174.3 | 173.5 | 166.1 | 166.7 | 165.7 |
| B(7)-B(8) | 166.1 | 167.9 | 165.3 | 166.3 | 165.4 |
| B(7)-B(10) | 166.1 | 167.9 | 171.5 | 171.2 | 172.4 |
| Energy[a] | -30969.1526 | -31085.9482 | -31109.4550 | -31138.7105 | -31088.1906 |

[a] absolute energy in Hartrees.

**Table 7**. Calculated ($r_e$) B-B bond lengths (pm) for $B_{10}I_{12}$ (pm).

| Geometric parameter | Level of theory / Basis set | | | | |
|---|---|---|---|---|---|
| | HF | | B3LYP | | MP2 |
| | 3-21G* | 6-31G*[a] | 6-31G*[a] | 6-311G*[b] | 6-31G*[a] |
| B(1)-B(2) | 167.7 | 169.4 | 167.3 | 167.0 | 173.6 |
| B(1)-B(4) | 267.5 | 267.2 | 257.1 | 257.4 | 176.6 |
| B(2)-B(3) | 178.6 | 176.7 | 171.2 | 171.2 | 164.8 |
| B(2)-B(4) | 178.6 | 177.8 | 171.4 | 171.4 | 163.2 |
| B(2)-B(5) | 167.7 | 169.3 | 167.2 | 166.8 | 166.2 |
| B(2)-B(7) | 267.4 | 272.5 | 259.9 | 260.5 | 227.2 |
| B(3)-B(4) | 156.1 | 155.8 | 162.8 | 162.3 | 183.1 |
| B(3)-B(7) | 178.6 | 177.8 | 171.4 | 171.4 | 163.2 |
| B(3)-B(9) | 169.5 | 172.0 | 170.0 | 169.4 | 169.4 |
| B(3)-B(10) | 267.5 | 267.2 | 257.1 | 257.4 | 176.6 |
| B(4)-B(6) | 169.5 | 172.0 | 170.0 | 169.4 | 169.4 |
| B(4)-B(7) | 178.6 | 176.7 | 171.2 | 171.2 | 164.8 |
| B(7)-B(8) | 167.7 | 169.3 | 167.2 | 166.8 | 166.2 |
| B(7)-B(10) | 167.7 | 169.4 | 167.3 | 167.0 | 173.5 |
| Energy[c] | -82900.5828 | -380.9400 | -385.3987 | -385.4466 | -382.4412 |

[a] 6-31G* on B atoms and lanl2dz on I atoms.
[b] 6-311G* on B atoms and lanl2dz on I atoms.
[c] absolute energy in Hartrees.

At the MP2 level of theory $B_{10}Cl_{12}$ reverts to the structure that is seen in Figure 1. This is highlighted by the reformation of the bridging bonds B(1)-B(4) and B(3)-B(10), and the core B(2)-B(7) bond. These bonds are 254.3 pm and 244.8 pm respectively at the B3LYP level of theory using the 6-311G* basis set, a massive increase of 76.5 pm and 64.6 pm respectively when compared to the MP2/6-31G* calculated values.

For X = Br, increasing the basis set from 3-21G* to 6-31G* at the HF level of theory resulted in increased terminal B-B bond distances (by 1.8 pm and 2.8 pm for B(1)-B(2) and B(3)-B(9) respectively). This increase of basis set also resulted in decreased distances for the bridging B-B bonds (by 0.8 pm). The incorporation of electron correlation resulted in $B_{10}Br_{12}$ adopting the structure found in Figure 1. The central tetrahedron is most strongly bound at the MP2/6-31G* level with shorter core bond distances than those found at the DFT level using the B3LYP functional. For example, the B(2)-B(7) bond is 20.2 pm and 35.2 pm shorter at the MP2/6-31G*

level compared to the B3LYP/6-31G* and B3LYP/6-311G* levels respectively. Indeed, this bond distance at the B3LYP/6-311G* (244.8 pm) level indicates that the structure more closely resembles that seen in Figure 2 at this level with only a weak interaction between atoms B(2) and B(7). However, the bridging bonds B(1)-B(2), B(1)-B(4), B(3)-B(10) and B(7)-B(10) remain intact despite the fact that they exhibit extreme asymmetry. It is therefore more accurate to describe the demonstrated structure of $B_{10}Br_{12}$ at the MP2 and B3LYP levels as that observed in Figure 1.

Similarly to $B_{10}Cl_{12}$, $B_{10}I_{12}$ forms the structure seen in Figure 2 according to calculations at the HF and B3LYP levels. The structure at the MP2 level more closely resembles that found in Figure 1. Increasing the size of the basis set from 3-21G* to 6-31G*, using the lanl2dz basis set on the I atoms, at the HF level resulted in the terminal B-B bond distances increasing in length (by 1.7 pm for the B(1)-B(2) distance). The opposite trend is found at the DFT level when the basis set on the B atoms is increased from 6-31G* to 6-311G*, with the lanl2dz basis set on the I atoms, using the B3LYP functional. The B(1)-B(2) bond at this level decreases by 0.3 pm whilst the bonds B(2)-B(5) and B(3)-B(9) decrease by 0.4 pm and 0.6 pm respectively. The bridge bonds are over-estimated using the 3-21G* basis set at the HF level when compared to the equivalent distances using the 6-31G* with lanl2dz basis sets. For example the B(2)-B(3) bond length decreases by 1.9 pm when the basis set on the B atoms is increased to 6-31G*. The 6-31G* basis set at the B3LYP level is in very good agreement with the 6-311G* when estimating the B-B bond distances in $B_{10}I_{12}$. The tetrahedron in $B_{10}I_{12}$ determined at the MP2/6-31G* level shows only a weak interaction between B(2) and B(7), with a distance of 227.2 pm. This is 33.3 pm and 45.3 pm shorter than the values at the B3LYP/6-311G* (with lanl2dz on the I atoms) and HF/6-31G* (with lanl2dz on the I atoms) levels respectively. The B(1)-B(4) and B(3)-B(10) bonds at the MP2/6-31G* level are 80.8 pm and 90.6 pm shorter than the equivalent bonds at the B3LYP/6-311G* and HF/6-31G* levels respectively.

The calculated structure of $B_{10}H_{12}$ is dependent upon the level of theory used, or more accurately, upon the inclusion of electron correlation. The structure at the HF

level of theory using the 3-21G* and 6-31G* basis sets represents that shown in Figure 2. However, the inclusion of electron correlation by utilising DFT and MP2 methods results in a very different structure to those of its halogen analogues (see Figure 3). Six adjacent deltahedra form an extended open framework of boron atoms. Atoms B(3) and B(4) are five-coordinate but are not involved in bonding to anything other than boron atoms in the framework. Atoms B(2) and B(7) are four coordinate connected to one bridging $BH_2$ and one terminal $BH_2$ group. These terminal $BH_2$ groups lie only 0.7° (at MP2/6-31G*) away from a linear configuration to the adjacent B-B bond. The calculated B-B bond distances are shown in Table 8.

**Figure 3**. Molecular framework for calculated structure of $B_{10}H_{12}$.

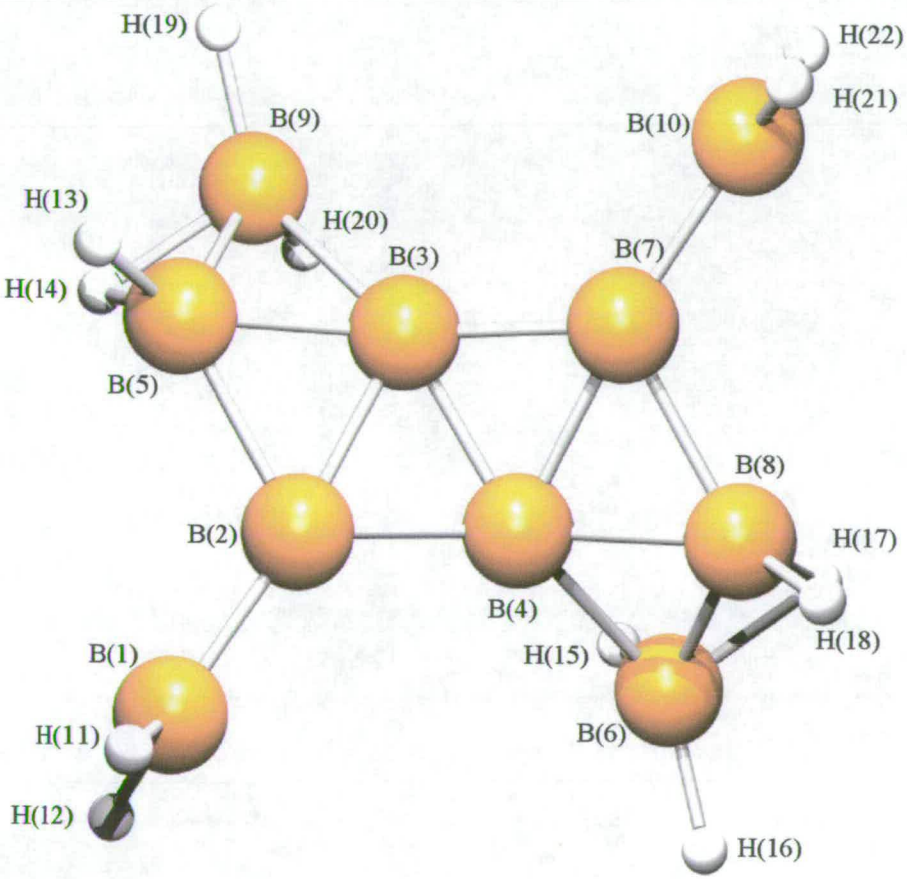

**Table 8**. Calculated ($r_e$) B-B bond lengths (pm) for $B_{10}H_{12}$ (pm).

| Geometric parameter | Level of theory / Basis set | | | | | | |
|---|---|---|---|---|---|---|---|
| | HF | | B3LYP | | | MP2 | |
| | 3-21G* | 6-31G* | 6-31G* | 6-311G* | 6-311+G* | 6-31G* | 6-311G* |
| B(1)-B(2) | 164.4 | 165.4 | 162.1 | 161.4 | 161.4 | 163.1 | 163.1 |
| B(2)-B(3) | 175.0 | 172.3 | 167.0 | 166.8 | 166.8 | 166.8 | 167.6 |
| B(2)-B(4) | 175.0 | 172.3 | 165.6 | 165.3 | 165.3 | 165.2 | 165.8 |
| B(2)-B(5) | 164.4 | 165.4 | 174.3 | 174.1 | 174.1 | 174.1 | 174.8 |
| B(3)-B(4) | 160.6 | 161.1 | 163.9 | 163.5 | 163.5 | 164.9 | 166.1 |
| B(3)-B(5) | 243.6 | 242.8 | 167.0 | 166.8 | 166.8 | 166.8 | 167.7 |
| B(3)-B(7) | 175.0 | 172.3 | 165.6 | 166.8 | 165.3 | 165.2 | 165.8 |
| B(3)-B(9) | 167.6 | 169.6 | 184.5 | 184.6 | 184.6 | 183.6 | 183.9 |
| B(4)-B(6) | 167.6 | 169.7 | 184.6 | 184.6 | 184.6 | 183.6 | 183.9 |
| B(4)-B(7) | 175.0 | 172.3 | 165.6 | 166.8 | 166.8 | 166.8 | 167.6 |
| B(4)-B(8) | 243.5 | 242.8 | 167.0 | 166.8 | 166.8 | 166.8 | 167.8 |
| B(5)-B(9) | 316.0 | 315.3 | 173.3 | 172.9 | 172.9 | 173.3 | 174.2 |
| B(6)-B(8) | 315.9 | 315.3 | 173.3 | 172.9 | 172.9 | 173.3 | 174.2 |
| B(7)-B(8) | 164.4 | 165.4 | 174.3 | 174.1 | 174.1 | 174.1 | 174.8 |
| B(7)-B(10) | 164.4 | 165.4 | 162.1 | 161.4 | 161.4 | 163.1 | 163.1 |
| Energy[a] | -252.1900 | -253.6299 | -255.6562 | -255.6930 | -255.6934 | -254.5167 | -254.5898 |

[a] absolute energy in Hartrees.

The inclusion of electron correlation when calculating the structure of $B_{10}H_{12}$ is essential. Without such treatment, the structure is fundamentally different. Without experimental collaboration it is impossible to say definitively which *ab initio* method gives the 'correct' structure but experience tells us that the DFT and MP2 methods are generally more precise in estimating experimental structures than HF methods. Yet, the calculations described for the halogen analogues show that the DFT and MP2 calculations can give very different structures. Table 8 shows that the results of the B3LYP/6-31G* calculation are in good agreement with those using larger basis sets (6-311G* and 6-311+G*) at the same level. This is less true for the MP2/6-31G* level calculation compared to MP2/6-311G*. The MP2/6-31G* calculation underestimates the central B(3)-B(4) bond length by 1.2 pm compared to the MP2/6-311G* level, but in general there can be regarded as negligible difference between the 6-31G* and 6-311G* basis sets. At the DFT (using the B3LYP functional) and MP2 levels the terminal B-B bonds are shorter than both the central B(3)-B(4) and bridging B-B bonds. This is perhaps not surprising since the greatest electron deficiency exists in the central core of this molecule.

## 5.4. Discussion

The compound $B_4Cl_4$ was first synthesised by Schlesinger and co-workers in 1952.[1] Its crystal structure was determined by M. Atoji and W. N. Lipscomb to contain a tetrahedron of boron atoms surrounded by a larger tetrahedron of chlorine atoms.[4] A remarkable aspect of boron subhalide chemistry is that fluorine does not appear to support a series of monohalides as do chlorine, bromine and iodine.[3] There exist no experimentally determined structures of monofluorides. Despite many attempts, the monofluoride $B_4F_4$ has yet to be synthesised.[3,5] The inability to synthesise $B_4F_4$ has been explained in the past to be due to relatively weak back-bonding from the F *p* orbitals into cage bonding orbitals compared to the chlorine analogue.[3,7] However, this is not the whole story. The synthesis of $B_{10}F_{12}$ and alkyl-substituted cages such as $B_4(^tBu)_4$ and mass spectral evidence for the ions $B_9F_9^+$, $B_{11}F_{11}^+$ and $B_{12}F_{12}^+$ show that such clusters are stable under certain conditions.[3] Further to this, an *ab initio*

study by Hall and Lipscomb advocates that there is greater back-donation in $B_4F_4$ than in $B_4Cl_4$, thus suggesting that the non-existence of $B_4F_4$ is due to the lack of synthetic routes.[5]

The crystal structure of $B_{10}F_{12}$ is based on a central distorted tetrahedron of boron atoms each with a terminal $BF_2$ group, similar to the known $B_4X_4$ tetrahedra,[7] but with $BF_2$ bridges across the B(2)-B(4) and B(3)-B(7) edges. Formally, $B_{10}F_{12}$ belongs to the *closo*-$B_4H_6$ family of boranes.[27] A computational study of $B_4H_6$ derivatives by A. Neu *et al.* shows its ground state to be a tetrahedral $B_4H_4(\mu\text{-}H)_2$ structure,[28] i.e. equivalent to $B_{10}F_{12}$ if H were replaced with $BF_2$. Calculations on the family of compounds $B_{10}X_{12}$ (X = Cl, Br and I) at the MP2/6-31G* level indicate such systems adopt a similar structure to that found by X-ray crystallography for $B_{10}F_{12}$. Comparing the solid phase of $B_{10}F_{12}$ to these systems, with the exception of bonds B(2)-B(3) and B(4)-B(7) in the chloro analogue, the bridged edges of the central tetrahedron are shorter than the four non-bridged edges. For example, the bridged edges [B(2)-B(4) and B(3)-B(7)] are shorter than the non-bridged B(2)-B(3) and B(4)-B(7) edges by 15.4, 10.2, 5.7 and 1.6 pm for $B_{10}F_{12}$, $B_{10}Cl_{12}$, $B_{10}Br_{12}$ and $B_{10}I_{12}$ respectively. In the cases of X = Cl, Br and I two of the non-bridged edges are much longer than the other two. The edge B(2)-B(7) is longer than B(2)-B(3) by 20.7, 30.2 and 62.4 pm for $B_{10}Cl_{12}$, $B_{10}Br_{12}$ and $B_{10}I_{12}$ respectively. The edge B(3)-B(4) is longer than B(2)-B(3) by 20.7, 16.7 and 18.3 pm for $B_{10}Cl_{12}$, $B_{10}Br_{12}$ and $B_{10}I_{12}$ respectively.

In the crystal phase of $B_{10}F_{12}$ (Figure 1), the $BF_2$ bridges across the B(2)-B(4) and B(3)-B(7) edges are symmetric. This is not so for the other halogen analogues, whereby the asymmetric nature of these bridges increases in the sequence I < Br < Cl. The B(1)-B(2) and B(7)-B(10) bonds in $B_{10}Cl_{12}$, at the MP2/6-31G* level, are 9.9 pm shorter than the corresponding B(1)-B(4) and B(3)-B(10) bonds. For $B_{10}Br_{12}$ and $B_{10}I_{12}$, this difference is less pronounced, being 7.7 and 3.0 pm respectively.

The calculated structures of $B_{10}F_{12}$ (at all levels of theory), $B_{10}Cl_{12}$ and $B_{10}I_{12}$ (using HF and DFT methods), and $B_{10}Br_{12}$ and $B_{10}H_{12}$ (at the HF level) are very different to

the crystal structure of $B_{10}F_{12}$ and MP2/6-31G* calculated structures of $B_{10}X_{12}$ (X = Cl, Br and I). Figure 2 shows such systems bond as $(X_2B)B[\mu\text{-}B(BX_2)_2]_2B(BX_2)$. *Ab initio* calculations on $B_{10}F_{12}$ show the $S_4$ structure to be a transition state and that it relaxes into the energy minimum $C_{2v}$ structure. Contrastingly, a computational study of $B_4H_6$ shows that the energy difference between energy minima of $D_{2d}$ and $C_{2v}$ symmetry is +38.5 kJ $mol^{-1}$.[28]

Comparison of the molecules $B_{10}X_{12}$ at the HF/6-31G* level, where the structural motif is $(X_2B)B[\mu\text{-}B(BX_2)_2]_2B(BX_2)$, shows the central B(3)-B(4) bond length to be similar for the halogen species (with a difference of only 0.7 pm), and to be only 4.6 pm longer in the hydrogen compound. The largest length for this bond is found for the hydride (161.1 pm), and the shortest for the iodo compound (155.8 pm). The corresponding bond in $B_8F_{12}$ (see Chapter 3) is found by calculation to be 18.3 pm longer than in $B_{10}F_{12}$, at the same level of theory and basis set. The lengths of the bridging and terminal bonds in this family of compounds are similar. The shortest bridge bond, found for the fluoro compound, is 5.8 pm shorter than the equivalent bond in $B_{10}I_{12}$, but only 1.8, 1.5 and 0.3 pm shorter than in $B_{10}Cl_{12}$, $B_{10}Br_{12}$ and $B_{10}H_{12}$ respectively. In $B_{10}H_{12}$, the B-B bonds that belong to the terminal B-$BX_2$ groups connected to the apex of the bridging B-B-B bonds are shorter than in the halogen compounds (by 4.4, 4.0, 2.5 and 4.0 pm for $B_{10}F_{12}$, $B_{10}Cl_{12}$, $B_{10}Br_{12}$ and $B_{10}I_{12}$ respectively). The differences between B-B distances belonging to the terminal B-$BX_2$ groups that are bonded directly to the central B(3)-B(4) bond are less pronounced. In $B_{10}H_{12}$, such bonds are 1.5, 1.8, 0.7 and 2.4 pm shorter than when X = F, Cl, Br and I respectively.

The B-B bond lengths in the crystal structure of $B_4Cl_4$ are 171(4) and 169(4) pm.[4] The crystal structures of the much larger clusters $B_8Cl_8$ and $B_9Cl_9$ show B-B bond lengths of 178(5) – 207(5)[29] and 173.3(6) – 206.1(7) pm respectively.[14] These compare to values of 159.5 – 180.2 pm for the core boron fragment in $B_{10}Cl_{12}$ at the MP2/6-31G* level. The B-B bond distances in $B_9Br_9$ range from 173.5 – 201.0 pm by crystallography and 175.5 – 204.0 pm by calculation.[14] This compares to values of 160.0 – 195.9 pm for $B_{10}Br_{12}$ at the MP2/6-31G* level. Calculated values for the

B-B bond distances in $B_9I_9$ range from 176.0 – 203.2 pm[14] compared to 163.2 – 227.2 pm in $B_{10}I_{12}$ at the MP2/6-31G* level. It can therefore be seen that the shortest bonds in $B_{10}X_{12}$ (X = F, Cl, Br and I) are shorter than in any known B*n*X*n* cluster.

The debate that rages as to the strength of the back-bonding from F *p* orbitals into cage bonding orbitals compared to that from Cl is further clouded by the structure determination of $B_{10}F_{12}$. Whilst the crystal structure seems to concur with the calculations (albeit to a low level) carried out on $B_4F_4$ by Hill and Lipscomb,[5] *ab initio* calculations carried out on $B_{10}F_{12}$ (where the molecule is free from crystal packing forces) seem to disprove this same theory. $B_8F_{12}$, in both the crystal and gas phases, adopts an open diborane-type structure, which is also closely favoured by $B_{10}F_{12}$ in the gas phase. In $B_{10}F_{12}$ there are fewer fluorine atoms per boron available to provide extra electron density via $p\pi$-$\pi$ bonding than in $B_8F_{12}$. To circumvent this, $B_{10}F_{12}$ forms a central tetrahedral core of B atoms in the crystal phase. It is something of a quandary to the author as to why, in the gas phase, $B_{10}F_{12}$ would adopt a structure as that seen in Figure 2. It has been suggested that the reason for this is that the global minimum has not been determined and that by twisting the terminal $BF_2$ groups in the crystal geometry we will determine the true global minimum.[27] Whilst this may be valid, calculations carried out on both $S_4$ and $D_2$ isomers starting with the crystal geometry resulted in the relaxation to the structure in Figure 2.

## 5.5. References


1. G. Urry, T. Wartik and H. I. Schlesinger, *J. Am. Chem. Soc.*, 1952, **74**, 5809; G. Urry, A. G. Garrett and H. I. Schlesinger, *Inorg. Chem.*, 1963, **2**, 396.
2. L. Trefonas and W. N. Lipscomb, *J. Chem. Phys.*, 1958, **28**, 54.
3. A. G. Massey, *Adv. Inorg. Chem. Radiochem.*, 1983, **26**, 1.
4. M. Atoji and W. N. Lipscomb, *Acta Cryst.*, 1953, **6**, 547.
5. J. H. Hall, Jr., and W. N. Lipscomb, *Inorg. Chem.*, 1974, **13**, 710.
6. A. K. Holliday and A. G. Massey, *J. Inorg. Nucl. Chem.*, 1961, **18**, 108.
7. J. A. Morrison, *Chem. Rev.*, 1991, **91**, 35.
8. S. L. Emery and J. A. Morrison, *J. Am. Chem. Soc.*, 1982, **104**, 6790.
9. A. J. Markwell, A. G. Massey and P. J. Portal, *Polyhedron*, 1982, **1**, 134.
10. J. Kane and A. G. Massey, *J. Inorg. Nucl. Chem.*, 1971, **33**, 1195.
11. T. Davan and J. A. Morrison, *Inorg. Chem.*, 1986, **25**, 2366.
12. N. A. Kutz and J. A. Morrison, *Inorg. Chem.*, 1980, **19**, 3295.
13. L. Ahmed, J. Castillo and J. A. Morrison, *Inorg. Chem.*, 1992, **31**, 1858.
14. W. Hönle, Y. Grin, A. Burkhardt, U. Wedig, M. Schultheiss and H. G. von Schnering, *J. Solid State Chem.*, 1997, 59; H. Binder, R. Kellner, K. Vaas, M. Hein, F. Baumann, M. Wanner, R. Winter, W. Kaim, W. Hönle, Y. Grin, U. Wedig, M. Schultheiss, R. K. Kremer, H. G. von Schnering, O. Groeger and G. Engelhardt, *Z. Anorg. Allg. Chem.*, 1999, **625**, 1059; H. Binder, R. Kellner, K. Vaas, M. Hein, F. Baumann, M. Wanner, W. Kaim, U. Wedig, W. Hönle, H. G. von Schnering, O. Groeger and G. Engelhardt, *Z. Anorg. Allg. Chem.*, 1999, **625**, 1638.
15. J. A. J. Pardoe, N. C. Norman, P. L. Timms, S. Parsons, I. Mackie, C. R. Pulham and D. W. H. Rankin, *Angew. Chem. Int. Ed.*, 2003, **42**, 571.
16. R. Boese and M. Nussbaumer, in *Correlations, Transformations and Interactions in Organic Crystal Chemistry, IUCr Crystallographic Symposia, Vol. 7 (Eds.: D. W. Jones and A. Katrusiak)*, pp.20-37, Oxford, 1994.
17. Gaussian 98, Revision A.7, M. J. Frisch, G. W. Trucks, H. B. Schlegel, G. E. Scuseria, M. A. Robb, J. R. Cheeseman, V. G. Zakrzewski, J. A. Montgomery, R. E. Stratmann Jr, J. C. Burant, S. Dapprich, J. M. Millam, A. D. Daniels, K. N.

Kudin, M. C. Strain, O. Farkas, J. Tomasi, V. Barone, M. Cossi, R. Cammi, B. Mennucci, C. Pomelli, C. Adamo, S. Clifford, J. Ochterski, G. A. Petersson, P. Y. Ayala, Q. Cui, K. Morokuma, D. K. Malick, A. D. Rabuck, K. Raghavachari, J. B. Foresman, J. Cioslowski, J. V. Ortiz, A. G. Baboul, B. B. Stefanov, G. Liu, A. Liashenko, P. Piskorz, I. Komaromi, R. Gomperts, R. L. Martin, D. J. Fox, T. Keith, M. A. Al-Laham, C. Y. Peng, A. Nanayakkara, C. Gonzalez, M. Challacombe, P. M. W. Gill, B. Johnson, W. Chen, M. W. Wong, J. L. Andres, C. Gonzalez, M. Head-Gordon, E. S. Replogle and J. A. Pople, Gaussian, Inc., Pittsburgh PA, 1998.

18. W. J. Hehre, L. Radom, P. v. R. Schleyer and J. A. Pople, *Ab initio Molecular Orbital Theory*, J . Wiley & Sons, 1986, p.71; D. R. Hartree, *Proc. Camb. Phil. Soc.*, 1928, **24**, 89; V. Fock, *Z. Physik*, 1930, **61**, 126 and *Z. Physik*, 1930, **62**, 795.
19. J. S. Binkley, J. A. Pople and W. J. Hehre, *J. Am. Chem. Soc.*, 1980, **102**, 939; M. S. Gordon, J. S. Binkley, J. A. Pople, W. J. Pietro and W. J. Hehre, *J. Am. Chem. Soc.*, 1982, **104**, 2797; W. J. Pietro, M. M. Francl, W. J. Hehre, D. J. Defrees, J. A. Pople and J. S. Binkley, *J. Am. Chem. Soc.*, 1982, **104**, 5039.
20. W. J. Hehre, R. Ditchfield and J. A. Pople, *J. Chem. Phys.*, 1972, **56**, 2257; P. C. Hariharan and J. A. Pople, *Mol. Phys.*, 1974, **27**, 209; M. S. Gordon, *Chem. Phys. Lett.*, 1980, **76**, 163.
21. C. Møller and M. S. Plesset, *Phys. Rev.*, 1934, **46**, 618; P. Hohenburg, W. Kohn, *Phys. Rev.*, 1964, **B136**, 864.
22. P. J. Knowles, K. Somasundram, N. C. Handy and K. Hirao, *Chem. Phys. Lett.*, 1993, **211**, 272; W. Kohn and L. J. Sham, *Phys. Rev.*,1965, **A140**, 1133.
23. A. D. McLean and G. S. Chandler, *J. Chem. Phys.*, 1980, **72**, 5639; R. Krishnan, J. S. Binkley, R. Seeger and J. A. Pople, *J. Chem. Phys.*, 1980, **72**, 650.
24. A. D. Becke, *Phys. Rev.*, 1988, **A38**, 3098; A. D. Becke, *J. Chem. Phys.*, 1993, **98**, 5648; J. P. Perdew, *Phys. Rev.*, 1986, **B33**, 8822; L. A. Curtiss, K. Raghavachari, G. W. Trucks and J. A. Pople, *J. Chem. Phys.*, 1991, **94**, 7221.
25. T. H. Dunning Jr. and P. J. Hay, *Modern Theoretical Chemistry*, Vol. 3, Ed. H. F. Schaefer III, Plenum, 1976, p.1; P. J. Hay and W. R. Wadt, *J. Chem. Phys.*, 1985, **82**, pp. 270, 284 and 299.

26. D. J. Watkin, C. K. Prout, J. R. Carruthers, P. W. Betteridge and R. I. Cooper, CRYSTALS issue 11, Chemical Crystallography Lab., University of Oxford.
27. Personal communication from Prof. K. Wade and Dr. M. A. Fox.
28. A. Neu, T. Mennekes, P. Paetzold, U. Englert, M. Hofmann, P. v. R. Schleyer, *Inorg. Chim. Acta*, 1999, **289**, 58.
29. R. A. Jacobson and W. N. Lipscomb, *J. Am. Chem. Soc.*, 1958, **80**, 5571.

# Chapter Six

## The Molecular Structures of Substituted Boranes $B_8X_4H_8$, $B_8X_8H_4$, $B_4X_4H_4$, $B_{10}X_4H_8$, $B_{10}X_8H_4$ and $B_6X_4H_4$ (X = F, Cl, Br and I) studied by Theoretical Calculations

## 6.1. Introduction

Our knowledge of polyboron halides has improved with the discovery of the unique molecular structures of $B_8F_{12}$ (see Chapter 3) and $B_{10}F_{12}$ (see Chapter 5), and subsequent theoretical investigation of their halogen analogues (see Chapters 4 and 5). In order to rationalise these extraordinary structures a theoretical study was instigated on substituted halogenated boranes to determine the ability of hydrogen to replace both bridging and terminal -$BX_2$ groups in the structures discovered in Chapters 3 -5. Work in this chapter has focussed on the study of $B_8X_4H_8$, $B_8X_8H_4$, $B_4X_4H_4$, $B_{10}X_4H_8$, $B_{10}X_8H_4$ and $B_6X_4H_4$ (X = F, Cl, Br and I) through *ab initio* and DFT calculations. Each of these molecules utilises the framework generated from the determination of $B_8F_{12}$ and $B_{10}F_{12}$, replacing bridging and terminal $BX_2$ groups with $BH_2$ or hydrogen substituents.

The diboron tetrahalides $B_2Cl_4$ and $B_2Br_4$ react with common boranes regioselectively to form many examples of halogenated boranes.[1] For example, the propensity for $B_8Cl_8$ to accept hydrogen is utilised in its reaction with excess pentane to form $H_nB_9Cl_{9-n}$ ($n$ = 0 - 5) cluster compounds.[1] Also, when excess of the *nido*-boranes $B_5H_9$ and $B_{10}H_{14}$ reacts with $B_2Cl_4$ and $B_2Br_4$ the compounds $(BCl_2)B_5H_8$, $(BBr_2)B_5H_8$, $(BCl_2)B_{10}H_{13}$ and $(BBr_2)B_{10}H_{13}$ are formed.[2,3] In each of these cases, the presence of the halogen does not alter the boron framework drastically, whether this is the case with the unusual boron frameworks in $B_8F_{12}$ and $B_{10}F_{12}$ will be determined theoretically.

## 6.2. Experimental

### 6.2.1 Theory

All calculations were performed, unless otherwise stated, with Gaussian 98[4] using resources of the EPSRC National Service for Computational Chemistry Software, on a

cluster of 6 HP ES40 computers. Each Alphaserver ES40 machine has four 833 MHz EV68 CPUs and 8 Gbytes of memory. In all cases where X = I, the lanl2dz[5] basis set was used on I above HF/3-21G*. This is implied wherever the 6-31G* or 6-311G* basis sets are referred to for the iodo compounds.

### 6.2.2. *Ab initio* and DFT calculations on $B_8X_8H_4$ (X = F, Cl, Br and I)

Calculations were performed on the system $B_8X_8H_4$ (X = F, Cl, Br and I), with starting geometry $(X_2B)_2B[\mu\text{-}BH_2]_2B(BX_2)_2$. For all cases of X, calculations were performed using HF[6] (3-21G*[7] and 6-31G*[8] basis sets), DFT[9] (6-31G*, 6-311G*[10] basis sets using the B3LYP[9] functional). In addition, for X = F, Cl and Br calculations were performed using the B3LYP functional with the 6-311+G* basis set. For X = F, Cl and I the 6-31G* and 6-311G* basis sets were employed using the MP2[11] method.

### 6.2.3. *Ab initio* and DFT calculations on $B_8X_4H_8$ (X = F, Cl, Br and I)

Calculations were performed on the system $B_8X_4H_8$ (X = F, Cl, Br and I), with starting geometry $(H_2B)_2B[\mu\text{-}BX_2]_2B(BH_2)_2$. For all cases of X, calculations were performed using HF (3-21G* and 6-31G* basis sets) and MP2 (6-31G* and 6-311G* basis sets) methods. Calculations using the B3LYP functional were carried out for X = F, Cl and Br using the 6-31G*, 6-311G* and 6-311+G* basis sets. For X = I, the 6-31G* and 6-311G* basis sets were employed.

### 6.2.4. *Ab initio* and DFT calculations on $B_4X_4H_4$ (X = F, Cl, Br and I)

Two isomers of $B_4X_4H_4$ were considered for each case of X: $X_2B(\mu\text{-}BH_2)_2BX_2$ and $H_2B(\mu\text{-}BX_2)_2BH_2$. The results for the lowest energy isomer are reported in section 6.3.3.

For all cases of X, calculations were performed using HF (3-21G* and 6-31G* basis sets), DFT (6-31G* and 6-311G* basis sets using the B3LYP functional) and MP2 (6-31G* and 6-311G* basis sets) methods. For X = F a further calculation was carried out using the MP2 method with the 6-311+G* basis set. For X = Cl and Br, additional calculations were performed using the B3LYP functional with the 6-311+G* basis set to include diffuse functionality.

### 6.2.5. *Ab initio* and DFT calculations on $B_{10}X_8H_4$ (X = F, Cl, Br and I)

Calculations on the system $B_{10}X_8H_4$ (X = F, Cl, Br and I) were performed with starting geometry $(H_2B)B[\mu\text{-}B(BX_2)_2]_2B(BH_2)$. For X = F, Cl and Br, HF and DFT methods were used with the PQS[12] computer program on a linux cluster. For all cases of X, HF (3-21G* and 6-31G* basis sets), DFT (6-31G* and 6-311G* basis sets) and MP2 (6-31G* basis set) methods were employed. For X = F additional calculations were performed using HF/6-311+G** and MP2/6-311G* methods. For X = Cl further calculations were carried out using HF and MP2 methods using the 6-311G* basis set. For X = Br a further calculation at the HF/6-311G* level was performed. For X = I the 6-311G* basis set was used at the correlated MP2 level.

### 6.2.6. *Ab initio* and DFT calculations on $B_{10}X_4H_8$ (X = F, Cl, Br and I)

The systems $B_{10}X_4H_8$ (X = F, Cl, Br and I) with starting geometry $(X_2B)B[\mu\text{-}B(BH_2)_2]_2B(BX_2)$ have been calculated *ab initio* at different levels. For X = F, Cl and Br, HF and DFT methods were used with the PQS[12] computer program on a linux cluster. For all cases of X, HF (3-21G* and 6-31G* basis sets), DFT (6-31G* and 6-311G* basis sets) and MP2 (6-31G* basis set) methods were employed. For X = F further calculations were performed at the HF level using the 6-311+G** basis set and at the MP2 level using the 6-311G* level. For X = Cl and I calculations were carried out

using HF and MP2 methods with the 6-311G* basis set. A calculation at the HF/6-311G* level was performed for X = Br.

### 6.2.7. *Ab initio* and DFT calculations on $B_6X_4H_4$ (X = F, Cl, Br and I)

Calculations on the system $B_6X_4H_4$ (X = F, Cl, Br and I) were performed with starting geometry $(H_2B)B[\mu\text{-}BX_2]_2B(BH_2)$. For X = F, Cl and Br, HF and DFT methods were used with the PQS[12] computer program on a linux cluster. HF (3-21G* and 6-31G* basis sets), DFT (6-31G* basis set with the B3LYP functional) and MP2 (6-31G* and 6-311G* basis sets) methods were employed for all cases of X. For X = F, the 6-311+G** basis set was utilised using HF and DFT (using the B3LYP functional) methods, whilst for X = Cl, Br and I the 6-311G* basis set was used at these levels of theory.

For sections 6.2.2 – 6.2.7 frequency calculations allowed the nature of any stationary points to be determined, confirming the structures as local minima, transition states or higher order stationary points on the potential-energy surfaces.

## 6.3. Results

For each of the molecules studied in this chapter, no imaginary frequencies were returned, indicating that these structures are minima on their respective potential energy surfaces (see Tables 1 - 24).

### 6.3.1. *Ab initio* and DFT calculations on $B_8X_8H_4$ (X = F, Cl, Br and I)

In $B_8F_8H_4$ the bridging $BF_2$ groups of $B_8F_{12}$ (see Chapter 3) are replaced by bridging $BH_2$ groups to reveal a symmetrically bridged structure with a planar central $B_4$ unit (see

Figure 1). Review of the resultant geometric parameters recorded in Table 1 shows that any symmetry exhibited in the central $B_4$ unit is broken when diffuse functions are employed on the boron and fluorine atoms (B3LYP/6-311+G*). The length of the bonds involved in the central fragment range from 162.8 to 186.8 pm [B(1)-B(2), B(1)-B(4), B(2)-B(3) and B(3)-B(4)] at this level of theory and basis set. This compares to values of 179.0 – 179.4 without the inclusion of diffuse functions using the B3LYP functional (6-311G*) and the value of 180.0 pm at the MP2/6-311G* level. The length of the central B(2)-B(4) core bond is greatest when DFT (using the B3LYP functional) methods are employed with the 6-311+G* basis set. The value of 174.9 pm at this level of theory and basis set is 3.1 and 4.4 pm longer than when the 6-311G* basis set is used at the B3LYP and MP2 methods respectively. With the exception of the B3LYP/6-311+G* structure, all calculations return B-B bond distances for the terminal $BF_2$ groups that are equivalent, i.e. B(2)-B(5) = B(2)-B(6) = B(4)-B(7) = B(4)-B(8). These bonds are less sensitive to the inclusion of electron correlation or a large basis set than the central boron core. For example, the distances obtained with the B3LYP are and MP2 methods using the 6-31G* basis set are 1.3 and 2.0 pm shorter respectively than with HF method. When the size of the basis set is increased to 6-311G* the difference between the B3LYP and MP2 calculated values reduces to 0.2 pm.

**Figure 1**. Molecular framework for $B_8F_8H_4$.

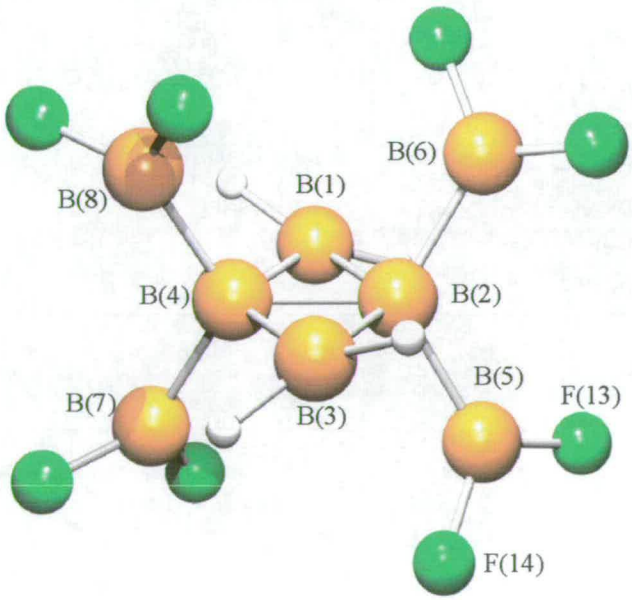

**Table 1**. Selected calculated ($r_e$) bond lengths for $B_8F_8H_4$.[a]

| Geometric parameter | Level of theory / Basis set | | | | | | |
|---|---|---|---|---|---|---|---|
| | HF | | B3LYP | | | MP2 | |
| | 3-21G* | 6-31G* | 6-31G* | 6-311G* | 6-311+G* | 6-31G* | 6-311G* |
| B(1)-B(2) | 186.8 | 186.0 | 179.1 | 179.4 | 186.8 | 179.5 | 180.0 |
| B(1)-B(4) | 186.8 | 186.0 | 179.2 | 179.0 | 162.8 | 179.5 | 180.0 |
| B(2)-B(3) | 186.8 | 186.0 | 179.1 | 179.4 | 182.0 | 179.5 | 180.0 |
| B(2)-B(4) | 173.0 | 172.3 | 171.8 | 171.8 | 174.9 | 169.9 | 170.5 |
| B(2)-B(5) | 168.8 | 172.7 | 171.4 | 171.2 | 173.9 | 170.7 | 171.0 |
| B(2)-B(6) | 168.8 | 172.7 | 171.4 | 171.2 | 170.8 | 170.7 | 171.0 |
| B(3)-B(4) | 186.8 | 186.0 | 179.2 | 179.0 | 174.7 | 179.5 | 180.0 |
| B(4)-B(7) | 168.8 | 172.7 | 171.4 | 171.2 | 172.2 | 170.7 | 171.0 |
| B(4)-B(8) | 168.8 | 172.7 | 171.4 | 171.2 | 168.5 | 170.7 | 171.0 |
| B(5)-F(13) | 133.8 | 131.2 | 132.5 | 132.6 | 132.6 | 133.1 | 132.5 |
| B(5)-F(14) | 136.7 | 132.2 | 133.7 | 133.7 | 133.0 | 134.6 | 133.8 |
| Energy[b] | -990.4154 | -995.7262 | -1000.3664 | -1000.6532 | -1000.6772 | -997.7252 | -998.2778 |

[a] distances in pm.

[b] absolute energy in Hartrees.

In $B_8F_8H_4$ the planes of the $BH_2$ and $BF_2$ groups are significantly twisted with respect to the central $B_4$ unit. This allows intramolecular interactions between the highly electron-deficient bridging boron atoms and the fluorine atoms of the terminal $BF_2$ groups. The bonds to those fluorine atoms involved in such stabilising interactions are inherently longer than those to atoms that take no part. For example, the interaction between B(3) and F(14) results in the lengthening of the B(5)-F(14) bond compared to B(5)-F(13). The difference between these B-F bonds is 1.0, 1.1 and 1.3 pm at the HF/6-31G*, B3LYP/6-311G* and MP2/6-311G* levels respectively.

The structures of $B_8Cl_8H_4$ and $B_8Br_8H_4$ differ significantly from that of $B_8F_8H_4$. Whereas in $B_8F_8H_4$ the central $B_4$ unit is planar, in the chloro and bromo analogues this unit involves a folded asymmetric butterfly with fold angles of 29.1° (for the chloro molecule calculated at the MP2/6-311G* level) and 28.3° (for the bromo molecule calculated at the B3LYP/6-311+G* level) respectively (see Figure 2). Two of the terminal $BX_2$ groups [involving B(5) and B(7)] twist in such a way as to form deltahedra with the central boron framework. Also, two of the hydrogen atoms formerly involved in $BH_2$ bridges twist in order to facilitate B-H-B bridges along the edges of B(1)-B(2) and B(3)-B(7). The resultant parameters for $B_8Cl_8H_4$ and $B_8Br_8H_4$ are shown in Tables 2 and 3.

**Figure 2**. Molecular framework for $B_8X_8H_4$ (X = Cl and Br).

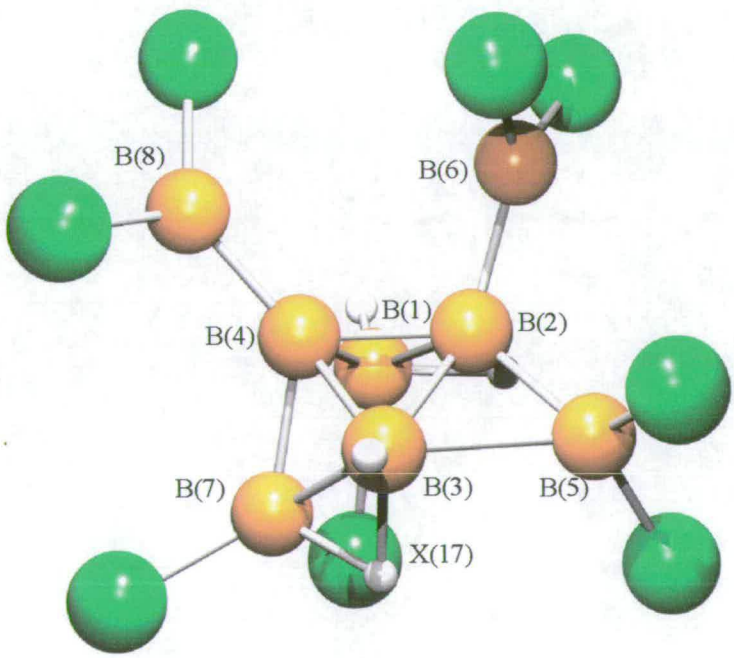

**Table 2.** Selected calculated ($r_e$) bond lengths for $B_8Cl_8H_4$.[a]

| Geometric parameter | Level of theory / Basis set | | | | | | |
|---|---|---|---|---|---|---|---|
| | HF | | B3LYP | | | MP2 | |
| | 3-21G* | 6-31G* | 6-31G* | 6-311G* | 6-311+G* | 6-31G* | 6-311G* |
| B(1)-B(2) | 180.0 | 178.5 | 183.7 | 183.9 | 183.8 | 181.7 | 181.9 |
| B(1)-B(4) | 169.8 | 168.0 | 171.5 | 171.1 | 171.2 | 171.4 | 171.7 |
| B(1)-B(7) | 230.7 | 224.8 | 222.1 | 223.8 | 223.5 | 213.5 | 216.8 |
| B(2)-B(3) | 210.0 | 200.5 | 178.9 | 179.0 | 179.1 | 176.7 | 176.8 |
| B(2)-B(4) | 181.1 | 179.4 | 173.6 | 173.9 | 173.9 | 170.5 | 171.3 |
| B(2)-B(5) | 174.2 | 177.2 | 178.2 | 177.6 | 177.7 | 177.0 | 176.0 |
| B(2)-B(6) | 170.9 | 172.9 | 170.6 | 170.1 | 170.1 | 168.6 | 168.0 |
| B(3)-B(4) | 174.1 | 173.0 | 169.0 | 168.7 | 168.7 | 168.9 | 169.9 |
| B(3)-B(7) | 226.5 | 222.6 | 178.3 | 177.7 | 177.8 | 178.1 | 178.2 |
| B(3)-B(8) | 249.5 | 238.0 | 212.2 | 214.1 | 213.7 | 204.6 | 205.5 |
| B(4)-B(7) | 170.9 | 170.6 | 174.5 | 175.0 | 174.9 | 172.2 | 173.3 |
| B(4)-B(8) | 169.0 | 171.3 | 168.1 | 167.3 | 167.3 | 166.8 | 166.1 |
| B(1)-Cl(17) | 263.4 | 260.5 | 202.1 | 202.3 | 202.5 | 195.5 | 195.7 |
| B(7)-Cl(17) | 180.7 | 180.1 | 197.0 | 196.5 | 196.6 | 193.9 | 193.3 |
| Energy[b] | -3858.0974 | -3875.8910 | -3883.0873 | -3883.3485 | -3883.3595 | -3877.6647 | -3878.0133 |

[a] distances in pm.

[b] absolute energy in Hartrees.

**Table 3**. Selected calculated ($r_e$) bond lengths for $B_8Br_8H_4$.[a]

| Geometric parameter | Level of theory / Basis set | | | | |
|---|---|---|---|---|---|
| | HF | | B3LYP | | |
| | 3-21G* | 6-31G* | 6-31G* | 6-311G* | 6-311+G* |
| B(1)-B(2) | 183.4 | 186.0 | 183.7 | 183.6 | 183.7 |
| B(1)-B(4) | 176.3 | 175.4 | 171.7 | 171.2 | 171.2 |
| B(1)-B(7) | 215.1 | 208.3 | 230.7 | 223.4 | 223.3 |
| B(2)-B(3) | 215.5 | 209.9 | 178.6 | 178.3 | 178.4 |
| B(2)-B(4) | 177.9 | 176.9 | 174.1 | 173.7 | 173.7 |
| B(2)-B(5) | 172.6 | 174.8 | 177.1 | 178.5 | 178.6 |
| B(2)-B(6) | 169.2 | 171.4 | 169.9 | 170.4 | 170.4 |
| B(3)-B(4) | 173.0 | 172.1 | 168.7 | 169.0 | 169.0 |
| B(3)-B(7) | 219.1 | 210.8 | 177.1 | 178.3 | 178.3 |
| B(3)-B(8) | 252.6 | 247.4 | 211.7 | 210.7 | 210.7 |
| B(4)-B(7) | 165.2 | 164.6 | 176.0 | 173.8 | 173.8 |
| B(4)-B(8) | 167.2 | 170.0 | 167.1 | 167.6 | 167.7 |
| B(1)-Br(17) | 221.2 | 222.2 | 216.9 | 219.4 | 219.4 |
| B(7)-Br(17) | 200.4 | 201.9 | 210.8 | 214.5 | 214.5 |
| Energy[b] | -20681.0924 | -20759.1503 | -20775.1548 | -20794.6689 | -20794.6730 |

[a] distances in pm.

[b] absolute energy in Hartrees.

For $B_8Cl_8H_4$ and $B_8Br_8H_4$ the asymmetry in the central boron core is evident at all levels of theory and basis set (see Tables 2 and 3) including those that incorporate correlation and diffuse functions. The core bonds that involve B(4) are shorter than those incorporating B(2), thus suggesting reduced electron deficiency in this region of the molecule. This can be explained by the developing interaction between B(1), X(17) and B(7). For X = Cl, the difference between the lengths of B(7)-Cl(17) and B(1)-Cl(17) is 80.4 pm at the HF/6-31G* level but only 5.9 and 2.4 pm at the B3LYP/6-311+G* and MP2/6-311G* levels respectively. Similarly, for X = Br, the differences are 20.3, 6.1 and 4.9 pm at the HF/6-31G*, B3LYP/6-31G* and B3LYP/6-311+G* levels respectively. In $B_8Cl_8H_4$ the asymmetry exhibited at the MP2/6-311G* level ranges from 169.9 – 181.9 pm in the order B(3)-B(4) [169.9 pm] < B(1)-B(4) [171.7 pm] < B(2)-B(3) [176.8 pm] < B(1)-B(2) [181.9 pm]. Equivalent ordering exists for $B_8Br_8H_4$ with the differences between the lengths of B(3)-B(4) and the other core bonds equalling 2.2, 8.5 and 13.8 pm respectively at the B3LYP/6-311+G* level.

The structure of $B_8I_8H_4$ (see Figure 3) is based upon a boron framework of four triangles incorporating atoms B(1), B(2), B(3), B(4), B(5) and B(7). Involved in this extraordinary structure are bridging $BH_2$ [on atoms B(1) and B(3)] and $BI_2$ groups [on atoms B(5) and B(7)] and terminal $BI_2$ groups [on atoms B(6) and B(8)]. These terminal $BI_2$ groups provide important electron density to atoms B(2) and B(4) which are only directly bonded to boron atoms.

The interaction B(1)...B(5), which leads to the formation of the fourth triangle, is incredibly sensitive to levels of theory. This interaction cannot be critically described as a bond when HF and B3LYP methods are employed, with lengths of 254.7 and 232.3 pm at the HF/6-31G* and B3LYP/6-311G* levels respectively. However, when the MP2 method is used with the 6-311G* basis set, this distance decreases by 19.8 pm compared to the B3LYP/6-311G* calculated value.

**Figure 3**. Molecular framework for $B_8I_8H_4$.

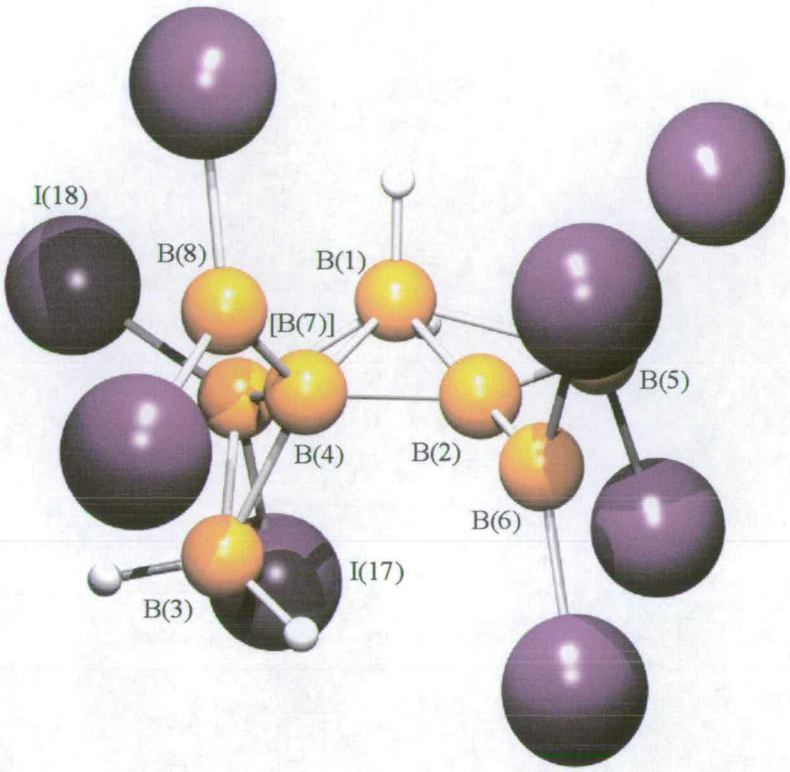


The triangle B(1)-B(2)-B(4) in $B_8I_8H_4$ is asymmetric at all levels of theory and basis set. The level of this asymmetry is dependent upon the inclusion of electron correlation when calculating the structure. When no account of correlation is taken, the bonds involved in this triangle range by 29.9 pm (HF/6-31G*). However, when correlated methods are employed (B3LYP and MP2) with a larger basis set (6-311G*), this range falls to 10.8 and 3.8 pm for the B3LYP and MP2 levels respectively.

The B(7)-I(17) bond is longer than classical B-I bonds which have typical values of c.a. 210 pm.[13] The lengths of B(7)-I(17) and B(7)-I(18) equal 227.3 and 213.6 pm at the MP2/6-311G* level. This suggests reduced electron density formulated in the bond with I(17), which is a direct result of the development of a bridging B(7)-I(17)-B(3) interaction.

**Table 4**. Selected calculated ($r_e$) bond lengths for $B_8I_8H_4$.[a]

| Geometric parameter | Level of theory / Basis set | | | | | |
|---|---|---|---|---|---|---|
| | HF | | B3LYP | | MP2 | |
| | 3-21G* | 6-31G*[b] | 6-31G*[b] | 6-311G*[c] | 6-31G*[b] | 6-311G*[c] |
| B(1)-B(2) | 205.4 | 203.1 | 182.5 | 182.5 | 174.9 | 175.4 |
| B(1)-B(4) | 175.6 | 173.2 | 172.1 | 171.7 | 173.7 | 174.6 |
| B(1)-B(5) | 254.7 | 254.7 | 230.8 | 232.3 | 209.0 | 212.5 |
| B(1)-B(7) | 191.1 | 191.1 | 187.3 | 187.1 | 187.0 | 188.9 |
| B(2)-B(4) | 178.0 | 181.6 | 176.9 | 176.9 | 171.5 | 171.6 |
| B(2)-B(5) | 168.5 | 170.2 | 167.9 | 167.5 | 167.2 | 167.0 |
| B(2)-B(6) | 167.6 | 169.2 | 165.8 | 165.3 | 163.7 | 163.6 |
| B(3)-B(4) | 196.4 | 195.3 | 188.6 | 188.9 | 185.3 | 186.1 |
| B(3)-B(7) | 184.3 | 183.5 | 181.0 | 180.2 | 183.4 | 184.3 |
| B(4)-B(7) | 167.3 | 166.3 | 167.0 | 166.7 | 167.3 | 167.8 |
| B(4)-B(8) | 170.7 | 173.3 | 171.0 | 170.5 | 169.1 | 168.8 |
| B(3)-I(17) | 251.3 | 257.8 | 243.1 | 240.9 | 238.9 | 234.4 |
| B(7)-I(17) | 230.6 | 230.3 | 236.0 | 236.5 | 230.5 | 227.3 |
| Energy[d] | -55302.0474 | -289.1521 | -292.4499 | -292.4860 | -290.2576 | -290.3733 |

[a] distances in pm.

[b] 6-31G*on B and H atoms, lanl2dz on I atoms.

[c] 6-311G*on B and H atoms, lanl2dz on I atoms.

[d] absolute energy in Hartrees.

### 6.3.2. *Ab initio* and DFT calculations on $B_8X_4H_8$ (X = F, Cl, Br and I)

Structural parameters obtained by theoretical calculations on the system $B_8F_4H_8$ are summarised in Table 5. The molecular framework at the MP2 level (see Figure 4) shows a central distorted tetrahedron of boron atoms [B(2), B(4), B(5) and B(6)]. Bridging the edge B(2)-B(4) is a $BH_2$ group whilst along the edges B(4)-B(5) and B(5)-B(6) there are bridging hydrogen atoms. Additional electron density is supplied to the central B(2)-B(4) bond *via* two $BF_2$ substituents on B(2) and a single $BH_2$ on B(4). However at the HF and B3LYP levels of theory the molecule adopts a $(BF_2)_2B[\mu\text{-}BH_2,\mu\text{-}B(BH_2)_2]BH_2$ structure (see Figure 4).

**Figure 4**. Molecular framework for $B_8F_4H_8$ calculated at the (a) HF and B3LYP, (b) MP2 levels.

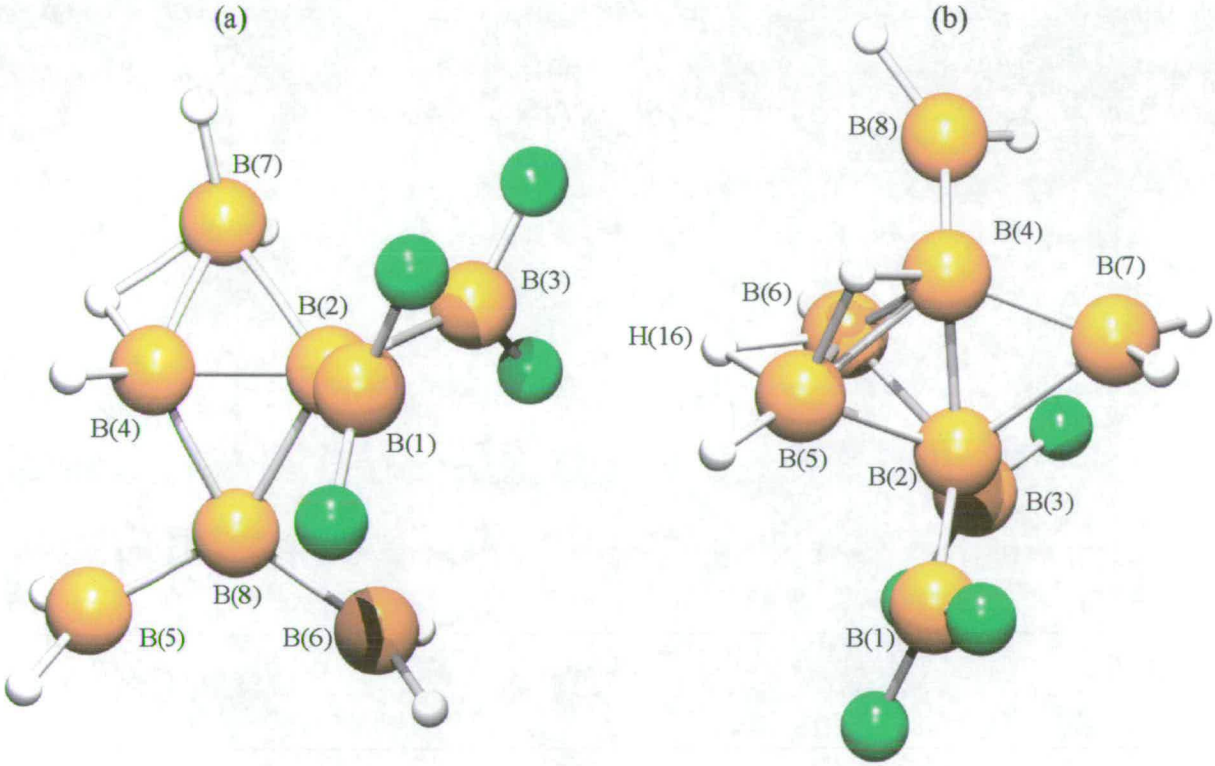

**Table 5**. Selected calculated ($r_e$) bond lengths for $B_8F_4H_8$.[a]

| Geometric parameter | Level of theory / Basis set | | | | | | |
|---|---|---|---|---|---|---|---|
| | HF | | B3LYP | | | MP2 | |
| | 3-21G* | 6-31G* | 6-31G* | 6-311G* | 6-311+G* | 6-31G* | 6-311G* |
| B(1)-B(2) | 168.8 | 171.1 | 170.4 | 169.9 | 169.9 | 169.0 | 169.3 |
| B(2)-B(3) | 168.6 | 171.1 | 169.9 | 169.4 | 169.5 | 171.2 | 171.2 |
| B(2)-B(4) | 175.8 | 184.8 | 173.6 | 174.1 | 174.4 | 169.3 | 170.0 |
| B(2)-B(5) | 180.9 | 195.5 | 187.5 | 188.2 | 188.6 | 173.9 | 174.6 |
| B(2)-B(6) | 175.4 | 167.2 | 167.8 | 167.7 | 167.8 | 172.3 | 173.5 |
| B(2)-B(7) | 270.2 | 262.8 | 237.9 | 245.7 | 252.5 | 190.4 | 191.9 |
| B(4)-B(5) | 322.4 | 289.2 | 274.6 | 274.4 | 274.8 | 175.7 | 176.7 |
| B(4)-B(6) | 179.5 | 177.7 | 172.9 | 172.7 | 172.6 | 171.6 | 172.3 |
| B(4)-B(7) | 166.7 | 165.4 | 161.3 | 160.8 | 160.8 | 170.5 | 170.4 |
| B(4)-B(8) | 167.1 | 165.7 | 161.2 | 161.0 | 161.3 | 165.9 | 166.1 |
| B(5)-B(6) | 199.3 | 174.2 | 176.8 | 176.5 | 176.4 | 171.3 | 172.3 |
| B(5)-H(16) | 243.8 | 138.8 | 137.4 | 137.3 | 137.4 | 131.6 | 132.6 |
| B(6)-H(16) | 119.5 | 127.9 | 129.5 | 129.7 | 129.6 | 133.6 | 134.6 |
| Energy[b] | -596.7791 | -600.0244 | -603.1712 | -603.3285 | -603.3390 | -601.4026 | -601.7114 |

[a] distances in pm.

[b] absolute energy in Hartrees.

Differences between MP2 and HF calculated structures can usually be attributed to electronic correlation. B3LYP, however, also models correlative effects. The vast difference in structure found for $B_8F_4H_8$ using MP2 and B3LYP methodologies must therefore be due to the semi-empirical nature of the functional used in the hybrid-DFT method. The structural differences exhibited are neatly highlighted by the interactions B(4)-B(5) and B(2)-B(7). In the MP2 structure these represent B-B bonds in the central tetrahedron and to the bridging $BH_2$ group respectively. The B(4)-B(5) interaction in the B3LYP structure corresponds to the distance between corners of a butterfly [B(4)-B(2)-B(5)-B(6)] and B(2)-B(7) the distance between a terminal $BH_2$ group and B(2). Accordingly, the B(4)-B(5) distance at the MP2/6-311G* level (176.6 pm) is 98.1 and 112.5 pm shorter than in the B3LYP/6-311+G* and HF/6-31G* calculations respectively. In addition the distance B(2)-B(7) is 60.6 and 70.9 pm longer at the B3LYP/6-311+G* and HF/6-31G* levels respectively compared to MP2/6-311G*.

Interestingly, the shortest B-B bonds in the MP2 structure of $B_8F_4H_8$ are those belonging to the terminal $BH_2$ [B(4)-B(8)] and $BF_2$ [B(1)-B(2)] groups. The use of the larger 6-311G* basis set increases the length of these bonds by only 0.2 and 0.3 pm respectively compared to the 6-31G* basis set. The $\mu$-$BH_2$ group is asymmetric in nature with the interaction toward B(2) 21.5 pm longer than the corresponding B(4)-B(7) distance calculated at the MP2/6-311G* level.

The calculated structures of $B_8Cl_4H_8$ and $B_8Br_4H_8$ (see Figure 5) are very different to that determined for $B_8F_4H_8$. The chloro and bromo analogues contain a distorted square-based pyramid of boron atoms. The apical position of the pyramid is inhabited by a terminal $BX_2$ substituent. Along the edge of the cap is a bridging $BH_2$ group, the plane of which lies perpendicular to the terminal $BX_2$ substituent. Along the pyramidal base lie a bridging halogen and two bridging hydrogens. The basal edge that does not possess a bridging substituent instead connects to a terminal $BH_2$ group. Resultant geometric parameters are summarised in Tables 6 and 7.

**Figure 5**. Molecular framework for $B_8X_4H_8$ (X = Cl and Br).

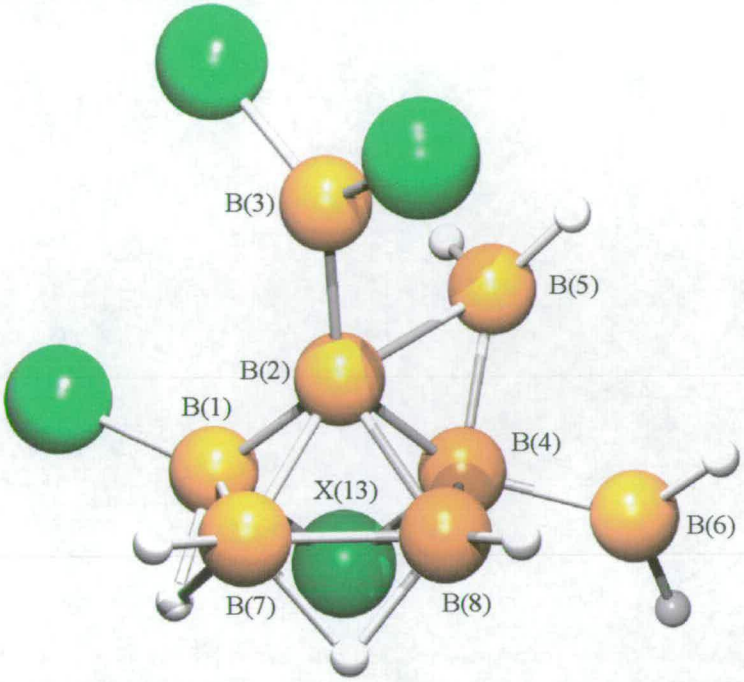


The lengths of the basal B-B bonds of the distorted pyramid in $B_8Cl_4H_8$ range from 171.3 to 229.5 pm at the MP2/6-311G* level, in the sequence B(4)-B(8) < B(7)-B(8) < B(1)-B(7) << B(1)-B(4). For $B_8Br_4H_8$ such bonds range from 171.3 to 235.0 pm at the MP2/6-311G* level in the same sequence. This arrangement is also determined using the 6-31G* at the MP2 level, and using the B3LYP method with 6-31G*, 6-311G* and 6-311+G* basis sets. The presence of the bulky $BX_2$ group forces asymmetry in the bridging interaction between B(2)-B(5)-B(4). For example, at the MP2/6-311G* level, the difference between distances B(2)-B(5) and B(4)-B(5) is 32.9 pm for the chloro analogue and 33.5 pm for the bromo such that B(2)-B(5), which lies closest to the $BX_2$ substituent, is longer.

**Table 6**. Selected calculated ($r_e$) bond lengths for $B_8Cl_4H_8$.[a]

| Geometric parameter | Level of theory / Basis set | | | | | | |
|---|---|---|---|---|---|---|---|
| | HF | | B3LYP | | | MP2 | |
| | 3-21G* | 6-31G* | 6-31G* | 6-311G* | 6-311+G* | 6-31G* | 6-311G* |
| B(1)-B(2) | 171.0 | 172.3 | 183.1 | 182.9 | 183.0 | 175.0 | 175.3 |
| B(1)-B(4) | 276.2 | 281.7 | 273.5 | 273.5 | 274.0 | 228.7 | 229.5 |
| B(1)-B(7) | 264.8 | 264.8 | 184.7 | 184.3 | 184.3 | 179.2 | 179.6 |
| B(2)-B(3) | 169.1 | 171.4 | 168.3 | 167.6 | 167.6 | 168.5 | 168.1 |
| B(2)-B(4) | 182.7 | 183.4 | 169.3 | 169.3 | 169.3 | 170.2 | 170.8 |
| B(2)-B(5) | 274.7 | 281.5 | 279.0 | 277.6 | 277.3 | 203.9 | 200.6 |
| B(2)-B(7) | 205.4 | 203.8 | 177.6 | 177.5 | 177.6 | 172.2 | 172.8 |
| B(2)-B(8) | 170.5 | 169.6 | 171.0 | 170.7 | 170.7 | 174.7 | 175.8 |
| B(4)-B(5) | 165.9 | 166.9 | 163.5 | 163.0 | 163.0 | 166.7 | 167.7 |
| B(4)-B(6) | 166.5 | 167.6 | 164.7 | 164.3 | 164.3 | 164.0 | 164.2 |
| B(4)-B(8) | 176.0 | 176.3 | 169.5 | 169.4 | 169.4 | 171.1 | 171.3 |
| B(6)-B(8) | 246.9 | 243.8 | 216.4 | 217.1 | 217.2 | 220.3 | 223.8 |
| B(7)-B(8) | 172.3 | 170.8 | 174.4 | 174.3 | 174.3 | 175.5 | 177.1 |
| B(1)-Cl(13) | 178.1 | 177.8 | 183.2 | 183.1 | 183.1 | 194.3 | 194.3 |
| B(4)-Cl(13) | 312.8 | 323.1 | 305.4 | 304.3 | 305.4 | 191.4 | 190.7 |
| Energy[b] | -2030.6265 | -2040.1051 | -2044.5101 | -2044.6550 | -2044.6605 | -2041.3244 | -2041.5330 |

[a] distances in pm.

[b] absolute energy in Hartrees.

**Table 7**. Selected calculated ($r_e$) bond lengths for $B_8Br_4H_8$.[a]

| Geometric parameter | Level of theory / Basis set | | | | | | |
|---|---|---|---|---|---|---|---|
| | HF | | B3LYP | | | MP2 | |
| | 3-21G* | 6-31G* | 6-31G* | 6-311G* | 6-311+G* | 6-31G* | 6-311G* |
| B(1)-B(2) | 170.7 | 171.5 | 176.2 | 176.1 | 176.1 | 175.5 | 175.5 |
| B(1)-B(4) | 264.7 | 278.2 | 250.8 | 249.5 | 249.4 | 238.9 | 235.0 |
| B(1)-B(7) | 279.4 | 264.2 | 180.0 | 180.9 | 180.9 | 178.8 | 180.2 |
| B(2)-B(3) | 167.9 | 170.6 | 166.6 | 166.9 | 167.0 | 168.5 | 168.5 |
| B(2)-B(4) | 175.6 | 183.2 | 175.5 | 174.7 | 174.6 | 170.6 | 171.3 |
| B(2)-B(5) | 276.2 | 281.8 | 276.9 | 275.8 | 275.8 | 198.0 | 201.3 |
| B(2)-B(7) | 192.6 | 202.5 | 175.9 | 176.4 | 176.4 | 171.6 | 172.9 |
| B(2)-B(8) | 175.0 | 169.2 | 169.6 | 170.4 | 170.4 | 174.6 | 176.9 |
| B(4)-B(5) | 167.0 | 167.5 | 167.2 | 166.3 | 166.3 | 168.0 | 167.8 |
| B(4)-B(6) | 167.4 | 167.8 | 168.6 | 168.3 | 168.3 | 164.1 | 164.6 |
| B(4)-B(8) | 180.9 | 176.9 | 173.2 | 172.4 | 172.4 | 171.0 | 171.3 |
| B(6)-B(8) | 237.3 | 244.7 | 209.1 | 208.2 | 208.2 | 226.5 | 222.2 |
| B(7)-B(8) | 187.5 | 170.8 | 174.7 | 174.1 | 174.0 | 175.5 | 176.1 |
| B(1)-Br(13) | 190.8 | 193.3 | 208.1 | 209.8 | 209.7 | 210.2 | 211.1 |
| B(4)-Br(13) | 332.9 | 324.2 | 227.1 | 231.7 | 232.2 | 207.7 | 205.9 |
| Energy[b] | -10442.1167 | -10481.7313 | -10490.5440 | -10500.3164 | -10500.3187 | -10482.8842 | -10492.9042 |

[a] distances in pm.

[b] absolute energy in Hartrees.

Like the chloro and bromo members of the family $B_8X_4H_8$, $B_8I_4H_8$ contains a distorted square-based pyramid of boron atoms (see Figure 6). Along the four basal edges of this pyramid lie a bridging iodine, two bridging hydrogens and a bridging $BI_2$ substituent which has a relatively wide fold angle of 6.2° (i.e. the fold of the butterfly wings) at the MP2/6-311G* level (with lanl2dz on the I atoms). This $\mu$-$BI_2$ substituent itself has a bridging $BH_2$ group along its B(1)-B(4) edge and one of the iodine atoms lies close to B(8). The fold angle made by these coupled deltahedra is narrower with a value of 16.3° at the MP2/6-311G* level (with lanl2dz on the I atoms). Connected to the B(2) corner of the pyramid lies a terminal $BH_2$ substituent. The terminal I atom on the apical position of the pyramid lies 42.1° away from parallel to the terminal $BH_2$ (at the MP2/6-311G* level using the lanl2dz basis set for the I atoms). The geometric parameters determined for $B_8I_4H_8$ are summarised in Table 8.

**Figure 6**. Molecular framework for $B_8I_4H_8$.

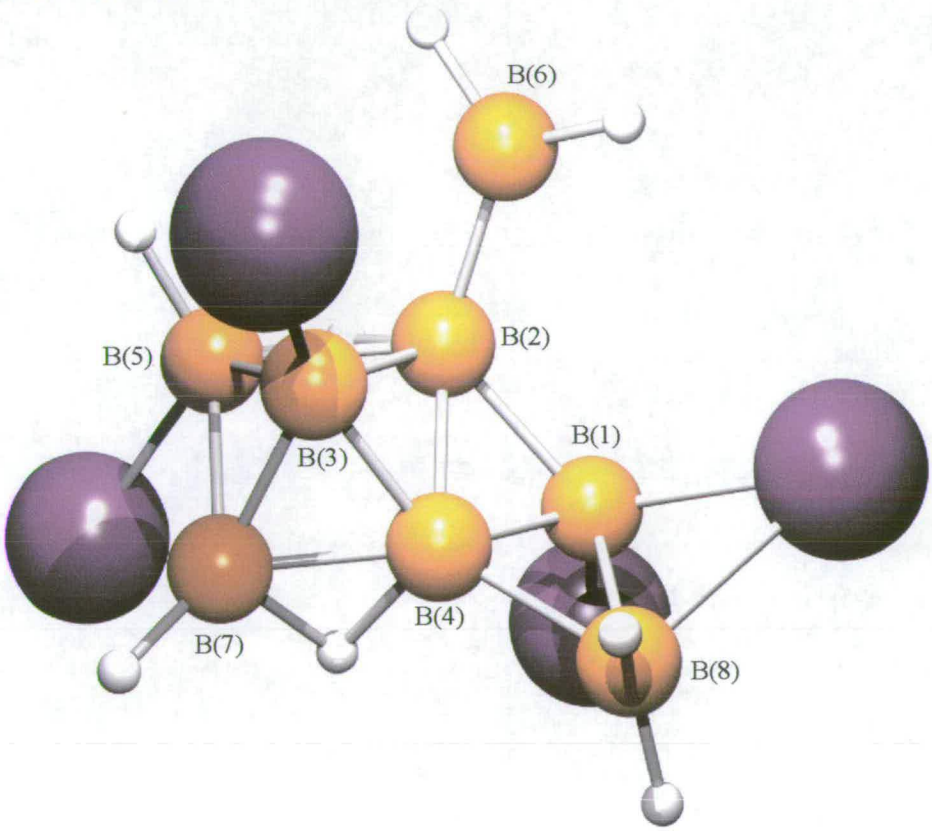

**Table 8**. Selected calculated ($r_e$) bond lengths for $B_8I_4H_8$.[a]

| Geometric parameter | Level of theory / Basis set | | | | | |
|---|---|---|---|---|---|---|
| | HF | | B3LYP | | MP2 | |
| | 3-21G* | 6-31G*[b] | 6-31G*[b] | 6-311G*[c] | 6-31G*[b] | 6-311G*[c] |
| B(1)-B(2) | 171.2 | 173.5 | 182.6 | 183.1 | 180.0 | 180.2 |
| B(1)-B(4) | 283.5 | 285.2 | 169.8 | 169.4 | 168.9 | 169.7 |
| B(1)-B(8) | 315.0 | 318.3 | 199.5 | 198.4 | 195.0 | 195.7 |
| B(2)-B(3) | 173.9 | 173.3 | 173.5 | 173.6 | 172.7 | 173.9 |
| B(2)-B(4) | 184.0 | 182.9 | 175.6 | 175.5 | 174.4 | 175.5 |
| B(2)-B(5) | 207.0 | 201.3 | 190.4 | 190.8 | 187.1 | 188.6 |
| B(2)-B(6) | 170.9 | 172.8 | 167.6 | 166.8 | 167.5 | 167.0 |
| B(3)-B(4) | 175.1 | 175.9 | 168.1 | 168.1 | 167.0 | 168.0 |
| B(3)-B(5) | 180.6 | 181.0 | 179.0 | 179.4 | 177.4 | 179.2 |
| B(3)-B(7) | 261.8 | 266.1 | 164.9 | 164.7 | 166.1 | 167.2 |
| B(4)-B(7) | 167.3 | 168.6 | 173.9 | 173.8 | 173.0 | 173.7 |
| B(4)-B(8) | 166.7 | 168.2 | 179.1 | 178.9 | 178.6 | 178.6 |
| B(5)-B(7) | 422.1 | 432.4 | 195.7 | 195.4 | 192.3 | 191.7 |
| Energy[d] | -27752.5811 | -246.7055 | -249.1922 | -249.2234 | -247.6324 | -247.7254 |

[a] distances in pm.
[b] 6-31G* on B, H atoms; lanl2dz on I atoms.
[c] 6-311G* on B, H atoms; lanl2dz on I atoms.
[d] absolute energy in Hartrees.

The base of the boron pyramid in $B_8I_4H_8$ is distorted to afford a bridging B-I-B across the B(5)-B(7) edge. The result is this B-B bond is longer than the other basal bonds. For example, such bonds, at the MP2/6-311G* level (with lanl2dz on the I atoms), range from 173.7 to 191.7 pm in the sequence B(4)-B(7) [173.7 pm] < B(2)-B(4) [175.5 pm] << B(2)-B(5) [188.6 pm] < B(5)-B(7) [191.7].

### 6.3.3. *Ab initio* and DFT calculations on $B_4X_4H_4$ (X = F, Cl, Br and I)

$B_4F_4H_4$ exists as a weakly bound $H_2BBF_2$ dimer at all levels of theory and basis set (see Figure 7 and Table 9). At the MP2/6-311+G* level the monomers are positioned 9.9° away from a parallel arrangement. The $BH_2$ groups lie only slightly away from a perpendicular configuration to the $BF_2$ substituents. This is to facilitate a B...F interaction between the monomeric species. Such an interaction has a distance of 224.5 pm at the MP2/6-311+G* level, and the bonded B-F distance involved is lengthened in comparison to the B-F that is not. For example, for the fluorines attached to B(2), the B-F that forms part of the B-F...B interaction is 2.8 pm longer than its adjacent B-F bond.

**Figure 7**. Molecular framework for $B_4F_4H_4$.

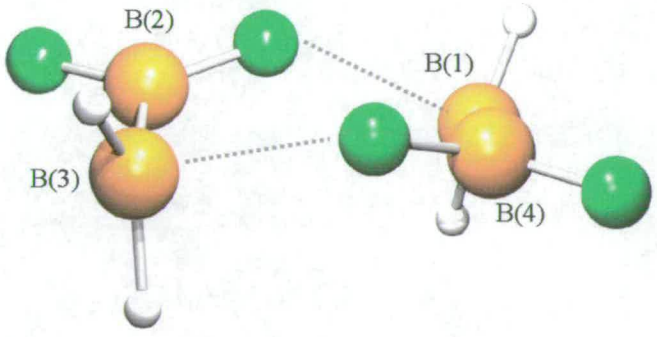

**Table 9**. Selected calculated ($r_e$) bond lengths for $B_4F_4H_4$.[a]

| Geometric parameter | Level of theory / Basis set | | | | | | |
|---|---|---|---|---|---|---|---|
| | HF | | B3LYP | | MP2 | | |
| | 3-21G* | 6-31G* | 6-31G* | 6-311G* | 6-31G* | 6-311G* | 6-311+G* |
| B(1)-B(2) | 296.4 | 372.6 | 300.8 | 328.6 | 300.0 | 317.7 | 330.3 |
| B(1)-B(4) | 168.0 | 170.8 | 168.5 | 167.9 | 169.2 | 169.4 | 169.5 |
| B(2)-B(3) | 168.0 | 170.8 | 168.5 | 167.9 | 169.2 | 169.4 | 169.5 |
| B(2)-B(4) | 321.4 | 382.8 | 328.1 | 348.6 | 328.8 | 343.0 | 351.6 |
| B(3)-B(4) | 296.5 | 327.3 | 300.8 | 328.6 | 300.0 | 317.8 | 330.4 |
| Energy[b] | -496.3528 | -499.0097 | -501.3497 | -501.4912 | -499.9843 | -500.2547 | -500.2728 |

[a] distances in pm.

[b] absolute energy in Hartrees.

The shortest separation distances between monomers in $B_4F_4H_4$ [B(1)-B(2) and B(3)-B(4)] occur when smaller basis sets are employed. These distances increase by 76.2 pm when the size of the basis set is increased from 3-21G* to 6-31G* at the HF level of theory. When the size of the basis set is increased from 6-31G* to 6-311G* using the correlated B3LYP and MP2 methods, these distances increase by 28.6 and 17.7 pm respectively. The inclusion of diffuse functions, which is important when modelling dimeric or weakly bound species, at the MP2 level, increases this distance by a further 12.6 pm compared to the 6-311G* basis set.

The structures of $B_4Cl_4H_4$ and $B_4Br_4H_4$ are essentially the same as each other (see Figure 8) with the resultant geometric parameters summarised in Tables 10 and 11. Each molecule retains the central folded butterfly of boron atoms (with fold angles of 14.6° and 12.7° for X = Cl and Br respectively at the MP2/6-311G* level) but there is significant twisting of the planes of the $BH_2$ groups with respect to the butterfly. The $B_4$ butterfly possesses $BH_2$ wing tips with terminal and bridging X atoms on the centre borons. It can be considered as like $B_4H_{10}$ without two bridging hydrogens. The reason for such a structure could be the intramolecular interactions that exist between the highly electron-deficient bridging boron atoms and halogens. This is evident in the accommodating twisting of the halogens as they utilise their $\pi$-donating ability to form bridging interactions along the edges B(1)-B(2) and B(3)-B(4) of the central butterfly.

**Figure 8**. Molecular framework for $B_4X_4H_4$ (X = Cl and Br).

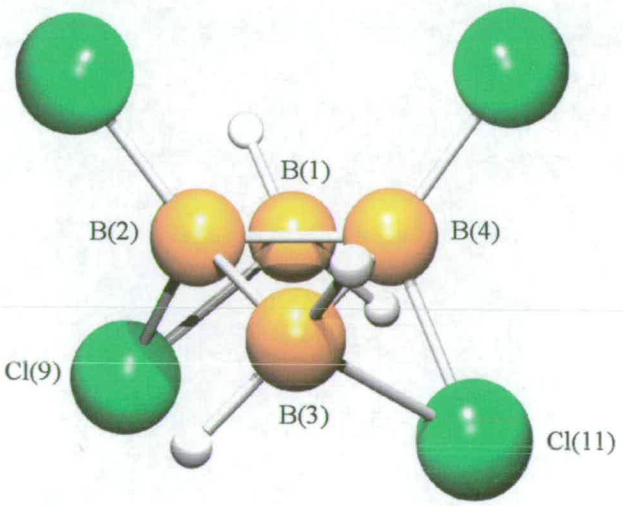

**Table 10**. Selected calculated ($r_e$) bond lengths for $B_4Cl_4H_4$.[a]

| Geometric parameter | Level of theory / Basis set | | | | | | |
|---|---|---|---|---|---|---|---|
| | HF | | B3LYP | | | MP2 | |
| | 3-21G* | 6-31G* | 6-31G* | 6-311G* | 6-311+G* | 6-31G* | 6-311G* |
| B(1)-B(2) | 188.6 | 188.9 | 185.6 | 185.5 | 185.5 | 183.9 | 185.0 |
| B(1)-B(4) | 191.1 | 189.4 | 186.0 | 185.6 | 185.6 | 185.1 | 185.0 |
| B(2)-B(3) | 188.5 | 189.4 | 186.0 | 185.6 | 185.6 | 185.1 | 185.0 |
| B(2)-B(4) | 169.0 | 168.8 | 167.1 | 166.8 | 166.8 | 166.2 | 166.8 |
| B(3)-B(4) | 191.2 | 188.9 | 185.6 | 185.5 | 185.5 | 183.9 | 185.0 |
| B(1)-Cl(9) | 256.1 | 259.4 | 205.5 | 205.7 | 206.1 | 198.6 | 200.0 |
| B(2)-Cl(9) | 182.2 | 181.4 | 189.6 | 189.6 | 189.6 | 186.4 | 186.3 |
| B(3)-Cl(11) | 261.9 | 259.3 | 205.5 | 205.7 | 206.1 | 198.6 | 200.0 |
| B(4)-Cl(11) | 181.5 | 181.4 | 189.6 | 189.6 | 189.6 | 186.4 | 186.3 |
| Energy[b] | -1930.1412 | -1939.0565 | -1942.7055 | -1942.8368 | -1942.8417 | -1939.9534 | -1940.1296 |

[a] distances in pm.

[b] absolute energy in Hartrees.

**Table 11**. Selected calculated ($r_e$) bond lengths for $B_4Br_4H_4$.[a]

| Geometric parameter | Level of theory / Basis set | | | | | | |
|---|---|---|---|---|---|---|---|
| | HF | | B3LYP | | | MP2 | |
| | 3-21G* | 6-31G* | 6-31G* | 6-311G* | 6-311+G* | 6-31G* | 6-311G* |
| B(1)-B(2) | 187.8 | 186.9 | 184.3 | 183.5 | 183.5 | 183.9 | 184.0 |
| B(1)-B(4) | 190.8 | 191.1 | 186.0 | 185.8 | 185.8 | 185.6 | 185.6 |
| B(2)-B(3) | 190.7 | 191.0 | 186.0 | 185.8 | 185.8 | 185.6 | 185.6 |
| B(2)-B(4) | 166.8 | 165.6 | 166.2 | 166.8 | 166.8 | 165.7 | 167.0 |
| B(3)-B(4) | 187.9 | 186.9 | 184.3 | 183.5 | 183.5 | 183.9 | 184.0 |
| B(1)-Br(9) | 223.6 | 230.5 | 221.0 | 223.8 | 224.1 | 216.9 | 217.2 |
| B(2)-Br(9) | 200.9 | 201.0 | 204.4 | 206.1 | 206.0 | 202.4 | 202.8 |
| B(3)-Br(11) | 223.8 | 230.5 | 221.0 | 223.8 | 224.1 | 216.9 | 217.2 |
| B(4)-Br(11) | 200.8 | 201.0 | 204.4 | 206.1 | 206.0 | 202.4 | 202.8 |
| Energy[b] | -10341.6521 | -10380.6991 | -10388.7498 | -10398.5070 | -10398.5089 | -10381.5195 | -10391.5081 |

[a] distances in pm.

[b] absolute energy in Hartrees.

The electron deficiency evident in the bridging $BH_2$ groups of $B_4Cl_4H_4$ and $B_4Br_4H_4$ is shown by the B-B bond distances involved in these bridge formations compared to the central B(2)-B(4) bond. For example, at the MP2/6-311G* level, the B(2)-B(4) bonds are 18.2 and 17.0 pm shorter than B(1)-B(2) for $B_4Cl_4H_4$ and $B_4Br_4H_4$ respectively. B-B bond distances are relatively insensitive to increases in the size of the basis set. For example, increasing the basis set from 6-31G* to 6-311+G* (at the B3LYP level) decreases B(1)-B(2) by 0.1 and 0.8 pm for $B_4Cl_4H_4$ and $B_4Br_4H_4$ respectively. The B(2)-B(4) central bond length decreases by 0.3 pm for X = Cl and increases by 0.6 pm for X = Br when the size of the basis set is increased from 6-31G* to 6-311+G* at the B3LYP level. Comparison of the correlated methods using the 6-311G* basis set shows that the differences between B3LYP and MP2 calculated values for B(1)-B(2) and B(2)-B(4) distances are 0.5 and 0.0 pm respectively in $B_4Cl_4H_4$. For X = Br, the differences are 0.5 and 0.2 pm for the equivalent bonds.

$B_4I_4H_4$ subsists as a diborane-type derivative, bonding as $(I_2B)B(H)[\mu\text{-}H]_2B(H)(BI_2)$ [see Figure 9]. The terminal $BI_2$ substituents lie in an anti-periplanar arrangement across the central B(2)-B(4) bond, with a B(1)-B(4)-B(2) angle of 123.4° at the MP2/6-311G* level (using the lanl2dz basis set on the I atoms). In addition to this $\sigma$ bond the two boron atoms are joined to symmetric bridging hydrogens by three-centre, two-electron bonds.

The core region of $B_4I_4H_4$ shows the greatest degree of electron deficiency since the B(2)-B(4) bond is longer than B(1)-B(4) and B(2)-B(3) at all levels of theory and basis set used (see Table 12). B(1)-B(4) is 6.9, 9.2 and 7.1 pm shorter than B(2)-B(4) at the HF/6-31G*, B3LYP/6-311G* and MP2/6-311G* levels respectively (using the lanl2dz basis set on the I atoms). Using the 6-31G* basis set for the B and H atoms and the lanl2dz basis set on the I atoms, B(2)-B(4) at the MP2 level is 2.4 and 2.1 pm shorter than the HF and B3LYP values respectively.

**Figure 9**. Molecular framework for $B_4I_4H_4$.

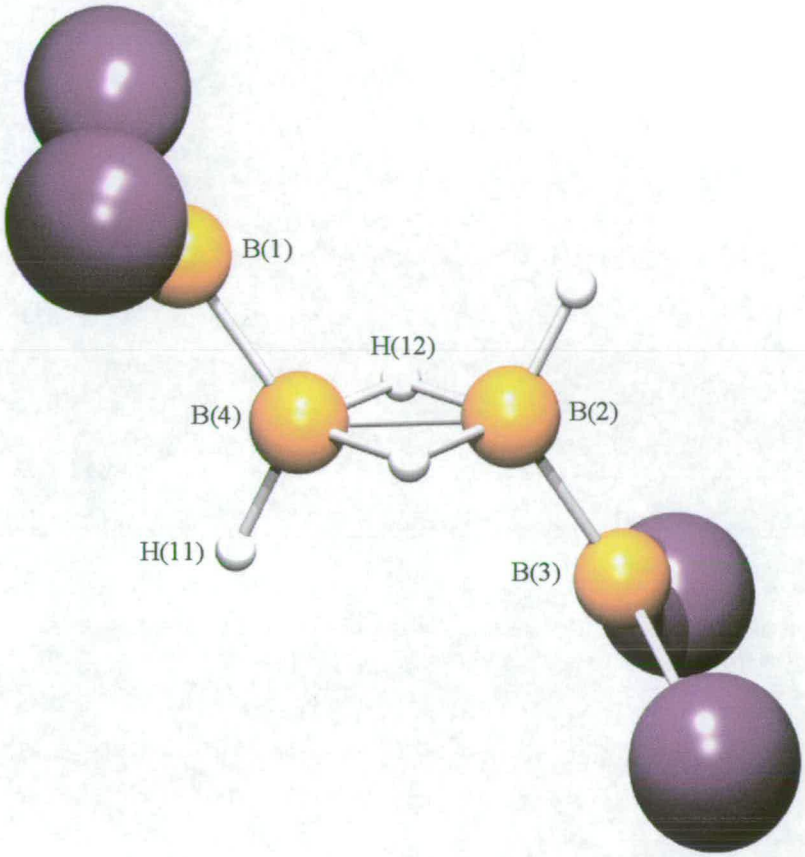

**Table 12**. Selected calculated ($r_e$) bond lengths for $B_4I_4H_4$.[a]

| Geometric parameter | Level of theory / Basis set | | | | | |
|---|---|---|---|---|---|---|
| | HF | | B3LYP | | MP2 | |
| | 3-21G* | 6-31G*[b] | 6-31G*[b] | 6-311G*[c] | 6-31G*[b] | 6-311G*[c] |
| B(1)-B(4) | 168.6 | 170.4 | 168.6 | 167.7 | 168.8 | 168.5 |
| B(2)-B(4) | 178.4 | 177.3 | 177.0 | 176.9 | 174.9 | 175.6 |
| B(2)-B(3) | 168.6 | 170.4 | 168.6 | 167.7 | 168.8 | 168.5 |
| B(2)-H(12) | 131.6 | 131.6 | 132.0 | 132.1 | 131.4 | 132.3 |
| B(4)-H(11) | 118.6 | 118.7 | 119.6 | 119.4 | 119.7 | 119.9 |
| B(4)-H(12) | 131.6 | 131.6 | 132.0 | 132.1 | 131.4 | 132.3 |
| Energy[d] | -27652.1781 | -145.7540 | -147.4314 | -147.4505 | -146.2694 | -146.3259 |

[a] distances in pm.
[b] 6-31G* on B, H atoms; lanl2dz on I atoms.
[c] 6-311G* on B, H atoms; lanl2dz on I atoms.
[d] absolute energy in Hartrees.

### 6.3.4. *Ab initio* and DFT calculations on $B_{10}X_8H_4$ (X = F, Cl, Br and I)

When HF methods are employed, $B_{10}F_8H_4$ bonds as $(BH_2)B[\mu\text{-}B(BF_2)_2]_2B(BH_2)$, similar to $B_{10}F_{12}$ (see Chapter 5, Figure 2). Central to this motif is an incredibly short B-B bond that is only 158.1 pm long when the 6-311+G** basis set is used. This bond forms the backbone of a folded butterfly with fold angle 34.4°. However, when the correleted B3LYP and MP2 methods are used, this structural motif is radically transformed into an incredible sheet of six conjoined boron triangles (see Figure 10). At the MP2/6-311G* level these deltahedra possess fold angles of 6.7° [B(1)-B(2)-B(6)-B(4) and B(3)-B(7)-B(9)-B(10)], 4.2° [B(2)-B(7)-B(3)-B(9) and B(6)-B(2)-B(4)-B(7)] and 13.9° [B(4)-B(2)-B(7)-B(3)]. Atoms B(2) and B(7) are not directly bonded to anything other than boron atoms, but they are involved in interactions with bridging $BF_2$ and $BH_2$ substituents. For a summary of the resulting geometric parameters see Table 13.

**Figure 10**. Molecular framework for $B_{10}F_8H_4$.

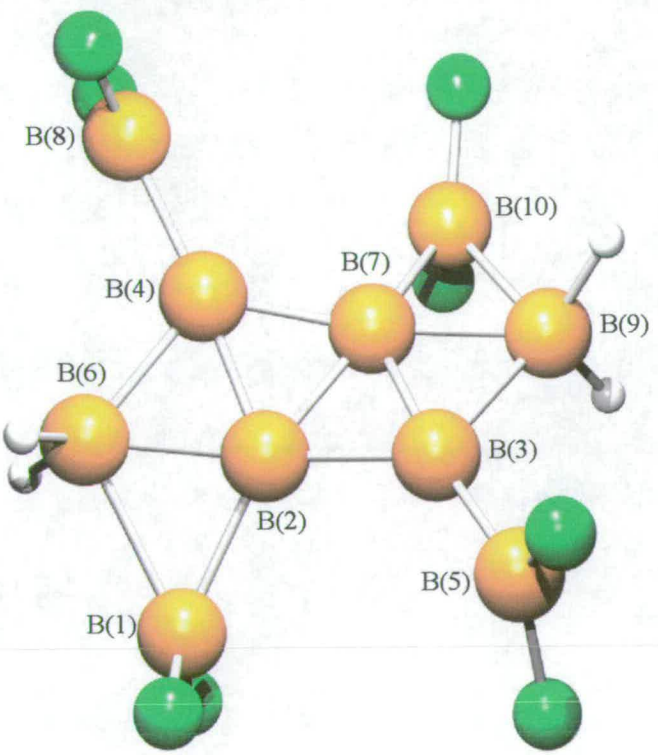

**Table 13**. Calculated ($r_e$) B-B bond lengths for $B_{10}F_8H_4$.[a]

| Geometric parameter | Level of theory / Basis set | | | | | | |
|---|---|---|---|---|---|---|---|
| | HF | | | B3LYP | | MP2 | |
| | 3-21G* | 6-31G* | 6-311+G** | 6-31G* | 6-311G* | 6-31G* | 6-311G* |
| B(1)-B(2) | 167.3 | 169.3 | 168.9 | 179.2 | 179.1 | 179.5 | 179.7 |
| B(1)-B(6) | 286.3 | 299.0 | 301.8 | 200.1 | 200.2 | 197.4 | 198.8 |
| B(2)-B(3) | 174.4 | 172.0 | 172.5 | 164.9 | 164.2 | 165.1 | 165.0 |
| B(2)-B(4) | 174.4 | 172.0 | 172.5 | 161.8 | 161.8 | 161.4 | 162.3 |
| B(2)-B(6) | 304.8 | 308.1 | 308.8 | 171.0 | 170.7 | 169.8 | 170.2 |
| B(2)-B(7) | 275.0 | 256.6 | 258.9 | 164.4 | 165.2 | 163.9 | 166.1 |
| B(3)-B(4) | 157.4 | 158.0 | 158.1 | 272.0 | 269.8 | 275.1 | 273.9 |
| B(3)-B(5) | 249.6 | 251.3 | 252.8 | 166.9 | 166.1 | 167.2 | 167.0 |
| B(3)-B(7) | 174.4 | 172.0 | 172.5 | 161.8 | 161.7 | 161.5 | 162.3 |
| B(3)-B(9) | 170.5 | 171.5 | 171.1 | 175.1 | 174.8 | 175.8 | 176.5 |
| B(4)-B(6) | 170.5 | 171.5 | 171.1 | 175.1 | 174.7 | 175.8 | 176.5 |
| B(4)-B(7) | 174.4 | 172.0 | 172.5 | 165.0 | 164.3 | 165.1 | 165.0 |
| B(4)-B(8) | 249.6 | 251.3 | 252.8 | 166.9 | 166.1 | 167.2 | 167.0 |
| B(7)-B(9) | 304.8 | 308.1 | 308.7 | 171.0 | 170.9 | 169.7 | 170.2 |
| B(7)-B(10) | 167.3 | 169.3 | 168.9 | 179.0 | 178.8 | 179.6 | 179.7 |
| B(9)-B(10) | 286.3 | 299.0 | 301.5 | 200.5 | 201.0 | 197.3 | 198.8 |
| Energy[b] | -1039.4562 | -1045.0686 | -1045.3393 | -1050.1028 | -1050.3955 | -1047.2842 | -1047.8471 |

[a] distances in pm.

[b] absolute energy in Hartrees.

$B_{10}F_8H_4$ contains a two-fold axis of symmetry with the origin at the mid-point of B(2)-B(7). It possesses two bridging $BF_2$, two bridging $BH_2$ and two terminal $BF_2$ substituents. These terminal $BF_2$ groups lie 7.6° away from a linear configuration to their adjacent B-B bonds at the MP2/6-311G* level. B-B bond lengths (see Table 13) are dependent on the type of interaction involved. At the MP2 and B3LYP levels, there exists a sequence of increasing B-B bond length from core B-B [B(2)-B(3), B(2)-B(4), B(2)-B(7), B(3)-B(7) and B(4)-B(7)] < B-$BF_2$ (terminal) [B(3)-B(5) and B(4)-B(8)] < B-$BH_2$ (bridging) [B(2)-B(6), B(3)-B(9), B(4)-B(6) and B(7)-B(9)] < B-$BF_2$ (bridging) [B(1)-B(2), B(1)-B(6), B(7)-B(10) and B(9)-B(10)]. These bonds range from 162.3 [B(2)-B(4)] to 198.8 pm [B(1)-B(6)] at the MP2/6-311G* level. Table 13 shows that there is negligible difference between the B3LYP and MP2 structures, or the 6-31G* and 6-311G* basis sets at these levels.

The structures of $B_{10}X_8H_4$ (X = Cl, Br and I) at the MP2 level are very similar to that found for $B_{10}F_8H_4$ except that the bridging $BX_2$ and $BH_2$ substituents have exchanged positions (see Figure 11). The boron sheets in $B_{10}X_8H_4$ (X = Cl, Br and I) are less planar than in $B_{10}F_8H_4$. For example, the fold angles involved in the B(2)-B(3)-B(5)-B(9) triangles are 15.2° (for X = Cl at the MP2/6-311G* level), 15.1° (for X = Br at the MP2/6-31G* level) and 14.8° (for X = I at the MP2 level using the 6-311G* basis set on the B and H atoms, and lanl2dz on the I atoms). The equivalent triangles in $B_{10}F_8H_4$ contain a fold angle of only 6.7°. The primary reason for the narrow fold angles in $B_{10}X_8H_4$ (X = Cl, Br and I) is that it allows the accommodation of a B...X interaction between the boron on bridging $BH_2$ groups to a halogen on the bridging $BX_2$ group. There is twisting of said bridging $BH_2$ substituent to facilitate such an interaction. The structural motif of $B_{10}X_8H_4$ at the HF level is also found for X = Cl, Br and I using the HF method and for X = Cl using the B3LYP functional. Selected bond distances for these systems are listed in Tables 14 - 16.

**Figure 11**. Molecular framework for $B_{10}X_8H_4$ (X = Cl, Br and I).

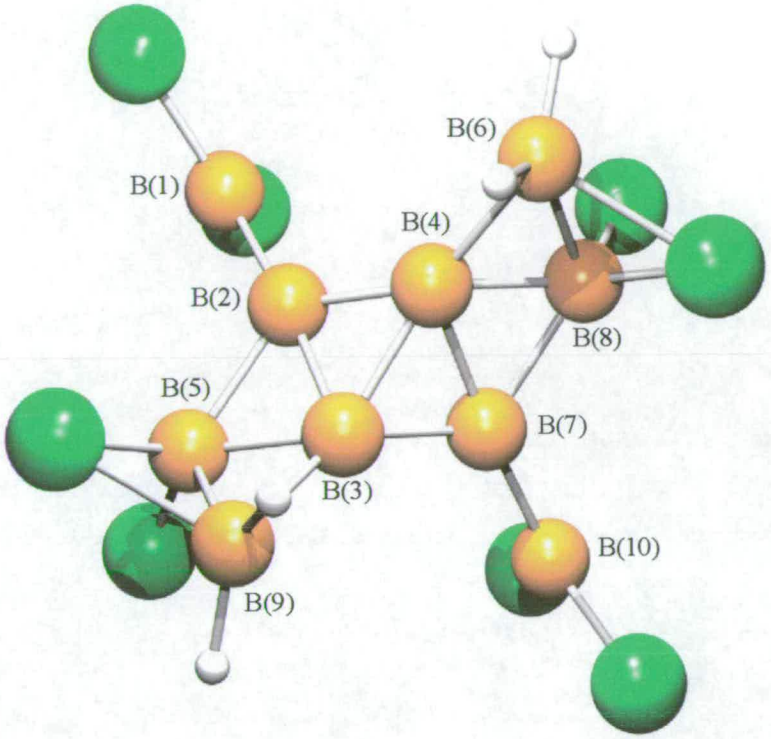


Geometry changes for X = Cl are found as a result of the inclusion of electron correlation when the B3LYP functional is used in place of HF methods (see Table 14). Comparison of the B-B bond distances determined using the 6-311G* basis set at these levels shows that they are all shorter at the B3LYP level with the exception of B(3)-B(4) – the spinal bond of the butterfly. This bond actually increases by 6.2 pm when the B3LYP level is used instead of HF methods, and increases by a further 5.7 pm when the MP2 method is utilised using the 6-311G* basis set. B(1)-B(2), B(2)-B(3), B(3)-B(5), B(3)-B(9) and B(5)-B(9) are 2.3, 5.8, 14.1, 2.4 and 9.8 pm shorter at the B3LYP level compared to the HF calculation using the 6-311G* basis set. The $B(5)F_2$ and $B(8)F_2$ groups twist from their positions in the HF and B3LYP calculated structures to form closer interactions with $B(9)H_2$ and $B(6)H_2$ respectively at the MP2 level. The bonds B(5)-B(9) and B(6)-B(8) shorten from 294.2 and 294.1 pm at the B3LYP/6-311G* level to 194.2 and 194.2 pm respectively at the MP2/6-311G* level. This MP2 value reflects

the bridging involvement of these bonds with the said $BH_2$ groups. The bonds B(3)-B(9) and B(4)-B(6) lengthen by 10.7 pm when comparing the B3LYP and MP2 levels, using the 6-311G* basis set, as their function alters from being terminal to bridging $BH_2$ groups.

For X = Br, the inclusion of electron correlation when calculating structural properties results in the structure changing from the butterfly motif discussed at the beginning of section 6.3.4 (and found for $B_{10}F_{12}$ in Chapter 5, Figure 2) to that seen in Figure 11. As a result there are significant differences in B-B bond distances when the HF structures are compared to B3LYP and MP2 (see Table 15). For example, B(3)-B(4) is 156.1 pm at the HF/6-311G* level, but is 6.9 and 11.9 pm longer at the B3LYP/6-311G* and MP2/6-31G* levels respectively. B(3)-B(5) is 90.5 and 91.1 pm shorter at the B3LYP/6-311G* and MP2/6-31G* levels respectively compared to the HF/6-311G* value. Also, B(5)-B(9) at the HF/6-311G* level is 112.1 and 110.0 pm longer than when the B3LYP/6-311G* and MP2/6-31G* calculations are employed respectively.

The structure determination of $B_{10}I_8H_4$ using theoretical calculations shows that correlated methods (B3LYP and MP2) give the structure shown in Figure 11, whilst non-correlated methods (HF) give the butterfly structure discussed in section 6.3.4. Table 16 shows that the B(3)-B(4) distance is 155.8 pm at the HF/6-31G* level (with lanl2dz on the I atoms), but is 6.1 and 10.1 pm longer at the B3LYP and MP2 levels respectively using the 6-311G* basis set on the B and H atoms and the lanl2dz on the I atoms. B(3)-B(5) is 91.0 and 90.2 pm shorter at the B3LYP and MP2 levels respectively, using the 6-311G* basis set on the B and H atoms and the lanl2dz on the I atoms, compared to the HF/6-31G* value (with lanl2dz on the I atoms). In addition to this, B(5)-B(9) at the HF/6-31G* level (with lanl2dz on the I atoms) is 115.1 and 113.0 pm longer than when the B3LYP/6-311G* and MP2/6-31G* calculations are employed respectively.

**Table 14**. Calculated ($r_e$) B-B bond lengths for $B_{10}Cl_8H_4$.[a]

| Geometric parameter | Level of theory / Basis set | | | | | | |
|---|---|---|---|---|---|---|---|
| | HF | | | B3LYP | | MP2 | |
| | 3-21G* | 6-31G* | 6-311G* | 6-31G* | 6-311G* | 6-31G* | 6-311G* |
| B(1)-B(2) | 166.9 | 168.5 | 168.2 | 166.2 | 165.9 | 165.1 | 164.8 |
| B(2)-B(3) | 177.2 | 174.4 | 174.5 | 168.8 | 168.7 | 164.1 | 164.4 |
| B(2)-B(4) | 177.2 | 174.4 | 174.5 | 168.8 | 168.7 | 164.0 | 164.5 |
| B(2)-B(5) | 166.9 | 168.5 | 168.2 | 166.2 | 165.9 | 175.6 | 175.5 |
| B(3)-B(4) | 156.6 | 156.5 | 156.6 | 163.1 | 162.8 | 166.6 | 168.5 |
| B(3)-B(5) | 257.7 | 256.9 | 257.2 | 242.4 | 243.1 | 167.1 | 168.1 |
| B(3)-B(7) | 177.2 | 174.4 | 174.5 | 168.8 | 168.7 | 164.0 | 164.5 |
| B(3)-B(9) | 170.2 | 171.9 | 171.4 | 169.8 | 169.0 | 180.4 | 179.7 |
| B(4)-B(6) | 170.2 | 171.9 | 171.4 | 169.8 | 169.0 | 180.4 | 179.7 |
| B(4)-B(7) | 177.2 | 174.4 | 174.5 | 168.8 | 168.7 | 164.1 | 164.4 |
| B(4)-B(8) | 257.7 | 256.9 | 257.2 | 242.3 | 243.1 | 167.1 | 168.1 |
| B(5)-B(9) | 302.6 | 303.6 | 303.9 | 293.2 | 294.2 | 192.0 | 194.2 |
| B(6)-B(8) | 302.6 | 303.6 | 303.9 | 293.1 | 294.1 | 192.0 | 194.2 |
| B(7)-B(8) | 166.9 | 168.5 | 168.2 | 166.2 | 165.9 | 175.6 | 175.5 |
| B(7)-B(10) | 166.9 | 168.5 | 168.2 | 166.2 | 165.9 | 165.1 | 164.8 |
| Energy[b] | -3907.1679 | -3925.2443 | -3925.4838 | -3932.7502 | -3933.0196 | -3927.1641 | -3927.5231 |

[a] distances in pm.

[b] absolute energy in Hartrees.

**Table 15**. Calculated ($r_e$) B-B bond lengths for $B_{10}Br_8H_4$.[a]

| Geometric parameter | Level of theory / Basis set | | | | | |
|---|---|---|---|---|---|---|
| | HF | | | B3LYP | | MP2 |
| | 3-21G* | 6-31G* | 6-311G* | 6-31G* | 6-311G* | 6-31G* |
| B(1)-B(2) | 165.2 | 167.2 | 168.0 | 164.0 | 164.2 | 164.1 |
| B(2)-B(3) | 175.5 | 174.2 | 175.6 | 164.7 | 165.3 | 163.3 |
| B(2)-B(4) | 175.5 | 174.2 | 175.6 | 165.4 | 165.4 | 164.0 |
| B(2)-B(5) | 165.2 | 167.2 | 168.0 | 174.9 | 176.1 | 174.8 |
| B(3)-B(4) | 157.1 | 156.7 | 156.1 | 163.6 | 163.0 | 168.0 |
| B(3)-B(5) | 251.7 | 254.2 | 257.7 | 167.4 | 167.2 | 166.6 |
| B(3)-B(7) | 175.5 | 174.2 | 175.6 | 165.4 | 165.5 | 164.0 |
| B(3)-B(9) | 170.4 | 172.2 | 171.6 | 181.6 | 182.2 | 180.3 |
| B(4)-B(6) | 170.4 | 172.2 | 171.6 | 181.5 | 182.2 | 180.3 |
| B(4)-B(7) | 175.5 | 174.2 | 175.6 | 164.7 | 165.3 | 163.3 |
| B(4)-B(8) | 251.7 | 254.2 | 257.7 | 167.5 | 167.2 | 166.6 |
| B(5)-B(9) | 297.4 | 301.2 | 302.5 | 192.2 | 190.4 | 192.5 |
| B(6)-B(8) | 297.4 | 301.2 | 302.5 | 192.3 | 190.4 | 192.6 |
| B(7)-B(8) | 165.2 | 167.2 | 168.0 | 174.8 | 176.1 | 174.8 |
| B(7)-B(10) | 165.2 | 167.2 | 168.0 | 164.0 | 164.2 | 164.1 |
| Energy[b] | -20730.1627 | -20808.5048 | -20828.3344 | -20824.8497 | -20844.3781 | -20810.2912 |

[a] distances in pm.

[b] absolute energy in Hartrees.

**Table 16**. Calculated ($r_e$) B-B bond lengths for $B_{10}I_8H_4$.[a]

| Geometric parameter | Level of theory / Basis set | | | | | |
|---|---|---|---|---|---|---|
| | HF | | B3LYP | | MP2 | |
| | 3-21G* | 6-31G*[b] | 6-31G*[b] | 6-311G*[c] | 6-31G*[b] | 6-311G*[c] |
| B(1)-B(2) | 166.0 | 167.8 | 164.4 | 163.7 | 163.4 | 163.0 |
| B(2)-B(3) | 178.4 | 176.5 | 165.6 | 165.4 | 164.6 | 165.3 |
| B(2)-B(4) | 178.4 | 176.6 | 166.9 | 166.4 | 165.6 | 165.8 |
| B(2)-B(5) | 166.0 | 167.8 | 175.9 | 175.6 | 173.8 | 174.3 |
| B(3)-B(4) | 156.1 | 155.8 | 162.1 | 161.9 | 164.4 | 165.9 |
| B(3)-B(5) | 257.2 | 257.9 | 167.0 | 166.9 | 166.8 | 167.7 |
| B(3)-B(7) | 178.4 | 176.5 | 166.9 | 166.4 | 165.6 | 165.8 |
| B(3)-B(9) | 170.7 | 172.5 | 182.6 | 182.5 | 180.5 | 180.5 |
| B(4)-B(6) | 170.7 | 172.4 | 182.6 | 182.5 | 180.5 | 180.5 |
| B(4)-B(7) | 178.4 | 176.6 | 165.6 | 165.4 | 164.6 | 165.3 |
| B(4)-B(8) | 257.2 | 258.0 | 167.0 | 166.9 | 166.8 | 167.7 |
| B(5)-B(9) | 302.0 | 301.3 | 186.8 | 186.2 | 187.3 | 188.3 |
| B(6)-B(8) | 302.0 | 301.4 | 186.8 | 186.2 | 187.3 | 188.3 |
| B(7)-B(8) | 166.0 | 167.8 | 175.9 | 175.6 | 173.7 | 174.3 |
| B(7)-B(10) | 166.0 | 167.8 | 164.4 | 163.7 | 163.4 | 163.0 |
| Energy[d] | -55351.1257 | -338.5093 | -342.1746 | -342.2182 | -339.8084 | -339.9359 |

[a] distances in pm.
[b] 6-31G* on B, H atoms; lanl2dz on I atoms.
[c] 6-311G* on B, H atoms; lanl2dz on I atoms.
[d] absolute energy in Hartrees.

### 6.3.5. *Ab initio* and DFT calculations on $B_{10}X_4H_8$ (X = F, Cl, Br and I)

Calculations on $B_{10}X_4H_8$ (X = F, Cl, Br and I) using the correlated B3LYP and MP2 methodologies give structures as illustrated in Figure 12. Hence, we can see that $B_{10}X_8H_4$ (see section 6.3.4) and $B_{10}X_4H_8$ (X = F, Cl, Br and I) share a common structural pattern with six conjoined boron deltahedra possessing four bridging $BY_2$ groups and two terminal $BY_2$ substituents (where Y is a halogen or hydrogen). For each case of X, HF methods fail to model this motif, thus emphasising the importance of correlation in determining the structures of substituted boron halides by theoretical methods. B-B bond distances for $B_{10}X_4H_8$ (X = F, Cl, Br and I) are recorded in Tables 17 – 20.

**Figure 12**. Molecular framework for $B_{10}X_4H_8$ (X = F, Cl, Br and I).

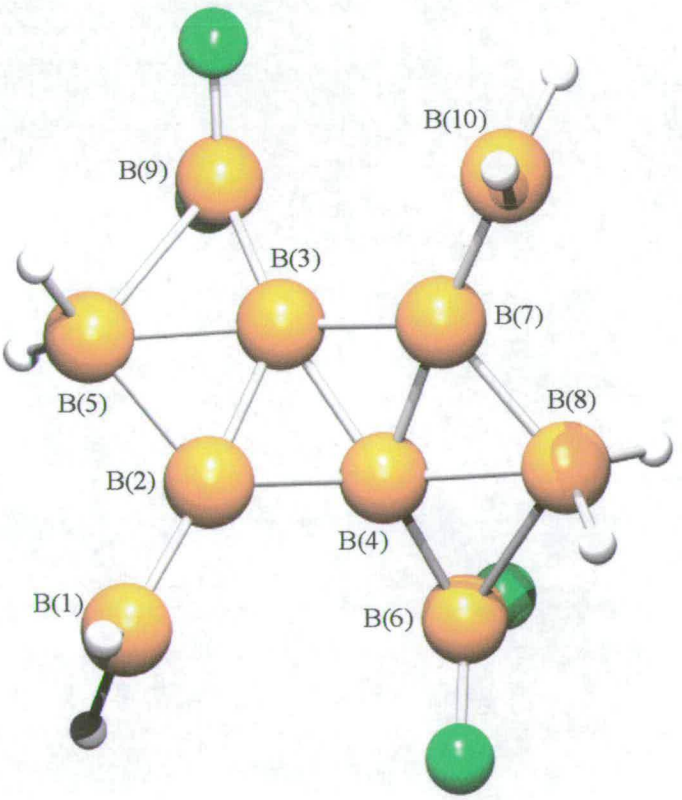

**Table 17**. Calculated ($r_e$) B-B bond lengths for $B_{10}F_4H_8$.[a]

| Geometric parameter | Level of theory / Basis set | | | | | | |
|---|---|---|---|---|---|---|---|
| | HF | | | B3LYP | | MP2 | |
| | 3-21G* | 6-31G* | 6-311+G** | 6-31G* | 6-311G* | 6-31G* | 6-311G* |
| B(1)-B(2) | 165.3 | 165.7 | 165.4 | 162.4 | 161.8 | 163.6 | 163.4 |
| B(2)-B(3) | 175.2 | 170.8 | 170.8 | 163.2 | 163.1 | 162.5 | 163.2 |
| B(2)-B(4) | 175.2 | 170.8 | 170.8 | 166.1 | 165.9 | 165.2 | 165.7 |
| B(2)-B(5) | 165.3 | 165.9 | 165.8 | 172.9 | 171.6 | 174.9 | 174.7 |
| B(3)-B(4) | 155.9 | 160.7 | 161.0 | 165.9 | 166.9 | 164.9 | 167.9 |
| B(3)-B(5) | 249.8 | 237.4 | 238.4 | 175.4 | 177.3 | 171.2 | 173.5 |
| B(3)-B(7) | 175.2 | 170.8 | 170.8 | 166.1 | 165.9 | 165.2 | 165.7 |
| B(3)-B(9) | 167.3 | 170.3 | 169.6 | 174.7 | 172.8 | 177.5 | 175.5 |
| B(4)-B(6) | 167.3 | 170.3 | 169.6 | 174.7 | 172.8 | 177.4 | 175.5 |
| B(4)-B(7) | 175.2 | 170.7 | 170.8 | 163.2 | 163.1 | 162.5 | 163.2 |
| B(4)-B(8) | 249.7 | 236.9 | 238.3 | 175.4 | 177.3 | 171.2 | 173.5 |
| B(5)-B(9) | 293.6 | 304.0 | 306.6 | 214.0 | 221.0 | 201.4 | 209.5 |
| B(6)-B(8) | 293.5 | 303.3 | 306.5 | 214.0 | 221.0 | 201.6 | 209.5 |
| B(7)-B(8) | 165.3 | 165.9 | 165.8 | 172.9 | 171.6 | 174.9 | 174.7 |
| B(7)-B(10) | 165.3 | 165.3 | 165.4 | 162.4 | 161.8 | 163.6 | 163.4 |
| Energy[b] | -645.8509 | -649.3717 | -649.5320 | -652.8621 | -653.0268 | -650.8784 | -651.1963 |

[a] distances in pm.

[b] absolute energy in Hartrees.

**Table 18**. Calculated ($r_e$) B-B bond lengths for $B_{10}Cl_4H_8$.[a]

| Geometric parameter | Level of theory / Basis set | | | | | | |
|---|---|---|---|---|---|---|---|
| | HF | | | B3LYP | | MP2 | |
| | 3-21G* | 6-31G* | 6-311G* | 6-31G* | 6-311G* | 6-31G* | 6-311G* |
| B(1)-B(2) | 164.9 | 165.7 | 165.5 | 162.6 | 161.9 | 163.6 | 163.4 |
| B(2)-B(3) | 171.7 | 168.6 | 168.9 | 163.8 | 163.7 | 162.9 | 163.4 |
| B(2)-B(4) | 171.7 | 168.7 | 169.0 | 165.9 | 165.7 | 165.1 | 165.7 |
| B(2)-B(5) | 164.9 | 165.7 | 165.5 | 171.1 | 170.6 | 174.8 | 174.8 |
| B(3)-B(4) | 159.5 | 160.9 | 160.9 | 170.3 | 170.3 | 166.6 | 168.8 |
| B(3)-B(5) | 244.0 | 241.9 | 242.7 | 179.9 | 180.3 | 171.3 | 173.3 |
| B(3)-B(7) | 175.5 | 172.1 | 172.2 | 165.9 | 165.8 | 165.1 | 165.7 |
| B(3)-B(9) | 167.6 | 170.3 | 169.8 | 171.4 | 170.6 | 174.9 | 172.8 |
| B(4)-B(6) | 167.6 | 170.3 | 169.8 | 171.4 | 170.7 | 174.9 | 172.8 |
| B(4)-B(7) | 175.5 | 172.1 | 172.2 | 163.7 | 163.7 | 162.9 | 163.4 |
| B(4)-B(8) | 260.6 | 257.5 | 257.9 | 179.9 | 180.2 | 171.3 | 173.3 |
| B(5)-B(9) | 306.3 | 303.0 | 303.3 | 230.1 | 232.5 | 204.4 | 211.7 |
| B(6)-B(8) | 331.9 | 328.4 | 329.1 | 230.2 | 232.4 | 204.3 | 211.7 |
| B(7)-B(8) | 165.6 | 166.4 | 166.1 | 171.2 | 170.6 | 174.7 | 174.8 |
| B(7)-B(10) | 165.5 | 166.4 | 166.1 | 162.6 | 161.9 | 163.6 | 163.4 |
| Energy[b] | -2079.6952 | -2089.4521 | -2089.5881 | -2094.2048 | -2094.3571 | -2090.8196 | -2091.0329 |

[a] distances in pm.

[b] absolute energy in Hartrees.

**Table 19**. Calculated ($r_e$) B-B bond lengths for $B_{10}Br_4H_8$.[a]

| Geometric parameter | Level of theory / Basis set | | | | | |
|---|---|---|---|---|---|---|
| | HF | | | B3LYP | | MP2 |
| | 3-21G* | 6-31G* | 6-311G* | 6-31G* | 6-311G* | 6-31G* |
| B(1)-B(2) | 165.9 | 166.2 | 165.4 | 162.4 | 161.9 | 164.0 |
| B(2)-B(3) | 175.7 | 170.0 | 169.3 | 163.8 | 163.8 | 167.3 |
| B(2)-B(4) | 173.0 | 170.1 | 169.5 | 166.3 | 165.9 | 166.8 |
| B(2)-B(5) | 165.2 | 166.5 | 166.8 | 172.0 | 170.2 | 172.2 |
| B(3)-B(4) | 158.1 | 160.9 | 163.1 | 168.1 | 171.1 | 161.6 |
| B(3)-B(5) | 237.8 | 228.2 | 223.8 | 177.9 | 181.2 | 167.3 |
| B(3)-B(7) | 173.1 | 170.0 | 169.5 | 166.3 | 165.8 | 166.8 |
| B(3)-B(9) | 166.8 | 169.7 | 169.7 | 170.4 | 170.1 | 181.6 |
| B(4)-B(6) | 166.8 | 169.7 | 169.7 | 170.4 | 170.1 | 181.6 |
| B(4)-B(7) | 175.7 | 170.0 | 169.3 | 163.8 | 163.8 | 167.3 |
| B(4)-B(8) | 237.9 | 228.2 | 223.8 | 177.9 | 181.2 | 167.3 |
| B(5)-B(9) | 289.4 | 283.3 | 286.7 | 225.0 | 233.7 | 176.6 |
| B(6)-B(8) | 289.4 | 283.3 | 286.7 | 225.0 | 233.8 | 176.6 |
| B(7)-B(8) | 165.2 | 166.6 | 166.8 | 172.0 | 170.3 | 172.2 |
| B(7)-B(10) | 165.9 | 166.2 | 165.4 | 162.4 | 162.0 | 164.0 |
| Energy[b] | -10491.1898 | -10531.0781 | -10541.0137 | -10540.2330 | -10550.0172 | -10532.3836 |

[a] distances in pm.

[b] absolute energy in Hartrees.

**Table 20**. Calculated ($r_e$) B-B bond lengths for $B_{10}I_4H_8$.[a]

| Geometric parameter | Level of theory / Basis set | | | | | | |
|---|---|---|---|---|---|---|---|
| | HF | | | B3LYP | | MP2 | |
| | 3-21G* | 6-31G*[b] | 6-311G*[c] | 6-31G*[b] | 6-311G*[c] | 6-31G*[b] | 6-311G*[c] |
| B(1)-B(2) | 164.9 | 165.9 | 165.5 | 162.8 | 162.1 | 164.1 | 163.8 |
| B(2)-B(3) | 173.0 | 168.7 | 168.9 | 164.1 | 164.0 | 167.8 | 168.4 |
| B(2)-B(4) | 172.0 | 168.9 | 169.1 | 166.2 | 165.9 | 167.0 | 167.5 |
| B(2)-B(5) | 165.9 | 167.4 | 167.1 | 170.9 | 170.2 | 171.9 | 172.6 |
| B(3)-B(4) | 161.0 | 164.1 | 164.1 | 171.6 | 171.8 | 163.6 | 164.6 |
| B(3)-B(5) | 229.7 | 218.8 | 220.5 | 180.6 | 181.2 | 168.0 | 168.6 |
| B(3)-B(7) | 172.0 | 168.9 | 169.1 | 166.2 | 165.9 | 167.0 | 167.5 |
| B(3)-B(9) | 167.4 | 169.8 | 169.6 | 170.3 | 169.8 | 180.7 | 181.2 |
| B(4)-B(6) | 167.4 | 169.8 | 169.6 | 170.3 | 169.8 | 180.7 | 181.2 |
| B(4)-B(7) | 173.0 | 168.7 | 168.9 | 164.1 | 164.0 | 167.8 | 168.4 |
| B(4)-B(8) | 229.7 | 218.8 | 220.5 | 180.6 | 181.2 | 168.0 | 168.6 |
| B(5)-B(9) | 288.3 | 281.9 | 283.1 | 229.8 | 232.4 | 175.4 | 176.7 |
| B(6)-B(8) | 288.3 | 281.9 | 283.1 | 229.8 | 232.4 | 175.4 | 176.7 |
| B(7)-B(8) | 165.9 | 167.4 | 167.1 | 170.9 | 170.2 | 171.9 | 172.6 |
| B(7)-B(10) | 164.9 | 165.9 | 165.5 | 162.8 | 162.1 | 164.1 | 163.8 |
| Energy[d] | -27801.6686 | -296.0810 | -296.1269 | -298.8904 | -298.9321 | -297.1380 | -297.2389 |

[a] distances in pm.

[b] 6-31G* on B, H atoms; lanl2dz on I atoms.

[c] 6-311G* on B, H atoms; lanl2dz on I atoms.

[d] absolute energy in Hartrees.

Focussing on the central B(3)-B(4) bond, for each case of X in $B_{10}X_4H_8$ we can see that, at the MP2/6-31G* level (using the lanl2dz basis set on I atoms), this bond length increases in the sequence Br < I (+2.0 pm) < F (+1.3 pm) < Cl (+1.7 pm). In other words, there is more electron density in this bond when the bulkier Br and I halogens occupy bridging positions compared to the smaller F and Cl substituents. However, analysis of the B(2)-B(4) bond at the same level shows an opposing trend. The chloro analogue has B(2)-B(4) 0.1, 1.7 and 1.9 pm shorter than the fluoro, bromo and iodo compounds respectively.

Comparison of the bridging $BX_2$ interactions for X = F, Cl, Br and I shows that there is greater symmetry in the bromo and iodo compounds than in their fluoro and chloro analogues. Examination of B(5)-B(9) and B(3)-B(9) distances at the MP2/6-31G* level (using the lanl2dz basis set on I atoms), shows that the differences between them are 32.0, 36.8, 5.0 and 5.3 pm for X = F, Cl, Br and I respectively. For X = F and Cl, B(5)-B(9) is greater than B(3)-B(9), but for X = Br and I, the opposite is true.

### 6.3.6. *Ab initio* and DFT calculations on $B_6X_4H_4$ (X = F, Cl, Br and I)

Calculations on $B_6X_4H_4$ (X = F, Cl, Br and I) show a symmetrically bridged structure with a planar central $B_4$ unit (see Figure 13). The bridging $BH_2$ groups are twisted resulting in shortened X...H interactions. For example, at the MP2/6-311G* level of theory, X...H distances of 265.5, 298.2 and 309.1 pm are calculated for X = F, Cl and Br respectively. For X = F, Cl and Br the terminal B-B bonds lie in a linear arrangement with respect to the central boron core. B-B-X angles for X = Br equal the classic $sp^2$ hybrid angle of 120.0°, whilst angles of 121.5° and 120.3° prevail for the fluoro and chloro analogues respectively at the MP2/6-311G* level of theory.

**Figure 13**. Molecular framework for $B_6X_4H_4$ (X = F, Cl and Br).

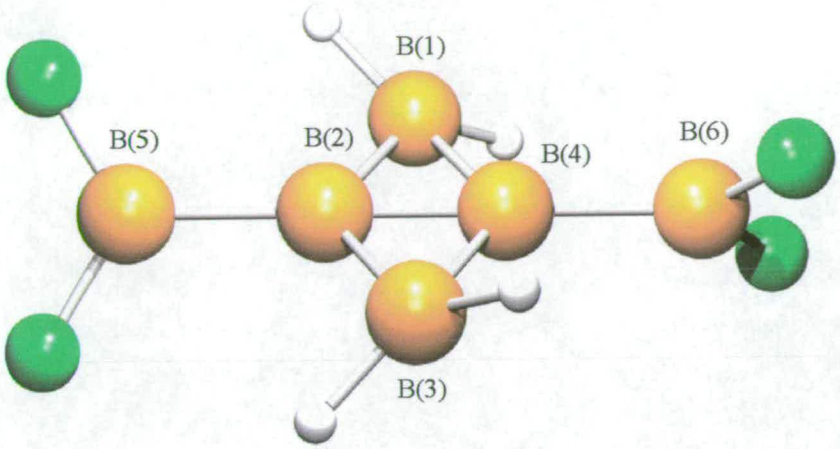


Review of Tables 21 - 23 shows that the B-B bonds in $B_6X_4H_4$ (X = F, Cl and Br) are sensitive to the level of theory and basis set used. For X = F (see Table 21), the bridging B-B bonds [B(1)-B(2), B(1)-B(4), B(2)-B(3) and B(3)-B(4)] are 4.5 and 2.6 pm longer at the HF/6-311+G** level than the B3LYP/6-311+G** and MP2/6-311G* levels respectively. Differences for X = Cl (see Table 22) equate to 4.1 and 2.7 pm, and for X = Br (see Table 23) equal 4.2 and 2.7 pm respectively, when the 6-311G* basis set is used at each level of theory. In $B_6F_4H_4$ the central B(2)-B(4) is 1.7 and 1.9 pm longer at the B3LYP/6-311+G** and MP2/6-311G* levels respectively than the HF/6-311+G** value. Differences for X = Cl (see Table 22) equate to 2.1 and 2.2 pm, and for X = Br (see Table 23) equal 2.2 and 2.3 pm respectively when the 6-311G* basis set is used at each level of theory. The terminal B-B bonds in $B_6F_4H_4$ [B(2)-B(3) and B(4)-B(6)] are 1.8 pm shorter at the B3LYP level than at the HF level when the 6-311+G** basis set is employed. Using the 6-311G* basis set at the MP2 level results in this bond being 1.2 pm longer than at the B3LYP/6-311+G** level. In $B_6Cl_4H_4$ the terminal B-B bonds are 2.2 and 1.5 pm shorter at the B3LYP and MP2 levels respectively compared to HF when the 6-311G* basis set is used. Similarly, for X = Br, these bonds are 2.6 and 1.7 pm shorter at the B3LYP and MP2 levels respectively compared to HF when the 6-311G* basis set is used.

**Table 21**. Calculated ($r_e$) geometric parameters for $B_6F_4H_4$.[a]

| Geometric parameter | Level of theory / Basis set | | | | | | |
|---|---|---|---|---|---|---|---|
| | HF | | | B3LYP | | MP2 | |
| | 3-21G* | 6-31G* | 6-311+G** | 6-31G* | 6-311+G** | 6-31G* | 6-311G* |
| B(1)-B(2) | 177.5 | 175.7 | 175.9 | 172.0 | 171.4 | 172.5 | 173.3 |
| B(1)-B(4) | 177.1 | 175.7 | 175.9 | 172.0 | 171.4 | 172.5 | 173.3 |
| B(2)-B(3) | 177.1 | 175.7 | 175.9 | 172.0 | 171.4 | 172.5 | 173.3 |
| B(2)-B(4) | 150.7 | 151.4 | 151.4 | 153.4 | 153.1 | 153.0 | 153.6 |
| B(3)-B(4) | 177.5 | 175.7 | 175.9 | 172.0 | 171.4 | 172.5 | 173.3 |
| B(2)-B(5) | 166.3 | 169.0 | 168.4 | 167.3 | 166.6 | 167.7 | 167.8 |
| B(4)-B(6) | 166.2 | 169.0 | 168.4 | 167.3 | 166.6 | 167.7 | 167.8 |
| ∠BBB[b] | 171.3 | 180.0 | 180.0 | 179.9 | 180.0 | 180.0 | 180.0 |
| Energy[c] | -545.3935 | -548.3756 | -548.5005 | -551.0712 | -551.2425 | -549.5206 | -549.8122 |

[a] distances in pm, angles in °.

[b] angle B(5)-B(2)-B(4).

[c] absolute energy in Hartrees.

**Table 22**. Calculated ($r_e$) geometric parameters for $B_6Cl_4H_4$.[a]

| Geometric parameter | Level of theory / Basis set | | | | | | |
|---|---|---|---|---|---|---|---|
| | HF | | | B3LYP | | MP2 | |
| | 3-21G* | 6-31G* | 6-311G* | 6-31G* | 6-311G* | 6-31G* | 6-311G* |
| B(1)-B(2) | 175.0 | 175.3 | 175.4 | 171.8 | 171.3 | 172.1 | 172.7 |
| B(1)-B(4) | 174.9 | 175.3 | 175.4 | 171.8 | 171.3 | 172.1 | 172.7 |
| B(2)-B(3) | 174.9 | 175.3 | 175.4 | 171.8 | 171.3 | 172.1 | 172.7 |
| B(2)-B(4) | 153.5 | 152.2 | 152.1 | 154.5 | 154.2 | 153.8 | 154.3 |
| B(3)-B(4) | 175.0 | 175.3 | 175.4 | 171.8 | 171.3 | 172.1 | 172.7 |
| B(2)-B(5) | 165.9 | 168.3 | 167.9 | 166.4 | 165.7 | 166.5 | 166.4 |
| B(4)-B(6) | 165.9 | 168.3 | 167.9 | 166.4 | 165.7 | 166.5 | 166.4 |
| ∠BBB[b] | 180.0 | 180.0 | 180.0 | 180.0 | 179.9 | 180.0 | 180.0 |
| Energy[c] | -1979.2441 | -1988.4424 | -1988.5651 | -1992.4185 | -1992.5581 | -1989.4221 | -1989.6033 |

[a] distances in pm, angles in °.

[b] angle B(5)-B(2)-B(4).

[c] absolute energy in Hartrees.

**Table 23**. Calculated ($r_e$) geometric parameters for $B_6Br_4H_4$.[a]

| Geometric parameter | Level of theory / Basis set | | | | | | |
|---|---|---|---|---|---|---|---|
| | HF | | | B3LYP | | MP2 | |
| | 3-21G* | 6-31G* | 6-311G* | 6-31G* | 6-311G* | 6-31G* | 6-311G* |
| B(1)-B(2) | 174.7 | 175.5 | 175.5 | 172.0 | 171.3 | 172.3 | 172.8 |
| B(1)-B(4) | 174.7 | 175.5 | 175.5 | 172.0 | 171.3 | 172.3 | 172.8 |
| B(2)-B(3) | 174.7 | 175.5 | 175.5 | 172.0 | 171.3 | 172.3 | 172.8 |
| B(2)-B(4) | 153.9 | 152.4 | 152.4 | 154.8 | 154.6 | 154.1 | 154.7 |
| B(3)-B(4) | 174.7 | 175.5 | 175.5 | 172.0 | 171.3 | 172.3 | 172.8 |
| B(2)-B(5) | 165.1 | 167.8 | 167.8 | 165.7 | 165.2 | 166.1 | 166.1 |
| B(4)-B(6) | 165.1 | 167.8 | 167.8 | 165.7 | 165.2 | 166.1 | 166.1 |
| ∠BBB[b] | 179.9 | 180.0 | 180.0 | 180.0 | 180.0 | 179.9 | 180.0 |
| Energy[c] | -10390.7331 | -10430.0640 | -10439.9896 | -10438.4429 | -10448.2192 | -10431.0073 | -10441.0125 |

[a] distances in pm, angles in °.

[b] angle B(5)-B(2)-B(4).

[c] absolute energy in Hartrees.

Unlike the other members of the $B_6X_4H_4$ family, $B_6I_4H_4$ adopts an unusual structure based on a network of irregular boron triangles, as illustrated in Figure 14. Attached to B(1), B(2) and B(6) are terminal I, $BI_2$ and H substituents respectively. B(5) contains two hydrogen substituents. Along the edges B(1)-B(5) and B(4)-B(6) there are bridging I and H respectively.

**Figure 14**. Molecular framework for $B_6I_4H_4$.

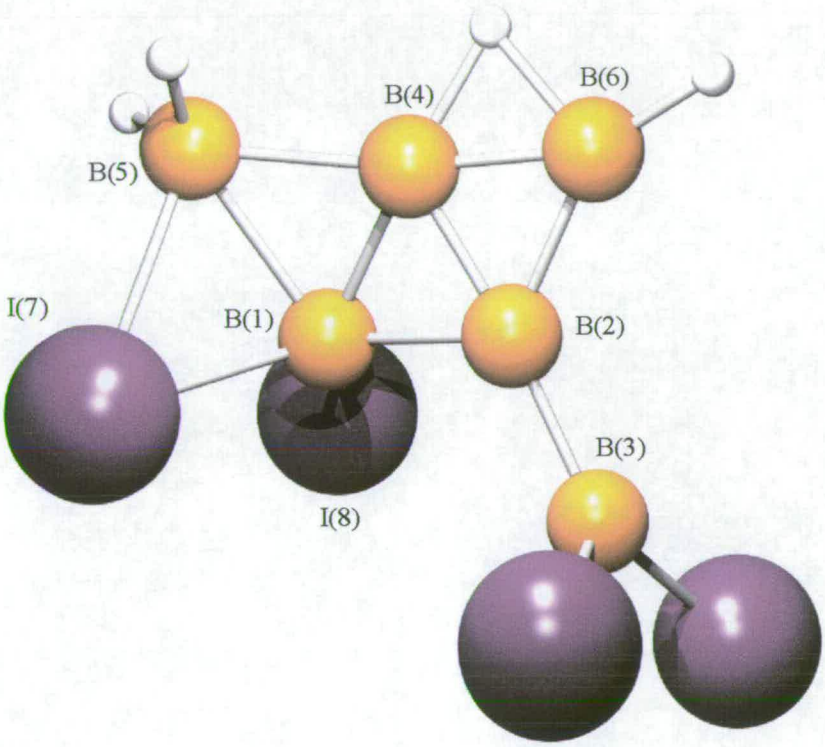


The size of the basis set at the HF level of theory is crucial in its structure determination. For example, using the larger 6-311G* basis set on the B and H atoms results in a decrease of 101.7 pm for B(1)-B(5) compared to when the 6-31G* basis set is employed. The inclusion of correlation decreases this bond even further, with the values at the B3LYP and MP2 levels being 48.7 and 48.8 pm shorter respectively than the HF value, using the 6-311G* basis set for the B and H atoms, and the lanl2dz basis set on the I atoms.

**Table 24**. Calculated ($r_e$) geometric parameters for $B_6I_4H_4$.[a]

| Geometric parameter | Level of theory / Basis set | | | | | | |
|---|---|---|---|---|---|---|---|
| | HF | | | B3LYP | | MP2 | |
| | 3-21G* | 6-31G*[b] | 6-311G*[c] | 6-31G*[b] | 6-311G*[c] | 6-31G*[b] | 6-311G*[c] |
| B(1)-B(2) | 168.2 | 169.0 | 169.3 | 174.9 | 174.8 | 174.3 | 175.1 |
| B(1)-B(4) | 242.8 | 220.0 | 218.8 | 165.8 | 165.5 | 165.4 | 166.7 |
| B(1)-B(5) | 358.4 | 343.1 | 241.4 | 192.9 | 192.7 | 191.0 | 192.6 |
| B(2)-B(3) | 167.4 | 169.3 | 169.1 | 164.4 | 163.7 | 163.8 | 163.6 |
| B(2)-B(4) | 160.3 | 154.8 | 154.3 | 158.4 | 158.1 | 157.9 | 158.7 |
| B(2)-B(6) | 175.9 | 176.0 | 176.0 | 163.0 | 162.5 | 162.2 | 162.2 |
| B(4)-B(5) | 167.5 | 170.4 | 170.1 | 179.8 | 179.7 | 180.1 | 180.4 |
| B(4)-B(6) | 251.8 | 215.9 | 213.8 | 156.6 | 156.4 | 157.9 | 158.9 |
| B(1)-I(7) | 230.7 | 223.9 | 222.7 | 234.2 | 233.2 | 229.1 | 225.0 |
| B(5)-I(7) | 279.3 | 309.8 | 307.8 | 240.1 | 238.7 | 237.4 | 233.1 |
| B(1)-I(8) | 215.1 | 216.2 | 215.4 | 218.0 | 217.4 | 217.0 | 214.8 |
| Energy[d] | -27701.2028 | -195.0367 | -195.0682 | -197.1063 | -197.1333 | -195.7820 | -195.8543 |

[a] 6-31G* on B and H atoms, lanl2dz on I atoms.

[b] 6-311G* on B and H atoms, lanl2dz on I atoms.

[c] distances in pm, angles in °.

[d] absolute energy in Hartrees.

In each calculation of $B_6I_4H_4$ the B(2)-B(4) bond remains relatively short – the longest value (160.3 pm) returned when the inadequate 3-21G* basis set is used for the B and H atoms at the HF level. Even this value suggests a region of high electron density, but bond distances found utilising the 6-311G* basis set on the B and H atoms show values 6.0, 2.2 and 1.6 pm shorter when the HF, B3LYP and MP2 methods are employed. The construction of a bridging B-I-B interaction between B(1) and B(5) is manifested in the B(1)-I(7) and B(5)-I(7) bond distances. B(1)-I(7) at the MP2/6-311G* level (with lanl2dz on the I atoms) is 10.2 pm longer than the terminal B(1)-I(8) bond distance at the same level.

## 6.4. Discussion

The structures discussed in sections 6.3.1 – 6.3.6 highlight the extraordinary bonding abilities of boranes, especially when they are mixed with halogens. The theoretical study of $B_8X_8H_4$ and $B_8X_4H_8$ (X = F, Cl, Br and I), with starting geometries derived from $B_8F_{12}$, has produced a wide variety of interesting bonding motifs. However these structures are not global minima. $B_8F_8H_4$ is interesting as it reinforces the reasoning behind the unusual structure adopted by $B_8F_{12}$ (see Chapter 3). As in the case of $B_8F_{12}$, terminal $BF_2$ substituents, attached to the central $B_4$ rhomboid, twist in such a way as to introduce hyperconjugative effects with the bridging groups of the rhomboid. In the case of $B_8F_{12}$ these bridging groups are $BF_2$, but for $B_8F_8H_4$ they are replaced by $BH_2$. As a result, the central butterfly is flattened in $B_8F_8H_4$ and the hydrogens show more pronounced twisting to accommodate the hyperconjugative interaction between B and F.

For X = Cl, Br and I in $B_8X_8H_4$, we encounter structures very different from that found for the fluoro analogue. In the cases of X = Cl and Br, the folded central $B_4$ butterfly is retained from the parent $B_8X_{12}$ (X = Cl and Br) molecules (see Chapter 4). The increased electron deficiency of the bridging ($BH_2$) region compared to their parents is evident by the introduction of bonding between the terminal $BX_2$ groups to B(3) and a bridging

B-H-B interaction between B(1) and B(2) [see Figure 2]. The cases of X = Cl and Br suggest that polyboron halides of these nature are more capable of forming polyhedral boron clusters and that polyboron fluorides prefer to adopt more open-type structures as has been found experimentally for $B_8F_{12}$. The boron framework of $B_8I_8H_4$ can also be classified as an open-type structure. Perhaps the steric bulk of iodine precludes the formation of structures such as those found for X = F, Cl and Br.

Further substitution of hydrogen for halogens in $B_8X_4H_8$ (X = F, Cl, Br and I) changes the structure of the boron framework beyond recognition. The halogens no longer dominate the molecule. For example, in the case of X = F, the boron framework is based on a distorted tetrahedron supplemented by bridging hydrogens and a bridging $BH_2$. Comparison of the tetrahedra found for $B_8F_4H_8$ to the crystal structure of $B_{10}F_{12}$ (see Chapter 5) shows that the borons in $B_{10}F_{12}$ belong to a region of greater electron density with B-B bond distances in this area ranging from 160.5 – 175.9 pm compared to 170.0 – 176.7pm for $B_8F_4H_8$ (calculated at MP2/6-311G*). The terminal $BF_2$ groups in $B_8F_4H_8$, whilst they are not irrelevant, do not control the nature of boron bonding. In the case of $B_8F_8H_4$, a planar $B_4$ rhomboid is determined, but for $B_8F_4H_8$ a $B_4$ tetrahedron is favoured.

Known tetraboranes(6) tend to be derivatives of a distorted tetrahedral isomer of $B_4H_6$ containing hydrogen bridges across two of the edges.[14] Computational studies carried out, at the MP2/6-311G* level, on this model compound show the tetrahedral arrangement to be 38.5 kJ $mol^{-1}$ lower in energy than a planar formation.[14] However the recent structure determination of such compounds as the *bicyclo*-tetraborane(4), $B_6(NMe_2)_6$, show a planar $B_4$ diamond to be attainable experimentally.[15,16] Further evidence for the existence of such an arrangement can be seen from the computational study of the tetrahedrane molecule $B_4H_4$.[15] It has been found that a $D_{4h}$ isomer of this species is 272.0 kJ $mol^{-1}$ higher in energy than its $T_d$ form (see Figure 15).[15] However, when the $\pi$ molecular orbital, made up of four $p_z$ atomic orbitals, is occupied with an electron pair that formally originates from one of the four $\sigma$ molecular orbitals of the $B_4$

framework, Jahn-Teller distortion leads to the lowering of symmetry from $D_{4h}$ to $D_{2h}$.[15] The $D_{2h}$ structure lies 338.9 kJ mol$^{-1}$ lower in energy than the $D_{4h}$.[15] This geometric reorganisation, which plays a central role in isomerisation of boranes, carboranes and metalloboranes (commonly referred to as the diamond-square-diamond rearrangement),[16] results in rehybridisation of B(1) and B(3) from $sp^2$ to $sp$.[15] For $B_4H_4$, hyperconjugation leads to the formation of a three-centre two-electron B-H-B bridge but it has been noted that for less effective $\sigma$ donors there is only a shift of the substituents at B(1) and B(3) towards B(2) and B(4).[15] Compare this to $B_8X_8H_4$ (X = Cl, Br and I), where terminal substituents on B(2) and B(4) shift towards the bridging B(1) and B(3) atoms.

**Figure 15.** $B_4$ unit in $B_4H_4$ with $T_d$, $D_{4h}$ and $D_{2h}$ symmetry.

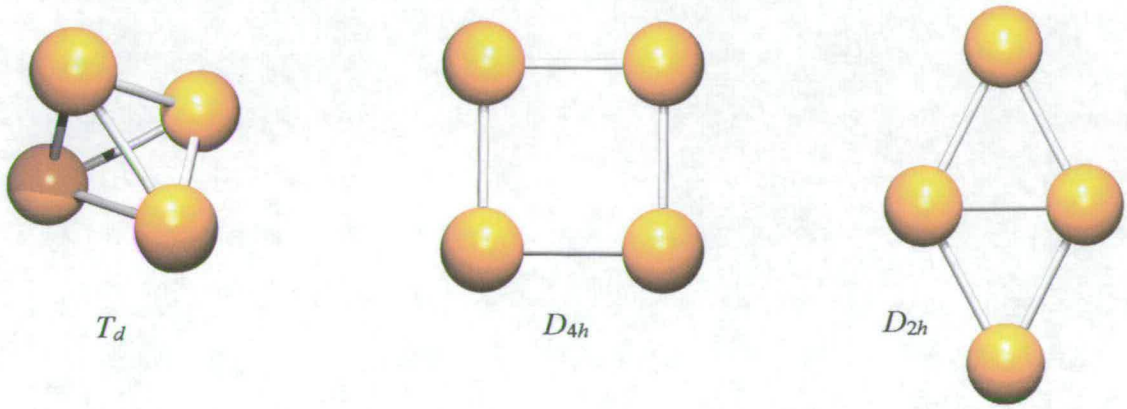


The boron framework of *arachno*-$B_5H_{11}$[17] has long been established as that of an open-sided tetragonal pyramid comparable to that found for $B_8X_4H_8$ (X = Cl, Br and I). Table 25 compares the B-B bond distances in the boron framework of pentaborane(11)[17] to those found in $B_8X_4H_8$ (X = Cl, Br and I). For clarity the atom numbering has been changed from those in Figures 5 and 6 to conform to the published structure of *arachno*-$B_5H_{11}$.[17]

**Table 25**. Selected B-B bond lengths in $B_5H_{11}$ and $B_8X_4H_8$ (X = Cl, Br and I).

| Bond[a] | $B_5H_{11}$[b] | $B_8Cl_4H_8$[c] | $B_8Br_4H_8$[c] | $B_8I_4H_8$[d] |
|---|---|---|---|---|
| B(1)-B(2) | 189.2(6) | 170.8 | 171.3 | 179.2 |
| B(1)-B(3) | 174.2(8) | 172.8 | 172.9 | 173.9 |
| B(1)-B(4) | 174.2(8) | 175.8 | 176.9 | 168.0 |
| B(1)-B(5) | 189.2(6) | 175.3 | 175.5 | 167.2 |
| B(2)-B(3) | 181.2(7) | 171.3 | 171.3 | 188.6 |
| B(2)-B(5) | 309.1(10) | 229.5 | 235.0 | 191.7 |
| B(3)-B(4) | 176.0(12) | 177.1 | 176.1 | 175.5 |
| B(4)-B(5) | 181.2(7) | 179.6 | 180.2 | 173.7 |

[a] For atom numbering see Ref 17.
[b] Geometry from Ref 17.
[c] MP2/6-311G*.
[d] MP2/6-311G* on B and H atoms, lanl2dz on I atoms.

The lengths of the basal bonds of the pyramid, with the exclusion of the open face, range from 176.0(12) – 181.2(7) for $B_5H_{11}$,[17] 171.3 – 179.6 pm for $B_8Cl_4H_8$, 171.3 – 180.2 pm for $B_8Br_4H_8$ and 173.7 – 188.6 pm for $B_8I_4H_8$. However, the distance of the open face in $B_5H_{11}$[17] is 79.6, 74.1 and 117.4 pm longer than in $B_8X_4H_8$ (X = Cl, Br and I respectively).

The determination of the structure of the family of compounds $B_8X_8H_4$ and $B_8X_4H_8$ (X = F, Cl, Br and I) by theoretical calculations has provided an interesting array of different structural motifs. The experimental *nido* structure of $B_8H_{12}$ was established by X-ray crystallography in 1964.[18] Substitution of eight (for $B_8X_8H_4$) or four (for $B_8X_4H_8$) of the hydrogens with X = F, Cl, Br or I provides the opportunity for comparison with the structures found in Figures 1 – 6. Similarly, the experimental structures of hexaborane(10),[19] pentaborane(9),[20] tetraborane(8),[21,22] and the theoretically studied triborane(7)[21,23] can be used as structural blueprints, with the addition of further boron and halogens to make up the $B_8X_8H_4$ or $B_8X_4H_8$ (X = F, Cl, Br and I) formulae. In other words, they have terminal H replaced by $BX_2$ (or $BH_2$) so that, for example, the $B_5H_9$ derivatives of $B_8X_8H_4$ are 1,2,3-, 1,2,4- and 2,3,4-$(BF_2)_3B_5H_9$. To that end, MP2/6-31G* calculations on the systems $B_8X_8H_4$ and $B_8X_4H_8$ (X = F, Cl, Br and I) were performed

using the Gaussian 98 computer program[4] as described in section 6.2.1. In the case of X = I the 6-31G* basis set was used for the B and H atoms, and the lanl2dz basis set was used for the I atoms. For $B_8X_8H_4$ (X = F, Cl, Br and I) one isomer based on the geometry of $B_8H_{12}$ (**2**), four based on $B_6H_{10}$ (**3a-d**), three derived from $B_5H_9$ (**4a-c**), three from $B_4H_8$ (**5a-c**) and five from $B_3H_7$ (**6a-e**) were calculated (see Figures 16 – 20) and compared to the structures found in Figures 1 – 3 (denoted **1** in the following discussion). For $B_8X_8H_4$ (X = F, Cl, Br and I) two isomers derived from the geometry of $B_8H_{12}$ (**8a-b**), four based on $B_6H_{10}$ (**9a-d**), three on $B_5H_9$ (**10a-c**), two on $B_4H_8$ (**11a-b**) and two on $B_3H_7$ (**12a-b**) were calculated (see Figures 21 – 25) and compared to the structures found in Figures 4 – 6 (denoted **7**). These structures are illustrated in Figures 26 – 33 with their relative energies given in Tables 26 – 27. All systems returned no imaginary frequencies, indicating that these structures are minima on their respective potential energy surfaces.

**Figure 16**. Isomer of $B_8X_8H_4$ (X = F, Cl, Br and I) based on $B_8H_{12}$.

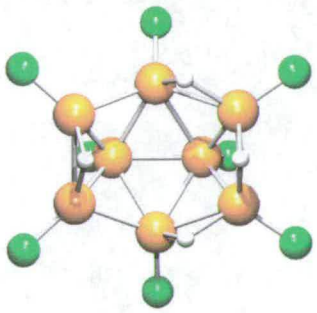

**2**

**Figure 17**. Isomers of $B_8X_8H_4$ (X = F, Cl, Br and I) based on $B_6H_{10}$.

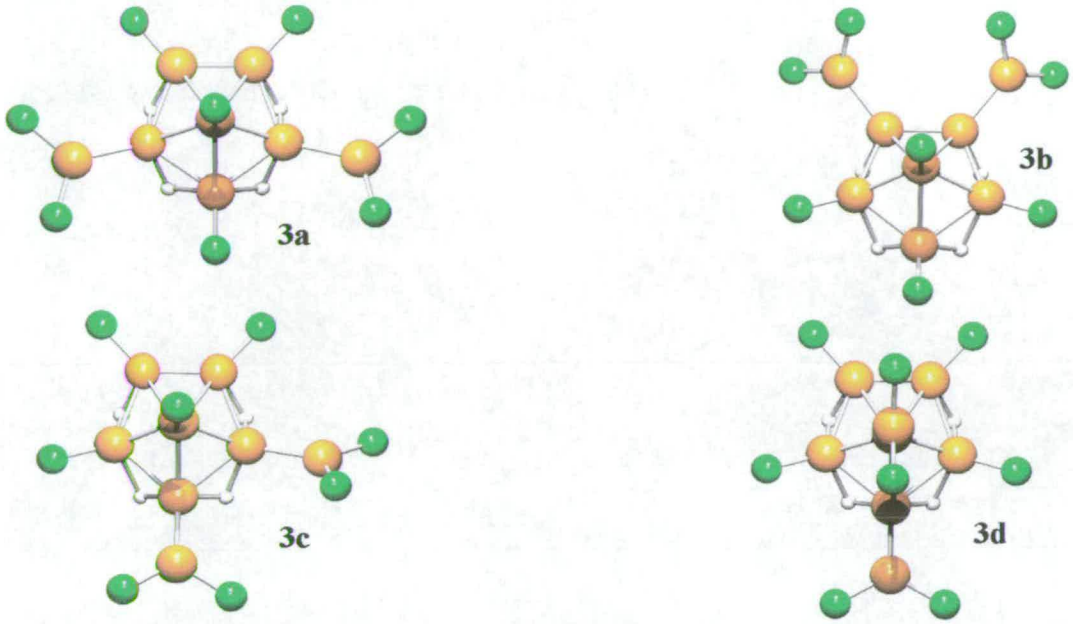


**Figure 18**. Isomers of $B_8X_8H_4$ (X = F, Cl, Br and I) based on $B_5H_9$.

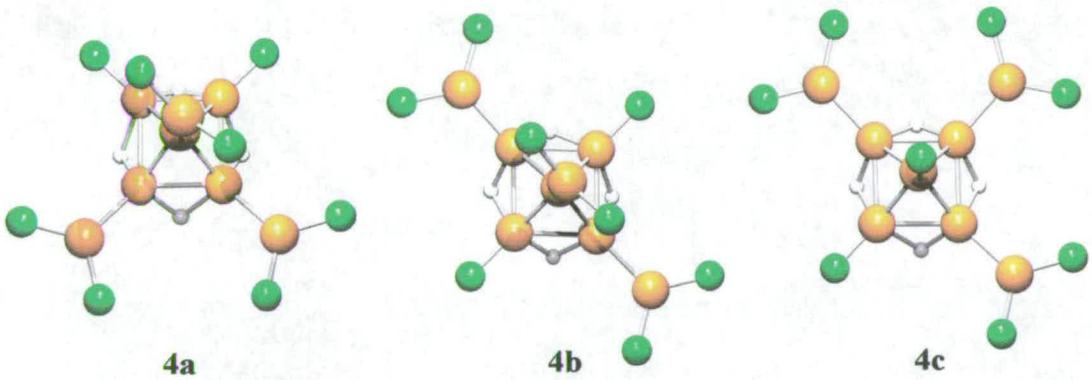

**Figure 19**. Isomers of $B_8X_8H_4$ (X = F, Cl, Br and I) based on $B_4H_8$.

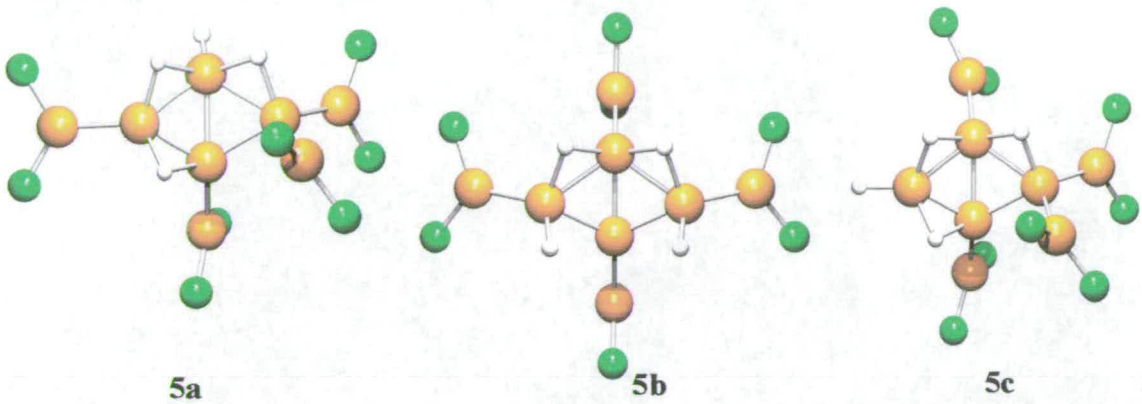

**5a** **5b** **5c**

**Figure 20**. Isomers of $B_8X_8H_4$ (X = F, Cl, Br and I) based on $B_3H_7$.

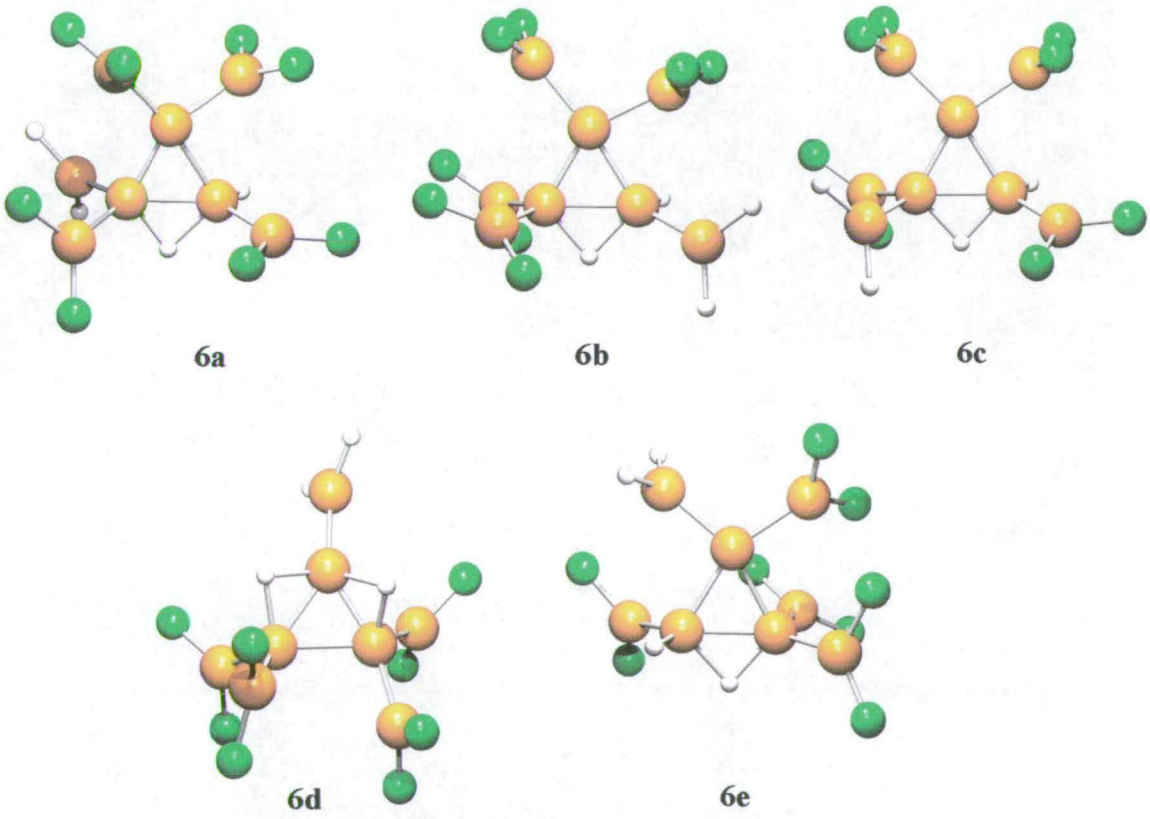

**6a** **6b** **6c**

**6d** **6e**

**Figure 21**. Isomers of $B_8X_4H_8$ (X = F, Cl, Br and I) based on $B_8H_{12}$.

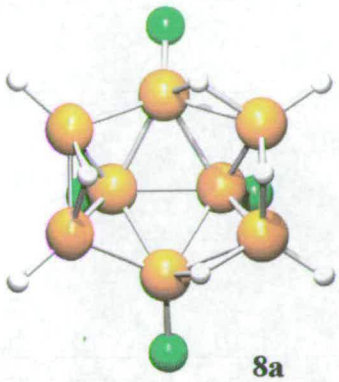

**8a**

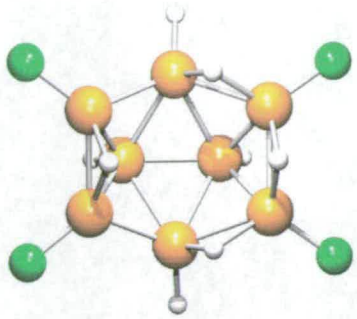

**8b**

**Figure 22**. Isomers of $B_8X_4H_8$ (X = F, Cl, Br and I) based on $B_6H_{10}$.

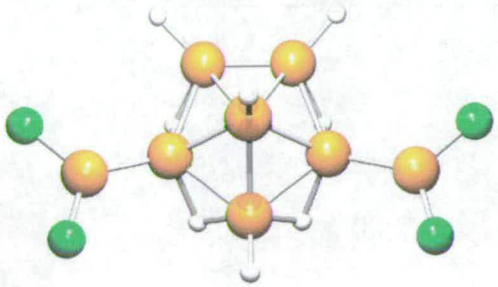

**9a**

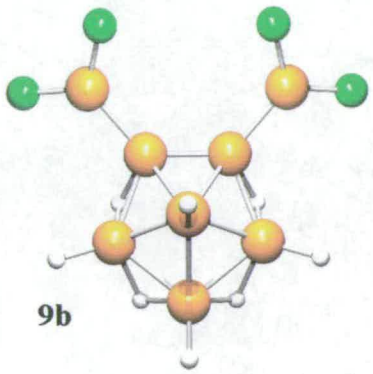

**9b**

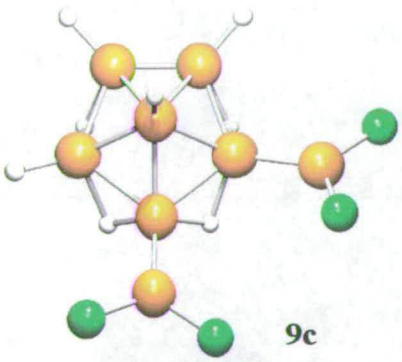

**9c**

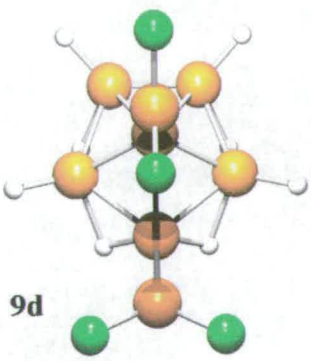

**9d**

**Figure 23**. Isomers of $B_8X_4H_8$ (X = F, Cl, Br and I) based on $B_5H_9$.

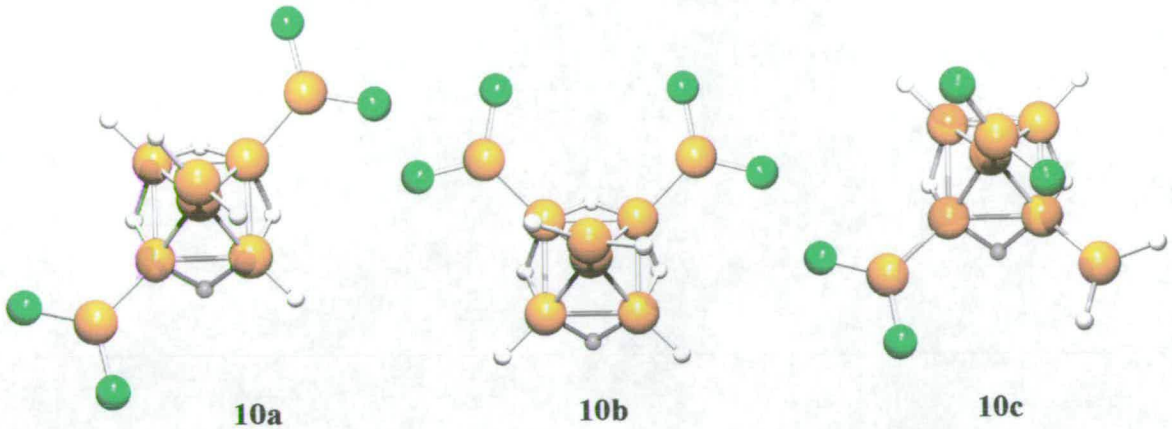

**10a** **10b** **10c**

**Figure 24**. Isomers of $B_8X_4H_8$ (X = F, Cl, Br and I) based on $B_4H_8$.

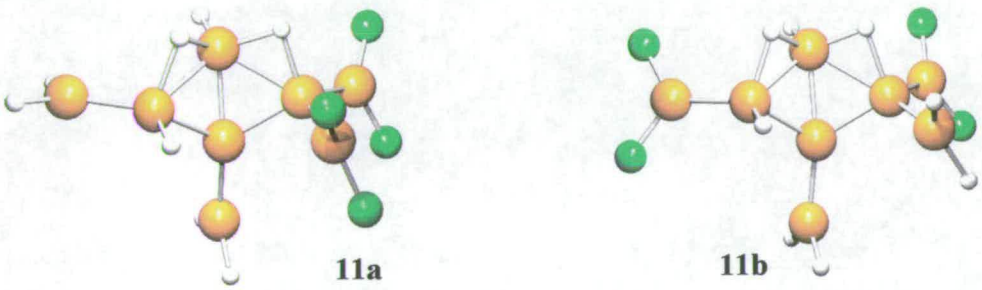

**11a** **11b**

**Figure 25**. Isomers of $B_8X_4H_8$ (X = F, Cl, Br and I) based on $B_3H_7$.

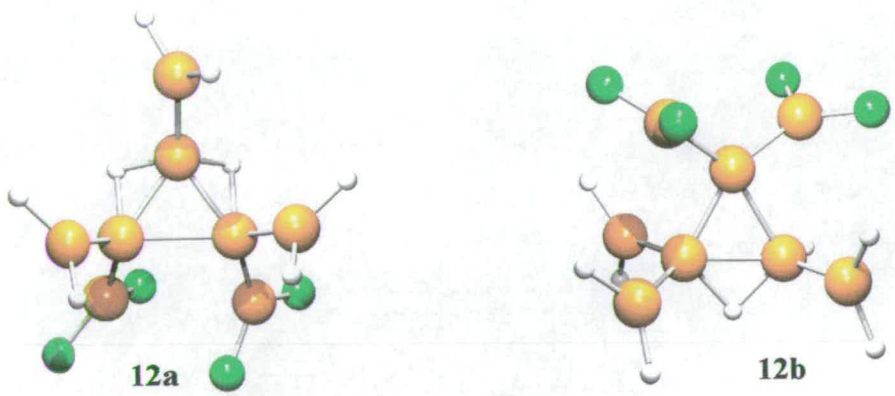

**12a** **12b**

**Table 26**. Relative energies (MP2/6-31G*) for $B_8X_8H_4$ (X = F, Cl, Br and I).[a]

| Isomer | X = F | X = Cl | X = Br | X = I |
|---|---|---|---|---|
| **1** | 160.2 | 114.63 | 92.8 | 328.5 |
| **2** | 254.5 | **0.0** | 31.3 | **0.0** |
| **3a** | 131.5 | 85.1 | 35.6 | 159.3 |
| **3b** | 91.9 | 59.3 | 31.2 | 144.5 |
| **3c** | 109.5 | 68.1 | 28.6 | 154.2 |
| **3d** | 70.7 | 56.1 | 23.9 | 154.4 |
| **4a** | **0.0** | 56.4 | **0.0** | 184.7 |
| **4b** | 18.2 | 60.3 | 2.3 | 179.4 |
| **4c** | 40.0 | 76.8 | 11.1 | 193.0 |
| **5a** | 9.2 | 119.3 | 47.8 | 278.7 |
| **5b** | 40.7 | 154.6 | 50.2 | 289.6 |
| **5c** | -[b] | 128.4 | 28.1 | 317.5 |
| **6a** | 141.2 | -[b] | 52.7 | 251.1 |
| **6b** | 145.1 | 186.1 | 122.1 | 305.9 |
| **6c** | 102.4 | 187.4 | 143.8 | 340.2 |
| **6d** | 139.3 | 201.7 | 122.1 | 302.8 |
| **6e** | 18.0 | 132.1 | 62.4 | 298.3 |

[a] Energies in kJ $mol^{-1}$

[b] Structure failed to optimise.

**Table 27**. Relative energies (MP2/6-31G*) for $B_8X_4H_8$(X = F, Cl, Br and I).[a]

| Isomer | X = F | X = Cl | X = Br | X = I |
|---|---|---|---|---|
| **7** | 144.5 | 239.5 | 247.4 | 296.3 |
| **8a** | -[b] | 0.3 | **0.0** | **0.0** |
| **8b** | 102.2 | **0.0** | 20.3 | 12.6 |
| **9a** | 29.3 | 82.5 | 121.5 | 165.2 |
| **9b** | **0.0** | 46.1 | 76.8 | 124.2 |
| **9c** | 22.4 | 74.2 | 102.6 | 153.9 |
| **9d** | 8.0 | 61.2 | 86.4 | 137.1 |
| **10a** | 102.6 | 150.9 | 190.8 | 231.0 |
| **10b** | 104.4 | 154.6 | 186.8 | 235.5 |
| **10c** | 91.0 | 138.4 | 162.0 | 211.1 |
| **11a** | 249.5 | 297.7 | 318.4 | 374.7 |
| **11b** | 240.7 | 286.7 | 317.4 | 363.3 |
| **12a** | 237.7 | 269.5 | 296.2 | 173.8 |
| **12b** | 280.3 | 291.5 | 293.2 | 340.1 |

[a] Energies in kJ $mol^{-1}$

[b] Structure failed to optimise.

**Figure 26**. Relative energies of $B_8X_8H_4$ (X = F).

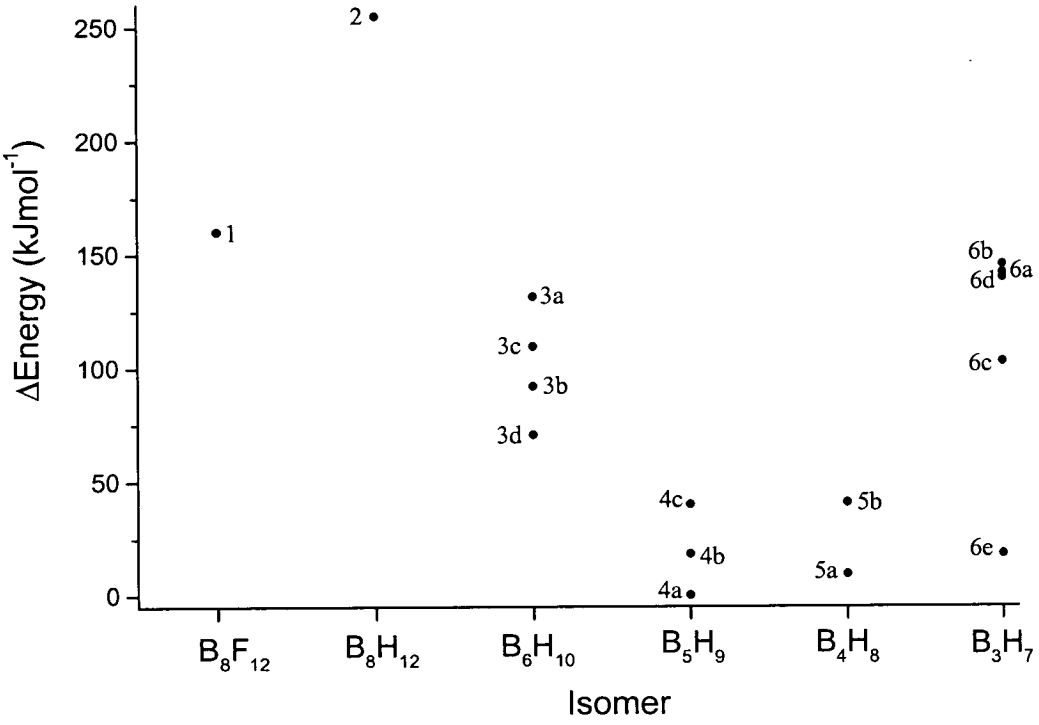


**Figure 27**. Relative energies of $B_8X_8H_4$ (X = Cl).

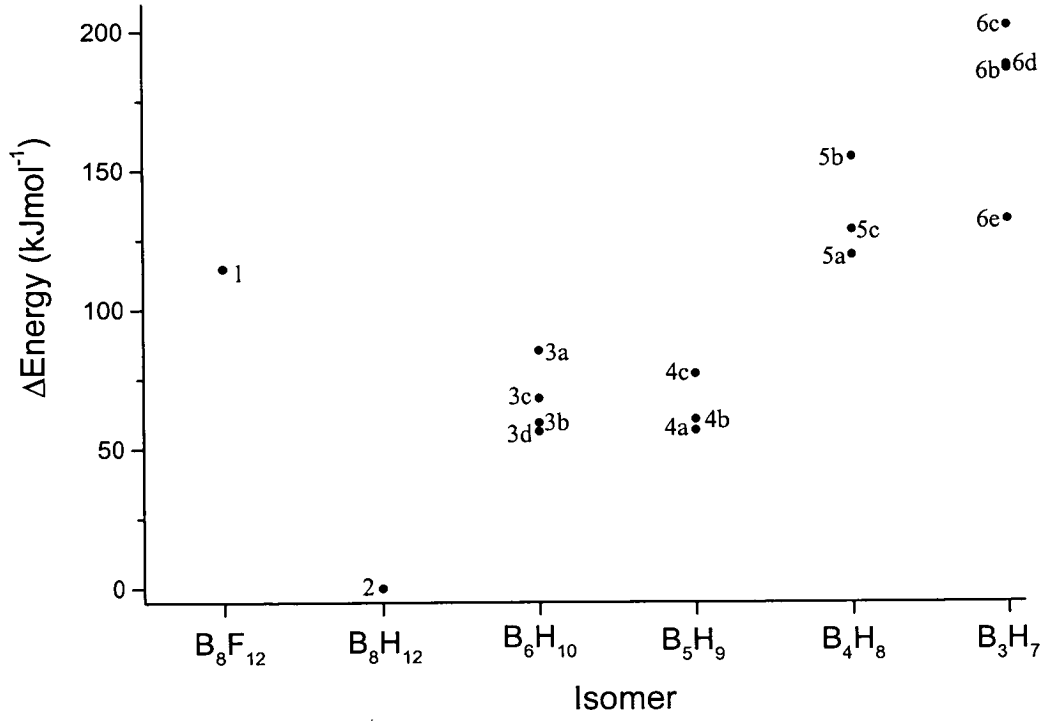

**Figure 28**. Relative energies of $B_8X_8H_4$ (X = Br).

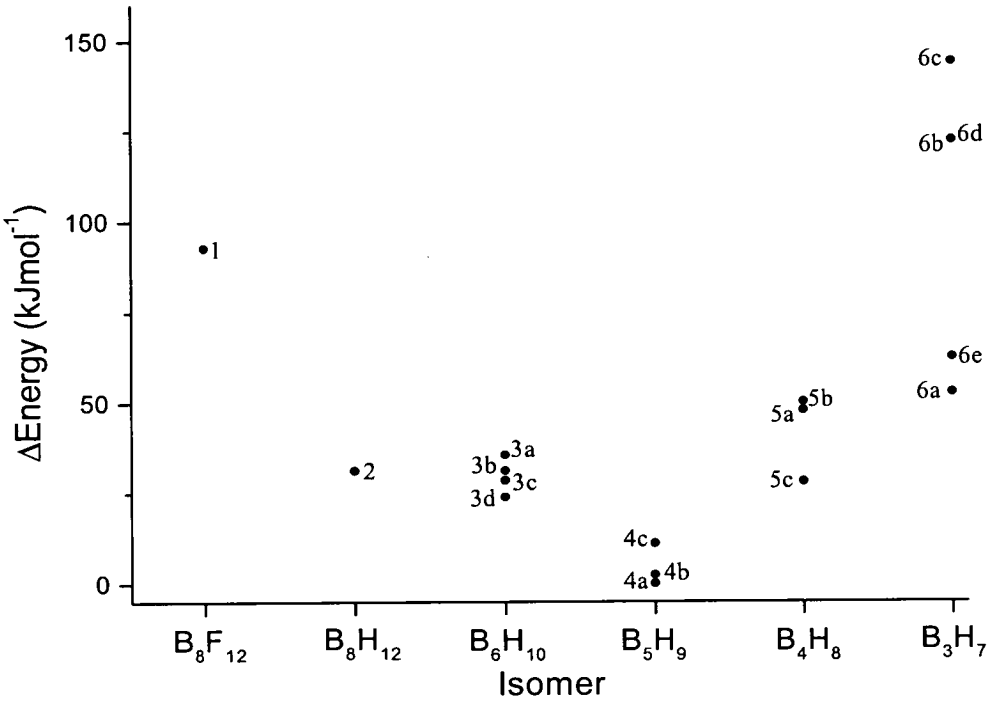


**Figure 29**. Relative energies of $B_8X_8H_4$ (X = I).

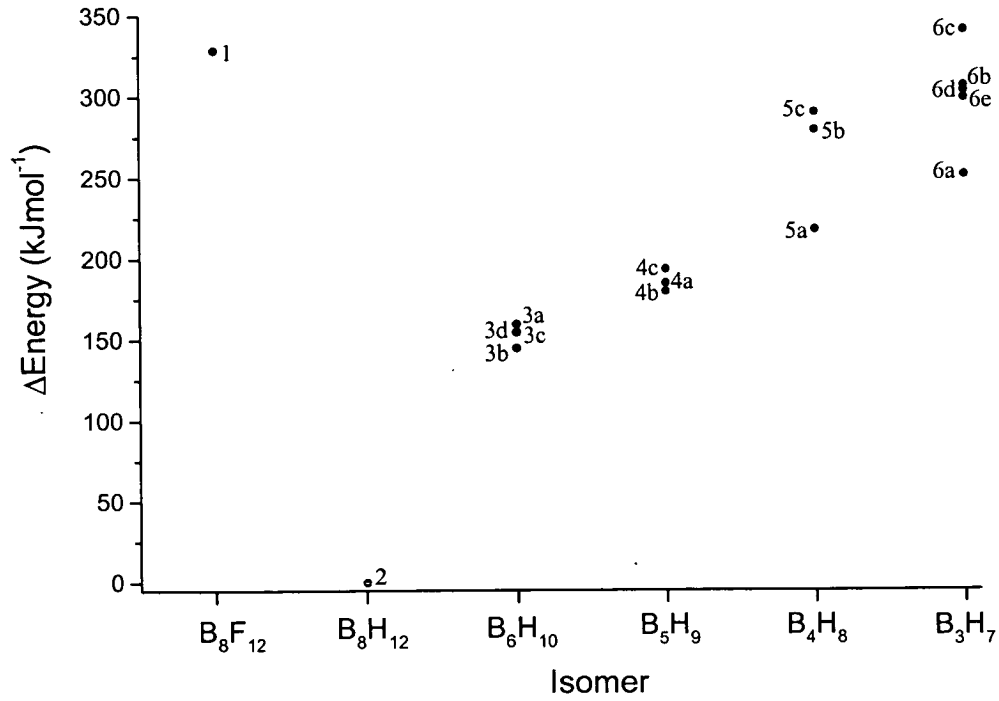

**Figure 30**. Relative energies of $B_8X_4H_8$ (X = F).

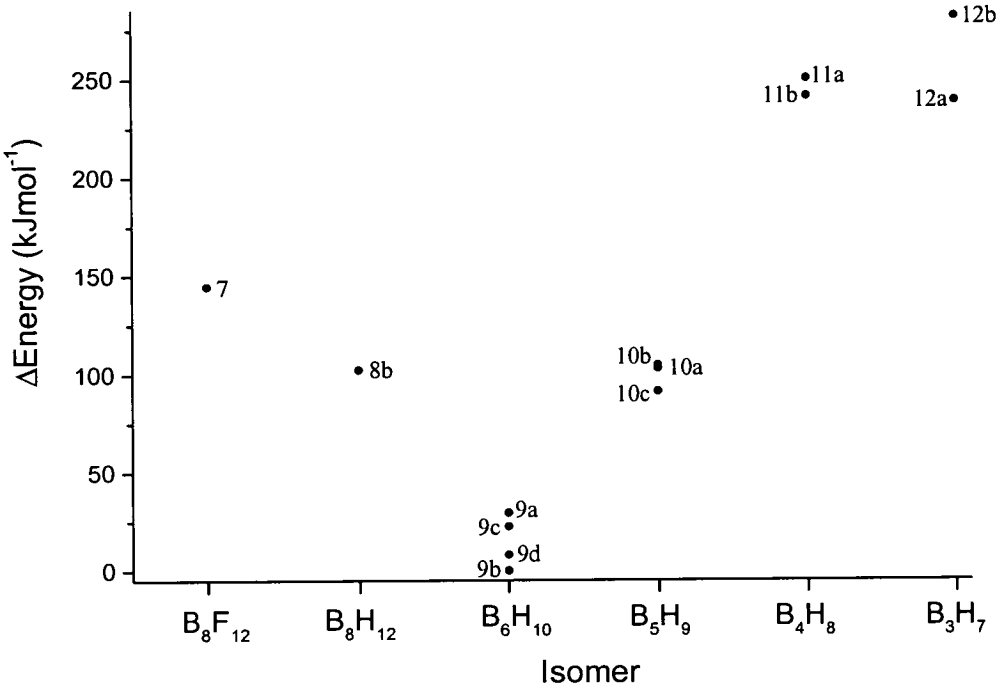


**Figure 31**. Relative energies of $B_8X_4H_8$ (X = Cl).

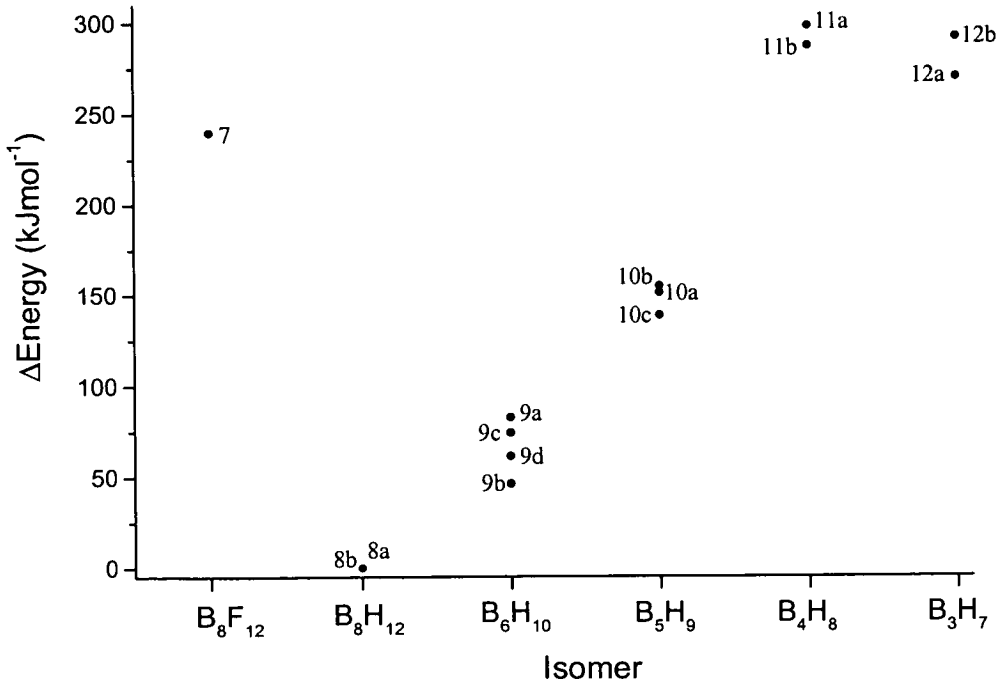

**Figure 32**. Relative energies of $B_8X_4H_8$ (X = Br).

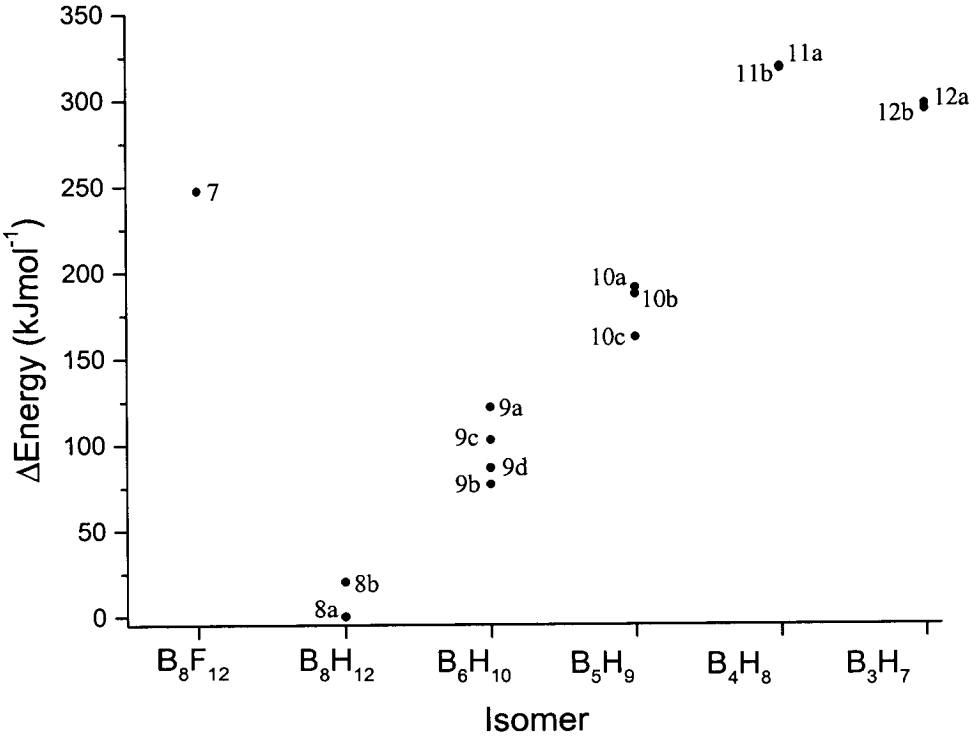


**Figure 33**. Relative energies of $B_8X_4H_8$ (X = I).

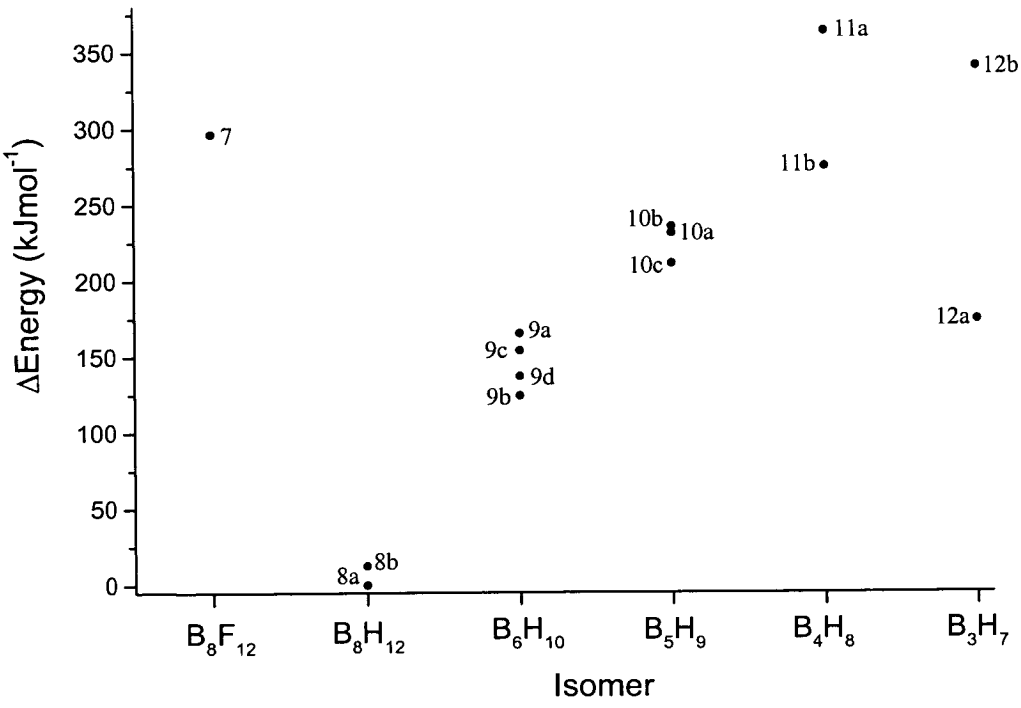

For X = F and Br in $B_8X_8H_4$, the lowest energy isomer utilises the recognised boron framework of $B_5H_9$ (**4a**). However, for X = Cl and I the $B_8H_{12}$ (**2**) isomer is favoured. For X = F seven further isomers lie less than 100 kJ $mol^{-1}$ higher than **4a**. The closest of these, **5a**, is only 9.2 kJ $mol^{-1}$ higher. Whilst isomer **2** is the most stable for X = Cl and I, in the case of X = F it is a massive 254.5 kJ $mol^{-1}$ higher in energy than **4a**. For X = Br, it is only 31.3 kJ $mol^{-1}$ higher than **4a**. The bromo molecules have many energy minima in close proximity – a problem that also affects the area of theoretical crystal structure determination.[24,25] It therefore highlights the importance of experimental data to corroborate theoretical structures. Indeed **4b** is only 2.3 kJ $mol^{-1}$ higher than **4a**. In contrast, the second lowest isomer (**3b**) for X = I is 144.5 kJ $mol^{-1}$ higher in energy. For X = Cl, seven isomers lie less than 100 kJ $mol^{-1}$ higher than **2**, but the second lowest energy isomer (**3d**) is 56.1 kJ $mol^{-1}$ higher in energy.

The reasoning behind the favourability of certain geometric isomers for $B_8X_8H_4$ (X = F, Cl, Br and I) is unclear. If you take the point of view that B atoms in polyboron fluoride clusters are less capable of delocalisation than in other halogenated species, then the adoption of a $B_5H_9$ isomer for $B_8F_8H_4$ can be explained since the boron cluster in such a molecule is smaller than in $B_8H_{12}$ and $B_6H_{10}$ isomers. This would also neatly explain the preference of $B_8H_{12}$ isomers for X = Cl and I. However the validity of this explanation is impaired by the fact that $B_8Br_8H_4$ also prefers the $B_5H_9$ isomer. One characteristic that is common to these isomers (**4a** and **2**) is that the hydrogen atoms are all positioned in B-H-B bridge formations – a position commonly regarded as the favoured site for H in boranes.

In $B_8X_4H_8$ (X = F, Cl, Br and I) there are fewer halogens available to provide $\pi$ bonding than in $B_8X_8H_4$. For X = Cl, Br and I in $B_8X_4H_8$, $B_8H_{12}$ (**8a-b**) isomers are the most stable. For X = Br and I, **8a** is favoured and for X = Cl this isomer is only 0.3 kJ $mol^{-1}$ higher in energy than its lowest energy isomer (**8b**). Contrastingly, **8b** is 20.3 and 12.6 kJ $mol^{-1}$ higher in energy than **8a** for X = Br and I respectively. It is perhaps not so surprising that such systems adopt $B_8H_{12}$ isomers. The crystal structure of $B_8H_{12}$ is well

established and hence the substitution of four of its hydrogens by halogen atoms can be seen to have little effect on the boron framework. However, $B_8F_4H_8$ prefers to adopt the $B_6H_{10}$ (**9b**) motif which lies 102.2 kJ $mol^{-1}$ lower in energy than isomer **8b**. All the other $B_6H_{10}$ derived isomers are also much more stable than those derived from $B_8H_{12}$. In **9b** $BF_2$ substituents are attached to borons that possess only one B-H-B bridge in the pentagonal boron cluster. All three of the other basal borons in this pyramid contain two B-H-B bridges.

The dimeric structure of $B_4F_4H_4$ is stable with respect to each $B_2F_2H_2$ monomer, but the generation of such a structure is puzzling given that the chloro and bromo analogues produce vastly different bonding schemes. $B_4Cl_4H_4$ and $B_4Br_4H_4$ contain a central $B_4$ butterfly with fold angles of 14.6° and 12.7° respectively at the MP2/6-311G* level. In comparison, $B_8Cl_8H_4$ and $B_8Br_8H_4$ possess fold angles of 29.1° and 28.3° respectively (calculated at MP2/6-311G* for $B_8Cl_8H_4$ and B3LYP/6-311+G* for $B_8Br_8H_4$). This narrower fold angle allows the formation of bridging B-X-B between terminal $BX_2$ and bridging $BH_2$ groups in $B_8X_8H_4$ (X = Cl and Br). $B_2F_4$ adopts a planar configuration and whilst $B_2Cl_4$ is also planar in the solid state, it possesses $D_{2d}$ symmetry in the gas phase.[26] The increased steric interaction relative to F and Cl for the larger halides means that $B_2Br_4$ also prefers the $D_{2d}$ staggered conformation.[26] Calculations on $B_2I_4$ (see Chapter 2) determine the staggered $D_{2d}$ conformation with a B-B bond distance of 166.4 pm (MP2/6-311G* with lanl2dz on the I atoms). In contrast the central B(2)-B(4) bond in $B_4I_4H_4$ is 175.6 pm at the same level of theory and basis set, and the substituents lie eclipsed albeit with the bulky $BI_2$ groups in an anti-periplanar fashion. The terminal B-B [B(1)-B(4) and B(2)-B(3)] bonds in $B_4I_4H_4$ exhibit a pronounced shortening compared to the central B(2)-B(4) bond. For example, at the MP2/6-311G* level (with lanl2dz on the I atoms) B(1)-B(4) equals 168.5 pm compared to 175.6 pm for B(2)-B(4).

The structures of $B_{10}X_8H_4$ and $B_{10}X_4H_8$ (X = F, Cl, Br and I) share a common motif – six conjoined boron triangles supplemented by bridging and terminal $BY_2$ substituents (where Y = halogen or hydrogen). Polyhedral boranes are considered to be 3D aromatics

and in non-classical systems there is potential for double aromaticity, i.e., in addition to an aromatic $\pi$ system there is a bonding $\sigma$ system derived from unpaired electrons.[27] Alternatively it can be thought of as multiples of two orthogonal systems each with ($4n$ + 2) electrons.

1,3-diamino-2,4-diboryltetraborane(4), $B_6(NMe_2)_6$, possesses a planar $B_4$ diamond.[15,16] However, its dianion, formed through the reaction with lithium in DME, contains a puckered framework (with a fold angle of 29.5°) – characteristic of a four-membered, two-electron aromatic system.[28] Compare this fold angle to those found in the $B_{10}X_8H_4$ and $B_{10}X_4H_8$ (X = F, Cl, Br and I), for example angles of 34.4°, 33.7°, 22.9° and 23.7° in $B_{10}F_8H_4$, $B_{10}Cl_8H_4$, $B_{10}F_4H_8$ and $B_{10}Cl_4H_8$ respectively. It is noted that the narrowed angles are obtained for the molecules with the greatest number of halogen substituents.

In $B_6X_4H_4$ (X = F, Cl and Br) the central B(2)-B(4) bond length, at the MP2/6-311G* level, increases with increased steric bulk of the halogens. For X = F, B(2)-B(4) is 153.6 pm compared to 154.3 and 154.7 pm for X = Cl and Br respectively. The shortest distance ever measured between two boron atoms [151.1(3) pm] belongs to the pyridine adduct of a tetraalkyltetraborane.[14] It has been stated that cyclic delocalisation of two $\pi$ electrons over four boron centres is only possible when the axes of the $p$ orbitals of the boron atoms at the corners of the diamond are perpendicular to the plane formed by the boron triangle. The pyridine adduct of this tetraalkyltetraborane, characterised by Präsang *et al.*, results in the conversion of a four-centre two-electron aromatic into a three-centre two-electron aromatic system, puckering the planar ring in the parent compound by 12.8°.[14] Comparison of the central B-B bond in the parent molecule (with planar $B_4$ ring) to that found in $B_6X_4H_4$ (X = F, Cl and Br) shows it to be 1.2, 1.9 and 2.3 pm shorter than for X = F, Cl and Br respectively, at the MP2/6-311G* level. However, the boron atoms at the corners of the diamond in tetraalkyltetraborane are planar-tetracoordinate.[14] For $B_6X_4H_4$ (X = F, Cl and Br) there is significant twisting of the $BH_2$ bridging groups that occupy these positions. Calculations carried out on tetraborane(6) show the transformation of a planar-tetracoordinate boron into a tetrahedrally

coordinated one.[14] The species with tetrahedral coordination lies 186 kJ $mol^{-1}$ higher in energy than when it is planar.[14] However, the boron atoms in $B_6X_4H_4$ (X = F, Cl and Br) are not tetrahedrally coordinated - possessing B(2)-B(1)-H angles of 98.1°, 98.9° and 99.1° for X = F, Cl and Br respectively (calculated at the MP2/6-311G* level).

Another interesting feature in $B_6X_4H_4$ (X = F, Cl and Br) is the linearity of the substituent $BX_2$ groups to the central B(2)-B(4) bond. This feature is also evident in the calculated structures of $HB(\mu\text{-}BH)_2BH$, $(H_2B)B[\mu\text{-}BH]_2B(BH_2)$ and $[(H_2N)_2B]B[\mu\text{-}BH]_2B[B(NH_2)_2]$.[15] However, when amino substituents are in the bridging positions non-linear configurations are adopted, such as that determined by experiment in 1,3-diamino-2,4-diboryltetraborane(4), where the boron atoms concerned lie slightly above and below the $B_4$ plane (40 pm).[15]

There is a stark difference between the structure of the iodo member of the family $B_6X_4H_4$ and its lighter halogen analogues. $B_6I_4H_4$ is based on a distorted trapezium similar to that encountered in the known *bis*-homotriboriranide described in Ref. 27. Comparison of the central boron fragment in these species shows that $B_6I_4H_4$ (calculated at the MP2/6-311G* level using the lanl2dz basis set on the I atoms) contains B-B bonds which are changed by +2.7 [B(1)-B(2)], +6.5 [B(1)-B(4)] and -7.4 pm [B(2)-B(4)] relative to the triboriranide crystal structure.[27] B(4)-B(6) in $B_6I_4H_4$ is 4.4 pm longer than the B-C of the equivalent position in triboriranide. However, the B-C bond in triboriranide equivalent to B(4)-B(5) in $B_6I_4H_4$ is 27.9 pm longer, and the large B(1)-B(5) bond (192.6 pm) indicates the lack of electron density in this region of $B_6I_4H_4$.[27]

The structures discovered in this chapter are all the more remarkable given the relationship between currently known haloboranes and their parent borane structures. Known haloboranes include $B_3H_7Br^-$,[29] $B_4H_9X$ (X = F and Br),[30-32] $B_5H_7Br_2$,[33] $B_5H_8X$ (X = F, Br, I, $BF_2$ and $BCl_2$),[33-35] $B_9Br_9H_2$,[36] $B_{10}H_{13}I$,[37] $B_{10}H_{12}X_2$ (X = Br and I).[38,39] The structures of all of these systems do not significantly deviate from those of their parent unsubstituted borane molecules. Similarly for the halocarboranes $CB_9H_5X_5^-$ (X = Cl and

Br),[40,41] 3-X-1,2-*closo*-$C_2B_{10}H_{11}$[42] and $CB_{11}H_{11}X^-$ (X = F, Cl, Br and I),[43-45] which retain the structural features of the respective parent carboranes. The calculations carried out in this chapter show that the systems $B_8X_4H_8$, $B_8X_8H_4$, $B_4X_4H_4$, $B_{10}X_4H_8$, $B_{10}X_8H_4$ and $B_6X_4H_4$ bear little resemblance to the parent $B_8X_{12}$ and $B_{10}X_{12}$ (X = F, Cl, Br and I) molecules discussed in Chapters 3 – 5. At the same time these calculations have shed some light onto the explanations for the unusual bonding found in polyboron halides.

## 6.5. References


1. J. A. Morrison, *Chem. Rev.* 1991, **91**, 35.
2. D. F. Gaines, J. A. Heppert, D. E. Coons and M. W. Jorgensen, *Inorg. Chem.*, 1982, **21**, 3662.
3. D. A. Saulys and J. A. Morrison, *Inorg. Chem.*, 1990, **29**, 4174.
4. Gaussian 98, Revision A.7, M. J. Frisch, G. W. Trucks, H. B. Schlegel, G. E. Scuseria, M. A. Robb, J. R. Cheeseman, V. G. Zakrzewski, J. A. Montgomery, R. E. Stratmann Jr, J. C. Burant, S. Dapprich, J. M. Millam, A. D. Daniels, K. N. Kudin, M. C. Strain, O. Farkas, J. Tomasi, V. Barone, M. Cossi, R. Cammi, B. Mennucci, C. Pomelli, C. Adamo, S. Clifford, J. Ochterski, G. A. Petersson, P. Y. Ayala, Q. Cui, K. Morokuma, D. K. Malick, A. D. Rabuck, K. Raghavachari, J. B. Foresman, J. Cioslowski, J. V. Ortiz, A. G. Baboul, B. B. Stefanov, G. Liu, A. Liashenko, P. Piskorz, I. Komaromi, R. Gomperts, R. L. Martin, D. J. Fox, T. Keith, M. A. Al-Laham, C. Y. Peng, A. Nanayakkara, C. Gonzalez, M. Challacombe, P. M. W. Gill, B. Johnson, W. Chen, M. W. Wong, J. L. Andres, C. Gonzalez, M. Head-Gordon, E. S. Replogle and J. A. Pople, Gaussian, Inc., Pittsburgh PA, 1998.
5. T. H. Dunning Jr. and P. J. Hay, *Modern Theoretical Chemistry*, Vol. 3, Ed. H. F. Schaefer III, Plenum, 1976, p.1; P. J. Hay and W. R. Wadt, *J. Chem. Phys.*, 1985, **82**, pp. 270, 284 and 299.
6. W. J. Hehre, L. Radom, P. v. R. Schleyer and J. A. Pople, *Ab initio Molecular Orbital Theory*, J . Wiley & Sons, 1986, p.71; D. R. Hartree, *Proc. Camb. Phil. Soc.*, 1928, **24**, 89; V. Fock, *Z. Physik*, 1930, **61**, 126 and *Z. Physik*, 1930, **62**, 795.
7. J. S. Binkley, J. A. Pople and W. J. Hehre, *J. Am. Chem. Soc.*, 1980, **102**, 939; M. S. Gordon, J. S. Binkley, J. A. Pople, W. J. Pietro and W. J. Hehre, *J. Am. Chem. Soc.*, 1982, **104**, 2797; W. J. Pietro, M. M. Francl, W. J. Hehre, D. J. Defrees, J. A. Pople and J. S. Binkley, *J. Am. Chem. Soc.*, 1982, **104**, 5039.
8. W. J. Hehre, R. Ditchfield and J. A. Pople, *J. Chem. Phys.*, 1972, **56**, 2257; P. C. Hariharan and J. A. Pople, *Mol. Phys.*, 1974, **27**, 209; M. S. Gordon, *Chem. Phys. Lett.*, 1980, **76**, 163.

9. P. J. Knowles, K. Somasundram, N. C. Handy and K. Hirao, *Chem. Phys. Lett.*, 1993, **211**, 272; W. Kohn and L. J. Sham, *Phys. Rev.*,1965, **A140**, 1133.
10. A. D. McLean and G. S. Chandler, *J. Chem. Phys.*, 1980, **72**, 5639; R. Krishnan, J. S. Binkley, R. Seeger and J. A. Pople, *J. Chem. Phys.*, 1980, **72**, 650.
11. C. Møller and M. S. Plesset, *Phys. Rev.*, 1934, **46**, 618; P. Hohenburg, W. Kohn, *Phys. Rev.*, 1964, **B136**, 864.
12. PQS *Ab initio* Program Package version 2.4, Parallel Quantum Solutions, Fayetteville, Arkansas, 2001.
13. W. Hönle, Y. Grin, A. Burkhardt, U. Wedig, M. Schultheiss and H. G. von Schnering, *J. Solid State Chem.*, 1997, 59.
14. C. Präsang, M. Hofmann, G. Geiseler, W. Massa and A. Berndt, *Angew. Chem. Int. Ed.*, 2002, **41**, 1526.
15. A. Maier, M. Hofmann, H. Pritzkow and W. Siebert, *Angew. Chem. Int. Ed.*, 2002, **41**, 1529.
16. C. Präsang, M. Hofmann, G. Geiseler, W. Massa and A. Berndt, *Angew. Chem. Int. Ed.*, 2003, **42**, 1049.
17. R. Greatrex, N. N. Greenwood, D. W. H. Rankin and H. E. Robertson, *Polyhedron*, 1987, **6**, 1849.
18. R. E. Enrione, F. P. de Boer and W. N. Lipscomb, *J. Am. Chem. Soc.*, 1964, **86**, 1451.
19. I. R. Epstein, J. A. Tossell, E. Switkes, R. M. Stevens and W. N. Lipscomb, *Inorg. Chem.*, 1971, **10**, 171.
20. M. L. McKee, *J. Am. Chem. Soc.*, 1990, **112**, 6753.
21. M. L. McKee and W. N. Lipscomb, *Inorg. Chem.*, 1982, **21**, 2846.
22. M. Bühl and M. L. McKee, *Inorg. Chem.*, 1998, **37**, 4953.
23. J. F. Stanton, W. N. Lipscomb and R. J. Bartlett, *J. Am. Chem. Soc.*, 1989, **111**, 5165.
24. J. P. M. Lommerse, W. D. S. Motherwell, H. L. Ammon, J. D. Dunitz, A. Gavezzotti, D. W. M. Hofmann, F. J. J. Leusen, W. T. M. Mooij, S. L. Price, B.

Schweizer, M. U. Schmidt, B. P. van Eijck, P. Verwer and D. E. Williams, *Acta Cryst.*, 2000, **B56**, 697.

25. W. D. S. Motherwell, H. L. Ammon, J. D. Dunitz, A. Dzyabchenko, P. Erk, A. Gavezzotti, D. W. M. Hofmann, F. J. J. Leusen, J. P. M. Lommerse, W. T. M. Mooij, S. L. Price, H. Scheraga, B. Schweizer, M. U. Schmidt, B. P. van Eijck, P. Verwer and D. E. Williams, *Acta Cryst.*, 2002, **B58**, 647.
26. A. G. Massey, *Adv. Inorg. Chem and Radiochem.*, 1983, **26**, 1.
27. M. Unverzagt, G. Subramanian, M. Hofmann, P. v. R. Schleyer, S. Berger, K. Harms, W. Massa and A. Berndt, *Angew. Chem. Int. Ed.*, 1997, **36**, 1469.
28. W. Mesbah, C. Präsang, M. Hofmann, G. Geiseler, W. Massa and A. Berndt, *Angew. Chem. Int. Ed.*, 2003, **42**, 1717.
29. G. E. Ryschkewitsch and V. H. Miller, *J. Am. Chem. Soc.*, 1975, **97**, 6258.
30. M. A. Fox, R. Greatrex and D. L. Ormsby, *Chem. Commun.*, 2002, 2052.
31. M. A. Toft, J. B. Leach, F. L. Himpsl and S. G. Shore, *Inorg. Chem.*, 1982, **21**, 1952.
32. J. Dobson and R. Schaeffer, *Inorg. Chem.*, 1965, **4**, 593.
33. B. Johnston and D. W. H. Rankin, *manuscript in preparation.*
34. A. B. Berg, *J. Am. Chem. Soc.*, 1968, **90**, 1407.
35. L. H. Hall, S. Block and A. Perloff, *Acta Cryst.*, 1965, **19**, 658.
36. H. Binder, R. Kellner, K. Vaas, M. Hein, F. Baumann, M. Wanner, R. Winter, W. Kaim, W. Hönle, Y. Grin, U. Wedig, M. Schultheiss, R. K. Kremer, H. G. von Schnering, O. Groeger and G. Engelhardt, *Z. Anorg. Allg. Chem.*, 1999, **625**, 1059.
37. A. Sequiera and W. C. Hamilton, *Inorg. Chem.*, 1967, **6**, 1281.
38. T. J. Dupont, R. E. Loffredo, R. C. Haltiwanger, C. A. Turner and A. D. Norman, *Inorg. Chem.*, 1978, **17**, 2062.
39. R. Schaeffer, J. N. Shoolery and R. Jones, *J. Am. Chem. Soc.*, 1958, **80**, 2670.
40. Z. Xie, R. Bau and C. A. Reed, *Inorg. Chem.*, 1995, **34**, 5403.
41. R. J. Wiersema and M. F. Hawthorne, *Inorg. Chem.*, 1973, **12**, 785.
42. C. Viñas, G. Barberà, J. M. Oliva, F. Teixidor, A. J. Welch and G. M. Rosair, *Inorg. Chem.*, 2001, **40**, 6555.

43. S. V. Ivanov, A. J. Lupinetti, S. M. Miller, O. P. Anderson, K. A. Solntsez and S. H. Strauss, *Inorg. Chem.*, 1995, **34**, 6419.
44. T. Jelinek, P. Baldwin, W. R. Scheidt and C. A. Reed, *Inorg. Chem.*, 1993, **32**, 1982.
45. T. Jelinek, J. Plešak, S. Heřmánek and B. Štibr, *Collect. Czech. Chem. Commun.*, 1986, **51**, 819.

# Chapter Seven

## The Molecular Structures of Carboranes *closo*-2,3-$C_2B_9H_{11}$, *nido*-2,9-$C_2B_9H_{13}$ and *arachno*-6,9-$C_2B_8H_{14}$ studied by Gas-phase Electron Diffraction and Theoretical Calculations

## 7.1. Introduction

Carboranes are molecular boron clusters that contain at least one carbon atom bound into an electron-delocalised "non-classical" cage skeleton.[1] Such systems have a wide range of practical uses, such as in the areas of liquid crystal technology and boron neutron capture therapy of malignant tumours.[1] Work in this chapter investigates the gas-phase structures of *closo*-2,3-$C_2B_9H_{11}$, *nido*-2,9-$C_2B_9H_{13}$ and *arachno*-6,9-$C_2B_8H_{14}$ by both gas-phase electron diffraction and *ab initio* molecular orbital calculations.

Closed cage (*closo*) carboranes are a widely studied class of polyhedral boron cluster that possess high stability.[2] The 11-vertex *closo*-structure, an octadecahedron, has the lowest symmetry of all known *closo*-structures and is the only deltahedron to contain vertices of three different connectivities.[2] The carborane cluster *closo*-2,3-$C_2B_9H_{11}$ (Figure 1) was first synthesised in 1964 and is produced from the thermolysis of the 7,9-isomer of the *nido*-carborane $C_2B_9H_{13}$.[3] The configuration was confirmed by $^{11}B$ and $^{1}H$ NMR studies carried out at the time along with X-ray diffraction studies on the 2,3-dimethyl derivative.[4] However, until now, no diffraction studies have been carried out on the neutral carborane itself.

The *nido*-carboranes $C_2B_9H_{13}$ are isolated as either the neutral species *nido*-$C_2B_9H_{13}$ or the mono-anion *nido*-$C_2B_9H_{12}^-$, which can be deprotonated to the di-anion *nido*-$C_2B_9H_{11}^{2-}$.[5-7] These species can act as precursors to many *closo* icosahedral metallocarboranes with the twelfth vertex occupied by a metal ion. Of the nine possible cage conformations for *nido*-$C_2B_9H_{13}$, three are known, the 7,8-, 7,9- and 2,9-isomers.[5,6] These species are produced from their respective parent dicarbadodecaborane *closo*-$C_2B_{10}H_{12}$.[5] In 1964, Wiesbock and Hawthorne discovered that degradation of the *closo* icosahedral carborane 1,2-$C_2B_{10}H_{12}$ by ethanolic KOH produces the *nido*-carborane anion 7,8-$C_2B_9H_{12}^-$.[8] Similar treatment of 1,7-$C_2B_{10}H_{12}$ leads more slowly to the isomeric 7,9-$C_2B_9H_{12}^-$.[9] Plešek and Heřmánek (1973)[10] obtained the third isomer 2,9-

$C_2B_9H_{12}^-$ from 1,12-$C_2B_{10}H_{12}$, under more forcing conditions (20% KOH in propanediol, 170°C). To date, the structural characterisation of the *nido*-carboranes has relied upon *ab initio* methods and NMR evidence for the solution state geometries.[5] Experimental structure determination has been hampered by the inability of these systems to form single crystals; the reliance being upon the characterisation of various salts, for example, $(Me_2SO)_2H^+$, $(Me_2N)_3PNH_2^+$ and $(C_5H_{10}NH)_2H^+$ salts.[5] In this chapter, the first experimental structure determination of *nido*-2,9-$C_2B_9H_{13}$ (Figure 2), by gas-phase electron diffraction supplemented with high level *ab initio* calculations, is reported.

**Figure 1**. Molecular framework for *closo*-2,3-$C_2B_9H_{11}$.

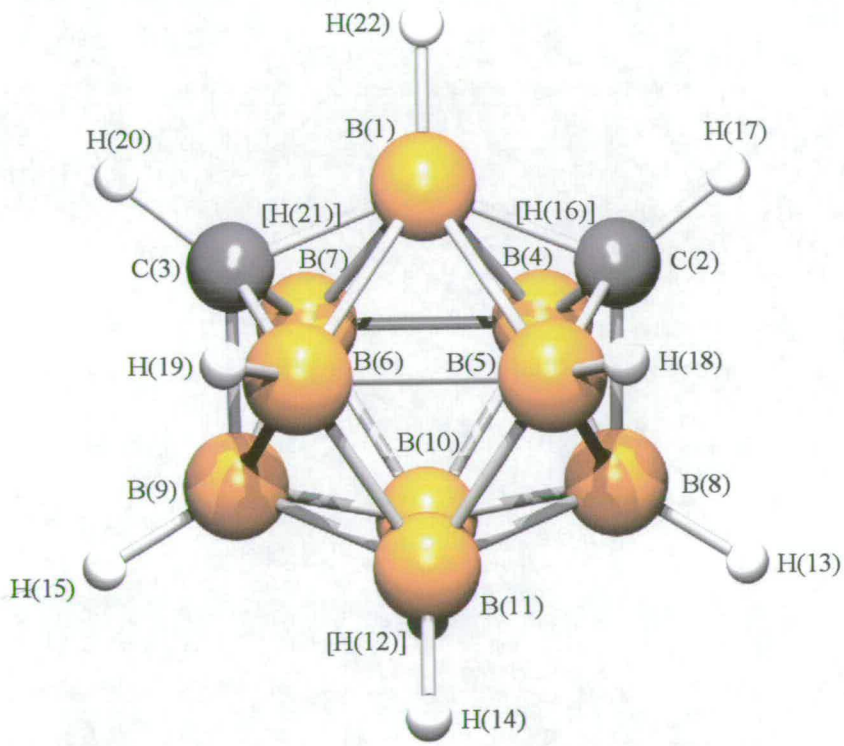

**Figure 2**. Molecular framework for *nido*-2,9-$C_2B_9H_{13}$.

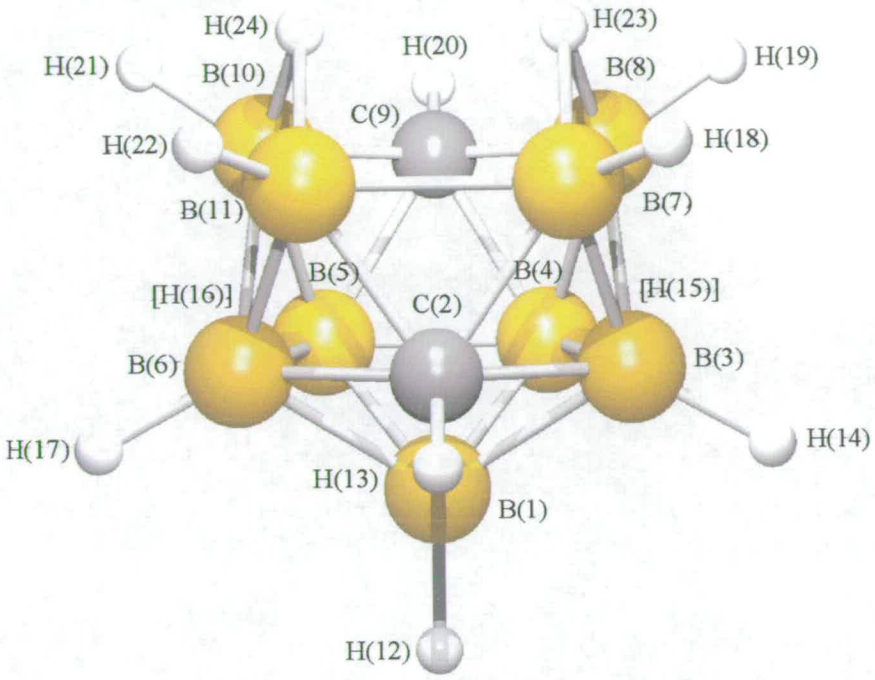


A variety of *arachno* boranes exist, perhaps the most well-known being $B_4H_{10}$ and $B_5H_{11}$, which were among the six original boranes discovered by Stock.[2] The structures of these *arachno* boranes consist of open triangulated boron networks derived from closed deltahedra by removal of two adjacent vertices.[2] *Arachno* boranes are of specific interest due to their more open structures and lower chemical stabilities compared to *closo* and *nido*-boranes.[2] One such system is *arachno*-6,9-$C_2B_8H_{14}$ (Figure 3), which has been studied by gas-phase electron diffraction and *ab initio* calculations.

**Figure 3**. Molecular framework for *arachno*-6,9-$C_2B_8H_{14}$.

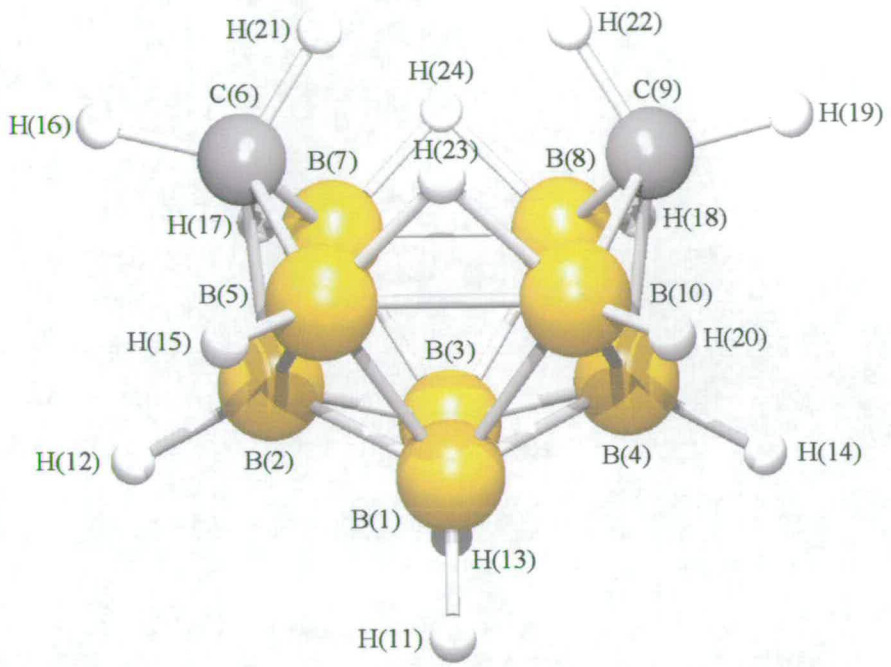


## 7.2. Experimental

### 7.2.1. Compound Synthesis

The compounds *closo*-2,3-$C_2B_9H_{11}$ and *nido*-2,9-$C_2B_9H_{13}$ were prepared by M. A. Fox (University of Durham) using literature methods.[5] The compound *arachno*-6,9-$C_2B_8H_{14}$ was prepared by J. Holub (Academy of Sciences of the Czech Republic, Rez) using literature methods.[11] The samples provided were used for GED without further purification.

### 7.2.2. Gas-phase Electron Diffraction (GED) Studies of *closo*-2,3-$C_2B_9H_{11}$, *nido*-2,9-$C_2B_9H_{13}$ and *arachno*-6,9-$C_2B_8H_{14}$

Data for *closo*-2,3-$C_2B_9H_{11}$, *nido*-2,9-$C_2B_9H_{13}$ and *arachno*-6,9-$C_2B_8H_{14}$ were collected at two different camera distances (93.9 and 257.7 mm) using the Edinburgh apparatus.[12]

Data for the *closo* and *nido* compounds were recorded photographically on Kodak Electron Image films, which were converted into digital form using a PDS densitometer at the Institute of Astronomy in Cambridge with a scanning program described elsewhere.[13] The electron scattering patterns for the *arachno* compound were converted into digital form using an Epson Expression 1600 Scanner with a scanning program described elsewhere.[14] The weighting points for the off-diagonal weight matrices, correlation parameters and scale factors for the two camera distances are given in Tables 1 - 3, together with the electron wavelengths, which were determined from the scattering patterns of benzene vapour.[13] The data reduction and analysis were performed using standard programs,[15] employing the scattering factors of Ross *et al.*[16]

**Table 1**. GED data analysis parameters for *closo*-2,3-$C_2B_9H_{11}$.

| | | |
|---|---|---|
| Camera distance /mm | 257.75 | 93.92 |
| $T_{sample}$ /K | 440 | 400 |
| $T_{nozzle}$ /K | 453 | 423 |
| $\Delta s$ /nm$^{-1}$ | 2 | 4 |
| $s_{min}$ /nm$^{-1}$ | 20 | 80 |
| $sw_1$ /nm$^{-1}$ | 40 | 100 |
| $sw_2$ /nm$^{-1}$ | 112 | 276 |
| $s_{max}$ /nm$^{-1}$ | 130 | 320 |
| Correlation parameter | 0.4497 | 0.4223 |
| Scale factor, $k^a$ | 0.722(6) | 0.612(13) |
| Electron wavelength /pm | 6.02 | 6.02 |

[a] Figures in parenthesis are the estimated standard deviations.

**Table 2**. GED data analysis parameters for *nido*-2,9-$C_2B_9H_{13}$.

| | | |
|---|---|---|
| Camera distance /mm | 257.73 | 93.71 |
| $T_{sample}$ /K | 465 | 455 |
| $T_{nozzle}$ /K | 473 | 473 |
| $\Delta s$ /nm$^{-1}$ | 2 | 4 |
| $s_{min}$ /nm$^{-1}$ | 20 | 80 |
| $sw_1$ /nm$^{-1}$ | 40 | 100 |
| $sw_2$ /nm$^{-1}$ | 112 | 276 |
| $s_{max}$ /nm$^{-1}$ | 130 | 320 |
| Correlation parameter | 0.4408 | 0.3817 |
| Scale factor, $k^a$ | 0.678(4) | 0.603(10) |
| Electron wavelength /pm | 6.02 | 6.02 |

[a] Figures in parenthesis are the estimated standard deviations.

**Table 3**. GED data analysis parameters for *arachno*-6,9-$C_2B_8H_{14}$.

| | | |
|---|---|---|
| Camera distance /mm | 257.08 | 95.99 |
| $T_{sample}$ /K | 453 | 416 |
| $T_{nozzle}$ /K | 493 | 458 |
| $\Delta s$ /nm$^{-1}$ | 2 | 4 |
| $s_{min}$ /nm$^{-1}$ | 20 | 80 |
| $sw_1$ /nm$^{-1}$ | 40 | 100 |
| $sw_2$ /nm$^{-1}$ | 112 | 276 |
| $s_{max}$ /nm$^{-1}$ | 130 | 320 |
| Correlation parameter | 0.4236 | 0.4761 |
| Scale factor, $k^a$ | 0.677(5) | 0.5443(9) |
| Electron wavelength /pm | 6.02 | 6.02 |

[a] Figures in parenthesis are the estimated standard deviations.

On the basis of the *ab initio* calculations described in section 7.2.3, electron diffraction refinements[17] were carried out for *closo*-2,3-$C_2B_9H_{11}$, *nido*-2,9-$C_2B_9H_{13}$ and *arachno*-6,9-$C_2B_8H_{14}$.

The structure of *closo*-2,3-$C_2B_9H_{11}$ was refined using twenty-two geometric parameters with a model of $C_{2v}$ symmetry. See Figure 1 for the general molecular structure and atom numbering of *closo*-2,3-$C_2B_9H_{11}$. Parameter $p_1$ defines the average of the bond

distances B(5)-B(11), B(10)-B(11) and B(8)-B(10). The differences associated with them are defined by parameters $p_2$ and $p_3$ such that $p_2$ is the difference between B(5)-B(11) and B(10)-B(11), and $p_3$ is the difference between B(5)-B(11) and B(8)-B(10). With the origin placed at the mid-point of the B(10)-B(11) bond, the fold angle for atom B(8) is defined by $p_4$. The distances between the origin and atoms B(1) and C(2) are described by parameters $p_5$ and $p_6$. Parameter $p_7$ defines the angle made between atom B(1), the origin and atom C(2), whilst the angle B(5)-B(11)-B(10) is defined by $p_8$. Parameter $p_9$ describes the torsional angle B(5)-B(11)-B(10)-B(1). The mean of the bond distances B(1)-H(22), C(2)-H(17) and B(5)-H(18), and the subsequent associated differences are defined by parameters $p_{10}$ - $p_{12}$. $p_{11}$ is the difference between B(1)-H(22) and C(2)-H(17), and $p_{12}$ is the difference between B(1)-H(22) and B(5)-H(18).The angle that H(22) makes with B(1) and B(11) is included as $p_{13}$, with the associated torsion with B(10) defined as $p_{14}$. Angle H(17)-C(2)-B(8) and torsion H(17)-C(2)-B(8)-B(9) are defined as parameters $p_{15}$ and $p_{16}$. The angle made by H(18)-B(5)-B(6) and torsion H(18)-B(5)-B(6)-B(7) are described by $p_{17}$ and $p_{18}$. Angle H(13)-B(8)-C(2) and the associated torsion with B(9) are defined by $p_{19}$ and $p_{20}$ respectively. The final two parameters, $p_{21}$ and $p_{22}$, define the angle H(14)-B(11)-B(10) and torsion H(14)-B(11)-B(10)-B(1) respectively.

The structure of *nido*-2,9-$C_2B_9H_{13}$ was refined with a model of $C_s$ symmetry using twenty-five geometric parameters. The structure of *nido*-2,9-$C_2B_9H_{13}$ obtained in the GED refinement is shown in Figure 2. Parameter $p_1$ defines the average of the bond distances B(7)-B(11), B(4)-B(5), B(5)-B(6), C(2)-B(6), B(7)-B(8), B(8)-C(9), B(1)-B(5) and B(1)-B(6). The differences between B(7)-B(11) and each of these bond distances are defined by parameters $p_2$ – $p_8$ respectively. Parameter $p_9$ describes the terminal B-H bond distances, whilst the C-H and bridging B-H distances are defined by $p_{10}$ and $p_{11}$. The angles B(4)-B(5)-B(6), C(2)-B(3)-B(6), B(8)-B(7)-B(11) and C(9)-B(10)-B(8) are defined as $p_{12}$ – $p_{15}$ respectively. Parameter $p_{16}$ defines the angle B(7)-H(23)-B(8). The angle B(5)-B(1)-H(12) is defined by $p_{17}$. To move the origin from the mid-point of B(3)-B(6) to the mid-point of B(7)-B(11) parameters $p_{18}$ and $p_{19}$ describe the displacements in

the $y$ (perpendicular to the plane of the paper in Figure 2) and $z$ (vertical) directions. The torsional angles C(2)-B(3)-B(6)-B(5) and C(9)-B(8)-B(10)-B(11), which describe the movement of each carbon out of the plane of their respective rings, are defined by $p_{20}$ and $p_{21}$. In addition to the displacement between the rings, on the basis of *ab initio* calculations (see section 7.3.2.), there exists a significant tilt of the upper ring such that atoms B(8), C(9) and B(10) move away from the lower ring. This tilt is defined by $p_{22}$. Moving the origin to the centre of the boron cage, the angles origin-B(5)-H(16) and origin-B(4)-H(15) are defined by $p_{23}$, whilst the angles origin-B(3)-H(14) and origin-B(6)-H(17) are defined by $p_{24}$. Parameter $p_{25}$ describes the torsion B(4)-B(5)-B(1)-H(12).

The structure of *arachno*-6,9-$C_2B_8H_{14}$ was refined in $C_{2v}$ symmetry using twenty-two geometric parameters. The structure of *arachno*-6,9-$C_2B_8H_{14}$ obtained in the GED refinement is shown in Figure 3. The mean of the bond distances B(1)-B(3), B(1)-B(2) and B(1)-B(5) is defined by $p_1$. Parameters $p_2$ and $p_3$ define the differences between B(1)-B(3) and B(1)-B(2) and between B(1)-B(3) and B(1)-B(5), respectively. With the origin placed at the mid-point of B(1)-B(3), the basal butterfly is formed with atoms B(2) and B(4) through the fold angle defined by $p_4$. The distance from the origin to C(6), and the fold angle required to put C(6) into position are described by $p_5$ and $p_6$. $p_7$ defines the angle B(5)-B(1)-B(3). Average and difference values were used for B-H(bridge), C-H and B-H(terminal) [$p_8 - p_{10}$]. The difference between B-H(bridge) and C-H is defined by $p_9$, and the difference between B-H(bridge) and B-H(terminal) is defined by $p_{10}$. The angles B(3)-B(1)-H(11), B(4)-B(2)-H(12), B(1)-B(5)-H(15), B(2)-C(6)-H(16), B(2)-C(6)-H(21) and B(10)-B(5)-H(23) are defined by $p_{11} - p_{16}$ respectively. Parameters $p_{17} - p_{22}$ define the torsional angles B(4)-B(3)-B(1)-B(5), B(1)-B(4)-B(2)-H(12), B(3)-B(1)-B(5)-H(15), B(4)-B(2)-C(6)-H(16), B(4)-B(2)-C(6)-H(21) and B(8)-B(10)-B(5)-H(23) respectively.

### 7.2.3. *Ab initio* and DFT Calculations

All calculations were performed using the Gaussian 98 computer program.[18] Calculations were performed for the compounds *closo*-2,3-$C_2B_9H_{11}$ and *nido*-2,9-$C_2B_9H_{13}$ using HF[19] (3-21G*[20] and 6-31G*[21] basis sets), DFT[22] (6-31G* and 6-311G*[23] basis sets using the B3LYP[24] functional) and MP2[25] (6-31G*, 6-311G* and 6-311+G* basis sets) methods. Calculations were performed for the compound *arachno*-6,9-$C_2B_8H_{14}$ using HF (3-21G* and 6-31G* basis sets), DFT (6-31G*, 6-311G* and 6-311+G* basis sets using the B3LYP functional) and MP2 (6-31G* and 6-311G* basis sets) methods.

Frequency calculations allowed the nature of any stationary points to be determined, confirming the structures as local minima, transition states or higher order stationary points on the potential-energy surfaces. The starting parameters for the $r_{h1}$ refinement were taken from the theoretical geometry at the HF/6-31G* level. Theoretical (HF/6-31G*) Cartesian force fields were obtained and converted into force fields described by sets of symmetry coordinates using the SHRINK[26] program. All geometric parameters were then refined.

## 7.3. Results

### 7.3.1. GED Refinements for *closo*-2,3-$C_2B_9H_{11}$, *nido*-2,9-$C_2B_9H_{13}$ and *arachno*-6,9-$C_2B_8H_{14}$

The model used for the GED refinement of *closo*-2,3-$C_2B_9H_{11}$ was based upon the geometry obtained from the optimised *ab initio* calculations. The least-squares refinement of the structure resulted in an $R_G$ factor of 0.041, with the resultant parameter values listed in Table 4. A summary of final bond distances and amplitudes of vibration are recorded in Table 5. Of the twenty-two parameters, eight refined without the

application of restraints. The restraints applied using the SARACEN method[27] are detailed in Appendix D. For a full list of final bond distances and amplitudes of vibration, see Appendix D. The least-squares correlation matrix for the structural refinement is given in Table 6. The success of the final refinement can be assessed on the basis of the molecular scattering curves (Figure 4) and the radial distribution curve (Figure 5).

**Table 4**. Geometrical parameters ($r_{h1}$ structure) for *closo*-2,3-$C_2B_9H_{11}$.[a,b]

| | Parameter | GED | MP2/6-311+G* |
|---|---|---|---|
| $p_1$ | $rB_m$[c] | 182.8(3) | 180.1 |
| $p_2$ | $d1$[c] | -5.9(5) | -6.2 |
| $p_3$ | $d2$[c] | -0.4(1) | -0.4 |
| $p_4$ | ∠B(8) | 16.9(4) | 14.7 |
| $p_5$ | $r$oB(1) | 271.2(5) | 270.9 |
| $p_6$ | $r$oC(2) | 259.6(11) | 254.1 |
| $p_7$ | ∠C(2) | 35.3(3) | 39.3 |
| $p_8$ | ∠BBB | 103.1(2) | 103.9 |
| $p_9$ | BBBB | -32.7(2) | -32.8 |
| $p_{10}$ | $rH_m$[c] | 117.2(3) | 115.4 |
| $p_{11}$ | $d3$[c] | 11.4(4) | 10.6 |
| $p_{12}$ | $d4$[c] | 0.3(1) | 0.3 |
| $p_{13}$ | ∠HBB1 | 161.2(1) | 161.2 |
| $p_{14}$ | ϕHBBB1 | 180.0(2) | 180.0 |
| $p_{15}$ | ∠HCB | 128.2(2) | 128.2 |
| $p_{16}$ | ϕHCBB | 180.0(2) | 180.0 |
| $p_{17}$ | ∠HBB2 | 114.6(2) | 114.6 |
| $p_{18}$ | ϕHBBB2 | 165.6(2) | 165.7 |
| $p_{19}$ | ∠HBC | 120.4(2) | 120.4 |
| $p_{20}$ | ϕHBCB | 180.0(2) | 180.0 |
| $p_{21}$ | ∠HBB3 | 127.6(2) | 127.6 |
| $p_{22}$ | ϕHBBB3 | 180.0(2) | 180.0 |

[a] distances in pm, angles in °.
[b] see text for parameter definitions.
[c] m = mean, d = difference.

**Table 5**. Bond distances ($r_{h1}$/pm) and amplitudes of vibration ($u$/pm) obtained in the GED refinement of *closo*-2,3-$C_2B_9H_{11}$.

| $u$ | Atom pair | $r_{h1}$ | Amplitude | MP2/6-311+G* |
|---|---|---|---|---|
| $u_1$ | B(1)-C(2) | 162.2(11) | 6.8(tied to $u_5$) | 163.1 |
| $u_3$ | B(1)-H(22) | 121.0(3) | 8.1(fixed) | 119.0 |
| $u_5$ | C(2)-B(5) | 157.9(5) | 7.2(1) | 157.9 |
| $u_6$ | C(2)-B(8) | 167.0(11) | 6.8(tied to $u_5$) | 166.8 |
| $u_7$ | C(2)-H(17) | 109.6(4) | 7.3(fixed) | 108.4 |
| $u_{12}$ | B(4)-B(7) | 188.6(11) | 13.5(5) | 187.0 |
| $u_{14}$ | B(4)-B(10) | 180.7(3) | 7.0(tied to $u_{23}$) | 177.9 |
| $u_{15}$ | B(4)-H(16) | 120.7(3) | 8.1(fixed) | 118.7 |
| $u_{23}$ | B(7)-B(9) | 177.4(6) | 6.7(2) | 180.1 |
| $u_{26}$ | B(8)-B(10) | 180.8(3) | 7.9(tied to $u_{23}$) | 178.3 |
| $u_{28}$ | B(8)-H(13) | 120.7(3) | 8.1(fixed) | 118.7 |
| $u_{32}$ | B(10)-B(11) | 186.6(5) | 7.4(tied to $u_{12}$) | 184.1 |
| $u_{33}$ | B(10)-H(12) | 121.0(3) | 8.1(fixed) | 119.0 |
| $u_{35}$ | B(1)-B(4) | 200.0(7) | 24.6(9) | 206.7 |

**Table 6**. Least-squares correlation matrix (x100) for GED structure refinement of *closo*-2,3-$C_2B_9H_{11}$.[a]

| | $p_1$ | $p_4$ | $p_7$ | $p_9$ | $u_{84}$ |
|---|---|---|---|---|---|
| $p_1$ | | 73 | | | |
| $p_6$ | 63 | 80 | -81 | | -56 |
| $p_8$ | -70 | | | | |
| $u_{69}$ | | 55 | -88 | | |
| $k_1$[b] | | | | -59 | |

[a] Only elements with absolute values >50% are shown.
[b] Scale factor.

**Figure 4**. Experimental and final weighted difference (experimental – theoretical) molecular scattering intensities for *closo*-2,3-$C_2B_9H_{11}$.

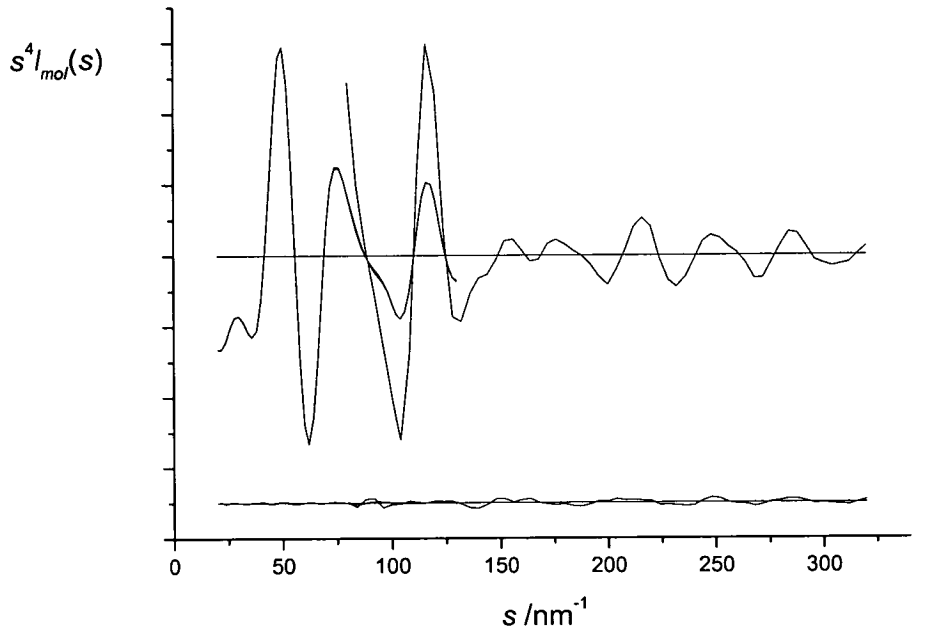


**Figure 5**. Experimental and difference (experimental – theoretical) radial distribution curves, $P(r)/r$ for *closo*-2,3-$C_2B_9H_{11}$. Before Fourier inversion the data were multiplied by $s.\exp(-0.00002s^2)/(Z_B-f_B)/(Z_C-f_C)$.

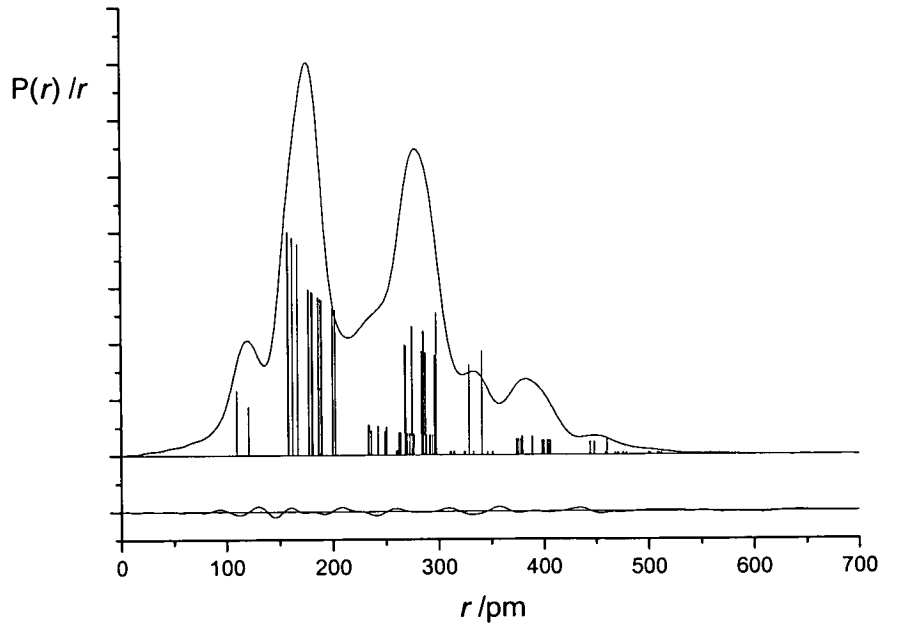

The model used for the GED refinement of *nido*-2,9-$C_2B_9H_{13}$ was based upon the geometry obtained from the optimised *ab initio* calculations. The least-squares refinement of the structure resulted in an $R_G$ factor of 0.035, with the resultant parameter values listed in Table 7. A summary of final bond distances and amplitudes of vibration are recorded in Table 8. Of the twenty-five parameters, five refined without the application of restraints. The restraints applied using the SARACEN method[27] are detailed in Appendix D. For a full list of final bond distances and amplitudes of vibration, see Appendix D. The least-squares correlation matrix for the structural refinement is labelled Table 9. The success of the final refinement can be assessed on the basis of the molecular scattering curves (Figure 6) and the radial distribution curve (Figure 7).

**Table 7**. Geometrical parameters ($r_{h1}$ structure) for *nido*-2,9-$C_2B_9H_{13}$.[a,b]

| | Parameter | GED | MP2/6-311+G* |
|---|---|---|---|
| $p_1$ | $r_m$ | 181.2(2) | 178.2 |
| $p_2$ | $d1^c$ | 17.5(1) | 17.5 |
| $p_3$ | $d2^c$ | 15.9(1) | 16.0 |
| $p_4$ | $d3^c$ | 20.7(1) | 20.8 |
| $p_5$ | $d4^c$ | 8.5(1) | 8.7 |
| $p_6$ | $d5^c$ | 27.9(1) | 28.0 |
| $p_7$ | $d6^c$ | 16.9(1) | 17.0 |
| $p_8$ | $d7^c$ | 13.6(1) | 13.7 |
| $p_9$ | *r*BH | 120.3(3) | 118.7 |
| $p_{10}$ | *r*CH | 111.6(5) | 108.7 |
| $p_{11}$ | *r*BH(br) | 134.2(6) | 127.2 |
| $p_{12}$ | ∠BBB1 | 108.9(2) | 109.3 |
| $p_{13}$ | ∠CBB1 | 29.9(3) | 31.9 |
| $p_{14}$ | ∠BBB2 | 100.2(3) | 102.7 |
| $p_{15}$ | ∠CBB2 | 32.9(4) | 33.8 |
| $p_{16}$ | ∠BBH(br) | 50.7(5) | 48.2 |
| $p_{17}$ | ∠BBH | 127.4(12) | 127.4 |
| $p_{18}$ | $dY^c$ | 83.9(4) | 81.7 |
| $p_{19}$ | $dZ^c$ | 142.6(5) | 149.3 |
| $p_{20}$ | ϕCBBB1 | 4.1(1) | 4.1 |
| $p_{21}$ | ϕCBBB2 | 11.7(1) | 11.8 |
| $p_{22}$ | ringTilt | -3.8(1) | -4.0 |

| | | | |
|---|---|---|---|
| $p_{23}$ | H(15)tilt | -47.8(11) | -48.0 |
| $p_{24}$ | H(14)tilt | -60.7(12) | -60.5 |
| $p_{25}$ | ϕBBBH | 64.0(12) | 63.9 |

[a] distances in pm, angles in °.
[b] see text for parameter definitions.
[c] differences as described in text.

**Table 8**. Bond distances ($r_{h1}$/pm) and amplitudes of vibration ($u$/pm) obtained in the GED refinement of *nido*-2,9-$C_2B_9H_{13}$.

| $u$ | Atom pair | $r_{h1}$ | Amplitude | MP2/6-311+G* |
|---|---|---|---|---|
| $u_1$ | B(1)-C(2) | 169.7(5) | 3.7(5) | 169.5 |
| $u_2$ | B(1)-B(3) | 182.8(3) | 3.9(tied to $u_1$) | 179.7 |
| $u_3$ | B(1)-B(4) | 179.6(3) | 3.7(tied to $u_1$) | 176.4 |
| $u_6$ | B(1)-H(12) | 120.2(3) | 7.5(tied to $u_{35}$) | 118.6 |
| $u_7$ | C(2)-B(3) | 171.9(8) | 4.0(tied to $u_1$) | 172.6 |
| $u_9$ | C(2)-B(7) | 168.2(4) | 3.7(tied to $u_1$) | 167.5 |
| $u_{11}$ | C(2)-H(13) | 111.5(5) | 6.8(tied to $u_{35}$) | 108.8 |
| $u_{12}$ | B(3)-B(4) | 180.6(2) | 3.8(tied to $u_1$) | 177.4 |
| $u_{13}$ | B(3)-B(7) | 173.0(4) | 3.8(tied to $u_1$) | 177.3 |
| $u_{14}$ | B(3)-B(8) | 185.2(5) | 3.9(tied to $u_1$) | 179.1 |
| $u_{15}$ | B(3)-H(14) | 120.2(3) | 7.5(tied to $u_{35}$) | 118.6 |
| $u_{16}$ | B(4)-B(5) | 179.0(3) | 3.6(tied to $u_1$) | 175.9 |
| $u_{17}$ | B(4)-B(8) | 175.4(6) | 4.0(tied to $u_1$) | 181.7 |
| $u_{18}$ | B(4)-C(9) | 169.5(4) | 3.7(tied to $u_1$) | 168.5 |
| $u_{27}$ | B(7)-B(8) | 187.8(3) | 4.1(tied to $u_1$) | 184.7 |
| $u_{28}$ | B(7)-B(11) | 196.1(2) | 8.4(10) | 193.4 |
| $u_{30}$ | B(7)-H(23) | 134.2(6) | 9.0(10) | 127.2 |
| $u_{31}$ | B(8)-C(9) | 160.3(7) | 3.7(tied to $u_1$) | 165.3 |
| $u_{38}$ | B(10)-H(24) | 139.6(13) | 12.3(12) | 137.8 |

**Table 9**. Least-squares correlation matrix (x100) for GED structure refinement of *nido*-2,9-$C_2B_9H_{13}$.[a]

| | $p_1$ | $p_{12}$ | $p_{14}$ | $p_{19}$ | $u_{62}$ | $u_{164}$ |
|---|---|---|---|---|---|---|
| $p_1$ | | | -56 | -63 | | |
| $p_{13}$ | | 66 | | -52 | -68 | 74 |
| $p_{15}$ | -55 | | | | | |
| $u_1$ | | | 55 | | | |
| $u_{62}$ | | -64 | | 56 | | -75 |

[a] Only elements with absolute values >50% are shown.

**Figure 6**. Experimental and final weighted difference (experimental – theoretical) molecular scattering intensities for *nido*-2,9-$C_2B_9H_{13}$.

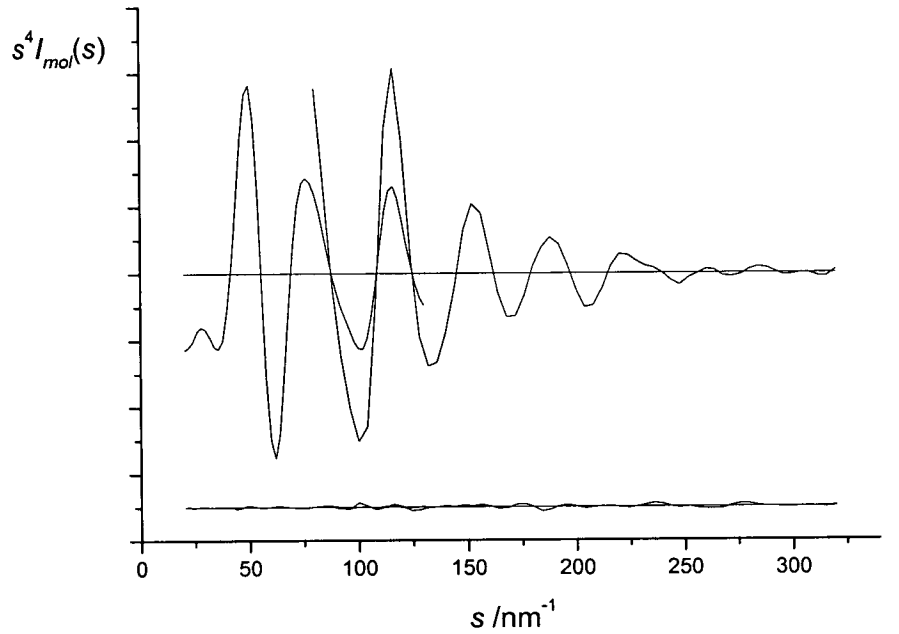

**Figure 7**. Experimental and difference (experimental – theoretical) radial distribution curves, $P(r)/r$ for *nido*-2,9-$C_2B_9H_{13}$. Before Fourier inversion the data were multiplied by $s.\exp(-0.00002s^2)/(Z_B-f_B)/(Z_C-f_C)$.

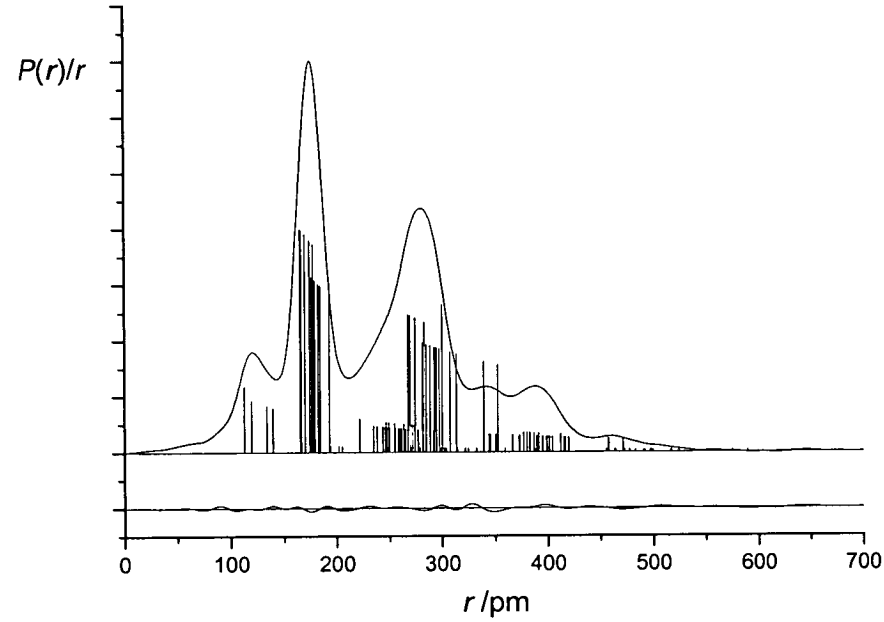


The model used for the GED refinement of *arachno*-6,9-$C_2B_8H_{14}$ was based upon the geometry obtained from the optimised *ab initio* calculations. The least-squares refinement of the structure resulted in an $R_G$ factor of 0.035, with the resultant parameter values listed in Table 10. A summary of final bond distances and amplitudes of vibration are recorded in Table 11. Of the twenty-five parameters, five refined without the application of restraints. The restraints applied using the SARACEN method[27] are detailed in Appendix D. For a full list of final bond distances and amplitudes of vibration, see Appendix D. The least-squares correlation matrix for the structural refinement is labelled Table 12. The success of the final refinement can be assessed on the basis of the molecular scattering curves (Figure 8) and the radial distribution curve (Figure 9).

**Table 10**. Geometrical parameters ($r_{h1}$ structure) for *arachno*-6,9-$C_2B_8H_{14}$.[a,b]

| | Parameter | GED | MP2/6-311G* |
|---|---|---|---|
| $p_1$ | $r$BB$_m$ | 176.2(5) | 178.9 |
| $p_2$ | $d1$[c] | 8.2(1) | 7.2 |
| $p_3$ | $d2$[c] | 2.2(1) | 1.9 |
| $p_4$ | ∠B(2) | 20.0(7) | 20.2 |
| $p_5$ | $r$oC | 269.7(1) | 268.4 |
| $p_6$ | ∠C(6) | 54.7(3) | 54.1 |
| $p_7$ | ∠BBB | 109.2(2) | 107.3 |
| $p_8$ | $r$H$_m$ | 122.9(2) | 119.9 |
| $p_9$ | $d3$[c] | 23.2(1) | 23.5 |
| $p_{10}$ | $d4$[c] | 13.4(1) | 13.4 |
| $p_{11}$ | ∠BBH1 | 120.3(5) | 120.3 |
| $p_{12}$ | ∠BBH2 | 152.4(5) | 153.2 |
| $p_{13}$ | ∠BBH3 | 120.4(5) | 120.0 |
| $p_{14}$ | ∠HCB1 | 109.9(5) | 110.0 |
| $p_{15}$ | ∠HCB2 | 140.7(5) | 140.4 |
| $p_{16}$ | ∠HCB3 | 44.4(4) | 45.0 |
| $p_{17}$ | ϕBBBB | 103.6(10) | 102.7 |
| $p_{18}$ | ϕHBBB1 | -61.1(5) | -60.5 |
| $p_{19}$ | ϕHBBB2 | 146.4(5) | 145.5 |
| $p_{20}$ | ϕHCBB1 | 180.0(5) | 180.0 |
| $p_{21}$ | ϕHCBB2 | 0.0(5) | 0.0 |
| $p_{22}$ | ϕHCBB3 | -107.0(5) | -106.9 |

[a] distances in pm, angles in °.
[b] see text for parameter definitions.
[c] differences as described in text.

**Table 11**. Bond distances ($r_{h1}$/pm) and amplitudes of vibration ($u$/pm) obtained in the GED refinement of *arachno*-6,9-$C_2B_9H_{13}$.

| $u$ | Atom pair | $r_{h1}$ | Amplitude | MP2/6-311G* |
|---|---|---|---|---|
| $u_1$ | B(1)-B(2) | 171.5(5) | 7.3(tied to $u_{17}$) | 174.7 |
| $u_2$ | B(1)-B(3) | 179.9(5) | 7.1(tied to $u_{20}$) | 181.9 |
| $u_4$ | B(1)-B(5) | 177.4(5) | 7.4(tied to $u_{20}$) | 180.0 |
| $u_6$ | B(1)-H(11) | 121.6(3) | 8.1(fixed) | 118.8 |
| $u_8$ | B(2)-B(5) | 178.9(8) | 7.0(tied to $u_{20}$) | 177.8 |
| $u_{11}$ | B(2)-H(12) | 121.63 () | 8.1(fixed) | 118.8 |
| $u_{17}$ | B(4)-C(9) | 171.2(13) | 7.6(4) | 166.8 |

| | | | | |
|---|---|---|---|---|
| $u_{20}$ | B(5)-C(6) | 179.9(8) | 8.4(2) | 174.0 |
| $u_{21}$ | B(5)-H(15) | 121.6(3) | 8.1(fixed) | 118.9 |
| $u_{22}$ | B(5)-H(23) | 135.3(3) | 10.2(fixed) | 132.1 |
| $u_{24}$ | C(6)-H(16) | 111.8(3) | 7.3(fixed) | 108.6 |
| $u_{25}$ | C(6)-H(21) | 111.8(3) | 7.4(fixed) | 108.8 |

**Table 12**. Least-squares correlation matrix (x100) for GED structure refinement of *arachno*-6,9-$C_2B_8H_{14}$.[a]

| | $p_1$ | $p_5$ | $p_7$ | $k_1$[b] |
|---|---|---|---|---|
| $p_1$ | | | -57 | |
| $p_4$ | 57 | 73 | | |
| $p_6$ | | 57 | | |
| $p_{17}$ | -63 | -68 | | |
| $k_2$[b] | | | | 54 |

[a] Only elements with absolute values >50% are shown.
[b] Scale factor.

**Figure 8**. Experimental and final weighted difference (experimental – theoretical) molecular scattering intensities for *arachno*-6,9-$C_2B_8H_{14}$.

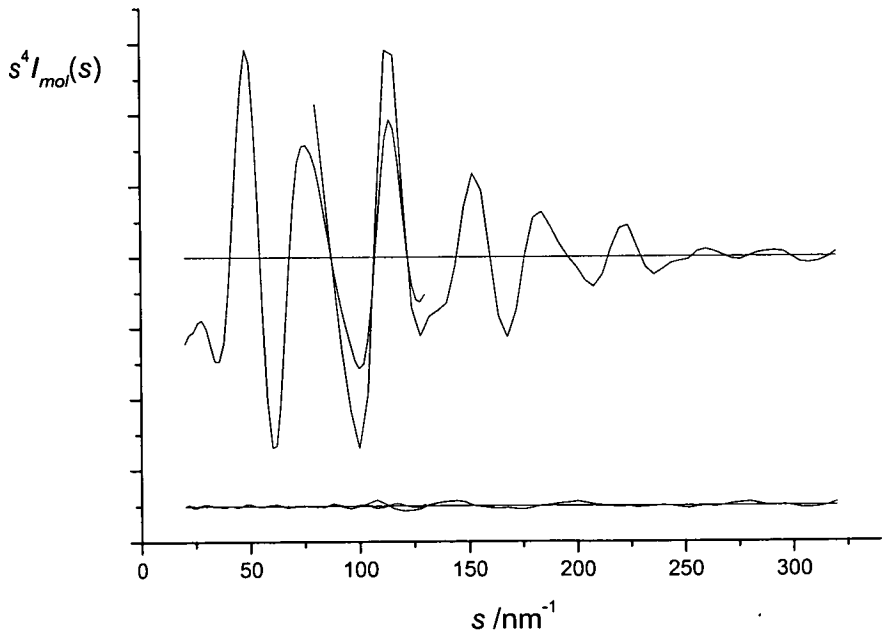

**Figure 9**. Experimental and difference (experimental – theoretical) radial distribution curves, $P(r)/r$ for *arachno*-6,9-$C_2B_8H_{14}$. Before Fourier inversion the data were multiplied by $s.\exp(-0.00002s^2)/(Z_B-f_B)/(Z_C-f_C)$.

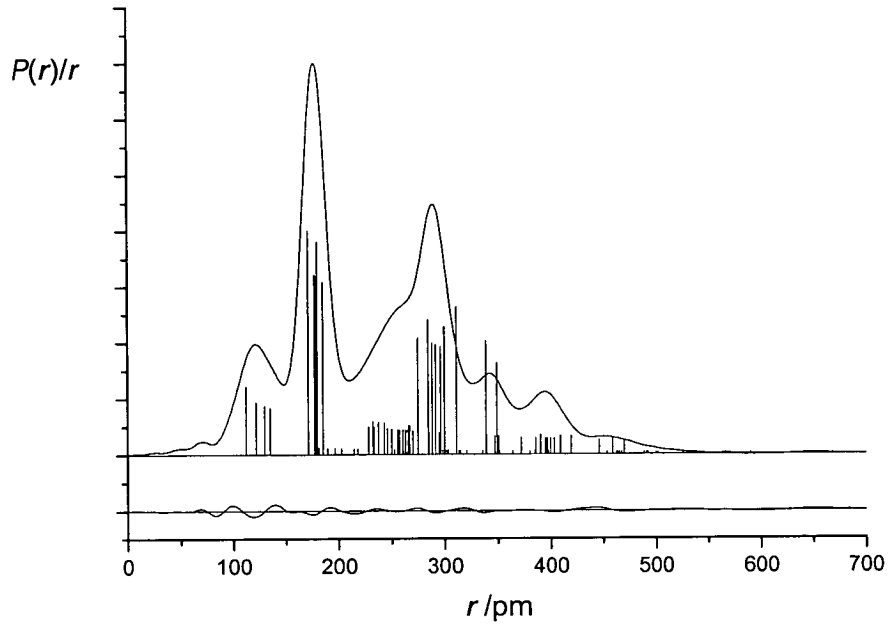


### 7.3.2. *Ab initio* and DFT calculations

For each of the three molecules studied in this chapter, no imaginary frequencies were returned, indicating that these structures are minima on their respective potential energy surfaces (see Tables 13 -15).

For *closo*-2,3-$C_2B_9H_{11}$ (see Table 13 and Figure 1, p. 212) cage distances are insensitive to improvements in basis set (from 6-31G* to 6-311G* and 6-311+G*), but do show some signs of sensitivity to increased levels of theory. In particular, HF methods generally overestimate the B-B and C-B bond distances and underestimate the B-H and C-H bond distances compared to the B3LYP and MP2 methods. For example, comparison of the B(1)-B(4) bond at the MP2/6-311+G* level to that calculated by HF methods shows that at the MP2 level it is 8.3 and 2.7 pm shorter than when the 3-21G*

and 6-31G* basis sets are used at the HF level respectively. Also, bonds B(4)-H(16) and B(8)-H(17) are longer at the MP2/6-311+G* level compared to the HF/3-21G* (+ 1.1 pm) and HF/6-31G* (+ 0.7 pm) calculated values. With the exception of the HF level, increasing the size of the basis set (from 6-31G* to 6-311G* at the B3LYP level, and from 6-31G* to 6-311G* to 6-311+G* at the MP2 level) has little effect on the structural parameters. Indeed there is negligible difference between the parameters calculated using the B3LYP functional and the more computationally demanding MP2 methodology. The largest difference between these methods arises for the B(1)-B(4) bond which is 1.9 pm longer at the B3LYP/6-311G* level compared to the MP2/6-311G* value.

Increasing the size of the basis set from 3-21G* to 6-31G* at the HF level reduces the length of each bond in *nido*-2,9-$C_2B_9H_{13}$ (see Table 14 and Figure 2, p. 213), with the exception of C(2)-H(13) and B(7)-H(23). These bonds increase by 0.3 and 0.1 pm respectively. The bond that decreases the most at this level is B(7)-B(11) – by 5.9 pm. When correlated methods are employed, increasing the size of the basis set (from 6-31G* to 6-311G* at the B3LYP level, and from 6-31G* to 6-311G* to 6-311+G* at the MP2 level) has little effect on the structural parameters.

The bond distance B(7)-B(11) in *nido*-2,9-$C_2B_9H_{13}$ is the most variant between the methodologies employed. Without the inclusion of electron correlation this bond is at its longest. For example, its value at the HF/6-31G* level is 5.2 and 10.0 pm longer than at the B3LYP and MP2 levels respectively, using equivalent basis sets. Comparison of the B3LYP/6-311G* and MP2/6-311G* values for this bond show the DFT calculated distance to be 4.5 pm longer.

**Table 13.** Calculated ($r_e$) and experimental ($r_{h1}$) structure of *closo*-2,3-$C_2B_9H_{11}$ (pm).

| Geometric parameter | Level of theory / Basis set | | | | | | | GED |
|---|---|---|---|---|---|---|---|---|
| | HF | | B3LYP | | MP2 | | | |
| | 3-21G* | 6-31G* | 6-31G* | 6-311G* | 6-31G* | 6-311G* | 6-311+G* | |
| B(1)-C(2) | 163.8 | 162.8 | 162.2 | 162.1 | 162.5 | 163.1 | 163.1 | 162.2(10) |
| B(1)-B(4) | 215.0 | 209.4 | 208.1 | 208.6 | 205.6 | 206.7 | 206.7 | 200.0(7) |
| C(2)-B(4) | 159.3 | 157.0 | 157.6 | 157.6 | 157.3 | 157.9 | 157.9 | 158.3(5) |
| C(2)-B(8) | 170.3 | 166.9 | 167.0 | 167.0 | 165.9 | 166.8 | 166.8 | 167.0(10) |
| B(4)-B(7) | 192.8 | 190.5 | 187.5 | 187.3 | 186.1 | 187.0 | 187.0 | 188.6(11) |
| B(7)-B(9) | 181.1 | 179.4 | 179.2 | 179.1 | 179.2 | 180.1 | 180.1 | 177.4(6) |
| B(4)-B(10) | 179.3 | 178.1 | 177.3 | 177.2 | 177.1 | 178.3 | 177.9 | 180.6(2) |
| B(8)-B(10) | 179.8 | 179.2 | 178.0 | 178.0 | 177.6 | 178.3 | 178.3 | 180.8(3) |
| B(10)-B(11) | 190.3 | 188.3 | 185.7 | 185.8 | 183.5 | 184.1 | 184.1 | 186.6(5) |
| B(1)-H(22) | 117.7 | 118.1 | 118.7 | 118.5 | 119.0 | 119.0 | 119.0 | 121.0(3) |
| C(2)-H(17) | 106.8 | 107.2 | 108.3 | 108.1 | 108.5 | 108.4 | 108.4 | 109.6(4) |
| B(4)-H(16) | 117.6 | 118.0 | 118.5 | 118.3 | 118.8 | 118.7 | 118.7 | 120.7(3) |
| B(8)-H(13) | 117.6 | 118.0 | 118.5 | 118.2 | 118.8 | 118.7 | 118.7 | 120.7(3) |
| B(10)-H(12) | 118.1 | 118.4 | 118.9 | 118.6 | 119.1 | 119.0 | 119.0 | 120.9(3) |
| Energy[a] | -302.6029 | -304.3337 | -306.6210 | -306.6608 | -305.4362 | -305.5245 | -305.5279 | |

[a] absolute energy in Hartrees.

**Table 14**. Calculated ($r_e$) and experimental ($r_{h1}$) structure of *nido*-2,9-$C_2B_9H_{13}$ (pm).

| Geometric Parameter | Level of theory / Basis set | | | | | | | GED |
|---|---|---|---|---|---|---|---|---|
| | HF | | B3LYP | | MP2 | | | |
| | 3-21G* | 6-31G* | 6-31G* | 6-311G* | 6-31G* | 6-311G* | 6-311+G* | |
| B(1)-C(2) | 170.7 | 169.9 | 169.7 | 169.7 | 168.9 | 169.6 | 169.5 | 169.7(5) |
| B(1)-B(3) | 183.3 | 180.8 | 179.9 | 179.8 | 178.8 | 179.7 | 179.7 | 182.8(2) |
| B(1)-B(4) | 177.0 | 175.9 | 175.9 | 175.8 | 175.5 | 176.3 | 176.4 | 179.5(2) |
| C(2)-B(3) | 178.2 | 174.2 | 173.4 | 173.3 | 171.9 | 172.6 | 172.6 | 171.9(8) |
| C(2)-B(7) | 169.4 | 167.5 | 167.2 | 167.1 | 166.9 | 167.5 | 167.5 | 168.2(4) |
| B(3)-B(4) | 178.6 | 178.2 | 177.3 | 177.2 | 176.7 | 177.4 | 177.4 | 180.6(2) |
| B(3)-B(7) | 176.6 | 175.5 | 175.7 | 175.7 | 176.3 | 177.3 | 177.3 | 173.0(4) |
| B(3)-B(8) | 180.8 | 180.2 | 179.3 | 179.3 | 178.4 | 179.1 | 179.1 | 185.2(5) |
| B(4)-B(5) | 175.3 | 174.2 | 174.7 | 174.6 | 174.9 | 175.8 | 175.9 | 179.0(3) |
| B(4)-B(8) | 187.6 | 184.5 | 182.2 | 182.2 | 180.9 | 181.7 | 181.7 | 175.4(6) |
| B(4)-C(9) | 172.9 | 168.9 | 168.5 | 168.5 | 167.6 | 168.5 | 168.5 | 169.5(4) |
| B(7)-B(8) | 186.2 | 185.2 | 185.3 | 185.1 | 184.2 | 184.7 | 184.7 | 187.7(3) |
| B(7)-B(11) | 209.1 | 203.2 | 198.0 | 197.7 | 193.2 | 193.2 | 193.4 | 196.1(2) |
| B(8)-C(9) | 164.2 | 164.6 | 164.9 | 164.7 | 165.0 | 165.3 | 165.3 | 160.3(7) |
| B(1)-H(12) | 117.5 | 117.8 | 118.4 | 118.1 | 118.7 | 118.6 | 118.6 | 120.2(3) |
| C(2)-H(13) | 107.1 | 107.4 | 108.6 | 108.3 | 108.9 | 108.8 | 108.8 | 111.5(5) |
| B(3)-H(14) | 117.6 | 118.0 | 118.5 | 118.2 | 118.7 | 118.6 | 118.6 | 120.2(3) |
| B(7)-H(23) | 124.3 | 124.4 | 125.9 | 126.0 | 126.5 | 127.3 | 127.2 | 134.2(6) |
| B(10)-H(24) | 143.3 | 140.8 | 139.1 | 139.1 | 137.0 | 137.8 | 137.8 | 139.5(12) |
| Energy[a] | -303.6921 | -305.4292 | -307.7789 | -307.8191 | -306.5616 | -306.6545 | -306.6585 | |

[a] absolute energy in Hartrees.

For *arachno*-6,9-$C_2B_8H_{14}$ (see Table 15 and Figure 3, p. 214) all B-B and C-B bond distances are overestimated by the 3-21G* basis set compared to the 6-31G*. The largest difference between the results obtained from the basis sets arises for the bond B(2)-B(6), which is 4.1 pm shorter when the 6-31G* basis set is used. The second largest difference occurs for B(2)-B(5), which is overestimated by 2.4 pm with the 3-21G* basis set. All other B-B or C-B bonds agree within 0.9 pm. Interestingly the B-H and C-H bond distances, with the exception of C(6)-H(21), are underestimated with the 3-21G* basis set compared to the 6-31G* at the HF level. The largest discrepancy is 0.4 pm – evident in bonds B(1)-H(11) and B(2)-H(12).

Using B3LYP methods, increasing the size of the basis set from 6-31G* to 6-311G* to 6-311+G* has negligible effect on the structural parameters. This is less true for the MP2 level, with which all the B-B and C-B bonds are underestimated with the 6-31G* basis set compared to the 6-311G*. For example, the B(2)-B(5) distance is 1.0 pm shorter using the 6-31G*, and bonds B(1)-B(3) and B(1)-B(5) are 0.9 pm shorter. The bridging B-H bonds are 0.7 pm shorter at the MP2/6-31G* level compared to the MP2/6-311G* value.

The longest bonded distance in this molecule is B(5)-B(10). This bond is 2.9 and 5.5 pm longer at the HF/6-31G* level than at the B3LYP/6-311+G* and MP2/6-311G* levels respectively.

**Table 15**. Calculated ($r_e$) and experimental ($r_{h1}$) structure of *arachno*-6,9-$C_2B_8H_{14}$ (pm).

| Geometric Parameter | Level of theory / Basis set | | | | | | | GED |
|---|---|---|---|---|---|---|---|---|
| | HF | | B3LYP | | | MP2 | | |
| | 3-21G* | 6-31G* | 6-31G* | 6-311G* | 6-311+G* | 6-31G* | 6-311G* | |
| B(1)-B(2) | 175.0 | 174.5 | 174.3 | 174.2 | 174.2 | 173.9 | 174.7 | 171.5(5) |
| B(1)-B(3) | 184.7 | 183.8 | 182.5 | 182.4 | 182.4 | 181.0 | 181.9 | 179.8(5) |
| B(1)-B(5) | 183.1 | 182.2 | 180.2 | 180.2 | 180.2 | 179.1 | 180.0 | 177.4(5) |
| B(2)-B(5) | 180.6 | 178.2 | 177.6 | 177.6 | 177.6 | 176.8 | 177.8 | 178.9(8) |
| B(2)-C(6) | 172.2 | 168.1 | 167.1 | 166.9 | 166.9 | 166.0 | 166.8 | 171.2(3) |
| B(5)-C(6) | 174.1 | 173.6 | 174.1 | 173.7 | 173.7 | 173.7 | 174.0 | 179.8(8) |
| B(5)-B(10) | 192.4 | 192.2 | 189.4 | 189.3 | 189.3 | 186.4 | 186.7 | 185.2(6) |
| B(1)-H(11) | 117.9 | 118.3 | 118.7 | 118.4 | 118.4 | 118.8 | 118.8 | 121.6(2) |
| B(2)-H(12) | 117.5 | 117.9 | 118.6 | 118.3 | 118.3 | 118.9 | 118.8 | 121.6(2) |
| B(5)-H(15) | 117.8 | 118.1 | 118.7 | 118.4 | 118.4 | 119.0 | 118.9 | 121.6(2) |
| B(5)-H(23) | 131.0 | 131.1 | 131.6 | 131.7 | 131.7 | 131.4 | 132.1 | 135.3(3) |
| C(6)-H(16) | 107.4 | 107.5 | 108.6 | 108.3 | 108.4 | 108.7 | 108.6 | 111.8(3) |
| C(6)-H(21) | 107.8 | 107.5 | 108.7 | 108.4 | 108.5 | 108.7 | 108.8 | 111.8(3) |
| Energy[a] | -279.7026 | -281.2992 | -283.4975 | -283.5380 | -283.5388 | -282.3348 | -282.4257 | |

[a] absolute energy in Hartrees.

## 7.4. Discussion

The chemistry of *closo*-$C_2B_9H_{11}$ has been widely investigated.[3,4,28-35] However, until now, no diffraction studies had been carried out on its structure. One reason its structure is of interest is due to the relationship with the isoelectronic *closo*-borate $B_{11}H_{11}^{2-}$.[36,38] The $C_{2v}$ structure of this anion was suggested by spectroscopic studies and through analogy to well-characterised isoelectronic species [for example, *closo*-$(MeC)_2B_9H_9$] as well as from *ab initio* calculations.[32,39-42] $B_{11}H_{11}^{2-}$ and $C_2B_9H_{11}$ have octadecahedral structures related to that of decaborane, $B_{10}H_{14}$, with the extra atom occupying the highly coordinated apical position.[30] Single hydrogen substituents are attached by a normal electron-pair bond in the *exo* position to each boron and/or carbon of the structural cage.[31]

$B_{11}H_{11}^{2-}$ in solution is fluxional on the NMR timescale,[3,39] with its structural reorganisation (or isomerisation) proposed to take place through a diamond-square-diamond process.[32] This process, first proposed by Lipscomb,[40,43] involves the breaking of a bond shared by two adjacent triangular faces and formation of a new bond, perpendicular to the broken bond, to join the pair of atoms in the two-triangle diamond. The activation barrier for rearrangement of $B_{11}H_{11}^{2-}$ is thought to be very low and has been estimated by Kleier *et al*[40] to be less than 12.6 kJ $mol^{-1}$.[32] This is of interest to $C_2B_9H_{11}$ since out of twenty possible geometric isomers, only the 2,3-isomer has been isolated and characterised.[32] However, it has been proposed through computational studies that further isomers may be isolable.[32,35] Using HF methods, with the STO-3G basis set, it has been found that the isomers 2,9-, 2,10- and 2,6- are 83.2, 102.9 and 103.3 kJ $mol^{-1}$ higher in energy respectively than the lowest energy 2,3-isomer.[32] Further investigation by Schleyer and Najafian (1998)[35] showed that, when correlated methods are employed (MP2/6-31G*), the 2,9- and 2,10-isomers are 73.3 and 76.3 kJ $mol^{-1}$ higher in energy than 2,3-$C_2B_9H_{11}$. The reason for the greater stability of the 2,3-isomer is linked to empirical valence rules – carbons prefer to occupy sites of lowest coordination in the polyhedral structure.[35] They prefer non-adjacent sites since B-C

bonds are inherently stronger than C-C bonds.[35] Another consideration is electrostatic repulsion – carbons in a boron framework should have negative charges. Separation of the carbons therefore reduces repulsion between like charges.[35]

Whilst no previous diffraction studies have been performed for *closo*-2,3-$C_2B_9H_{11}$, the structure of its dimethyl derivative[4] was determined by X-ray crystallography as far back as 1966. It is useful in this context to compare the detailed *closo* structures of 2,3-$C_2B_9H_{11}$ determined by GED with those of equivalent eleven-vertex clusters such as $C_2B_9H_9(CH_3)_2$ and the calculated (MP2/6-31G*) structure of $B_{11}H_{11}^{2-}$ (see Table 16).[4,35]

**Table 16.** Calculated ($r_e$) and experimental ($r_{h1}$) structure of *closo*-2,3-$C_2B_9H_{11}$, crystal structure of $C_2B_9H_9(CH_3)_2$ and calculated structure of $B_{11}H_{11}^{2-}$ (pm).

| Geometric parameter | $C_2B_9H_{11}$ GED | $C_2B_9H_{11}$ MP2/6-311+G* | $C_2B_9H_9(CH_3)_2$[a] | $B_{11}H_{11}^{2-}$[b] |
|---|---|---|---|---|
| B(1)-X(2)[c] | 162.2(10) | 163.1 | 168.0(1) | 174.6 |
| B(1)-B(4) | 200.0(7) | 206.7 | 205.0(1) | 200.4 |
| X(2)-B(4)[c] | 158.3(5) | 157.9 | 159.0(1) | 167.0 |
| X(2)-B(8)[c] | 167.0(10) | 166.8 | 170.0(1) | 175.3 |
| B(4)-B(7) | 188.6(11) | 187.0 | 187.0(1) | 185.6 |
| B(4)-B(8) | 177.4(6) | 180.1 | 181.0(1) | 179.1 |
| B(4)-B(10) | 180.6(2) | 177.9 | 178.0(1) | 178.0 |
| B(8)-B(10) | 180.8(3) | 178.3 | 179.0(1) | 178.5 |
| B(10)-B(11) | 186.6(5) | 184.1 | 185.0(1) | 181.4 |

[a] Geometry from Ref. 4.
[b] Geometry from Ref. 35.
[c] X = B or C.

Comparison of the carborane molecules shows that the presence of methyl substituents on the carbon atoms results in lengthening of the B(1)-C(2) bond.[4] The experimentally determined value for this bond length in *closo*-2,3-$C_2B_9H_{11}$ is 0.9 pm less than by calculation and 5.8 pm less than in its dimethyl derivative.[4] The relatively long B(1)-B(4) bond in $C_2B_9H_{11}$ is 6.7 pm longer by calculation (MP2/6-311+G*) than found

experimentally in the gas phase. In fact the length of this bond as determined by GED more closely resembles that found by calculation for the anion $B_{11}H_{11}^{2-}$ (+ 0.4 pm)[35] than the distance determined for its dimethyl derivative (+ 5.0 pm).[4] One consequence of this is that the B(4)-B(8) bond in *closo*-2,3-$C_2B_9H_{11}$ is 2.7 pm shorter by experiment than by calculation. The refined GED structure also has a B(4)-B(8) bond that is 3.6 and 1.7 pm shorter than those found in $C_2B_9H_9(CH_3)_2$ and $B_{11}H_{11}^{2-}$ respectively.[4,35] The opposite trend is found for the B(4)-B(10) bond; in the GED structure of *closo*-2,3-$C_2B_9H_{11}$ this bond is 2.7, 2.6 and 2.6 pm longer than in the MP2/6-311+G* calculated structure, $C_2B_9H_9(CH_3)_2$ and $B_{11}H_{11}^{2-}$ structures respectively.[4,35]

*Nido* boranes all have structures derived from the most spherical deltahedra by loss of a vertex of highest connectivity.[38] The result is that all but one of the faces is triangular with the unique non-triangular face being a hole.[5] This hole means that compounds such as the *nido*-$C_2B_9H_{11}^{2-}$ species can act as important precursors to many *closo* icosahedral metallocarboranes with addition to form a twelfth vertex.[5] Of the nine possible cage configurations for *nido*-$C_2B_9H_{13}$ three are known – *meta* (7,9-), *ortho* (7,8-) and *para* (2,9-) isomers.[5] The mono-anions of these species have been structurally determined through the analysis of various salts.[5,44-47]

The most widely studied structure is the 7,8- anion, for which ten salts have been studied experimentally, including the $(Me_2SO)_2H^+$, $(Me_2N)_3PNH_2^+$ and $(C_5H_{10}NH)_2H^+$ salts which contain well-defined carborane clusters.[5,44,45] A neutron diffraction study of its $(C_5H_{10}NH)_2H^+$ salt determined the unique hydrogen in the anion to be localised in an unsymmetric B-H-B bridging position over the B(10)-B(11) bond.[7] Calculation at the MP2/6-311++G* level on the neutral species (see Appendix D) confirm the conclusions from previous MP2/6-31G* calculations, that there is an unsymmetrical B-H-B arrangement of the two bridge hydrogens on adjacent edges of the open face.[7] These 7,6-bridge hydrogens, exemplified in compounds such as 2-$Me_2S{\cdot}B_{11}H_{13}$[48] and 7-Thx-$B_{11}H_{13}^-$ (Thx = 2,3-dimethyl-2-butyl group),[49] are so called because they lie between one 6-coordinated boron and one 7-coordinated boron.

The order of stability of the three *nido*-$C_2B_9H_{11}^-$ mono-anions is reported to be 7,9- (0.0 kJ $mol^{-1}$) > 7,8- (22.5 kJ $mol^{-1}$) > 2,9- (104.5 kJ $mol^{-1}$).[5] This has been attributed to carbon's preference for low connectivity and the fact that in the 7,9-isomer there exists only one B-B bond on the open face to accommodate the sole bridging hydrogen, as opposed to two or three in the 7,8- and 2,9-isomers.[5] The structures of the $(C_5H_{10}NH)_2H^+$ salt of *nido*-7,9-$C_2B_9H_{12}^-$ and two tri-substituted derivatives, in the form of 10-HO- and 3-OEt-7,9-$Ph_2$-*nido*-7,9-$C_2B_9H_9^-$, have been determined by X-ray crystallography.[5,50] The $(C_5H_{10}NH)_2H^+$ salt shows the *endo* hydrogen to be symmetrically bridging between adjacent boron atoms [B(10) and B(11)] on the open face.[5]

The opposite trend of stability is found for the neutral species, where the availability of non-adjacent B-B bonds to accommodate the two bridging hydrogens overrules the preference for low connectivity by the cage carbons.[5] Whilst no previous diffraction studies have been performed for *nido*-2,9-$C_2B_9H_{13}$, the structure of the salt $[(C_5H_{10}NH)_2H^+](nido\text{-}2,9\text{-}C_2B_9H_{12}^-)$ has been determined by X-ray crystallography.[5] The structure of *nido*-2,9-$C_2B_9H_{13}$ determined by GED is compared to the cage geometry found in the crystal structure of $[(C_5H_{10}NH)_2H^+](nido\text{-}2,9\text{-}C_2B_9H_{12}^-)$ in Table 17.

As in the case of 11-Me-2,7-$C_2B_9H_{12}$,[51] the structure of *nido*-2,9-$C_2B_9H_{13}$ is of particular interest because only one carbon is adjacent to the metal in metallocarboranes in contrast to the 7,8- and 7,9-isomers. Comparison of the intramolecular B-B bonds detailed in Table 17 shows some interesting differences between the experimental and calculated gas-phase structures of *nido*-2,9-$C_2B_9H_{13}$ and the solid-phase structure of *nido*-2,9-$C_2B_9H_{12}^-$.[5] In the mono-anion salt the longest bond [B(7)-B(11)] accommodates the bridging hydrogen.[5] This bond is longer in the neutral species by 7.0 and 4.3 pm using GED and calculation (MP2/6-311+G*) respectively. The B(7)-B(11) bond in each molecule is longer than the corresponding bond in the lower pentagonal ring [B(4)-

B(5)]. The differences between these bonds is 17.1, 17.5 and 9.7 pm for *nido*-2,9-$C_2B_9H_{13}$ (GED and MP2/6-311+G*) and *nido*-2,9-$C_2B_9H_{12}^-$ respectively.[5]

**Table 17**. Calculated ($r_e$) and experimental ($r_{h1}$) structure of *nido*-2,9-$C_2B_9H_{13}$ and crystal structure of $[(C_5H_{10}NH)_2H^+](nido\text{-}2,9\text{-}C_2B_9H_{12}^-)$.[a]

| Geometric parameter | $C_2B_9H_{13}$ GED | $C_2B_9H_{13}$ MP2/6-311+G* | $[(C_5H_{10}NH)_2H^+](nido\text{-}2,9\text{-}C_2B_9H_{12}^-)$[b] |
|---|---|---|---|
| B(1)-C(2) | 169.7(5) | 169.5 | 172.0(2) |
| B(1)-B(3) | 182.8(2) | 179.7 | 177.0(2) |
| B(1)-B(4) | 179.5(2) | 176.4 | 178.0(2) |
| C(2)-B(3) | 171.9(8) | 172.6 | 174.3(2) |
| C(2)-B(7) | 168.2(4) | 167.5 | 170.7(2) |
| B(3)-B(4) | 180.6(2) | 177.4 | 173.2(2) |
| B(3)-B(7) | 173.0(4) | 177.3 | 179.0(2) |
| B(3)-B(8) | 185.2(5) | 179.1 | 175.0(2) |
| B(4)-B(5) | 179.0(3) | 175.9 | 179.4(2) |
| B(4)-B(8) | 175.4(6) | 181.7 | 178.0(2) |
| B(4)-C(9) | 169.5(4) | 168.5 | 172.0(2) |
| B(7)-B(8) | 187.7(3) | 184.7 | 177.2(2) |
| B(7)-B(11) | 196.1(2) | 193.4 | 189.1(2) |
| B(8)-C(9) | 160.3(7) | 165.3 | 164.4(2) |

[a] Distances in pm.
[b] Geometry from Ref. 5.

Bonds B(3)-B(4), B(3)-B(8) and B(7)-B(8) are all longer in the GED structure of *nido*-2,9-$C_2B_9H_{13}$ than found by calculation or in the crystal structure of *nido*-2,9-$C_2B_9H_{12}^-$.[5] Bond B(3)-B(4) is 3.2 and 7.4 pm longer, B(3)-B(8) is 6.1 and 10.2 pm longer, and B(7)-B(8) is 3.0 and 10.5 pm longer than in the calculated structure (MP2/6-311+G*) and *nido*-2,9-$C_2B_9H_{12}^-$ correspondingly.[5] In contrast, B(8)-C(9) is 5.0 and 4.1 pm shorter in the GED structure of 2,9-$C_2B_9H_{13}$ than by calculation or in the solid-phase structure of 2,9-$C_2B_9H_{12}^-$.[5] Comparison of the two pentagonal rings within each carborane molecule shows that a common pattern is observed, namely that bond B(4)-C(9) is longer than C(2)-B(7), B(7)-B(11) is longer than B(4)-B(5), but B(8)-C(9) is shorter than C(2)-B(3). In the gas-phase structure differences of 1.3, 17.1 and 11.6 pm

are determined respectively. By calculation differences of 1.0, 17.5 and 7.3 pm occur compared to differences of 1.3, 9.7 and 9.9 pm in 2,9-$C_2B_9H_{12}^-$.[5]

Unsymmetric hydrogen bridges in *nido*-2,9-$C_2B_9H_{13}$ occupy atoms B(7)/B(8) and B(10)/B(11) compared to positions B(9)/B(10) and B(10)/B(11) in its 7,8-isomer. In the GED structure of *nido*-2,9-$C_2B_9H_{13}$ such bridges occur at lengths 134.2 [B(11)-H(24)] and 139.5 pm [B(10)-H(24)]. This compares to calculated values of 127.2 and 137.8 pm respectively, employing correlated methods and diffuse functions (MP2/6-311+G*).

When *arachno*-6,9-$C_2B_8H_{14}$ was first synthesised in 1973[52] it was hailed as the first representative of the ten-vertex *arachno*-dicarborane family. Since then the isoelectronic $CNB_8H_{13}$, $CSB_8H_{12}$, $N_2B_8H_{14}$ and $Se_2B_8H_{10}$ compounds have been isolated.[53,54] However, as is common with the *arachno* family of boranes, experimental characterisation of these molecules has been complicated due to their high reactivity toward, for example, disproportionation, decomposition and protonation.[55] Reported here is the experimental characterisation of *arachno*-6,9-$C_2B_8H_{14}$ by GED and high-level *ab initio* calculations. Janoušek *et al.*[11] suggest that the formation of this compound follows the reductive cleavage of the C(5)-C(6) bond in the cage of 5,6-$C_2B_8H_{12}$, followed by moving the C(6) vertex into a new position. This mechanism parallels that proposed by Bould *et al.*[56] for the rearrangement in 6-irida-*nido*-decaborane and is analogous to the reduction of $B_{10}H_{14}$ to its di-anion. Comparison of the calculated structure of $B_{10}H_{14}^{2-}$ with *arachno*-6,9-$C_2B_8H_{14}$ shows that the B(5)-B(10)/B(7)-B(8) bonds are equivalent (186.7 pm) when the MP2/6-311G* level is employed.[55] These bonds are 185.2(6) pm long for *arachno*-6,9-$C_2B_8H_{14}$ determined by GED. The distances B(5)...B(7)/B(8)...B(10) are longest for the GED structure of $C_2B_8H_{14}$ [296.3(11) pm] compared to the calculated structures of $B_{10}H_{14}^{2-}$ (293.2 pm)[55] and *arachno*-6,9-$C_2B_8H_{14}$ (288.7 pm). In contrast the X(6)...X(9) distance in these compounds, where X = B or C, is greatest when X = B (344.4 pm).[55] The corresponding distance is 310.7(18) (by GED) and 314.6 pm (MP2/6-311G*) in *arachno*-6,9-$C_2B_8H_{14}$.

The structure of *arachno*-6,9-$C_2B_8H_{14}$ determined by GED is compared to the cage geometry found in the crystal structures of *exo,exo*-6,9-$(PMe_2Ph)_2$-*arachno*-$B_{10}H_{12}$ and *exo,endo*-6,9-$(PMe_2Ph)_2$-*arachno*-$B_{10}H_{12}$ in Table 18.[57]

**Table 18**. Calculated ($r_e$) and experimental ($r_{h1}$) structure of *arachno*-6,9-$C_2B_8H_{14}$ and crystal structures of *exo,exo*-6,9-$(PMe_2Ph)_2$-*arachno*-$B_{10}H_{12}$ and *exo,endo*-6,9-$(PMe_2Ph)_2$-*arachno*-$B_{10}H_{12}$.[a,b]

| Geometric | $C_2B_8H_{14}$ | | $(PMe_2Ph)_2$-$B_{10}H_{12}$ | |
|---|---|---|---|---|
| parameter | GED | MP2/6-311G* | *exo,exo*-6,9- | *exo,endo*-6,9- |
| B(1)-B(2) | 171.5(5) | 174.7 | 176.9(5) | 176.9(2) |
| B(1)-B(3) | 179.8(5) | 181.9 | 181.2(5) | 181.6(2) |
| B(1)-B(5) | 177.4(5) | 180.0 | 176.6(5) | 177.9(2) |
| B(2)-B(5) | 178.9(8) | 177.8 | 175.1(4) | 176.5(2) |
| B(2)-X(6) | 171.2(3) | 166.8 | 174.4(5) | 173.5(2) |
| B(5)-X(6) | 179.8(8) | 174.0 | 186.5(5) | 185.1(2) |
| B(5)-B(10) | 185.2(6) | 186.7 | 186.9(4) | 189.2(2) |

[a] Distances in pm.
[b] Geometry from Ref. 57.

Inspection of the data in Table 18 shows that the experimental B(5)-B(10) connectivity in *arachno*-6,9-$C_2B_8H_{14}$ is shorter than those determined by calculation (by 7.0, 3.7 and 1.5 pm at HF/6-31G*, B3LYP/6-311+G* and MP2/6-311G* levels respectively) and than those found in the *exo,exo*- and *exo,endo*-isomers of 6,9-$(PMe_2Ph)_2$-$B_{10}H_{12}$ (by 1.7 and 3.6 pm respectively).[57] All examples are characteristically shorter than the corresponding distance in *nido*-decaboranyl clusters, where typical values are around 200 pm.[57] In contrast, bonds B(2)-C(6) and B(5)-C(6) are longer in the experimental gas-phase structure of $C_2B_8H_{14}$ compared to calculated values. For these bonds, the HF/3-21G* calculation most closely matches the experiment with differences of 1.0 and 5.7 pm respectively. The MP2/6-311G* calculation underestimates the B(2)-C(6) bond by 4.4 pm and the B(5)-C(6) bond by 5.8 pm.

Through the combination of gas-phase electron diffraction and *ab initio* calculations the molecular structures of *closo*-2,3-$C_2B_9H_{11}$, *nido*-2,9-$C_2B_9H_{13}$ and *arachno*-6,9-$C_2B_8H_{14}$ have been determined for the first time. *Closo*-2,3-$C_2B_9H_{11}$ was first synthesised in 1964,[3] and *nido*-2,9-$C_2B_9H_{13}$ and *arachno*-6,9-$C_2B_8H_{14}$ in 1973,[10,52] yet it has taken until now to characterise them fully.

A review of journals that discuss carborane chemistry highlights the amount of research undertaken on *closo*-2,3-$C_2B_9H_{11}$, particularly theoretical investigation.[3,4,28-35] This would lend credence to the idea that its structure is of importance in the understanding of eleven-vertex carboranes. We now know its experimental structure in the gas phase, which is major contribution to this area of boron cluster chemistry.

The *nido*-carborane 2,9-$C_2B_9H_{13}$ is recognised as important in the field of metallocarborane chemistry since it can act as a precursor to many *closo*-metallocarboranes that have only one carbon adjacent to the metal.[5,44-47] Knowledge of molecular structure assists with the understanding of chemical processes, and again, we have provided the gas-phase structure of this important molecule to aid future synthesis in this field.

*Arachno*-6,9-$C_2B_8H_{14}$ is the first ten-vertex *arachno*-dicarborane to be fully characterised. Experimental characterisation of *arachno* boranes is hampered by their reactivity and by the difficulty in forming single crystals.[55] However, if the reactivity can be controlled, we have shown that GED is an ideal technique for determination of their molecular structures.

## 7.5. References


1. R. N. Grimes, *Coord. Chem. Rev.*, 2000, **200-202**, 773.
2. R. B. King, *Chem. Rev.*, 2001, **101**, 1119.
3. (a) F. N. Tebbe, P. M. Garrett and M. F. Hawthorne, *J. Am. Chem. Soc.*, 1964, **86**, 4222; (b) P. M. Garrett, F. N. Tebbe and M. F. Hawthorne, *J. Am. Chem. Soc.*, 1964, **86**, 5016; (c) T. E. Berry, F. N. Tebbe and M. F. Hawthorne, *Tetrahedron Letters*, 1965, 716; (d) F. N. Tebbe, P. M. Garrett and M. F. Hawthorne, *J. Am. Chem. Soc.*, 1966, **88**, 607; (e) F. N. Tebbe, P. M. Garrett, D. C. Young and M. F. Hawthorne, *J. Am. Chem. Soc.*, 1966, **88**, 609.
4. C. D. Tsai and W. E. Streib, *J. Am. Chem. Soc.*, 1966, **88**, 4513.
5. M. A. Fox, A. E. Goeta, A. K. Hughes and A. L. Johnson, *J. Chem. Soc., Dalton Trans.*, 2002, 2132.
6. M. A. Fox, A. K. Hughes and J. M. Malget, *J. Chem. Soc., Dalton Trans.*, 2002, 3505.
7. M. A. Fox, A. E. Goeta, J. A. K. Howard, A. K. Hughes, A. L. Johnson, D. A. Keen, K. Wade and C. C. Wilson, *Inorg. Chem.*, 2001, **40**, 173.
8. R. A. Wiesbock and M. F. Hawthorne, *J. Am. Chem. Soc.*, 1964, **86**, 1642.
9. D. C. Busby and M. F. Hawthorne, *Inorg. Chem.*, 1982, **21**, 4101.
10. J. Plešek and S. Heřmánek, *Chem. Ind.*, 1973, 81.
11. Z. Janoušek, J. Plešek, S. Heřmánek and B. Štíbr, *Polyhedron*, 1985, **4**, 1797.
12. C. M. Huntley, G. S. Laurenson and D. W. H. Rankin, *J. Chem. Soc., Dalton Trans.*, 1980, 954.
13. J. R. Lewis, P. T. Brain and D. W. H. Rankin, *Spectrum*, 1997, **15**, 7.
14. J. R. Lewis, R. J. Mawhorter, S. L. Hinchley and D. W. H. Rankin, *Manuscript in preparation.*
15. S. Cradock, J. Koprowski and D. W. H. Rankin, *J. Mol. Struct.*, 1981, **77**, 113.
16. A. W. Ross, M. Fink and R. Hilderbrandt, *International Tables for Crystallography*, Ed. A. J. C. Wilson, Kluwer Academic Publishers, Dordrecht, Boston and London, 1992; Vol. C, p.245.

17. A. S. F. Boyd, G. S. Laurenson and D. W. H. Rankin, *J. Mol. Struct.*, 1981, **71**, 217.
18. Gaussian 98, Revision A.7, M. J. Frisch, G. W. Trucks, H. B. Schlegel, G. E. Scuseria, M. A. Robb, J. R. Cheeseman, V. G. Zakrzewski, J. A. Montgomery, R. E. Stratmann Jr, J. C. Burant, S. Dapprich, J. M. Millam, A. D. Daniels, K. N. Kudin, M. C. Strain, O. Farkas, J. Tomasi, V. Barone, M. Cossi, R. Cammi, B. Mennucci, C. Pomelli, C. Adamo, S. Clifford, J. Ochterski, G. A. Petersson, P. Y. Ayala, Q. Cui, K. Morokuma, D. K. Malick, A. D. Rabuck, K. Raghavachari, J. B. Foresman, J. Cioslowski, J. V. Ortiz, A. G. Baboul, B. B. Stefanov, G. Liu, A. Liashenko, P. Piskorz, I. Komaromi, R. Gomperts, R. L. Martin, D. J. Fox, T. Keith, M. A. Al-Laham, C. Y. Peng, A. Nanayakkara, C. Gonzalez, M. Challacombe, P. M. W. Gill, B. Johnson, W. Chen, M. W. Wong, J. L. Andres, C. Gonzalez, M. Head-Gordon, E. S. Replogle and J. A. Pople, Gaussian, Inc., Pittsburgh PA, 1998.
19. W. J. Hehre, L. Radom, P. v. R. Schleyer and J. A. Pople, *Ab initio Molecular Orbital Theory*, J . Wiley & Sons, 1986, p.71; D. R. Hartree, *Proc. Camb. Phil. Soc.*, 1928, **24**, 89; V. Fock, *Z. Physik*, 1930, **61**, 126 and *Z. Physik*, 1930, **62**, 795.
20. J. S. Binkley, J. A. Pople and W. J. Hehre, *J. Am. Chem. Soc.*, 1980, **102**, 939; M. S. Gordon, J. S. Binkley, J. A. Pople, W. J. Pietro and W. J. Hehre, *J. Am. Chem. Soc.*, 1982, **104**, 2797; W. J. Pietro, M. M. Francl, W. J. Hehre, D. J. Defrees, J. A. Pople and J. S. Binkley, *J. Am. Chem. Soc.*, 1982, **104**, 5039.
21. W. J. Hehre, R. Ditchfield and J. A. Pople, *J. Chem. Phys.*, 1972, **56**, 2257; P. C. Hariharan and J. A. Pople, *Mol. Phys.*, 1974, **27**, 209; M. S. Gordon, *Chem. Phys. Lett.*, 1980, **76**, 163.
22. P. J. Knowles, K. Somasundram, N. C. Handy and K. Hirao, *Chem. Phys. Lett.*, 1993, **211**, 272; W. Kohn, L. J. Sham, *Phys. Rev.*,1965, A**140**, 1133.
23. A. D. McLean and G. S. Chandler, *J. Chem. Phys.*, 1980, **72**, 5639; R. Krishnan, J. S. Binkley, R. Seeger and J. A. Pople, *J. Chem. Phys.*, 1980, **72**, 650.
24. A. D. Becke, *Phys. Rev.*, 1988, **A38**, 3098; A. D. Becke, *J. Chem. Phys.*, 1993, **98**, 5648; J. P. Perdew, *Phys. Rev.*, 1986, **B33**, 8822; L. A. Curtiss, K. Raghavachari, G. W. Trucks and J. A. Pople, *J. Chem. Phys.*, 1991, **94**, 7221.

25. C. Møller and M. S. Plesset, *Phys. Rev.*, 1934, **46**, 618; P. Hohenburg and W. Kohn, *Phys. Rev.*, 1964, **B136**, 864.
26. V. A. Sipachev, *J. Mol. Struct. (Theochem)*, 1985, **121**, 143.
27. A. J. Blake, P. T. Brain, H. McNab, J. Miller, C. A. Morrison, S. Parsons, D.W.H Rankin, H. E. Robertson and B. A. Smart, *J. Phys. Chem.*, 1996, **100**, 12280; P. T. Brain, C. A. Morrison, S. Parsons and D. W. H. Rankin, *J. Chem. Soc., Dalton Trans.*, 1996, 4589.
28. D. A. Dixon, D. A. Kleier, T. A. Halgreen, J. H. Hall and W. N. Lipscomb, *J. Am. Chem. Soc.*, 1977, **99**, 6226.
29. M. J. S. Dewar and M. L. McKee, *Inorg. Chem.*, 1980, **19**, 2662.
30. M. E. O'Neill and K. Wade, *Polyhedron*, 1984, **3**, 199.
31. B. M. Gimarc and J. J. Ott, *J. Am. Chem. Soc.*, 1987, **109**, 1388.
32. B. M. Gimarc, B. Dai, D. S. Warren and J. J. Ott, *J. Am. Chem. Soc.*, 1990, **112**, 2597.
33. K. Takano, M. Izubo and H. Hosoya, *J. Phys. Chem.*, 1992, **96**, 6962.
34. B. M. Gimarc and M. Zhao, *Inorg. Chem.*, 1996, **35**, 825.
35. P. v. R. Schleyer and K. Najafian, *Inorg. Chem.*, 1998, **37**, 3454.
36. J. Aihara, *Inorg. Chem.*, 2001, **40**, 5042.
37. W. W. Porterfield, M. E. Jones, W. R. Gill and K. Wade, *Inorg. Chem.*, 1990, **29**, 2914.
38. O. Volkov and P. Paetzold, *J. Organomet. Chem.*, 2003, **680**, 301.
39. E. F. Tolpin and W. N. Lipscomb, *J. Am. Chem. Soc.*, 1973, **95**, 2384.
40. D. A. Kleier, D. A. Dixon and W. N. Lipscomb, *Inorg. Chem.*, 1978, **17**, 166.
41. O. Volkov, K. Radacki, P. Paetzold and X. Zheng, *Z. Anorg. Allg. Chem.*, 2001, **627**, 1185.
42. R. Rousseau and S. Lee, *J. Chem. Phys.*, 1994, **101**, 10753.
43. W. N. Lipscomb, *Science*, 1966, **153**, 373.
44. J. Buchanan, E. J. M. Hamilton, D. Reed and A. J. Welch, *J. Chem. Soc., Dalton Trans.*, 1990, 677.

45. M. G. Davidson, M. A. Fox, T. H. Hibbert, J. A. K. Howard, A. MacKinnon, I. S. Neretin and K. Wade, *Chem. Commun.*, 1999, 1649.
46. R. C. B. Copley and D. M. P. Mingos, *J. Chem. Soc., Dalton Trans.*, 1996, 491.
47. K. Chiu, Z. Zhang, T. C. W. Mak and Z. Xie, *J. Organomet. Chem.*, 2000, **614-615**, 107.
48. D. L. Keller, J. G. Kester, J. C. Huffman and L. J. Todd, *Inorg. Chem.*, 1993, **32**, 5067.
49. D. F. Gaines, A. N. Bridges and R. K. Hayashi, *Inorg. Chem.*, 1994, **33**, 1243.
50. A. J. Welch and A. S. Weller, *J. Chem. Soc., Dalton Trans.*, 1997, 1205.
51. Y. T. Struchkov and M. Y. Antipin, *J. Organomet. Chem.*, 1977, **141**, 133.
52. B. Štibr, J. Plešek and S. Heřmánek, *Collect. Czech. Chem. Commun.* 1973, **38**, 338.
53. Personal communication from Dr. D. Hnyk, Prague.
54. J. Holub, T. Jelínek, J. Plešek, B. Štibr, S. Heřmánek and J. D. Kennedy, *J. Chem. Soc., Chem. Comm.*, 1991, 1389.
55. M. Hofmann and P. v. R. Schleyer, *Inorg. Chem.*, 1998, **37**, 5557.
56. J. Bould, N. N. Greenwood, J. D. Kennedy and W. S. McDonald, *J. Chem. Soc., Chem. Comm.*, 1982, 465.
57. U. Dörfler, T. D. McGrath, P. A. Cooke, J. D. Kennedy and M. Thornton-Pett, *J. Chem. Soc., Dalton Trans.*, 1997, 4739.

# Chapter Eight

Future Work

## 8.1. Halogen π back-bonding

The degree of back-donation by halogens to empty B 2*p* orbitals is worthy of further investigation. The extent of back donation is difficult to quantify. Pauling's original definition of back-bonding, based on valence bond formalism, refers to the extent to which the appropriate canonical resonance forms contribute to the B-X bonding, i.e., the difference in B-X bond strength relative to a hypothetical B-X bond with only $\sigma$ character.[1,2] However, the same terminology has also been employed when assessing the extent to which the B-B framework in a boron cluster has been altered by the introduction of back-bonding orbitals from halogens.[3]

Review of the literature in relation to the π-donor abilities of the halogens is confusing. $B_4Cl_4$ and $B_4Br_4$ are the only members of the tetraboron tetrahalide family to have been synthesised to date.[4,5] It has been suggested that $B_4F_4$ may be less stable than the corresponding chloride because of relatively weak back-bonding from F *p* orbitals into cage bonding orbitals.[6] Indeed, common undergraduate textbooks relay that the π-donor abilities of the halogens increase in the sequence F < Cl < Br < I.[7] This sequence of π-donor ability is supported by the studies of $CH_2X^+$, $BX_3$, $BH_2X$, and $X_3P{\cdot}BY_3$ complexes (X, Y = F, Cl, Br and I).[8-11]

Contrary to this, various *ab initio* studies[2,9,12] advocate that there is actually greater back-donation in $B_4F_4$ than in $B_4Cl_4$; an order corroborated by the investigation of halomethyl cations, $CX_3^+$ (X = F, Cl, Br and I).[13] Further to this, the reasoning given for the sequence of Lewis acidity of the boron trihalides towards strong bases ($BF_3$ < $BCl_3$ < $BBr_3$ < $BI_3$), is stronger back-donation from F, which decreases the availability of the otherwise empty B 2*p* orbital to accept an electron pair from the base.[14,15] In $BCl_3$ this back-donation is considered to be less important because of a poorer overlap between Cl 3*p* and B 2*p* orbitals.[15] The existence of larger boron halide clusters of the type $B_nX_n$ (X = Cl, Br and I; *n* = 8, 9) has been taken to imply that the boron cores in such species are stabilised by back-donation from the halogens.[16] That the presence of halides is not required has been demonstrated by the synthesis of such compounds as $B_9(^tBu)_9$.[17] It has therefore been concluded that there

are no inherent reasons why $B_4F_4$ should not have been synthesised and characterised.[18]

In the compounds $B_8X_{12}$ and $B_{10}X_{12}$ there are more halogens available to compete for the $2p_z$ orbital of boron compared to the monohalide species. Therefore the $\pi$-donor abilities of the halogens (regardless of the preferred order) may be offset by steric contributions in the determination of molecular structure. It has been said that the poorer $\pi$-donating ability of fluorine results in polyboron fluorides preferring more open frameworks compared to the other halogens, which adopt cage-like structures. It might be said that this is supported by the structures of $B_8X_{12}$ and $B_{10}X_{12}$. $B_8F_{12}$ (by experiment and calculation) and $B_{10}F_{12}$ (by calculation) adopt more open boron frameworks than $B_{10}X_{12}$ (X = Cl, Br and I) and $B_nX_n$ (X = Cl, Br and I; $n$ = 8, 9), which contain boron cages.[16,19-21] However, the crystalline form of $B_{10}F_{12}$ also adopts such a structure, thereby affecting the reliability of such a conclusion. Future focus must be on the synthesis, and hence experimental characterisation, of such boron halides to try and end the debate.

## 8.2. Modelling of dimer systems

The dimeric species of $B_8X_{12}$ (X = F, Cl, Br and I) [i.e. $(B_4X_6)_2$] studied in Chapters 3 and 4 illustrate possible bonding schemes for polyboron halide complexes. It is therefore important to be aware of difficulties related to calculation of their structures by quantum mechanical methods. Hartree-Fock and DFT procedures are recognised as being poor for modelling interaction energies, which exist in complexes containing non-bonded forces such as van der Waals or London forces. The phenomenon of basis set superposition error (BSSE)[22] should be corrected for before comparing relative energies. BSSE is the term given to the increase in calculated stability of systems formed by non-covalent interaction between two or more species, resulting from the basis set of such a system being larger than for the component subsystems.[22] In the examples of the $B_4X_6$ dimers, the BSSE arises from a lowering of the quantum mechanical energy when the electron density of each $B_4X_6$ spreads

into the basis functions provided by the alternative $B_4X_6$ molecule. In other words the wavefunction of the monomer is expanded in many fewer basis functions than the wavefunction of the complex. The counterpoise correction[23] is one approximation utilised to correct the overestimation of complex stability. This involves placing ghost orbitals on one monomer and calculating the energy of the second monomer and *vice versa*. The total energy is then formulated using the contributions made by each monomer and the resultant complex. A more obvious solution to counteract the BSSE is to use extremely large basis sets, but this is computationally prohibitive. Alternatively the introduction of diffuse orbitals can be used to estimate the geometries and energies of systems containing long-range interactions more accurately. Future research could scrutinise these $B_4X_6$ (X = F, Cl, Br and I) dimer systems more closely. One of these systems that we have studied is a transition state, yet is also lower in energy than the state with the minimum energy so far found. There is, therefore, a lower energy minimum on the potential energy surface still to be found. There are vast differences in energy between the species when they are calculated with varying methods, a phenomenon still to be explained.

## 8.3. Haloboranes

Calculations in Chapter 6 have brought to attention the multitude of chemically feasible structures that systems such as $B_8X_8H_4$ and $B_8X_4H_8$ (X = F, Cl, Br and I) can adopt. Further analysis is required on these systems to explain fully the different structures obtained for each halogen. For example, the movement of the bridging $BH_2$ substituent in $B_8X_4H_8$ (X = Cl and Br) to form a basal bridge on the pyramid of boron may result in the determination of further energy minima. Indeed it is this problem of multiple energy minima on the potential energy surfaces of the haloboranes that provides the greatest impetus for future theoretical research. If any of these systems are synthesised then they may be suitable for analysis by gas-phase electron diffraction, for which it is essential to have an appropriate geometrical model to describe the system. In other words it is essential that the correct isomer (or mix of isomers) is calculated to formulate our starting model.

The systems derived from $B_{10}X_{12}$ (X = F, Cl, Br and I) are also interesting. For example, one question that arises from the structure determination of $B_{10}X_8H_4$ is why the fluoro compound contains bridging $BF_2$ substituents but the other halogens produce bridging $BH_2$ groups. The substitution of F for Cl, Br and I, and *vice versa*, would determine if the character of the bridging groups is essential for the molecular stability of these systems.

The molecules studied in Chapters 3 – 6 result from the presence of an even number of halogens, but what if there were an odd stoichiometry such as $B_8H_3X_7$ or $B_8H_5X_7$? Most of the known haloboranes, such as $B_4H_9X$ (X = F and Br)[24-26] and $B_{10}H_{12}X_2$ (X = Br and I),[27,28] contain fewer halogens than those investigated in this thesis. It would be of interest to compare the structures of the systems $B_8H_3X_7$, $B_8H_5X_7$ and all other $B_8H_xX_y$ possibilities to those of the systems in this thesis. Of interest would be the determination of how many halogens are required before the borane-like structure changes to the haloborane one? In addition the calculation of $B_xMe_y$ systems could provide further understanding of the bonding in the boron halide molecules.

## 8.4. Alanes

Although aluminium is in close proximity to boron in the periodic table, it does not form many clusters that are analogous to the boranes (alanes). The range of aluminium hydrides is much more limited than that of boron yet the alkylaluminium hydrides, such as $Al_2(C_2H_5)_4H_2$,[29] are well known molecular compounds like $B_2H_6$ and contain Al-H-Al three-centre two-electron bonds. $(Al_{12}{}^{i}Bu_{12})^{2-}$ is a rare example of a deltahedral Al cluster.[30] In contrast to boron, elemental aluminium is definitely metallic. Nevertheless, in some of its compounds aluminium displays properties associated with the semi-metals. For example, it forms rather volatile halides. Aluminium fluoride is a high-melting compound of low volatility, but the other halides of aluminium melt at relatively low temperatures. In the gas phase the chloride, bromide and iodide of aluminium exist as $Al_2X_6$ molecules, which have

bridges similar to those in diborane.[7] Future work could be focussed on increasing the understanding of aluminium hydride clusters by utilising the unique geometries discovered in this thesis and replacing B by Al to determine new classes of alane cluster compounds.

## 8.5. References


1. H. C. Longuet-Higgins, *Q. Rev.*, 1957, **11**, 121; A. Kaczmarczyk and B. G. Kolski, *Inorg. Chem.*, 1965, **4**, 665; N. Lynaugh, D. R. Lloyd, M. F. Guest, B. M. Hall and I. H. Hillier, *J. Chem. Soc., Faraday Trans.*, 1972, **68**, 2192.
2. M. F. Guest and I. H. Hillier, *J. Chem. Soc., Faraday Trans.*, 1974, **70**, 398.
3. W. N. Lipscomb, *Boron Hydrides*, Ed. W. A. Benjamin, New York, 1963, p.89.
4. G. Urry, T. Wartik and H. I. Schlesinger, *J. Am. Chem. Soc.*, 1952, 74, 5809.
5. L. Ahmed, J. Castillo and J. A. Morrison, *Inorg. Chem.*, 1992, **31**, 1858.
6. A. G. Massey, *Adv. Inorg. Chem and Radiochem.*, 1983, **26**, 1.
7. D. F. Shriver, P. W. Atkins and C. H. Langford, *Inorganic Chemistry 2nd Edition*, Oxford University Press, 1994, pp.206, 261.
8. R. W. Taft, R. H. Martin and F. W. Lampe, *J. Am. Chem. Soc.*, 1965, 2490.
9. J. H. Hall and W. N. Lipscomb, *Inorg. Chem.*, 1974, **13**, 710.
10. G. Frenking, S. Fau, C. M. Marchand and H. Grützmacher, *J. Am. Chem. Soc.*, 1997, **119**, 6648.
11. Ch. Aubauer, T. M. Klapötke and A. Schulz, *J. Mol. Struct. (Theochem)*, 2001, **543**, 285.
12. M. L. McKee and W. N. Lipscomb, *Inorg. Chem.*, 1981, **20**, 4148.
13. G. Olah, G. Rasul, L. Heiliger and G. K. S. Prakash, *J. Am. Chem. Soc.*, 1996, **118**, 3580.
14. B. D. Rowsell, R. J. Gillespie and G. L. Heard, *Inorg. Chem.*, 1999, **38**, 4659.
15. B. J. van der Veken and E. J. Sluyts, *J. Am. Chem. Soc.*, 1997, **119**, 11516.
16. E. H. Wong, *Inorg. Chem.*, 1981, **20**, 1300.
17. S. L. Emery and J. A. Morrison, *J. Am. Chem. Soc.*, 1982, **104**, 6790.
18. P. R. LeBreton, S. Urano, M. Shabbaz, S. L. Emery and J. A. Morrison, *J. Am. Chem. Soc.*, 1986, **108**, 3937.
19. J. A. Morrison, *Chem. Rev.* 1991, **91**, 35.
20. W. Hönle, Y. Grin, A. Burkhardt, U. Wedig, M. Schultheiss and H. G. von Schnering, *J. Solid State Chem.*, 1997, 59.
21. H. Binder, R. Kellner, K. Vaas, M. Hein, F. Baumann, M. Wanner, R. Winter, W. Kaim, W. Hönle, Y. Grin, U. Wedig, M. Schultheiss, R. K. Kremer, H. G. von

Schnering, O. Groeger and G. Engelhardt, *Z. Anorg. Allg. Chem.*, 1999, **625**, 1059.

22. E. R. Davidson and D. Feller, *Chem. Rev.*, 1986, **86**, 681.
23. S. F. Boys and F. Bernardi, *Mol. Phys.*, 1970, **19**, 553.
24. M. A. Fox, R. Greatrex and D. L. Ormsby, *Chem. Commun.*, 2002, 2052.
25. J. Dobson and R. Schaeffer, *Inorg. Chem.*, 1965, **4**, 593.
26. M. A. Toft, J. B. Leach, F. L. Himpsl and S. G. Shore, *Inorg. Chem.*, 1982, **21**, 1952.
27. T. J. Dupont, R. E. Loffredo, R. C. Haltiwanger, C. A. Turner and A. D. Norman, *Inorg. Chem.*, 1978, **17**, 2062.
28. R. Schaeffer, J. N. Shoolery and R. Jones, *J. Am. Chem. Soc.*, 1958, **80**, 2670.
29. G. Vass, G. Tarczay, G. Magyarfalvi, A. Bödi, L. Szepes, *Organometallics*, 2002, **21**, 2751.
30. O. P. Charkin, N. M. Klimenko, D. Moran, A. M. Mebel, D. O. Charkin and P. v. R. Schleyer, *Inorg. Chem.*, 2001, **40**, 6913 and *J. Phys. Chem.*, 2002, **A106**, 11594.

# Appendix A

| | |
|---|---|
| **Table A** | Crystallographic fractional atomic coordinates of $B_8F_{12}$. |
| **Table B** | Crystallographic atomic displacement parameters for $B_8F_{12}$. |
| **Table C** | Crystallographic bond lengths in $B_8F_{12}$. |
| **Table D** | Crystallographic bond angles in $B_8F_{12}$. |
| **Table E** | Crystallographic fractional atomic coordinates of $(B_8F_{12})_2.BF_3$ |
| **Table F** | Crystallographic atomic displacement parameters for $(B_8F_{12})_2.BF_3$ |
| **Table G** | Crystallographic bond lengths in $(B_8F_{12})_2.BF_3$ |
| **Table H** | Crystallographic bond angles in $(B_8F_{12})_2.BF_3$ |
| **Table I** | Flexible restraints used in the GED refinement of $B_8F_{12}$. |
| **Table J** | Bond distances and amplitudes of vibration obtained in the GED refinement of $B_8F_{12}$. |
| **Table K** | Fluorine-Fluorine interactions in $B_8F_{12}$. |

**Table A**. Crystallographic fractional atomic coordinates of $B_8F_{12}$.

| Atom($ij$)[a] | $x$ | $y$ | $z$ | $U_{iso}$ |
|---|---|---|---|---|
| B(11) | 0.31332(7) | 1.1697(2) | 0.10576(6) | 0.0367 |
| B(21) | 0.33772(5) | 1.39834(18) | 0.13439(5) | 0.0255 |
| B(31) | 0.41230(6) | 1.3917(2) | 0.16900(6) | 0.0321 |
| B(41) | 0.35452(5) | 1.25351(18) | 0.18659(5) | 0.0246 |
| B(51) | 0.36258(6) | 1.4961(2) | 0.08376(6) | 0.0321 |
| B(61) | 0.28578(6) | 1.5433(2) | 0.14085(6) | 0.035 |
| B(71) | 0.41022(6) | 1.1109(2) | 0.21931(6) | 0.0315 |
| B(81) | 0.30598(6) | 1.2350(2) | 0.22275(6) | 0.0349 |
| F(11) | 0.25864(4) | 1.14622(16) | 0.08950(4) | 0.0577 |
| F(21) | 0.34671(4) | 1.05733(12) | 0.09034(4) | 0.0498 |
| F(31) | 0.43413(4) | 1.52300(13) | 0.20377(4) | 0.0497 |
| F(41) | 0.44726(3) | 1.29694(13) | 0.14750(4) | 0.0434 |
| F(51) | 0.35501(4) | 1.41026(13) | 0.03669(3) | 0.0434 |
| F(61) | 0.38185(5) | 1.66297(12) | 0.08725(4) | 0.0506 |
| F(71) | 0.23480(4) | 1.48336(13) | 0.14063(4) | 0.0498 |
| F(81) | 0.29427(4) | 1.71850(13) | 0.14908(5) | 0.0578 |
| F(91) | 0.41205(4) | 0.94381(12) | 0.20269(4) | 0.0494 |
| F(101) | 0.44749(3) | 1.16403(13) | 0.26474(4) | 0.0462 |
| F(111) | 0.26465(4) | 1.11538(17) | 0.20996(4) | 0.0589 |
| F(121) | 0.30894(5) | 1.34081(15) | 0.26454(4) | 0.062 |
| B(12) | 0.58640(5) | 0.20812(18) | 0.53575(5) | 0.0256 |
| B(22) | 0.59277(5) | 0.22561(16) | 0.60884(5) | 0.0228 |
| B(32) | 0.55804(6) | 0.41795(18) | 0.62634(6) | 0.0285 |
| B(42) | 0.62110(5) | 0.41836(16) | 0.59354(5) | 0.0223 |
| B(52) | 0.52814(6) | 0.12461(19) | 0.60859(6) | 0.0321 |
| B(62) | 0.64437(6) | 0.09347(18) | 0.65110(6) | 0.0292 |
| B(72) | 0.59609(5) | 0.63179(17) | 0.56875(6) | 0.0268 |
| B(82) | 0.69375(5) | 0.41320(18) | 0.60761(5) | 0.0269 |
| F(12) | 0.61690(3) | 0.0794(1) | 0.52288(3) | 0.0347 |
| F(22) | 0.54572(3) | 0.2849(1) | 0.49759(3) | 0.034 |
| F(32) | 0.57260(4) | 0.47038(12) | 0.67759(3) | 0.0433 |
| F(42) | 0.50873(3) | 0.4782(1) | 0.59327(3) | 0.0343 |
| F(52) | 0.49655(4) | 0.05017(12) | 0.56316(4) | 0.0465 |
| F(62) | 0.51319(4) | 0.10204(14) | 0.65321(4) | 0.0522 |
| F(72) | 0.69161(3) | 0.05020(11) | 0.63900(4) | 0.0398 |
| F(82) | 0.64126(4) | 0.03656(13) | 0.69937(3) | 0.0451 |
| F(92) | 0.57822(3) | 0.6663(1) | 0.51639(3) | 0.0364 |
| F(102) | 0.59833(4) | 0.7705(1) | 0.60292(4) | 0.0393 |
| F(112) | 0.71978(3) | 0.35388(11) | 0.57253(3) | 0.0359 |
| F(122) | 0.72584(3) | 0.46844(15) | 0.65520(4) | 0.0509 |
| B(13) | 0.13566(6) | 0.08552(18) | 0.45723(6) | 0.0279 |
| B(23) | 0.14822(5) | 0.31819(17) | 0.43273(5) | 0.0234 |
| B(33) | 0.13149(5) | 0.32199(18) | 0.35896(5) | 0.0259 |
| B(43) | 0.18542(5) | 0.16855(17) | 0.40769(5) | 0.0242 |
| B(53) | 0.08065(6) | 0.41659(19) | 0.41735(6) | 0.0294 |
| B(63) | 0.19122(6) | 0.4566(2) | 0.48179(6) | 0.0298 |

| | | | | |
|---|---|---|---|---|
| B(73) | 0.17518(6) | 0.0190(2) | 0.35309(6) | 0.036 |
| B(83) | 0.25488(5) | 0.14676(18) | 0.44537(5) | 0.0274 |
| F(13) | 0.16269(3) | 0.04464(12) | 0.50739(3) | 0.0399 |
| F(23) | 0.09090(4) | -0.00838(11) | 0.43092(3) | 0.0391 |
| F(33) | 0.15458(3) | 0.4528(1) | 0.33693(3) | 0.0357 |
| F(43) | 0.08453(3) | 0.24312(11) | 0.32781(3) | 0.034 |
| F(53) | 0.03865(3) | 0.33390(12) | 0.42926(4) | 0.04 |
| F(63) | 0.07302(4) | 0.58606(11) | 0.39988(4) | 0.043 |
| F(73) | 0.23490(3) | 0.38984(12) | 0.52107(3) | 0.0421 |
| F(83) | 0.18499(4) | 0.63413(11) | 0.48243(4) | 0.0423 |
| F(93) | 0.16030(5) | -0.14934(12) | 0.35973(4) | 0.0574 |
| F(103) | 0.18813(5) | 0.06218(15) | 0.30848(4) | 0.0569 |
| F(113) | 0.27189(3) | 0.01883(12) | 0.48199(3) | 0.042 |
| F(123) | 0.29490(3) | 0.25565(11) | 0.43719(4) | 0.0433 |
| B(14) | 1.14312(6) | 0.1452(2) | 0.65243(6) | 0.032 |
| B(24) | 1.10936(5) | 0.36816(18) | 0.65122(5) | 0.0247 |
| B(34) | 1.06664(6) | 0.38177(19) | 0.69638(6) | 0.0306 |
| B(44) | 1.05485(5) | 0.22217(17) | 0.63204(5) | 0.0243 |
| B(54) | 1.15861(7) | 0.4617(2) | 0.70860(6) | 0.0397 |
| B(64) | 1.11168(6) | 0.5086(2) | 0.59823(6) | 0.0307 |
| B(74) | 1.01903(6) | 0.07904(19) | 0.66477(6) | 0.0314 |
| B(84) | 1.03048(5) | 0.19415(19) | 0.56230(5) | 0.0285 |
| F(14) | 1.17142(3) | 0.12459(13) | 0.61684(4) | 0.0449 |
| F(24) | 1.14923(4) | 0.02654(13) | 0.69174(4) | 0.05 |
| F(34) | 1.02909(4) | 0.51428(11) | 0.68945(4) | 0.044 |
| F(44) | 1.08091(4) | 0.29518(12) | 0.74426(3) | 0.0397 |
| F(54) | 1.20229(4) | 0.36485(17) | 0.73604(4) | 0.0584 |
| F(64) | 1.15697(5) | 0.63396(13) | 0.72063(4) | 0.0593 |
| F(74) | 1.11496(4) | 0.44014(12) | 0.55064(3) | 0.0412 |
| F(84) | 1.10873(5) | 0.68683(12) | 0.60035(4) | 0.0505 |
| F(94) | 1.03410(4) | -0.09214(12) | 0.67120(5) | 0.0591 |
| F(104) | 0.97428(3) | 0.12819(11) | 0.67944(3) | 0.038 |
| F(114) | 1.05234(3) | 0.06473(12) | 0.53851(3) | 0.0438 |
| F(124) | 0.99115(3) | 0.29716(12) | 0.53016(3) | 0.0402 |

[a] $i$ = atom number, $j$ = residue number.

**Table B**. Crystallographic atomic displacement parameters for $B_8F_{12}$.

| Atom($ij$)[a] | $U_{11}$ | $U_{22}$ | $U_{33}$ | $U_{23}$ | $U_{13}$ | $U_{12}$ |
|---|---|---|---|---|---|---|
| B(11) | 0.0444(8) | 0.0353(7) | 0.0294(6) | -0.0033(6) | 0.0089(6) | -0.0081(6) |
| B(21) | 0.0234(5) | 0.0279(6) | 0.0245(5) | 0.0009(5) | 0.0061(4) | 0.0032(5) |
| B(31) | 0.0253(6) | 0.0334(7) | 0.0360(7) | 0.0102(5) | 0.0062(5) | -0.0025(5) |
| B(41) | 0.0218(5) | 0.0266(6) | 0.0248(5) | -0.0007(4) | 0.0057(4) | -0.0003(4) |
| B(51) | 0.0338(6) | 0.0334(7) | 0.0309(7) | 0.0067(5) | 0.0123(5) | 0.0081(5) |
| B(61) | 0.0340(7) | 0.0395(8) | 0.0322(7) | 0.0037(6) | 0.0105(5) | 0.0120(6) |
| B(71) | 0.0256(6) | 0.0352(7) | 0.0362(7) | 0.0121(6) | 0.0130(5) | 0.0044(5) |
| B(81) | 0.0269(6) | 0.0485(8) | 0.0319(6) | 0.0109(6) | 0.0123(5) | 0.0095(6) |

| | | | | | | |
|---|---|---|---|---|---|---|
| F(11) | 0.0446(5) | 0.0728(7) | 0.0509(5) | -0.0172(5) | 0.0060(4) | -0.0223(5) |
| F(21) | 0.0672(6) | 0.0378(4) | 0.0405(4) | -0.0118(4) | 0.0093(4) | 0.0066(4) |
| F(31) | 0.0447(5) | 0.0436(5) | 0.0509(5) | 0.0028(4) | -0.0022(4) | -0.0164(4) |
| F(41) | 0.0275(3) | 0.0540(5) | 0.0545(5) | 0.0219(4) | 0.0209(3) | 0.0102(3) |
| F(51) | 0.0547(5) | 0.0497(5) | 0.0294(4) | 0.0018(3) | 0.0177(3) | 0.0029(4) |
| F(61) | 0.0771(6) | 0.0314(4) | 0.0516(5) | 0.0082(4) | 0.0318(5) | 0.0002(4) |
| F(71) | 0.0353(4) | 0.0559(5) | 0.0649(6) | 0.0127(4) | 0.0250(4) | 0.0151(4) |
| F(81) | 0.0550(6) | 0.0396(5) | 0.0807(7) | -0.0108(5) | 0.0224(5) | 0.0121(4) |
| F(91) | 0.0578(5) | 0.0355(4) | 0.0583(5) | 0.0098(4) | 0.0223(4) | 0.0159(4) |
| F(101) | 0.0317(4) | 0.0552(5) | 0.0436(4) | 0.0185(4) | -0.0021(3) | -0.0012(4) |
| F(111) | 0.0317(4) | 0.0931(8) | 0.0513(5) | 0.0169(5) | 0.0111(4) | -0.0155(5) |
| F(121) | 0.0813(7) | 0.0666(6) | 0.0517(5) | -0.0058(5) | 0.0407(5) | 0.0112(5) |
| B(12) | 0.0259(6) | 0.0224(6) | 0.0284(6) | -0.0018(5) | 0.0076(5) | -0.0023(4) |
| B(22) | 0.0225(5) | 0.0193(5) | 0.0260(5) | 0.0028(4) | 0.0061(4) | 0.0020(4) |
| B(32) | 0.0295(6) | 0.0260(6) | 0.0340(6) | -0.0001(5) | 0.0153(5) | 0.0028(5) |
| B(42) | 0.0217(5) | 0.0195(5) | 0.0254(5) | -0.0005(4) | 0.0062(4) | 0.0009(4) |
| B(52) | 0.0259(6) | 0.0249(6) | 0.0450(8) | 0.0095(6) | 0.0095(5) | 0.0012(5) |
| B(62) | 0.0287(6) | 0.0245(6) | 0.0318(6) | 0.0050(5) | 0.0044(5) | 0.0018(5) |
| B(72) | 0.0220(5) | 0.0193(5) | 0.0402(7) | 0.0030(5) | 0.0107(5) | 0.0006(4) |
| B(82) | 0.0214(5) | 0.0280(6) | 0.0306(6) | 0.0010(5) | 0.0063(5) | 0.0006(5) |
| F(12) | 0.0390(4) | 0.0295(4) | 0.0378(4) | -0.0050(3) | 0.0146(3) | 0.0053(3) |
| F(22) | 0.0348(4) | 0.0335(4) | 0.0283(3) | -0.0000(3) | 0.0003(3) | 0.0021(3) |
| F(32) | 0.0506(5) | 0.0474(5) | 0.0353(4) | -0.0088(3) | 0.0178(4) | 0.0043(4) |
| F(42) | 0.0266(3) | 0.0312(4) | 0.0475(4) | 0.0045(3) | 0.0144(3) | 0.0089(3) |
| F(52) | 0.0369(4) | 0.0393(4) | 0.0590(5) | -0.0052(4) | 0.0068(4) | -0.0145(3) |
| F(62) | 0.0405(4) | 0.0659(6) | 0.0539(5) | 0.0214(5) | 0.0194(4) | -0.0079(4) |
| F(72) | 0.0293(4) | 0.0390(4) | 0.0500(4) | 0.0112(3) | 0.0098(3) | 0.0122(3) |
| F(82) | 0.0437(4) | 0.0535(5) | 0.0365(4) | 0.0194(4) | 0.0089(3) | 0.0089(4) |
| F(92) | 0.0381(4) | 0.0287(4) | 0.0413(4) | 0.0102(3) | 0.0095(3) | 0.0047(3) |
| F(102) | 0.0469(4) | 0.0199(3) | 0.0537(5) | -0.0035(3) | 0.0189(4) | 0.0012(3) |
| F(112) | 0.0294(3) | 0.0411(4) | 0.0402(4) | -0.0044(3) | 0.0148(3) | 0.0028(3) |
| F(122) | 0.0284(4) | 0.0840(7) | 0.0366(4) | -0.0175(4) | 0.0033(3) | -0.0056(4) |
| B(13) | 0.0303(6) | 0.0248(6) | 0.0304(6) | 0.0010(5) | 0.0115(5) | 0.0017(5) |
| B(23) | 0.0247(5) | 0.0214(5) | 0.0240(5) | -0.0024(4) | 0.0069(4) | -0.0003(4) |
| B(33) | 0.0265(6) | 0.0249(6) | 0.0262(6) | 0.0014(5) | 0.0072(5) | 0.0045(5) |
| B(43) | 0.0271(6) | 0.0207(5) | 0.0236(5) | -0.0007(4) | 0.0055(4) | 0.0019(4) |
| B(53) | 0.0267(6) | 0.0295(6) | 0.0324(6) | -0.0030(5) | 0.0090(5) | 0.0040(5) |
| B(63) | 0.0292(6) | 0.0315(7) | 0.0305(6) | -0.0072(5) | 0.0116(5) | -0.0036(5) |
| B(73) | 0.0332(7) | 0.0362(7) | 0.0315(7) | -0.0111(6) | -0.0017(5) | 0.0126(6) |
| B(83) | 0.0253(6) | 0.0279(6) | 0.0280(6) | -0.0041(5) | 0.0061(5) | 0.0027(5) |
| F(13) | 0.0430(4) | 0.0466(4) | 0.0306(4) | 0.0096(3) | 0.0115(3) | 0.0032(3) |
| F(23) | 0.0444(4) | 0.0311(4) | 0.0414(4) | -0.0020(3) | 0.0118(3) | -0.0124(3) |
| F(33) | 0.0404(4) | 0.0332(4) | 0.0342(4) | 0.0083(3) | 0.0121(3) | 0.0001(3) |
| F(43) | 0.0279(3) | 0.0389(4) | 0.0303(3) | -0.0022(3) | 0.0004(3) | 0.0006(3) |
| F(53) | 0.0289(4) | 0.0429(4) | 0.0512(5) | 0.0026(4) | 0.0161(3) | 0.0016(3) |
| F(63) | 0.0396(4) | 0.0293(4) | 0.0635(5) | 0.0060(4) | 0.0203(4) | 0.0119(3) |
| F(73) | 0.0356(4) | 0.0474(5) | 0.0362(4) | -0.0115(3) | -0.0012(3) | -0.0009(3) |
| F(83) | 0.0492(5) | 0.0269(4) | 0.0520(5) | -0.0126(3) | 0.0168(4) | -0.0071(3) |

| | | | | | | |
|---|---|---|---|---|---|---|
| F(93) | 0.0652(6) | 0.0340(4) | 0.0677(6) | -0.0221(4) | 0.0108(5) | -0.0007(4) |
| F(103) | 0.0707(6) | 0.0685(6) | 0.0309(4) | -0.0084(4) | 0.0134(4) | 0.0266(5) |
| F(113) | 0.0334(4) | 0.0521(5) | 0.0387(4) | 0.0141(4) | 0.0078(3) | 0.0129(4) |
| F(123) | 0.0307(4) | 0.0363(4) | 0.0654(5) | -0.0018(4) | 0.0179(4) | -0.0034(3) |
| B(14) | 0.0235(6) | 0.0353(7) | 0.0344(7) | -0.0044(6) | 0.0037(5) | 0.0005(5) |
| B(24) | 0.0241(5) | 0.0269(6) | 0.0232(5) | -0.0023(4) | 0.0069(4) | -0.0053(4) |
| B(34) | 0.0350(7) | 0.0293(6) | 0.0310(6) | -0.0074(5) | 0.0149(5) | -0.0084(5) |
| B(44) | 0.0233(5) | 0.0225(5) | 0.0275(6) | -0.0031(4) | 0.0077(4) | -0.0004(4) |
| B(54) | 0.0386(7) | 0.0521(9) | 0.0284(7) | -0.0075(6) | 0.0095(6) | -0.0222(7) |
| B(64) | 0.0304(6) | 0.0327(7) | 0.0292(6) | 0.0011(5) | 0.0091(5) | -0.0057(5) |
| B(74) | 0.0319(6) | 0.0273(6) | 0.0350(7) | -0.0022(5) | 0.0096(5) | -0.0075(5) |
| B(84) | 0.0232(6) | 0.0319(6) | 0.0298(6) | -0.0067(5) | 0.0067(5) | -0.0039(5) |
| F(14) | 0.0372(4) | 0.0559(5) | 0.0433(4) | -0.0088(4) | 0.0141(3) | 0.0093(4) |
| F(24) | 0.0412(4) | 0.0500(5) | 0.0579(5) | 0.0195(4) | 0.0125(4) | 0.0137(4) |
| F(34) | 0.0498(5) | 0.0333(4) | 0.0562(5) | -0.0086(4) | 0.0268(4) | 0.0019(3) |
| F(44) | 0.0449(4) | 0.0505(5) | 0.0259(3) | -0.0020(3) | 0.0136(3) | -0.0136(4) |
| F(54) | 0.0372(4) | 0.0879(8) | 0.0401(5) | -0.0081(5) | -0.0047(4) | -0.0132(5) |
| F(64) | 0.0861(7) | 0.0472(5) | 0.0423(5) | -0.0145(4) | 0.0149(5) | -0.0351(5) |
| F(74) | 0.0508(5) | 0.0467(5) | 0.0284(4) | 0.0004(3) | 0.0150(3) | -0.0086(4) |
| F(84) | 0.0727(6) | 0.0315(4) | 0.0492(5) | 0.0052(4) | 0.0207(4) | -0.0034(4) |
| F(94) | 0.0547(5) | 0.0269(4) | 0.1050(8) | 0.0109(5) | 0.0379(6) | 0.0003(4) |
| F(104) | 0.0323(4) | 0.0392(4) | 0.0469(4) | -0.0011(3) | 0.0182(3) | -0.0064(3) |
| F(114) | 0.0367(4) | 0.0507(5) | 0.0399(4) | -0.0205(4) | 0.0046(3) | 0.0063(4) |
| F(124) | 0.0376(4) | 0.0471(4) | 0.0323(4) | -0.0018(3) | 0.0046(3) | 0.0080(3) |

[a] $i$ = atom number, $j$ = residue number.

**Table C**. Crystallographic bond lengths (Å) in $B_8F_{12}$.

| | | | |
|---|---|---|---|
| B(11)-B(21) | 1.858(2) | B(12)-B(22) | 1.8290(18) |
| B(21)-B(31) | 1.7918(18) | B(22)-B(32) | 1.7710(18) |
| B(21)-B(41) | 1.6595(18) | B(22)-B(42) | 1.6708(17) |
| B(21)-B(51) | 1.7340(18) | B(22)-B(52) | 1.7511(18) |
| B(21)-B(61) | 1.7055(18) | B(22)-B(62) | 1.7096(17) |
| B(31)-B(41) | 1.9004(18) | B(32)-B(42) | 1.9612(18) |
| B(41)-B(71) | 1.7343(18) | B(42)-B(72) | 1.7332(17) |
| B(41)-B(81) | 1.7098(18) | B(42)-B(82) | 1.7174(17) |
| B(11)-F(11) | 1.2990(19) | B(12)-F(12) | 1.3045(15) |
| B(11)-F(21) | 1.3008(19) | B(12)-F(22) | 1.3054(15) |
| B(31)-F(31) | 1.3142(18) | B(32)-F(32) | 1.3095(16) |
| B(31)-F(41) | 1.3391(17) | B(32)-F(42) | 1.3368(16) |
| B(51)-F(61) | 1.3062(18) | B(52)-F(52) | 1.3136(18) |
| B(51)-F(51) | 1.3200(17) | B(52)-F(62) | 1.3024(18) |
| B(61)-F(81) | 1.3087(19) | B(62)-F(72) | 1.3227(16) |
| B(61)-F(71) | 1.3263(18) | B(62)-F(82) | 1.3224(16) |
| B(71)-F(91) | 1.3013(18) | B(72)-F(92) | 1.3043(16) |
| B(71)-F(101) | 1.3124(18) | B(72)-F(102) | 1.3302(16) |
| B(81)-F(111) | 1.3104(19) | B(82)-F(112) | 1.3143(15) |

| | | | |
|---|---|---|---|
| B(81)-F(121) | 1.3032(19) | B(82)-F(122) | 1.3068(16) |
| B(13)-B(23) | 1.8730(18) | B(14)-B(24) | 1.830(2) |
| B(23)-B(33) | 1.8061(17) | B(24)-B(34) | 1.7697(18) |
| B(23)-B(43) | 1.6683(17) | B(24)-B(44) | 1.6743(17) |
| B(23)-B(53) | 1.7488(18) | B(24)-B(54) | 1.7485(19) |
| B(23)-B(63) | 1.7183(18) | B(24)-B(64) | 1.7129(18) |
| B(33)-B(43) | 1.9026(17) | B(34)-B(44) | 1.9676(18) |
| B(43)-B(73) | 1.7325(18) | B(44)-B(74) | 1.7308(19) |
| B(43)-B(83) | 1.7088(18) | B(44)-B(84) | 1.7175(18) |
| B(13)-F(13) | 1.2954(16) | B(14)-F(14) | 1.3010(17) |
| B(13)-F(23) | 1.3078(16) | B(14)-F(24) | 1.3027(18) |
| B(33)-F(33) | 1.3196(15) | B(34)-F(34) | 1.3168(18) |
| B(33)-F(43) | 1.3305(15) | B(34)-F(44) | 1.3306(17) |
| B(53)-F(53) | 1.3060(16) | B(54)-F(54) | 1.310(2) |
| B(53)-F(63) | 1.3154(16) | B(54)-F(64) | 1.303(2) |
| B(63)-F(73) | 1.3330(17) | B(64)-F(74) | 1.3368(16) |
| B(63)-F(83) | 1.3114(17) | B(64)-F(84) | 1.3109(17) |
| B(73)-F(93) | 1.313(2) | B(74)-F(94) | 1.3058(17) |
| B(73)-F(103) | 1.305(2) | B(74)-F(104) | 1.3101(17) |
| B(83)-F(113) | 1.3047(16) | B(84)-F(114) | 1.3208(16) |
| B(83)-F(123) | 1.3292(16) | B(84)-F(124) | 1.3120(16) |

**Table D**. Crystallographic bond angles (°) for $B_8F_{12}$.

| | | | |
|---|---|---|---|
| B(11)-B(21)-B(31) | 109.75(9) | B(12)-B(22)-B(32) | 113.96(9) |
| B(11)-B(21)-B(41) | 73.44(8) | B(12)-B(22)-B(42) | 74.98(7) |
| B(11)-B(21)-B(51) | 102.93(9) | B(12)-B(22)-B(52) | 98.91(9) |
| B(11)-B(21)-B(61) | 115.8(1) | B(12)-B(22)-B(62) | 115.66(9) |
| B(21)-B(31)-B(41) | 53.32(7) | B(22)-B(32)-B(42) | 52.89(6) |
| B(21)-B(41)-B(31) | 59.99(7) | B(22)-B(42)-B(32) | 57.71(7) |
| B(21)-B(41)-B(71) | 138.7(1) | B(22)-B(42)-B(72) | 136.16(9) |
| B(21)-B(41)-B(81) | 115.59(9) | B(22)-B(42)-B(82) | 114.24(9) |
| B(31)-B(21)-B(41) | 66.69(7) | B(32)-B(22)-B(42) | 69.41(7) |
| B(31)-B(21)-B(51) | 81.27(8) | B(32)-B(22)-B(52) | 80.53(8) |
| B(31)-B(21)-B(61) | 131.11(11) | B(32)-B(22)-B(62) | 128.1(1) |
| B(31)-B(41)-B(71) | 83.98(8) | B(32)-B(42)-B(72) | 85.18(8) |
| B(31)-B(41)-B(81) | 148.66(11) | B(32)-B(42)-B(82) | 144.3(1) |
| B(41)-B(21)-B(51) | 143.3(1) | B(42)-B(22)-B(52) | 142.71(9) |
| B(41)-B(21)-B(61) | 110.02(9) | B(42)-B(22)-B(62) | 110.08(9) |
| B(51)-B(21)-B(61) | 104.3(1) | B(52)-B(22)-B(62) | 105.68(9) |
| B(71)-B(41)-B(81) | 105.63(9) | B(72)-B(42)-B(82) | 109.55(9) |
| B(21)-B(11)-F(11) | 115.61(12) | B(22)-B(12)-F(12) | 114.8(1) |
| B(21)-B(11)-F(21) | 122.00(12) | B(22)-B(12)-F(22) | 123.5(1) |
| F(11)-B(11)-F(21) | 120.29(13) | F(12)-B(12)-F(22) | 119.82(11) |
| B(21)-B(31)-F(31) | 118.28(11) | B(22)-B(32)-F(32) | 118.17(11) |
| B(21)-B(31)-F(41) | 119.90(11) | B(22)-B(32)-F(42) | 121.30(11) |
| B(41)-B(31)-F(31) | 114.80(11) | B(42)-B(32)-F(32) | 113.7(1) |

| | | | |
|---|---|---|---|
| B(41)-B(31)-F(41) | 115.51(11) | B(42)-B(32)-F(42) | 114.5(1) |
| F(31)-B(31)-F(41) | 118.08(12) | F(32)-B(32)-F(42) | 118.06(11) |
| B(21)-B(51)-F(51) | 119.46(12) | B(22)-B(52)-F(52) | 118.99(12) |
| B(21)-B(51)-F(61) | 122.35(11) | B(22)-B(52)-F(62) | 122.28(12) |
| F(61)-B(51)-F(51) | 117.53(12) | F(52)-B(52)-F(62) | 118.26(12) |
| B(21)-B(61)-F(71) | 121.67(12) | B(22)-B(62)-F(72) | 122.06(11) |
| B(21)-B(61)-F(81) | 122.57(13) | B(22)-B(62)-F(82) | 122.31(11) |
| F(81)-B(61)-F(71) | 115.67(12) | F(72)-B(62)-F(82) | 115.52(11) |
| B(41)-B(71)-F(91) | 120.52(12) | B(42)-B(72)-F(92) | 121.9(1) |
| B(41)-B(71)-F(101) | 119.95(12) | B(42)-B(72)-F(102) | 120.56(11) |
| F(101)-B(71)-F(91) | 119.10(12) | F(92)-B(72)-F(102) | 117.40(11) |
| B(41)-B(81)-F(111) | 122.01(12) | B(42)-B(82)-F(112) | 123.0(1) |
| B(41)-B(81)-F(121) | 120.65(13) | B(42)-B(82)-F(122) | 120.1(1) |
| F(121)-B(81)-F(111) | 117.33(12) | F(112)-B(82)-F(122) | 116.9(1) |
| B(13)-B(23)-B(33) | 110.57(8) | B(14)-B(24)-B(34) | 112.98(9) |
| B(13)-B(23)-B(43) | 71.90(8) | B(14)-B(24)-B(44) | 75.78(8) |
| B(13)-B(23)-B(53) | 102.35(9) | B(14)-B(24)-B(54) | 97.8(1) |
| B(13)-B(23)-B(63) | 114.92(9) | B(14)-B(24)-B(64) | 115.7(1) |
| B(23)-B(33)-B(43) | 53.39(6) | B(24)-B(44)-B(34) | 57.47(7) |
| B(23)-B(43)-B(33) | 60.34(7) | B(24)-B(34)-B(44) | 52.91(6) |
| B(23)-B(43)-B(73) | 139.0(1) | B(24)-B(44)-B(74) | 136.2(1) |
| B(23)-B(43)-B(83) | 114.54(9) | B(24)-B(44)-B(84) | 112.99(9) |
| B(33)-B(23)-B(43) | 66.27(7) | B(34)-B(24)-B(44) | 69.62(7) |
| B(33)-B(23)-B(53) | 80.96(8) | B(34)-B(24)-B(54) | 80.28(8) |
| B(33)-B(23)-B(63) | 131.1(1) | B(34)-B(24)-B(64) | 129.76(11) |
| B(33)-B(43)-B(73) | 86.38(8) | B(34)-B(44)-B(74) | 86.12(8) |
| B(33)-B(43)-B(83) | 144.9(1) | B(34)-B(44)-B(84) | 149.1(1) |
| B(43)-B(23)-B(53) | 140.8(1) | B(44)-B(24)-B(54) | 143.0(1) |
| B(43)-B(23)-B(63) | 112.16(9) | B(44)-B(24)-B(64) | 111.07(9) |
| B(53)-B(23)-B(63) | 105.37(9) | B(54)-B(24)-B(64) | 104.6(1) |
| B(73)-B(43)-B(83) | 106.46(9) | B(74)-B(44)-B(84) | 110.62(9) |
| B(23)-B(13)-F(13) | 117.0(1) | B(24)-B(14)-F(14) | 115.00(11) |
| B(23)-B(13)-F(23) | 120.2(1) | B(24)-B(14)-F(24) | 124.13(11) |
| F(13)-B(13)-F(23) | 120.09(11) | F(14)-B(14)-F(24) | 119.50(12) |
| B(23)-B(33)-F(33) | 117.2(1) | B(24)-B(34)-F(34) | 118.59(11) |
| B(23)-B(33)-F(43) | 120.9(1) | B(24)-B(34)-F(44) | 121.38(11) |
| B(43)-B(33)-F(33) | 113.81(9) | B(44)-B(34)-F(34) | 113.44(11) |
| B(43)-B(33)-F(43) | 117.0(1) | B(44)-B(34)-F(44) | 114.7(1) |
| F(33)-B(33)-F(43) | 117.9(1) | F(34)-B(34)-F(44) | 117.70(11) |
| B(23)-B(53)-F(53) | 121.29(11) | B(24)-B(54)-F(54) | 119.88(13) |
| B(23)-B(53)-F(63) | 119.97(11) | B(24)-B(54)-F(64) | 121.09(14) |
| F(63)-B(53)-F(53) | 118.18(11) | F(54)-B(54)-F(64) | 118.43(13) |
| B(23)-B(63)-F(73) | 121.58(11) | B(24)-B(64)-F(74) | 120.94(11) |
| B(23)-B(63)-F(83) | 123.09(11) | B(24)-B(64)-F(84) | 123.53(11) |
| F(83)-B(63)-F(73) | 115.29(11) | F(74)-B(64)-F(84) | 115.50(12) |
| B(43)-B(73)-F(93) | 118.25(13) | B(44)-B(74)-F(94) | 118.58(11) |
| B(43)-B(73)-F(103) | 122.09(13) | B(44)-B(74)-F(104) | 123.78(11) |
| F(103)-B(73)-F(93) | 119.16(12) | F(94)-B(74)-F(104) | 117.37(12) |

| | | | |
|---|---|---|---|
| B(43)-B(83)-F(113) | 122.16(11) | B(44)-B(84)-F(114) | 119.63(11) |
| B(43)-B(83)-F(123) | 121.35(11) | B(44)-B(84)-F(124) | 123.55(11) |
| F(123)-B(83)-F(113) | 116.43(11) | F(114)-B(84)-F(124) | 116.81(11) |

**Table E.** Crystallographic fractional atomic coordinates for $(B_8F_{12})_2.BF_3$

| Atom(*ij*)[a] | *x* | *y* | *z* | $U_{iso}$ |
|---|---|---|---|---|
| B(11) | 0.3224(4) | 0.1301(2) | 0.9786(2) | 0.0292 |
| B(21) | 0.2705(4) | 0.22256(19) | 0.84272(19) | 0.0224 |
| B(31) | 0.3863(4) | 0.3464(2) | 0.8014(2) | 0.0283 |
| B(41) | 0.2243(4) | 0.29160(19) | 0.92755(18) | 0.0227 |
| B(51) | 0.4582(4) | 0.1883(2) | 0.7565(2) | 0.0291 |
| B(61) | 0.0712(4) | 0.1970(2) | 0.8086(2) | 0.0303 |
| B(71) | 0.3416(4) | 0.3701(2) | 0.9718(2) | 0.0275 |
| B(81) | -0.0093(4) | 0.3030(2) | 0.9781(2) | 0.0258 |
| F(11) | 0.2021(2) | 0.05836(12) | 1.02970(12) | 0.0411 |
| F(21) | 0.4886(2) | 0.11478(12) | 1.00582(11) | 0.0356 |
| F(31) | 0.3123(2) | 0.43201(11) | 0.73066(11) | 0.0386 |
| F(41) | 0.5685(2) | 0.34072(12) | 0.80623(12) | 0.0364 |
| F(51) | 0.5810(2) | 0.10553(13) | 0.79084(13) | 0.0444 |
| F(61) | 0.4688(2) | 0.23702(13) | 0.65210(11) | 0.0399 |
| F(71) | 0.0549(2) | 0.20760(15) | 0.71037(12) | 0.0478 |
| F(81) | -0.0791(2) | 0.16967(15) | 0.87999(13) | 0.0459 |
| F(91) | 0.4555(2) | 0.32305(13) | 1.04345(12) | 0.0393 |
| F(101) | 0.3057(2) | 0.47571(12) | 0.94117(12) | 0.0394 |
| F(111) | -0.0831(2) | 0.23113(12) | 1.06718(11) | 0.0349 |
| F(121) | -0.1205(2) | 0.38586(12) | 0.92926(12) | 0.0387 |
| B(12) | -0.0205(4) | 0.2346(3) | 1.4724(2) | 0.0325 |
| B(22) | 0.1366(3) | 0.26490(19) | 1.34178(19) | 0.0213 |
| B(32) | 0.2219(4) | 0.3969(2) | 1.30156(19) | 0.0252 |
| B(42) | 0.2529(4) | 0.2794(2) | 1.43050(19) | 0.0231 |
| B(52) | -0.0151(4) | 0.3381(2) | 1.2503(2) | 0.0261 |
| B(62) | 0.2214(3) | 0.1522(2) | 1.3053(2) | 0.0262 |
| B(72) | 0.2795(4) | 0.3835(2) | 1.4767(2) | 0.0308 |
| B(82) | 0.3990(4) | 0.1674(2) | 1.48954(19) | 0.0249 |
| F(12) | -0.1372(2) | 0.31019(15) | 1.49642(13) | 0.0464 |
| F(22) | -0.0434(2) | 0.13255(13) | 1.52335(12) | 0.0447 |
| F(32) | 0.1088(2) | 0.48400(11) | 1.30930(11) | 0.0335 |
| F(42) | 0.3756(2) | 0.41323(11) | 1.23198(11) | 0.0342 |
| F(52) | -0.1959(2) | 0.34090(13) | 1.27978(12) | 0.0399 |
| F(62) | 0.0445(2) | 0.37774(12) | 1.14683(11) | 0.0368 |
| F(72) | 0.2407(2) | 0.15543(12) | 1.20531(11) | 0.0331 |
| F(82) | 0.2756(2) | 0.05854(11) | 1.37568(12) | 0.0374 |
| F(92) | 0.4342(2) | 0.43151(14) | 1.44656(13) | 0.0491 |
| F(102) | 0.1536(2) | 0.40859(13) | 1.54864(12) | 0.0441 |
| F(112) | 0.3411(2) | 0.08602(11) | 1.57468(11) | 0.0361 |
| F(122) | 0.57687(19) | 0.16154(13) | 1.45204(11) | 0.0376 |

| | | | | |
|---|---|---|---|---|
| B(13) | -0.2428(4) | 0.0848(2) | 1.2388(2) | 0.0325 |
| F(13) | -0.1107(2) | 0.08807(14) | 1.29001(13) | 0.0473 |
| F(23) | -0.2307(3) | 0.01458(14) | 1.19036(14) | 0.061 |
| F(33) | -0.3905(2) | 0.15404(16) | 1.23719(14) | 0.0525 |

[a] $i$ = atom number, $j$ = residue number.

**Table F**. Crystallographic atomic displacement parameters for $(B_8F_{12})_2.BF_3$

| Atom($ij$)[a] | $U_{11}$ | $U_{22}$ | $U_{33}$ | $U_{23}$ | $U_{13}$ | $U_{12}$ |
|---|---|---|---|---|---|---|
| B(11) | 0.0348(15) | 0.0233(12) | 0.0241(12) | -0.004(1) | -0.001(1) | -0.000(1) |
| B(21) | 0.0276(12) | 0.0192(11) | 0.0194(11) | -0.0038(9) | -0.0029(9) | -0.0058(9) |
| B(31) | 0.0368(14) | 0.0269(13) | 0.0220(12) | -0.008(1) | 0.001(1) | -0.0111(11) |
| B(41) | 0.0269(13) | 0.0191(11) | 0.017(1) | -0.0003(9) | -0.0000(9) | -0.0046(9) |
| B(51) | 0.0295(13) | 0.0330(14) | 0.0297(13) | -0.0156(11) | -0.002(1) | -0.0081(11) |
| B(61) | 0.0325(15) | 0.0284(13) | 0.0315(14) | -0.0098(11) | -0.0052(11) | -0.0066(11) |
| B(71) | 0.0281(13) | 0.0319(14) | 0.0253(12) | -0.013(1) | 0.003(1) | -0.0112(11) |
| B(81) | 0.0293(13) | 0.0256(12) | 0.0259(12) | -0.011(1) | -0.004(1) | -0.006(1) |
| F(11) | 0.0453(9) | 0.0257(7) | 0.0402(8) | 0.0037(6) | -0.0022(7) | -0.0083(6) |
| F(21) | 0.0364(8) | 0.0334(8) | 0.0333(8) | -0.0073(6) | -0.0099(6) | 0.0044(6) |
| F(31) | 0.055(1) | 0.0292(7) | 0.0253(7) | 0.0012(6) | -0.0030(6) | -0.0139(7) |
| F(41) | 0.0301(8) | 0.0432(8) | 0.0395(8) | -0.0181(7) | 0.0056(6) | -0.0168(6) |
| F(51) | 0.0458(9) | 0.0425(9) | 0.0407(9) | -0.0164(7) | -0.0014(7) | 0.0089(7) |
| F(61) | 0.0444(9) | 0.0497(9) | 0.0260(7) | -0.0161(6) | 0.0017(6) | -0.0052(7) |
| F(71) | 0.050(1) | 0.0635(11) | 0.0340(8) | -0.0132(8) | -0.0138(7) | -0.0149(8) |
| F(81) | 0.0349(9) | 0.0625(11) | 0.0468(9) | -0.0230(8) | 0.0004(7) | -0.0201(8) |
| F(91) | 0.0413(9) | 0.0470(9) | 0.0335(8) | -0.0122(7) | -0.0105(6) | -0.0123(7) |
| F(101) | 0.0521(9) | 0.0284(8) | 0.0414(8) | -0.0149(6) | -0.0018(7) | -0.0121(7) |
| F(111) | 0.0320(8) | 0.0391(8) | 0.0283(7) | -0.0054(6) | 0.0029(5) | -0.0106(6) |
| F(121) | 0.0326(8) | 0.0366(8) | 0.0401(8) | -0.0085(6) | -0.0043(6) | 0.0053(6) |
| B(12) | 0.0250(13) | 0.0429(16) | 0.0253(13) | -0.0047(11) | -0.001(1) | -0.0095(11) |
| B(22) | 0.0198(11) | 0.0211(11) | 0.0200(11) | -0.0018(9) | -0.0030(9) | -0.0055(9) |
| B(32) | 0.0338(14) | 0.0233(12) | 0.0208(11) | -0.0067(9) | -0.006(1) | -0.009(1) |
| B(42) | 0.0249(12) | 0.0234(12) | 0.018(1) | -0.0049(9) | 0.0006(9) | -0.0048(9) |
| B(52) | 0.0319(14) | 0.0173(11) | 0.0317(13) | -0.007(1) | -0.011(1) | -0.0030(9) |
| B(62) | 0.0213(12) | 0.0273(13) | 0.0288(13) | -0.007(1) | -0.001(1) | -0.008(1) |
| B(72) | 0.0443(16) | 0.0267(13) | 0.0230(12) | -0.008(1) | -0.0090(11) | -0.0052(11) |
| B(82) | 0.0292(13) | 0.0247(12) | 0.0227(12) | -0.008(1) | -0.007(1) | -0.004(1) |
| F(12) | 0.0320(8) | 0.0610(11) | 0.0432(9) | -0.0201(8) | 0.0053(7) | -0.0013(7) |
| F(22) | 0.0355(8) | 0.0454(9) | 0.0401(8) | 0.0045(7) | 0.0004(6) | -0.0178(7) |
| F(32) | 0.0434(9) | 0.0240(7) | 0.0319(7) | -0.0072(6) | -0.0076(6) | -0.0019(6) |
| F(42) | 0.0398(8) | 0.0321(7) | 0.0283(7) | -0.0069(6) | 0.0048(6) | -0.0157(6) |
| F(52) | 0.0269(8) | 0.0434(9) | 0.0440(9) | -0.0067(7) | -0.0104(6) | -0.0005(6) |
| F(62) | 0.0442(9) | 0.0390(8) | 0.0253(7) | -0.0049(6) | -0.0119(6) | -0.0045(7) |
| F(72) | 0.0317(7) | 0.0399(8) | 0.0309(7) | -0.0165(6) | -0.0024(6) | -0.0041(6) |
| F(82) | 0.0440(9) | 0.0245(7) | 0.0406(8) | -0.0064(6) | -0.0091(7) | -0.0013(6) |
| F(92) | 0.0604(11) | 0.053(1) | 0.0444(9) | -0.0207(8) | -0.0041(8) | -0.0294(9) |
| F(102) | 0.055(1) | 0.0469(9) | 0.0355(8) | -0.0229(7) | -0.0058(7) | 0.0023(7) |

| | | | | | | |
|---|---|---|---|---|---|---|
| F(112) | 0.0388(8) | 0.0308(7) | 0.0302(7) | 0.0025(6) | -0.0065(6) | -0.0064(6) |
| F(122) | 0.0255(7) | 0.0475(9) | 0.0351(8) | -0.0111(7) | -0.0013(6) | 0.0003(6) |
| B(13) | 0.0334(15) | 0.0364(15) | 0.0252(13) | -0.0043(11) | 0.0010(11) | -0.0162(12) |
| F(13) | 0.0351(8) | 0.0583(11) | 0.0427(9) | -0.0021(8) | -0.0087(7) | -0.0194(7) |
| F(23) | 0.1027(16) | 0.042(1) | 0.042(1) | -0.0153(8) | -0.001(1) | -0.026(1) |
| F(33) | 0.0293(8) | 0.0735(12) | 0.046(1) | -0.0121(9) | -0.0008(7) | -0.0043(8) |

[a] $i$ = atom number, $j$ = residue number.

**Table G**. Crystallographic bond lengths (Å) for $(B_8F_{12})_2.BF_3$

| | | | |
|---|---|---|---|
| B(11)-B(21) | 1.882(3) | B(12)-B(22) | 1.872(4) |
| B(21)-B(31) | 1.816(3) | B(22)-B(32) | 1.802(3) |
| B(21)-B(41) | 1.662(3) | B(22)-B(42) | 1.669(3) |
| B(21)-B(51) | 1.747(4) | B(22)-B(52) | 1.741(3) |
| B(21)-B(61) | 1.721(4) | B(22)-B(62) | 1.720(4) |
| B(31)-B(41) | 1.869(3) | B(32)-B(42) | 1.904(3) |
| B(41)-B(71) | 1.749(4) | B(42)-B(72) | 1.743(4) |
| B(41)-B(81) | 1.727(4) | B(42)-B(82) | 1.721(4) |
| B(11)-F(11) | 1.311(3) | B(12)-F(12) | 1.303(3) |
| B(11)-F(21) | 1.301(3) | B(12)-F(22) | 1.298(3) |
| B(31)-F(31) | 1.313(3) | B(32)-F(32) | 1.334(3) |
| B(31)-F(41) | 1.337(3) | B(32)-F(42) | 1.321(3) |
| B(51)-F(51) | 1.308(3) | B(52)-F(52) | 1.310(3) |
| B(51)-F(61) | 1.323(3) | B(52)-F(62) | 1.324(3) |
| B(61)-F(71) | 1.311(3) | B(62)-F(72) | 1.320(3) |
| B(61)-F(81) | 1.327(3) | B(62)-F(82) | 1.323(3) |
| B(71)-F(91) | 1.317(3) | B(72)-F(92) | 1.310(3) |
| B(71)-F(101) | 1.303(3) | B(72)-F(102) | 1.309(3) |
| B(81)-F(111) | 1.324(3) | B(82)-F(112) | 1.321(3) |
| B(81)-F(121) | 1.308(3) | B(82)-F(122) | 1.310(3) |
| | | | |
| B(13)-F(13) | 1.302(3) | | |
| B(13)-F(23) | 1.294(3) | | |
| B(13)-F(33) | 1.303(4) | | |

**Table H**. Crystallographic bond angles (°) for $(B_8F_{12})_2.BF_3$

| | | | |
|---|---|---|---|
| B(11)-B(21)-B(31) | 110.80(18) | B(12)-B(22)-B(32) | 111.54(18) |
| B(11)-B(21)-B(41) | 70.36(15) | B(12)-B(22)-B(42) | 72.23(15) |
| B(11)-B(21)-B(51) | 103.43(18) | B(12)-B(22)-B(52) | 102.75(18) |
| B(11)-B(21)-B(61) | 113.36(18) | B(12)-B(22)-B(62) | 114.31(17) |
| B(21)-B(31)-B(41) | 53.58(13) | B(22)-B(32)-B(42) | 53.44(12) |
| B(21)-B(41)-B(31) | 61.56(14) | B(22)-B(42)-B(32) | 60.16(13) |
| B(21)-B(41)-B(71) | 137.92(19) | B(22)-B(42)-B(72) | 136.8(2) |
| B(21)-B(41)-B(81) | 113.36(18) | B(22)-B(42)-B(82) | 115.02(18) |

| | | | |
|---|---|---|---|
| B(31)-B(21)-B(41) | 64.86(14) | B(32)-B(22)-B(42) | 66.40(14) |
| B(31)-B(21)-B(51) | 81.67(16) | B(32)-B(22)-B(52) | 81.16(15) |
| B(31)-B(21)-B(61) | 131.10(19) | B(32)-B(22)-B(62) | 131.09(18) |
| B(31)-B(41)-B(71) | 82.71(15) | B(32)-B(42)-B(72) | 83.13(15) |
| B(31)-B(41)-B(81) | 140.29(19) | B(32)-B(42)-B(82) | 143.93(19) |
| B(41)-B(21)-B(51) | 139.3(2) | B(42)-B(22)-B(52) | 141.2(2) |
| B(41)-B(21)-B(61) | 112.37(19) | B(42)-B(22)-B(62) | 113.03(18) |
| B(51)-B(21)-B(61) | 106.99(18) | B(52)-B(22)-B(62) | 104.10(18) |
| B(71)-B(41)-B(81) | 108.30(18) | B(72)-B(42)-B(82) | 107.99(18) |
| B(21)-B(11)-F(11) | 114.9(2) | B(22)-B(12)-F(12) | 121.4(2) |
| B(21)-B(11)-F(21) | 121.9(2) | B(22)-B(12)-F(22) | 115.8(2) |
| F(11)-B(11)-F(21) | 119.9(2) | F(12)-B(12)-F(22) | 120.2(2) |
| B(21)-B(31)-F(31) | 116.5(2) | B(22)-B(32)-F(32) | 121.4(2) |
| B(21)-B(31)-F(41) | 120.1(2) | B(22)-B(32)-F(42) | 116.7(2) |
| B(41)-B(31)-F(31) | 113.7(2) | B(42)-B(32)-F(32) | 117.15(18) |
| B(41)-B(31)-F(41) | 118.9(2) | B(42)-B(32)-F(42) | 113.71(19) |
| F(31)-B(31)-F(41) | 118.0(2) | F(32)-B(32)-F(42) | 117.9(2) |
| B(21)-B(51)-F(51) | 121.6(2) | B(22)-B(52)-F(52) | 120.3(2) |
| B(21)-B(51)-F(61) | 120.8(2) | B(22)-B(52)-F(62) | 121.6(2) |
| F(51)-B(51)-F(61) | 117.1(2) | F(52)-B(52)-F(62) | 117.3(2) |
| B(21)-B(61)-F(71) | 122.5(2) | B(22)-B(62)-F(72) | 121.9(2) |
| B(21)-B(61)-F(81) | 121.6(2) | B(22)-B(62)-F(82) | 121.6(2) |
| F(71)-B(61)-F(81) | 115.8(2) | F(72)-B(62)-F(82) | 116.5(2) |
| B(41)-B(71)-F(91) | 120.5(2) | B(42)-B(72)-F(92) | 120.1(2) |
| B(41)-B(71)-F(101) | 120.5(2) | B(42)-B(72)-F(102) | 120.9(2) |
| F(91)-B(71)-F(101) | 118.8(2) | F(92)-B(72)-F(102) | 118.7(2) |
| B(41)-B(81)-F(111) | 122.6(2) | B(42)-B(82)-F(112) | 122.8(2) |
| B(41)-B(81)-F(121) | 120.2(2) | B(42)-B(82)-F(122) | 120.1(2) |
| F(111)-B(81)-F(121) | 117.2(2) | F(112)-B(82)-F(122) | 117.1(2) |
| | | | |
| F(13)-B(13)-F(23) | 121.6(3) | | |
| F(13)-B(13)-F(33) | 118.6(3) | | |
| F(23)-B(13)-F(33) | 119.8(3) | | |

**Table I**. Flexible restraints used in the GED refinement of $B_8F_{12}$.

| Parameter | Value /pm or ° | Uncertainty /pm or ° |
|---|---|---|
| $p_{10}$ | 141.7 | 14.0 |
| $p_{12}$ | 153.8 | 15.0 |
| $p_{13}$ | -10.3 | 1.0 |
| $p_{14}$ | 1.1 | 1.5 |
| $p_{15}$ | 5.4 | 1.0 |
| $p_{16}$ | 7.8 | 1.0 |
| $p_{17}$ | -24.7 | 2.5 |
| $p_{18}$ | 10.2 | 1.0 |
| $p_{19}$ | 7.8 | 2.0 |
| $p_{21}$ | 0.99 | 0.02 |

| | | |
|---|---|---|
| $u_1$ | 6.8 | 0.7 |
| $u_3$ | 4.7 | 0.5 |
| $u_5$ | 7.2 | 0.8 |
| $u_6$ | 6.0 | 0.6 |
| $u_7$ | 5.4 | 0.6 |
| $u_{13}$ | 3.8 | 1.0 |
| $u_{23}$ | 11.0 | 1.2 |
| $u_{24}$ | 11.2 | 1.3 |
| $u_{28}$ | 15.5 | 1.7 |
| $u_{30}$ | 13.3 | 1.3 |
| $u_{36}$ | 7.3 | 0.8 |
| $u_{40}$ | 8.2 | 0.9 |
| $u_{42}$ | 9.3 | 0.8 |
| $u_{50}$ | 14.2 | 1.4 |
| $u_{56}$ | 17.3 | 2.0 |
| $u_{61}$ | 19.6 | 2.0 |
| $u_{67}$ | 11.5 | 1.1 |
| $u_{71}$ | 1.0 | 0.1 |
| $u_{73}$ | 14.9 | 1.6 |
| $u_{74}$ | 20.6 | 2.1 |
| $u_{79}$ | 11.3 | 1.1 |
| $u_{82}$ | 15.3 | 1.5 |
| $u_{84}$ | 18.9 | 5.0 |
| $u_{105}$ | 18.3 | 2.0 |
| $u_{109}$ | 18.9 | 4.0 |
| $u_{111}$ | 19.5 | 2.0 |
| $u_{112}$ | 24.8 | 6.5 |
| $u_{114}$ | 21.8 | 2.1 |
| $u_{116}$ | 9.9 | 0.1 |
| $u_{122}$ | 28.2 | 2.8 |
| $u_{125}$ | 6.2 | 0.6 |
| $u_{129}$ | 18.7 | 2.0 |
| $u_{135}$ | 11.0 | 2.0 |
| $u_{136}$ | 16.8 | 2.0 |
| $u_{145}$ | 11.0 | 2.0 |
| $u_{150}$ | 30.9 | 3.1 |
| $u_{151}$ | 22.8 | 3.0 |
| $u_{153}$ | 22.4 | 7.1 |
| $u_{156}$ | 25.3 | 2.8 |
| $u_{161}$ | 22.4 | 2.3 |
| $u_{163}$ | 5.4 | 0.6 |
| $u_{164}$ | 18.8 | 2.1 |
| $u_{167}$ | 24.9 | 2.4 |
| $u_{168}$ | 26.9 | 3.0 |
| $u_{173}$ | 33.7 | 3.3 |
| $u_{174}$ | 11.4 | 4.4 |
| $u_{179}$ | 29.3 | 7.6 |
| $u_{181}$ | 40.1 | 4.0 |

| | | |
|---|---|---|
| $u_{183}$ | 55.1 | 5.5 |

**Table J**. Bond distances ($r_a$/pm) and amplitudes of vibration ($u$/pm) obtained in the GED refinement of $B_8F_{12}$.

| $u$ | Atom pair | $r_a$ | Amplitude |
|---|---|---|---|
| $u_1$ | B(1) - B(2) | 183.9(21) | 6.8(7) |
| $u_2$ | B(1) - B(4) | 193.5(21) | 9.4(tied to $u_5$) |
| $u_3$ | B(1) – F(9) | 127.0(8) | 4.7(0) |
| $u_4$ | B(1) - F(10) | 127.0(8) | 4.5(tied to $u_3$) |
| $u_5$ | B(2) - B(3) | 189.5(21) | 7.2(8) |
| $u_6$ | B(2) - B(4) | 164.2(33) | 6.0(6) |
| $u_7$ | B(2) - B(5) | 174.9(9) | 5.4(5) |
| $u_8$ | B(2) - B(6) | 174.9(9) | 5.0(tied to $u_7$) |
| $u_9$ | B(3) - F(11) | 127.0(8) | 4.3(tied to $u_3$) |
| $u_{10}$ | B(3) - F(12) | 127.0(8) | 4.3(tied to $u_3$) |
| $u_{11}$ | B(4) - B(7) | 174.9(9) | 5.1(tied to $u_7$) |
| $u_{12}$ | B(4) - B(8) | 174.9(9) | 5.0(tied to $u_7$) |
| $u_{13}$ | B(5) - F(13) | 133.4(3) | 3.8(5) |
| $u_{14}$ | B(5) - F(14) | 133.4(3) | 3.8(tied to $u_{13}$) |
| $u_{15}$ | B(6) - F(15) | 133.4(3) | 3.8(tied to $u_{13}$) |
| $u_{16}$ | B(6) - F(16) | 133.4(3) | 3.7(tied to $u_{13}$) |
| $u_{17}$ | B(7) - F(17) | 133.4(3) | 3.7(tied to $u_{13}$) |
| $u_{18}$ | B(7) - F(18) | 133.4(3) | 3.7(tied to $u_{13}$) |
| $u_{19}$ | B(8) - F(19) | 133.4(3) | 3.7(tied to $u_{13}$) |
| $u_{20}$ | B(8) - F(20) | 133.4(3) | 3.8(tied to $u_{13}$) |
| $u_{21}$ | B(1) ... B(3) | 330.2(54) | 9.3(tied to $u_{84}$) |
| $u_{22}$ | B(1) ... B(5) | 278.3(33) | 10.3(tied to $u_{24}$) |
| $u_{23}$ | B(1) ... B(6) | 293.4(63) | 11.0(13) |
| $u_{24}$ | B(1) ... B(7) | 283.9(47) | 11.2(11) |
| $u_{25}$ | B(1) ... B(8) | 309.9(32) | 11.2(tied to $u_{36}$) |
| $u_{26}$ | B(1)... F(11) | 425.1(41) | 9.7(tied to $u_{61}$) |
| $u_{27}$ | B(1) ... F(12) | 364.6(68) | 16.4(tied to $u_{56}$) |
| $u_{28}$ | B(1) ... F(13) | 296.1(43) | 15.5(19) |
| $u_{29}$ | B(1) ... F(14) | 405.4(36) | 17.3(tied to $u_{56}$) |
| $u_{30}$ | B(1) ... F(15) | 410.7(66) | 13.3(14) |
| $u_{31}$ | B(1) ... F(16) | 328.1(82) | 23.4(tied to $u_{84}$) |
| $u_{32}$ | B(1) ... F(17) | 301.0(64) | 15.3(tied to $u_{23}$) |
| $u_{33}$ | B(1) ... F(18) | 409.1(49) | 18.8(tied to $u_{56}$) |
| $u_{34}$ | B(1) ... F(19) | 337.3(42) | 21.1(tied to $u_{179}$) |
| $u_{35}$ | B(1) ... F(20) | 433.3(30) | 12.1(tied to $u_{150}$) |
| $u_{36}$ | B(2) ... B(7) | 320.5(42) | 7.3(8) |
| $u_{37}$ | B(2) ... B(8) | 266.1(42) | 8.2(tied to $u_{24}$) |
| $u_{38}$ | B(2) ... B(9) | 257.3(31) | 7.8(tied to $u_{40}$) |
| $u_{39}$ | B(2) ... F(10) | 259.7(40) | 6.5(tied to $u_{24}$) |
| $u_{40}$ | B(2) ... F(11) | 256.8(27) | 8.2(9) |

| | | | |
|---|---|---|---|
| $u_{41}$ | B(2) ... F(12) | 270.6(35) | 7.7(tied to $u_{24}$) |
| $u_{42}$ | B(2) ... F(13) | 271.6(10) | 9.3(6) |
| $u_{43}$ | B(2) ... F(14) | 271.6(10) | 9.0(tied to $u_{42}$) |
| $u_{44}$ | B(2) ... F(15) | 271.6(10) | 8.4(tied to $u_{42}$) |
| $u_{45}$ | B(2) ... F(16) | 271.6(10) | 8.8(tied to $u_{42}$) |
| $u_{46}$ | B(2) ... F(17) | 401.8(48) | 10.5(tied to $u_{56}$) |
| $u_{47}$ | B(2) ... F(18) | 409.4(43) | 12.7(tied to $u_{56}$) |
| $u_{48}$ | B(2) ... F(19) | 340.8(51) | 17.7(tied to $u_{105}$) |
| $u_{49}$ | B(2) ... F(20) | 350.5(47) | 17.3(tied to $u_{105}$) |
| $u_{50}$ | B(3) ... B(4) | 215.4(23) | 14.2(15) |
| $u_{51}$ | B(3) ... B(5) | 268.7(34) | 14.3(tied to $u_{42}$) |
| $u_{52}$ | B(3) ... B(6) | 319.7(56) | 10.7(tied to $u_{36}$) |
| $u_{53}$ | B(3) ... B(7) | 307.2(50) | 17.1(tied to $u_{23}$) |
| $u_{54}$ | B(3) ... B(8) | 329.1(34) | 13.7(tied to $u_{84}$) |
| $u_{55}$ | B(3) ... F( 9) | 428.8(41) | 9.0(tied to $u_{61}$) |
| $u_{56}$ | B(3) ... F(10) | 359.0(73) | 17.3(16) |
| $u_{57}$ | B(3) ... F(13) | 390.1(40) | 12.0(tied to $u_{56}$) |
| $u_{58}$ | B(3) ... F(14) | 288.5(43) | 15.4(tied to $u_{24}$) |
| $u_{59}$ | B(3) ... F(15) | 355.1(89) | 17.2(tied to $u_{179}$) |
| $u_{60}$ | B(3) ... F(16) | 440.6(45) | 17.7(tied to $u_{150}$) |
| $u_{61}$ | B(3) ... F(17) | 423.0(59) | 19.6(21) |
| $u_{62}$ | B(3) ... F(18) | 332.4(64) | 25.6(tied to $u_{156}$) |
| $u_{63}$ | B(3) ... F(19) | 447.7(35) | 10.6(tied to $u_{135}$) |
| $u_{64}$ | B(3) ... F(20) | 358.2(42) | 26.2(tied to $u_{114}$) |
| $u_{65}$ | B(4) ... B(5) | 330.3(28) | 7.8(tied to $u_{73}$) |
| $u_{66}$ | B(4) ... B(6) | 284.6(53) | 11.3(tied to $u_{79}$) |
| $u_{67}$ | B(4) ... F( 9) | 267.6(32) | 11.5(13) |
| $u_{68}$ | B(4) ... F(10) | 267.2(38) | 7.4(tied to $u_{24}$) |
| $u_{69}$ | B(4) ... F(11) | 293.4(33) | 17.0(tied to $u_{24}$) |
| $u_{70}$ | B(4) ... F(12) | 282.7(43) | 15.3(tied to $u_{28}$) |
| $u_{71}$ | B(4) ... F(13) | 413.2(29) | 1.1(1) |
| $u_{72}$ | B(4) ... F(14) | 420.1(28) | 12.4(tied to $u_{71}$) |
| $u_{73}$ | B(4) ... F(15) | 348.9(76) | 14.9(17) |
| $u_{74}$ | B(4) ... F(16) | 382.1(55) | 20.6(23) |
| $u_{75}$ | B(4) ... F(17) | 271.6(10) | 9.5(tied to $u_{42}$) |
| $u_{76}$ | B(4) ... F(18) | 271.6(10) | 9.9(tied to $u_{42}$) |
| $u_{77}$ | B(4) ... F(19) | 271.6(10) | 9.7(tied to $u_{42}$) |
| $u_{78}$ | B(4) ... F(20) | 271.6(10) | 9.5(tied to $u_{42}$) |
| $u_{79}$ | B(5) ... B(6) | 251.5(66) | 11.3(13) |
| $u_{80}$ | B(5) ... B(7) | 459.6(54) | 8.4(tied to $u_{135}$) |
| $u_{81}$ | B(5) ... B(8) | 438.2(42) | 6.6(tied to $u_{135}$) |
| $u_{82}$ | B(5) ... F(9) | 349.5(45) | 15.3(17) |
| $u_{83}$ | B(5) ... F(10) | 301.9(81) | 14.0(tied to $u_{73}$) |
| $u_{84}$ | B(5) ... F(11) | 327.3(42) | 18.9(26) |
| $u_{85}$ | B(5) ... F(12) | 306.0(69) | 19.0(tied to $u_{73}$) |
| $u_{86}$ | B(5) ... F(15) | 351.8(79) | 13.6(tied to $u_{74}$) |
| $u_{87}$ | B(5) ... F(16) | 301.1(85) | 19.2(tied to $u_{156}$) |
| $u_{88}$ | B(5) ... F(17) | 525.4(73) | 14.9(tied to $u_{151}$) |

| | | | |
|---|---|---|---|
| $u_{89}$ | B(5) ... F(18) | 540.3(65) | 19.3(tied to $u_{151}$) |
| $u_{90}$ | B(5) ... F(19) | 500.6(56) | 23.6(tied to $u_{109}$) |
| $u_{91}$ | B(5) ... F(20) | 512.8(53) | 21.7(tied to $u_{109}$) |
| $u_{92}$ | B(6) ... B(7) | 458.9(52) | 12.2(tied to $u_{150}$) |
| $u_{93}$ | B(6) ... B(8) | 277.2(70) | 13.6(tied to $u_{24}$) |
| $u_{94}$ | B(6) ... F(9) | 290.9(92) | 17.7(tied to $u_{24}$) |
| $u_{95}$ | B(6) ... F(10) | 399.0(63) | 9.3(tied to $u_{71}$) |
| $u_{96}$ | B(6) ... F(11) | 321.3(88) | 17.1(tied to $u_{28}$) |
| $u_{97}$ | B(6) ... F(12) | 426.0(46) | 10.5(tied to $u_{116}$) |
| $u_{98}$ | B(6) ... F(13) | 330.0(81) | 16.9(tied to $u_{84}$) |
| $u_{99}$ | B(6) ... F(14) | 324.9(80) | 19.6(tied to $u_{82}$) |
| $u_{100}$ | B(6) ... F(17) | 537.4(51) | 16.5(tied to $u_{151}$) |
| $u_{101}$ | B(6) ... F(18) | 548.3(55) | 16.4(tied to $u_{109}$) |
| $u_{102}$ | B(6) ... F(19) | 307.8(90) | 28.7(tied to $u_{84}$) |
| $u_{103}$ | B(6) ... F(20) | 341.2(84) | 22.9(tied to $u_{179}$) |
| $u_{104}$ | B(7) ... B(8) | 295.0(66) | 14.0(tied to $u_{42}$) |
| $u_{105}$ | B(7) ... F(9) | 368.9(49) | 18.3(22) |
| $u_{106}$ | B(7) ... F(10) | 295.6(81) | 15.2(tied to $u_{156}$) |
| $u_{107}$ | B(7) ... F(11) | 402.2(44) | 28.3(tied to $u_{183}$) |
| $u_{108}$ | B(7) ... F(12) | 312.1(82) | 22.1(tied to $u_{72}$) |
| $u_{109}$ | B(7) ... F(13) | 526.8(67) | 18.9(39) |
| $u_{110}$ | B(7) ... F(14) | 543.9(60) | 26.4(tied to $u_{109}$) |
| $u_{111}$ | B(7) ... F(15) | 519.9(85) | 19.5(21) |
| $u_{112}$ | B(7) ... F(16) | 548.8(59) | 24.8(63) |
| $u_{113}$ | B(7) ... F(19) | 379.7(73) | 22.3(tied to $u_{114}$) |
| $u_{114}$ | B(7) ... F(20) | 370.8(74) | 21.8(22) |
| $u_{115}$ | B(8) ... F(9) | 315.6(47) | 17.8(tied to $u_{36}$) |
| $u_{116}$ | B(8) ... F(10) | 416.2(41) | 9.9(1) |
| $u_{117}$ | B(8) ... F(11) | 345.5(49) | 24.9(tied to $u_{179}$) |
| $u_{118}$ | B(8) ... F(12) | 428.7(45) | 27.2(tied to $u_{150}$) |
| $u_{119}$ | B(8) ... F(13) | 524.5(41) | 12.9(tied to $u_{112}$) |
| $u_{120}$ | B(8) ... F(14) | 519.8(43) | 12.4(tied to $u_{112}$) |
| $u_{121}$ | B(8) ... F(15) | 289.5(109) | 20.1(tied to $u_{24}$) |
| $u_{122}$ | B(8) ... F(16) | 368.5(92) | 28.2(32) |
| $u_{123}$ | B(8) ... F(17) | 381.7(71) | 23.1(tied to $u_{114}$) |
| $u_{124}$ | B(8) ... F(18) | 368.8(77) | 21.7(tied to $u_{114}$) |
| $u_{125}$ | F(9) ... F(10) | 232.5(17) | 6.2(6) |
| $u_{126}$ | F(9) ... F(11) | 503.4(57) | 10.3(tied to $u_{111}$) |
| $u_{127}$ | F(9) ... F(12) | 482.6(55) | 15.8(tied to $u_{136}$) |
| $u_{128}$ | F(9) ... F(13) | 348.5(57) | 23.1(tied to $u_{179}$) |
| $u_{129}$ | F(9) ... F(14) | 479.9(44) | 18.7(22) |
| $u_{130}$ | F(9) ... F(15) | 407.0(108) | 22.3(tied to $u_{56}$) |
| $u_{131}$ | F(9) ... F(16) | 282.6(123) | 36.7(tied to $u_{24}$) |
| $u_{132}$ | F(9) ... F(17) | 370.7(65) | 24.4(tied to $u_{105}$) |
| $u_{133}$ | F(9) ... F(18) | 499.1(46) | 22.8(tied to $u_{111}$) |
| $u_{134}$ | F(9) ... F(19) | 290.6(58) | 27.8(tied to $u_{23}$) |
| $u_{135}$ | F(9) ... F(20) | 445.9(46) | 11.0(16) |
| $u_{136}$ | F(10) ... F(11) | 474.2(60) | 16.8(21) |

| | | | |
|---|---|---|---|
| $u_{137}$ | F(10) ... F(12) | 347.9(121) | 29.9(tied to $u_{61}$) |
| $u_{138}$ | F(10) ... F(13) | 294.8(105) | 22.9(tied to $u_{36}$) |
| $u_{139}$ | F(10) ... F(14) | 419.4(87) | 27.1(tied to $u_{150}$) |
| $u_{140}$ | F(10) ... F(15) | 517.6(53) | 12.0(tied to $u_{109}$) |
| $u_{141}$ | F(10) ... F(16) | 433.1(89) | 19.6(tied to $u_{150}$) |
| $u_{142}$ | F(10) ... F(17) | 285.3(118) | 22.0(tied to $u_{23}$) |
| $u_{143}$ | F(10) ... F(18) | 409.4(89) | 29.9(tied to $u_{61}$) |
| $u_{144}$ | F(10) ... F(19) | 455.9(49) | 12.0(tied to $u_{135}$) |
| $u_{145}$ | F(10) ... F(20) | 532.9(35) | 11.0(12) |
| $u_{146}$ | F(11) ... F(12) | 232.5(17) | 5.8(tied t $u_{125}$) |
| $u_{147}$ | F(11) ... F(13) | 459.7(42) | 22.8(tied to $u_{164}$) |
| $u_{148}$ | F(11) ... F(14) | 313.0(53) | 29.7(tied to $u_{36}$) |
| $u_{149}$ | F(11) ... F(15) | 307.7(130) | 22.9(tied to $u_{24}$) |
| $u_{150}$ | F(11) ... F(16) | 451.3(88) | 30.9(32) |
| $u_{151}$ | F(11) ... F(17) | 527.3(47) | 22.8(29) |
| $u_{152}$ | F(11) ... F(18) | 411.4(53) | 36.3(tied to $u_{56}$) |
| $u_{153}$ | F(11) ... F(19) | 466.2(52) | 22.4(56) |
| $u_{154}$ | F(11) ... F(20) | 331.5(60) | 29.0(tied to $u_{84}$) |
| $u_{155}$ | F(12) ... F(13) | 405.8(78) | 20.9(tied to $u_{150}$) |
| $u_{156}$ | F(12) ... F(14) | 316.9(97) | 25.3(31) |
| $u_{157}$ | F(12) ... F(15) | 477.3(80) | 14.3(tied to $u_{153}$) |
| $u_{158}$ | F(12) ... F(16) | 534.6(35) | 12.2(tied to $u_{145}$) |
| $u_{159}$ | F(12) ... F(17) | 411.0(93) | 24.1(tied to $u_{150}$) |
| $u_{160}$ | F(12) ... F(18) | 318.3(113) | 27.9(tied to $u_{28}$) |
| $u_{161}$ | F(12) ... F(19) | 544.6(40) | 22.4(25) |
| $u_{162}$ | F(12) ... F(20) | 466.9(53) | 38.6(tied to $u_{164}$) |
| $u_{163}$ | F(13) ... F(14) | 223.9(6) | 5.4(4) |
| $u_{164}$ | F(13) ... F(15) | 447.2(93) | 18.8(23) |
| $u_{165}$ | F(13) ... F(16) | 328.4(121) | 24.1(tied to $u_{84}$) |
| $u_{166}$ | F(13) ... F(17) | 563.5(93) | 24.4(tied to $u_{168}$) |
| $u_{167}$ | F(13) ... F(18) | 621.9(79) | 24.9(25) |
| $u_{168}$ | F(13) ... F(19) | 563.2(58) | 26.9(33) |
| $u_{169}$ | F(13) ... F(20) | 616.8(50) | 11.3(tied to $u_{174}$) |
| $u_{170}$ | F(14) ... F(15) | 387.2(115) | 25.5(tied to $u_{61}$) |
| $u_{171}$ | F(14) ... F(16) | 385.3(106) | 37.9(tied to $u_{30}$) |
| $u_{172}$ | F(14) ... F(17) | 624.9(79) | 26.3(tied to $u_{167}$) |
| $u_{173}$ | F(14) ... F(18) | 600.7(76) | 33.7(37) |
| $u_{174}$ | F(14) ... F(19) | 597.0(58) | 11.4(26) |
| $u_{175}$ | F(14) ... F(20) | 567.9(58) | 25.0(tied to $u_{168}$) |
| $u_{176}$ | F(15) ... F(16) | 223.9(6) | 5.5(tied to $u_{163}$) |
| $u_{177}$ | F(15) ... F(17) | 615.7(58) | 24.9(tied to $u_{174}$) |
| $u_{178}$ | F(15) ... F(18) | 587.9(95) | 15.6(tied to $u_{145}$) |
| $u_{179}$ | F(15) ... F(19) | 328.2(129) | 29.3(44) |
| $u_{180}$ | F(15 ... F(20) | 299.1(131) | 28.7(tied to $u_{24}$) |
| $u_{181}$ | F(16 ... F(17) | 604.2(72) | 40.1(45) |
| $u_{182}$ | F(16 ... F(18) | 653.3(53) | 12.5(tied to $u_{174}$) |
| $u_{183}$ | F(16 ... F(19) | 353.6129) | 55.1(61) |
| $u_{184}$ | F(16 ... F(20) | 446.1(104) | 17.1(tied to $u_{135}$) |

| | | | |
|---|---|---|---|
| $u_{185}$ | F(17 ... F(18) | 223.9(6) | 5.5(tied to $u_{163}$) |
| $u_{186}$ | F(17 ... F(19) | 431.0(90) | 36.6(tied to $u_{183}$) |
| $u_{187}$ | F(17 ... F(20) | 475.5(81) | 18.8(tied to $u_{135}$) |
| $u_{188}$ | F(18 ... F(19) | 471.0(86) | 17.1(tied to $u_{135}$) |
| $u_{189}$ | F(18 ... F(20) | 403.4(100) | 34.8(tied to $u_{183}$) |
| $u_{190}$ | F(19 ... F(20) | 223.9(6) | 5.5(tied to $u_{163}$) |

**Table K**. Calculated F...F interactions (pm) in $B_8F_{12}$ (MP2/6-31G*).

| Atom pair | $r_e$ | Atom pair | $r_e$ |
|---|---|---|---|
| F(11)...F(12) | 226.3 | F(15)...F(16) | 227.5 |
| F(13)...F(14) | 228.1 | F(17)...F(18) | 228.6 |
| F(19)...F(20) | 228.6 | F(9)...F(10) | 230.0 |
| F(12)...F(18) | 286.4 | F(12)...F(14) | 290.5 |
| F(11)...F(15) | 292.0 | F(15)...F(19) | 296.4 |
| F(9)...F(13) | 299.1 | F(9)...F(17) | 299.2 |
| F(11)...F(20) | 300.7 | F(13)...F(16) | 301.3 |
| F(15)...F(20) | 304.3 | F(10)...F(14) | 306.7 |
| F(10)...F(12) | 307.6 | F(10)...F(18) | 310.8 |
| F(10)...F(17) | 311.4 | F(10)...F(13) | 316.2 |
| F(11)...F(14) | 364.0 | F(17)...F(19) | 369.6 |
| F(9)...F(16) | 381.3 | F(18)...F(20) | 383.6 |
| F(9)...F(19) | 399.3 | F(12)...F(20) | 404.6 |
| F(14)...F(16) | 412.1 | F(9)...F(14) | 419.5 |
| F(16)...F(19) | 422.2 | F(9)...F(18) | 423.5 |
| F(11)...F(16) | 427.6 | F(11)...F(18) | 428.1 |
| F(17)...F(20) | 430.3 | F(11)...F(19) | 444.2 |
| F(12)...F(17) | 447.3 | F(18)...F(19) | 448.7 |
| F(12)...F(13) | 451.5 | F(9)...F(15) | 454.5 |
| F(12)...F(15) | 456.1 | F(13)...F(15) | 456.7 |
| F(9)...F(12) | 459.7 | F(10)...F(11) | 461.2 |
| F(14)...F(15) | 473.7 | F(11)...F(13) | 487.6 |
| F(10)...F(16) | 494.2 | F(16)...F(20) | 499.8 |
| F(14)...F(18) | 509.8 | F(9)...F(20) | 514.0 |
| F(10)...F(19) | 514.2 | F(12)...F(19) | 518.4 |
| F(9)...F(11) | 521.6 | F(12)...F(16) | 525.4 |
| F(10)...F(15) | 529.7 | F(10)...F(20) | 533.1 |
| F(11)...F(17) | 545.1 | F(15)...F(18) | 557.0 |
| F(15)...F(17) | 555.7 | F(13)...F(17) | 557.5 |
| F(14)...F(17) | 577.3 | F(13)...F(19) | 579.0 |
| F(13)...F(18) | 582.5 | F(14)...F(20) | 588.9 |
| F(16)...F(17) | 598.3 | F(14)...F(19) | 622.3 |
| F(13)...F(20) | 630.7 | F(16)...F(18) | 641.2 |

# Appendix B

**Table A** Crystallographic fractional atomic coordinates of $B_{10}F_{12}$.

**Table B** Crystallographic atomic displacement parameters for $B_{10}F_{12}$.

**Table A.** Crystallographic fractional atomic coordinates of $B_{10}F_{12}$.

| Atom($i$)[a] | $x$ | $y$ | $z$ | $U_{iso}$ |
|---|---|---|---|---|
| F(1) | 0.35873(9) | 0.85580(10) | 0.01674(2) | 0.016738(18) |
| F(2) | 0.06928(9) | 0.52970(10) | 0.05802(2) | 0.05802(2) |
| F(3) | 0.27220(10) | 0.27726(9) | 0.08863(2) | 0.08863(2) |
| B(1) | 0.5 | 0.75 | 0.04187(4) | 0.0208 |
| B(2) | 0.41766(14) | 0.47731(15) | 0.10063(3) | 0.10063(3) |
| B(3) | 0.24195(15) | 0.60873(9) | 0.07994(3) | 0.07994(3) |
| F(1) | 0.39420(10) | 0.31928(9) | 0.23326(2) | 0.016738(18) |
| F(2) | 0.72030(10) | 0.52220(10) | 0.19198(2) | 0.05802(2) |
| F(3) | 0.97274(9) | 0.16137(2) | 0.16137(2) | 0.08863(2) |
| B(1) | 0.5 | 0.75 | 0.20813(4) | 0.0208 |
| B(2) | 0.59429(13) | 0.66766(14) | 0.14937(3) | 0.10063(3) |
| B(3) | 0.77269(15) | 0.49195(15) | 0.17006(3) | 0.07994(3) |
| F(1) | 0.64127(9) | 0.64420(10) | 0.01674(2) | 0.016738(18) |
| F(2) | 0.93072(9) | 0.97030(10) | 0.05802(2) | 0.05802(2) |
| F(3) | 0.72780(10) | 1.22274(9) | 0.08863(2) | 0.08863(2) |
| B(2) | 0.58234(14) | 0.84429(13) | 0.10063(3) | 0.10063(3) |
| B(3) | 0.75805(15) | 1.02269(15) | 0.07994(3) | 0.07994(3) |
| F(1) | 0.60580(10) | 0.89127(9) | 0.23326(2) | 0.016738(18) |
| F(2) | 0.27970(10) | 1.18072(9) | 0.19198(2) | 0.05802(2) |
| F(3) | 0.02726(9) | 0.97780(10) | 0.16137(2) | 0.08863(2) |
| B(2) | 0.40571(13) | 0.83234(14) | 0.14937(3) | 0.10063(3) |
| B(3) | 0.22731(15) | 1.00805(15) | 0.17006(3) | 0.07994(3) |

[a] $i$ = atom number.

**Table B**. Crystallographic atomic displacement parameters for $B_{10}F_{12}$.

| Atom($i$)[a] | $U_{11}$ | $U_{22}$ | $U_{33}$ | $U_{23}$ | $U_{13}$ | $U_{12}$ |
|---|---|---|---|---|---|---|
| B(1) | 0.02240(60) | 0.02480(60) | 0.01520(50) | 0.00000 | 0.00000 | -0.00700(50) |
| B(2) | 0.01820(40) | 0.01820(40) | 0.01630(30) | 0.00090(30) | -0.00070(30) | -0.00170(30) |
| B(3) | 0.02100(40) | 0.02180(40) | 0.01860(30) | -0.00070(30) | 0.00140(30) | -0.00560(30) |
| F(1) | 0.03040(30) | 0.03710(30) | 0.02330(20) | 0.01080(20) | -0.00710(20) | -0.00740(20) |
| F(2) | 0.02250(30) | 0.03450(30) | 0.03730(30) | 0.00110(20) | -0.00680(20) | -0.00350(20) |
| F(3) | 0.03670(30) | 0.02020(30) | 0.03470(30) | 0.00240(20) | -0.00290(30) | -0.00610(20) |

[a] $i$ = atom number.

# Appendix C

**Figure 1**. Molecular framework for $B_6X_8$ (X = F, Br and I).

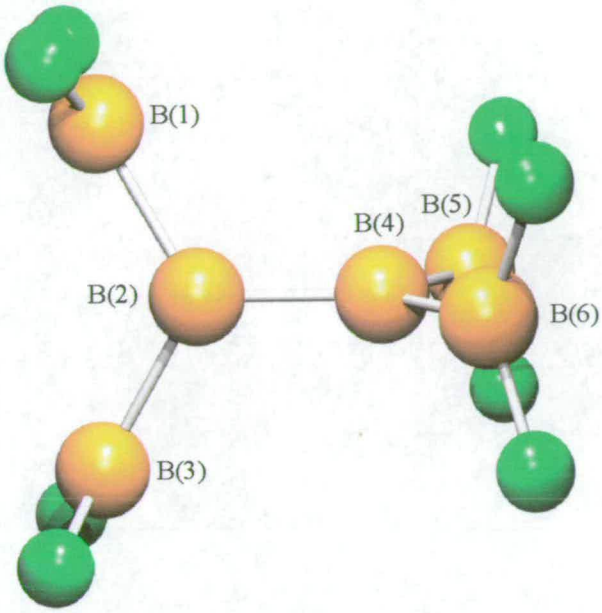


**Figure 2**. Molecular framework for $B_6Cl_8$.

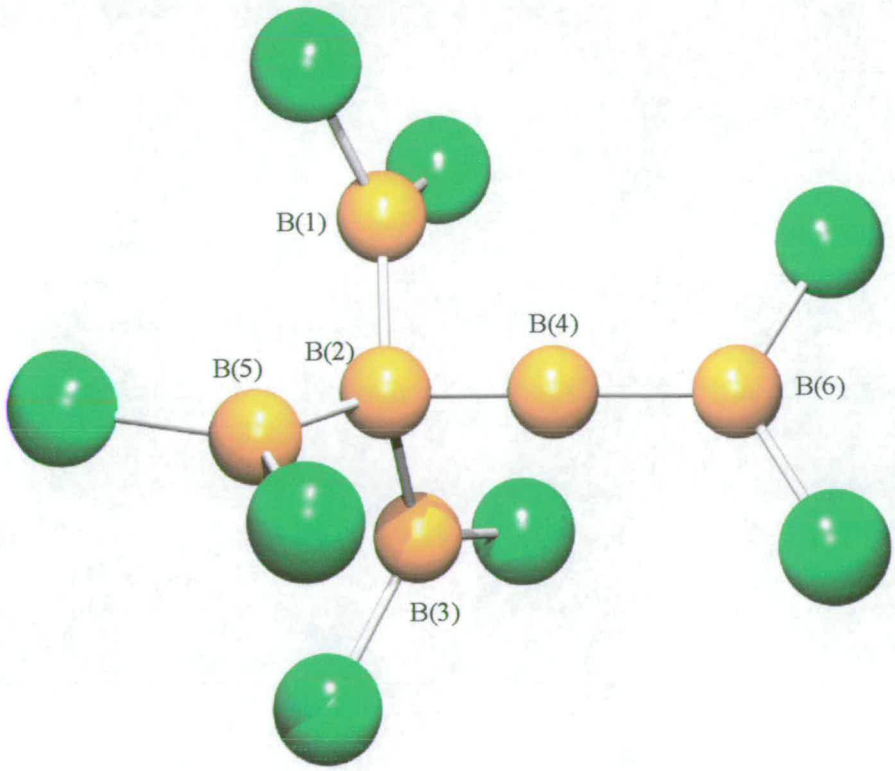

**Table A**. Calculated ($r_e$) geometric parameters for $B_6F_8$.[a]

| Geometric parameter | Level of theory / Basis set | | | | | | |
|---|---|---|---|---|---|---|---|
| | HF | | | B3LYP | | MP2 | |
| | 3-21G* | 6-31G* | 6-311+G** | 6-31G* | 6-311+G** | 6-31G* | 6-311G* |
| B(1)-B(2) | 168.1 | 170.7 | 170.3 | 168.7 | 168.1 | 168.8 | 168.8 |
| B(2)-B(4) | 163.4 | 164.7 | 164.4 | 159.3 | 158.6 | 159.9 | 159.7 |
| *r*BF | 134.2 | 131.1 | 131.0 | 132.5 | 132.5 | 133.1 | 132.4 |
| ϕBBBB[b] | 89.7 | 90.0 | 90.0 | 90.1 | 90.1 | 90.0 | 90.0 |
| Energy[c] | -939.0417 | -944.0909 | -944.3450 | -948.2840 | -948.5939 | -945.8823 | -946.4161 |

[a] distances in pm, angles in °.

[b] torsional angle B(1)-B(2)-B(4)-B(5).

[c] absolute energy in Hartrees.

**Table B**. Calculated ($r_e$) geometric parameters for $B_6Cl_8$.[a]

| Geometric parameter | Level of theory / Basis set | | | | | | |
|---|---|---|---|---|---|---|---|
| | HF | | | B3LYP | | MP2 | |
| | 3-21G* | 6-31G* | 6-311G* | 6-31G* | 6-311G* | 6-31G* | 6-311G* |
| B(1)-B(2) | 171.6 | 172.8 | 172.4 | 173.8 | 174.0 | 175.7 | 175.4 |
| B(1)-B(4) | 266.9 | 265.5 | 264.8 | 217.0 | 218.4 | 201.6 | 202.3 |
| B(2)-B(3) | 172.1 | 173.1 | 172.9 | 172.7 | 172.1 | 175.7 | 175.4 |
| B(2)-B(4) | 160.3 | 159.8 | 159.2 | 152.4 | 152.3 | 149.3 | 149.6 |
| B(3)-B(4) | 267.2 | 267.5 | 266.1 | 228.0 | 235.9 | 201.6 | 202.3 |
| B(2)-B(5) | 170.1 | 171.8 | 171.4 | 170.6 | 170.2 | 168.4 | 167.9 |
| B(4)-B(6) | 170.8 | 172.5 | 172.2 | 168.6 | 167.9 | 167.9 | 167.7 |
| ∠BBB[b] | 176.3 | 177.0 | 177.0 | 175.6 | 175.4 | 176.3 | 177.8 |
| Energy[c] | -3806.7209 | -3824.2164 | -3824.4425 | -3830.9474 | -3831.2026 | -3825.7478 | -3826.0710 |

[a] distances in pm, angles in °.

[b] angle B(2)-B(4)-B(6).

[c] absolute energy in Hartrees.

**Table C**. Calculated ($r_e$) geometric parameters for $B_6Br_8$.[a]

| Geometric parameter | Level of theory / Basis set | | | | | |
|---|---|---|---|---|---|---|
| | HF | | | B3LYP | | MP2 |
| | 3-21G* | 6-31G* | 6-311G* | 6-31G* | 6-311G* | 6-31G* |
| B(1)-B(2) | 166.0 | 167.8 | 168.6 | 165.3 | 166.0 | 164.8 |
| B(2)-B(4) | 164.7 | 166.6 | 166.6 | 162.8 | 162.1 | 161.7 |
| *r*BBr | 189.8 | 190.8 | 192.1 | 190.7 | 192.1 | 190.0 |
| ϕBBBB[b] | 90.0 | 90.0 | 90.0 | 90.0 | 90.0 | 85.7 |
| Energy[c] | -20629.7556 | -20707.5261 | -20707.3569 | -20723.0488 | -20742.5755 | -20708.8827 |

[a] distances in pm, angles in °.
[b] torsional angle B(1)-B(2)-B(4)-B(5).
[c] absolute energy in Hartrees.

**Table D**. Calculated ($r_e$) geometric parameters for $B_6I_8$.[a]

| Geometric parameter | Level of theory / Basis set | | | | | | |
|---|---|---|---|---|---|---|---|
| | HF | | | B3LYP | | MP2 | |
| | 3-21G* | 6-31G*[b] | 6-311G*[c] | 6-31G*[b] | 6-311G*[c] | 6-31G*[b] | 6-311G*[c] |
| B(1)-B(2) | 166.8 | 168.7 | 168.4 | 166.2 | 165.6 | 165.0 | 164.8 |
| B(2)-B(4) | 166.5 | 168.4 | 167.8 | 164.2 | 163.5 | 162.5 | 161.9 |
| *r*BI | 215.7 | 214.8 | 214.1 | 214.2 | 213.8 | 212.6 | 210.8 |
| ϕBBBB[d] | 90.0 | 90.0 | 90.0 | 90.0 | 90.0 | 90.0 | 90.0 |
| Energy[e] | -55250.7366 | -237.5500 | -237.5897 | -240.3788 | -240.4098 | -238.4035 | -238.4958 |

[a] distances in pm, angles in °.
[b] 6-31G* on B atoms, lanl2dz on I atoms.
[c] 6-311G* on B atoms, lanl2dz on I atoms.
[d] torsional angle B(1)-B(2)-B(4)-B(5).
[e] absolute energy in Hartrees.

# Appendix D

| | |
|---|---|
| **Table A** | Flexible restraints used in the GED refinement of *closo*-2,3-$C_2B_9H_{11}$. |
| **Table B** | Bond distances and amplitudes of vibration obtained in the GED refinement of *closo*-2,3-$C_2B_9H_{11}$. |
| **Table C** | Flexible restraints used in the GED refinement of *nido*-2,9-$C_2B_9H_{13}$. |
| **Table D** | Bond distances and amplitudes of vibration obtained in the GED refinement of *nido*-2,9-$C_2B_9H_{13}$. |
| **Table E** | Flexible restraints used in the GED refinement of *arachno*-6,9-$C_2B_9H_{13}$. |
| **Table F** | Bond distances and amplitudes of vibration obtained in the GED refinement of *arachno*-6,9-$C_2B_9H_{13}$. |
| **Table G** | Calculated ($r_e$) structure of *nido*-7,8-$C_2B_9H_{13}$. |

**Table A**. Flexible restraints used in the GED refinement of *closo*-2,3-$C_2B_9H_{11}$.

| Parameter | Value /pm or ° | Uncertainty /pm or ° |
|---|---|---|
| $p_2$ | -5.9 | 0.5 |
| $p_3$ | -0.4 | 0.1 |
| $p_5$ | 271.2 | 0.5 |
| $p_{11}$ | 11.4 | 0.5 |
| $p_{12}$ | 0.3 | 0.1 |
| $p_{14}$ | 180.0 | 0.2 |
| $p_{15}$ | 128.2 | 0.2 |
| $p_{16}$ | 180.0 | 0.2 |
| $p_{17}$ | 114.6 | 0.2 |
| $p_{18}$ | 165.3 | 0.2 |
| $p_{19}$ | 120.4 | 0.2 |
| $p_{20}$ | 180.0 | 0.2 |
| $p_{21}$ | 127.6 | 0.2 |
| $p_{22}$ | 180.0 | 0.2 |
| $u_5$ | 7.2 | 0.1 |
| $u_{12}$ | 13.5 | 0.5 |
| $u_{23}$ | 6.7 | 0.5 |
| $u_{38}$ | 23.8 | 1.0 |
| $u_{53}$ | 6.9 | 0.7 |
| $u_{69}$ | 8.7 | 0.8 |
| $u_{71}$ | 7.6 | 0.4 |
| $u_{73}$ | 7.4 | 0.7 |
| $u_{84}$ | 6.0 | 0.6 |

**Table B**. Bond distances ($r_{h1}$ /pm) and amplitudes of vibration ($u$ /pm) obtained in the GED refinement of *closo*-2,3-$C_2B_9H_{11}$.

| $u$ | Atom pair | $r_{h1}$ | Amplitude |
|---|---|---|---|
| $u_1$ | B(1)-C(2) | 162.2(11) | 6.8(tied to $u_5$) |
| $u_3$ | B(1)-H(22) | 121.0(3) | 8.1(fixed) |
| $u_5$ | C(2)-B(5) | 157.9(5) | 7.2(1) |
| $u_6$ | C(2)-B(8) | 167.0(11) | 6.8(tied to $u_5$) |
| $u_7$ | C(2)-H(17) | 109.6(4) | 7.3(fixed) |
| $u_{12}$ | B(4)-B(7) | 188.6(11) | 13.5(5) |
| $u_{14}$ | B(4)-B(10) | 180.7(3) | 7.0(tied to $u_{23}$) |
| $u_{15}$ | B(4)-H(16) | 120.7(3) | 8.1(fixed) |
| $u_{23}$ | B(7)-B(9) | 177.4(6) | 6.7(2) |
| $u_{26}$ | B(8)-B(10) | 180.8(3) | 7.9(tied to $u_{23}$) |
| $u_{27}$ | B(8)-B(11) | 181.3(3) | 7.9(tied to $u_{23}$) |
| $u_{28}$ | B(8)-H(13) | 120.7(3) | 8.1(fixed) |
| $u_{29}$ | B(9)-B(10) | 180.7(3) | 7.9(tied to $u_{23}$) |
| $u_{32}$ | B(10)-B(11) | 186.6(5) | 7.4(tied to $u_{12}$) |
| $u_{33}$ | B(10)-H(12) | 121.0(3) | 8.1(fixed) |
| $u_{35}$ | B(1)-B(4) | 200.0(7) | 24.6(9) |

| | | | |
|---|---|---|---|
| $u_{39}$ | B(1)...B(8) | 268.0(11) | 7.1(tied to $u_{84}$) |
| $u_{41}$ | B(1)...B(10) | 283.8(5) | 10.7(tied to $u_{69}$) |
| $u_{43}$ | B(1)...H(12) | 399.2(5) | 14.5(fixed) |
| $u_{44}$ | B(1)...H(13) | 379.4(10) | 11.0(fixed) |
| $u_{47}$ | B(1)...H(16) | 291.2(7) | 28.0(fixed) |
| $u_{48}$ | B(1)...H(17) | 236.2(10) | 11.0(fixed) |
| $u_{53}$ | C(2)...C(3) | 297.7(13) | 6.9(3) |
| $u_{60}$ | C(2)...H(13) | 250.5(10) | 11.4(fixed) |
| $u_{62}$ | C(2)...H(15) | 460.5(5) | 10.2(fixed) |
| $u_{63}$ | C(2)...H(16) | 242.5(6) | 11.1(fixed) |
| $u_{65}$ | C(2)...H(19) | 379.8(6) | 13.3(fixed) |
| $u_{66}$ | C(2)...H(20) | 389.0(15) | 11.1(fixed) |
| $u_{68}$ | C(2)...H(22) | 233.8(16) | 11.4(fixed) |
| $u_{69}$ | C(3)...B(4) | 285.3(5) | 8.7(5) |
| $u_{71}$ | C(3)...B(8) | 340.9(5) | 7.6(4) |
| $u_{73}$ | C(3)...B(11) | 274.6(10) | 7.4(5) |
| $u_{74}$ | C(3)...H(12) | 379.6(12) | 11.7(fixed) |
| $u_{84}$ | B(4)...B(5) | 268.8(9) | 6.0(4) |
| $u_{85}$ | B(4)...B(6) | 328.8(10) | 8.9(tied to $u_{71}$) |
| $u_{86}$ | B(4)...B(9) | 295.7(7) | 9.8(tied to $u_{53}$) |
| $u_{87}$ | B(4)...B(11) | 287.4(3) | 7.2(tied to $u_{69}$) |
| $u_{88}$ | B(4)...H(12) | 263.0(5) | 13.2(fixed) |
| $u_{89}$ | B(4)...H(13) | 263.9(8) | 12.2(fixed) |
| $u_{90}$ | B(4)...H(14) | 398.0(5) | 11.1(fixed) |
| $u_{91}$ | B(4)...H(15) | 405.5(7) | 12.8(fixed) |
| $u_{92}$ | B(4)...H(17) | 233.8(7) | 10.8(fixed) |
| $u_{93}$ | B(4)...H(18) | 378.1(9) | 11.1(fixed) |
| $u_{94}$ | B(4)...H(19) | 444.3(10) | 11.9(fixed) |
| $u_{95}$ | B(4)...H(20) | 378.2(7) | 12.8(fixed) |
| $u_{96}$ | B(4)...H(21) | 262.3(10) | 13.7(fixed) |
| $u_{97}$ | B(4)...H(22) | 287.9(9) | 26.5(fixed) |
| $u_{136}$ | B(8)...B(9) | 296.7(5) | 7.0(tied to $u_{53}$) |
| $u_{137}$ | B(8)...H(12) | 263.0(7) | 13.3(fixed) |
| $u_{139}$ | B(8)...H(15) | 404.1(6) | 11.2(fixed) |
| $u_{140}$ | B(8)...H(16) | 272.0(6) | 15.0(fixed) |
| $u_{141}$ | B(8)...H(17) | 249.2(11) | 10.9(fixed) |
| $u_{143}$ | B(8)...H(19) | 400.2(6) | 12.2(fixed) |
| $u_{144}$ | B(8)...H(20) | 448.3(6) | 9.8(fixed) |
| $u_{146}$ | B(8)...H(22) | 373.7(12) | 11.2(fixed) |
| $u_{157}$ | B(10)...H(13) | 268.3(4) | 12.4(fixed) |
| $u_{158}$ | B(10)...H(14) | 276.7(5) | 12.4(fixed) |
| $u_{160}$ | B(10)...H(16) | 270.3(4) | 12.0(fixed) |
| $u_{161}$ | B(10)...H(17) | 375.9(11) | 10.1(fixed) |
| $u_{162}$ | B(10)...H(18) | 402.8(4) | 10.9(fixed) |
| $u_{166}$ | B(10)...H(22) | 398.9(5) | 13.4(fixed) |
| $u_{177}$ | H(12)...H(13) | 310.4(7) | 20.0(fixed) |
| $u_{178}$ | H(12)...H(14) | 332.6(9) | 19.0(fixed) |
| $u_{180}$ | H(12)...H(16) | 314.8(6) | 20.1(fixed) |

| | | | |
|---|---|---|---|
| $u_{181}$ | H(12)...H(17) | 471.2(12) | 14.4(fixed) |
| $u_{182}$ | H(12)...H(18) | 508.3(7) | 14.4(fixed) |
| $u_{186}$ | H(12)...H(22) | 510.2(7) | 17.4(fixed) |
| $u_{188}$ | H(13)...H(15) | 501.8(10) | 15.3(fixed) |
| $u_{189}$ | H(13)...H(16) | 324.2(9) | 21.2(fixed) |
| $u_{190}$ | H(13)...H(17) | 295.7(12) | 17.7(fixed) |
| $u_{192}$ | H(13)...H(19) | 500.4(8) | 15.7(fixed) |
| $u_{193}$ | H(13)...H(20) | 567.9(7) | 12.4(fixed) |
| $u_{195}$ | H(13)...H(22) | 475.6(12) | 14.6(fixed) |
| $u_{211}$ | H(16)...H(17) | 275.3(7) | 18.4(fixed) |
| $u_{212}$ | H(16)...H(18) | 478.8(11) | 14.3(fixed) |
| $u_{213}$ | H(16)...H(19) | 558.6(11) | 14.7(fixed) |
| $u_{214}$ | H(16)...H(20) | 458.9(7) | 16.8(fixed) |
| $u_{215}$ | H(16)...H(21) | 287.8(13) | 20.9(fixed) |
| $u_{216}$ | H(16)...H(22) | 346.1(9) | 34.9(fixed) |
| $u_{219}$ | H(17)...H(20) | 468.3(20) | 14.9(fixed) |
| $u_{221}$ | H(17)...H(22) | 259.9(15) | 17.8(fixed) |

**Table C**. Flexible restraints used in the GED refinement of *nido*-2,9-$C_2B_9H_{13}$.

| Parameter | Value /pm or ° | Uncertainty /pm or ° |
|---|---|---|
| $p_2$ | 17.5 | 0.1 |
| $p_3$ | 15.9 | 0.1 |
| $p_4$ | 20.7 | 0.1 |
| $p_5$ | 8.5 | 0.1 |
| $p_6$ | 27.9 | 0.1 |
| $p_7$ | 16.9 | 0.1 |
| $p_8$ | 13.6 | 0.1 |
| $p_{16}$ | 50.7 | 0.5 |
| $p_{17}$ | 127.4 | 1.0 |
| $p_{20}$ | 4.1 | 0.1 |
| $p_{21}$ | 11.7 | 0.1 |
| $p_{22}$ | -3.8 | 0.1 |
| $p_{23}$ | -47.8 | 1.0 |
| $p_{24}$ | -60.7 | 1.0 |
| $p_{25}$ | 64.0 | 1.0 |
| $p_{10}$ | 111.6 | 0.5 |
| $p_{11}$ | 134.2 | 0.5 |
| $p_{18}$ | 83.9 | 0.5 |
| $p_{12}$ | 108.9 | 0.5 |
| $p_{13}$ | 29.9 | 0.5 |
| $u_{35}$ | 6.9 | 0.7 |
| $u_{30}$ | 9.0 | 0.9 |
| $u_{59}$ | 5.9 | 0.6 |
| $u_{61}$ | 6.4 | 0.2 |
| $u_{108}$ | 6.9 | 0.1 |

| | | |
|---|---|---|
| $u_{38}$ | 12.3 | 1.0 |
| $u_{28}$ | 8.3 | 0.9 |
| $u_{175}$ | 12.9 | 1.3 |

**Table D**. Bond distances ($r_{h1}$ /pm) and amplitudes of vibration ($u$ /pm) obtained in the GED refinement of *nido*-2,9-$C_2B_9H_{13}$.

| $u$ | Atom pair | $r_{h1}$ | Amplitude |
|---|---|---|---|
| $u_1$ | B(1)-C(2) | 169.7(5) | 3.7(5) |
| $u_2$ | B(1)-B(3) | 182.8(3) | 3.9(tied to $u_1$) |
| $u_3$ | B(1)-B(4) | 179.6(3) | 3.7(tied to $u_1$) |
| $u_6$ | B(1)-H(12) | 120.2(3) | 7.5(tied to $u_{35}$) |
| $u_7$ | C(2)-B(3) | 171.9(8) | 4.0(tied to $u_1$) |
| $u_9$ | C(2)-B(7) | 168.2(4) | 3.7(tied to $u_1$) |
| $u_{11}$ | C(2)-H(13) | 111.5(5) | 6.8(tied to $u_{35}$) |
| $u_{12}$ | B(3)-B(4) | 180.6(2) | 3.8(tied to $u_1$) |
| $u_{13}$ | B(3)-B(7) | 173.0(4) | 3.8(tied to $u_1$) |
| $u_{14}$ | B(3)-B(8) | 185.2(5) | 3.9(tied to $u_1$) |
| $u_{15}$ | B(3)-H(14) | 120.2(3) | 7.5(tied to $u_{35}$) |
| $u_{16}$ | B(4)-B(5) | 179.0(3) | 3.6(tied to $u_1$) |
| $u_{17}$ | B(4)-B(8) | 175.4(6) | 4.0(tied to $u_1$) |
| $u_{18}$ | B(4)-C(9) | 169.5(4) | 3.7(tied to $u_1$) |
| $u_{19}$ | B(4)-H(15) | 120.2(3) | 7.5(tied to $u_{35}$) |
| $u_{27}$ | B(7)-B(8) | 187.8(3) | 4.1(tied to $u_1$) |
| $u_{28}$ | B(7)-B(11) | 196.1(2) | 8.4(10) |
| $u_{29}$ | B(7)-H(18) | 120.2(3) | 7.5(tied to $u_{35}$) |
| $u_{30}$ | B(7)-H(23) | 134.2(6) | 9.0(10) |
| $u_{31}$ | B(8)-C(9) | 160.3(7) | 3.7(tied to $u_1$) |
| $u_{32}$ | B(8)-H(19) | 120.2(3) | 7.6(tied to $u_{35}$) |
| $u_{35}$ | C(9)-H(20) | 111.5(5) | 6.9(4) |
| $u_{38}$ | B(10)-H(24) | 139.6(13) | 12.3(12) |
| $u_{41}$ | B(1)...B(7) | 289.7(9) | 8.0(tied to $u_{62}$) |
| $u_{42}$ | B(1)...B(8) | 287.7(7) | 8.2(tied to $u_{62}$) |
| $u_{43}$ | B(1)...C(9) | 277.4(7) | 9.7(tied to $u_{164}$) |
| $u_{46}$ | B(1)...H(13) | 239.7(9) | 10.9(fixed) |
| $u_{47}$ | B(1)...H(14) | 266.8(6) | 11.9(fixed) |
| $u_{48}$ | B(1)...H(15) | 263.8(12) | 11.3(fixed) |
| $u_{51}$ | B(1)...H(18) | 389.8(12) | 11.4(fixed) |
| $u_{52}$ | B(1)...H(19) | 395.0(7) | 10.8(fixed) |
| $u_{53}$ | B(1)...H(20) | 374.8(8) | 10.0(fixed) |
| $u_{56}$ | B(1)...H(23) | 359.4(12) | 11.9(fixed) |
| $u_{59}$ | C(2)...B(5) | 273.0(7) | 5.9(5) |
| $u_{61}$ | C(2)...C(9) | 309.4(8) | 6.4(2) |
| $u_{62}$ | C(2)...B(10) | 272.9(6) | 7.5(5) |
| $u_{63}$ | C(2)...H(12) | 252.4(15) | 11.5(fixed) |

| | | | |
|---|---|---|---|
| $u_{64}$ | C(2)...H(14) | 262.9(9) | 11.5(fixed) |
| $u_{65}$ | C(2)...H(15) | 382.2(10) | 10.2(fixed) |
| $u_{68}$ | C(2)...H(18) | 253.2(11) | 11.3(fixed) |
| $u_{69}$ | C(2)...H(19) | 382.4(6) | 10.2(fixed) |
| $u_{70}$ | C(2)...H(20) | 420.1(9) | 9.4(fixed) |
| $u_{73}$ | C(2)...H(23) | 273.9(8) | 11.4(fixed) |
| $u_{75}$ | B(3)...B(5) | 292.2(5) | 7.7(tied to $u_{62}$) |
| $u_{76}$ | B(3)...B(6) | 295.6(12) | 9.0(tied to $u_{62}$) |
| $u_{77}$ | B(3)...C(9) | 279.9(6) | 10.0(tied to $u_{164}$) |
| $u_{78}$ | B(3)...B(10) | 334.7(7) | 6.4(tied to $u_{108}$) |
| $u_{79}$ | B(3)...B(11) | 296.3(4) | 9.3(tied to $u_{62}$) |
| $u_{80}$ | B(3)...H(12) | 262.5(15) | 11.7(fixed) |
| $u_{81}$ | B(3)...H(13) | 241.4(10) | 11.1(fixed) |
| $u_{82}$ | B(3)...H(15) | 263.9(8) | 11.4(fixed) |
| $u_{83}$ | B(3)...H(16) | 399.4(7) | 10.6(fixed) |
| $u_{84}$ | B(3)...H(17) | 402.7(13) | 11.5(fixed) |
| $u_{85}$ | B(3)...H(18) | 250.7(9) | 12.0(fixed) |
| $u_{86}$ | B(3)...H(19) | 267.6(6) | 11.6(fixed) |
| $u_{87}$ | B(3)...H(20) | 377.5(8) | 10.0(fixed) |
| $u_{88}$ | B(3)...H(21) | 453.9(7) | 10.2(fixed) |
| $u_{89}$ | B(3)...H(22) | 399.5(7) | 11.5(fixed) |
| $u_{90}$ | B(3)...H(23) | 251.6(10) | 10.5(fixed) |
| $u_{91}$ | B(3)...H(24) | 348.3(7) | 13.3(fixed) |
| $u_{93}$ | B(4)...B(7) | 291.9(4) | 8.3(tied to $u_{62}$) |
| $u_{94}$ | B(4)...B(10) | 278.8(7) | 7.9(tied to $u_{62}$) |
| $u_{96}$ | B(4)...H(12) | 268.8(11) | 11.2(fixed) |
| $u_{97}$ | B(4)...H(13) | 370.1(10) | 10.0(fixed) |
| $u_{98}$ | B(4)...H(14) | 264.1(4) | 11.4(fixed) |
| $u_{99}$ | B(4)...H(16) | 262.2(4) | 11.5(fixed) |
| $u_{100}$ | B(4)...H(17) | 399.3(7) | 10.8(fixed) |
| $u_{101}$ | B(4)...H(18) | 397.1(5) | 11.1(fixed) |
| $u_{102}$ | B(4)...H(19) | 256.5(8) | 11.9(fixed) |
| $u_{103}$ | B(4)...H(20) | 242.1(7) | 10.9(fixed) |
| $u_{104}$ | B(4)...H(21) | 383.8(8) | 10.9(fixed) |
| $u_{105}$ | B(4)...H(22) | 465.2(5) | 10.3(fixed) |
| $u_{106}$ | B(4)...H(23) | 299.8(13) | 12.9(fixed) |
| $u_{107}$ | B(4)...H(24) | 353.6(11) | 13.2(fixed) |
| $u_{108}$ | B(5)...B(7) | 346.8(4) | 6.9(1) |
| $u_{139}$ | B(7)...B(10) | 294.6(5) | 7.1(tied to $u_{61}$) |
| $u_{140}$ | B(7)...H(12) | 388.8(16) | 11.3(fixed) |
| $u_{141}$ | B(7)...H(13) | 234.1(6) | 11.0(fixed) |
| $u_{142}$ | B(7)...H(14) | 252.3(5) | 11.8(fixed) |
| $u_{143}$ | B(7)...H(15) | 397.1(5) | 11.2(fixed) |
| $u_{144}$ | B(7)...H(16) | 466.1(4) | 10.2(fixed) |
| $u_{145}$ | B(7)...H(17) | 402.1(5) | 11.7(fixed) |
| $u_{146}$ | B(7)...H(19) | 268.0(4) | 11.6(fixed) |
| $u_{147}$ | B(7)...H(20) | 390.1(11) | 10.5(fixed) |
| $u_{148}$ | B(7)...H(21) | 401.0(6) | 11.5(fixed) |

| | | | |
|---|---|---|---|
| $u_{149}$ | B(7)...H(22) | 279.7(4) | 13.3(fixed) |
| $u_{150}$ | B(7)...H(24) | 237.4(4) | 14.0(fixed) |
| $u_{151}$ | B(8)...B(10) | 263.0(15) | 8.7(tied to $u_{62}$) |
| $u_{153}$ | B(8)...H(12) | 397.1(10) | 10.6(fixed) |
| $u_{154}$ | B(8)...H(13) | 372.3(8) | 10.0(fixed) |
| $u_{155}$ | B(8)...H(14) | 272.5(7) | 11.3(fixed) |
| $u_{156}$ | B(8)...H(15) | 260.2(10) | 12.3(fixed) |
| $u_{157}$ | B(8)...H(16) | 384.4(9) | 10.8(fixed) |
| $u_{158}$ | B(8)...H(17) | 453.9(7) | 10.2(fixed) |
| $u_{159}$ | B(8)...H(18) | 280.1(7) | 11.6(fixed) |
| $u_{160}$ | B(8)...H(20) | 234.3(9) | 10.7(fixed) |
| $u_{161}$ | B(8)...H(21) | 366.1(17) | 11.4(fixed) |
| $u_{162}$ | B(8)...H(22) | 405.7(7) | 11.3(fixed) |
| $u_{163}$ | B(8)...H(24) | 266.9(9) | 13.7(fixed) |
| $u_{164}$ | C(9)...B(11) | 291.3(9) | 11.1(19) |
| $u_{165}$ | C(9)...H(12) | 389.2(10) | 10.1(fixed) |
| $u_{166}$ | C(9)...H(13) | 420.1(9) | 9.4(fixed) |
| $u_{167}$ | C(9)...H(14) | 387.3(6) | 10.2(fixed) |
| $u_{168}$ | C(9)...H(15) | 254.8(12) | 11.2(fixed) |
| $u_{171}$ | C(9)...H(18) | 404.2(10) | 10.4(fixed) |
| $u_{172}$ | C(9)...H(19) | 243.9(9) | 11.2(fixed) |
| $u_{175}$ | C(9)...H(23) | 238.3(14) | 12.9(15) |
| $u_{199}$ | H(12)...H(13) | 278.8(22) | 17.4(fixed) |
| $u_{200}$ | H(12)...H(14) | 305.5(21) | 18.6(fixed) |
| $u_{201}$ | H(12)...H(15) | 315.8(24) | 17.6(fixed) |
| $u_{204}$ | H(12)...H(18) | 473.9(21) | 16.1(fixed) |
| $u_{205}$ | H(12)...H(19) | 495.7(13) | 14.6(fixed) |
| $u_{206}$ | H(12)...H(20) | 478.2(13) | 13.5(fixed) |
| $u_{209}$ | H(12)...H(23) | 472.4(14) | 14.1(fixed) |
| $u_{211}$ | H13 ...H(14) | 293.5(12) | 17.6(fixed) |
| $u_{212}$ | H13 ...H(15) | 469.8(14) | 13.6(fixed) |
| $u_{215}$ | H13 ...H(18) | 274.8(16) | 17.5(fixed) |
| $u_{216}$ | H13 ...H(19) | 473.2(7) | 13.5(fixed) |
| $u_{217}$ | H13 ...H(20) | 530.7(13) | 11.6(fixed) |
| $u_{220}$ | H13 ...H(23) | 358.6(8) | 13.8(fixed) |
| $u_{222}$ | H(14)...H(15) | 307.0(11) | 17.8(fixed) |
| $u_{223}$ | H(14)...H(16) | 496.6(11) | 14.7(fixed) |
| $u_{224}$ | H(14)...H(17) | 500.5(16) | 15.8(fixed) |
| $u_{225}$ | H(14)...H(18) | 283.3(12) | 19.2(fixed) |
| $u_{226}$ | H(14)...H(19) | 316.7(10) | 17.8(fixed) |
| $u_{227}$ | H(14)...H(20) | 474.6(8) | 13.5(fixed) |
| $u_{228}$ | H(14)...H(21) | 572.9(9) | 12.7(fixed) |
| $u_{229}$ | H(14)...H(22) | 494.4(9) | 15.7(fixed) |
| $u_{230}$ | H(14)...H(23) | 336.3(9) | 13.9(fixed) |
| $u_{231}$ | H(14)...H(24) | 459.9(7) | 15.7(fixed) |
| $u_{232}$ | H(15)...H(16) | 303.9(6) | 18.3(fixed) |
| $u_{234}$ | H(15)...H(18) | 491.5(7) | 15.2(fixed) |
| $u_{235}$ | H(15)...H(19) | 299.2(14) | 19.1(fixed) |

| | | | |
|---|---|---|---|
| $u_{236}$ | H(15)...H(20) | 286.0(18) | 17.6(fixed) |
| $u_{237}$ | H(15)...H(21) | 477.6(12) | 14.9(fixed) |
| $u_{238}$ | H(15)...H(22) | 584.3(6) | 12.7(fixed) |
| $u_{239}$ | H(15)...H(23) | 397.3(15) | 16.3(fixed) |
| $u_{240}$ | H(15)...H(24) | 466.5()13 | 15.5(fixed) |
| $u_{256}$ | H(18)...H(19) | 324.8(11) | 17.3(fixed) |
| $u_{257}$ | H(18)...H(20) | 495.7(13) | 13.7(fixed) |
| $u_{258}$ | H(18)...H(21) | 504.6(10) | 15.1(fixed) |
| $u_{259}$ | H(18)...H(22) | 327.0(5) | 19.7(fixed) |
| $u_{260}$ | H(18)...H(23) | 202.0(16) | 13.3(fixed) |
| $u_{261}$ | H(18)...H(24) | 324.2(10) | 17.5(fixed) |
| $u_{262}$ | H(19)...H(20) | 273.9(11) | 17.3(fixed) |
| $u_{263}$ | H(19)...H(21) | 454.8(20) | 15.8(fixed) |
| $u_{265}$ | H(19)...H(23) | 192.7()11 | 15.4(fixed) |
| $u_{266}$ | H(19)...H(24) | 355.8()9 | 16.4(fixed) |
| $u_{269}$ | H(20)...H(23) | 311.9(16) | 15.6(fixed) |
| $u_{274}$ | H(22)...H(23) | 323.6(10) | 17.5(fixed) |
| $u_{276}$ | H(23)...H(24) | 196.9(2) | 16.5(fixed) |

**Table E**. Flexible restraints used in the GED refinement of *arachno*-6,9-$C_2B_9H_{13}$.

| Parameter | Value /pm or ° | Uncertainty /pm or ° |
|---|---|---|
| $p_2$ | 8.2 | 0.1 |
| $p_3$ | 2.2 | 0.1 |
| $p_9$ | 23.2 | 0.1 |
| $p_{10}$ | 13.4 | 0.1 |
| $p_{11}$ | 120.3 | 0.5 |
| $p_{12}$ | 152.4 | 0.5 |
| $p_{13}$ | 120.4 | 0.5 |
| $p_{14}$ | 109.9 | 0.5 |
| $p_{15}$ | 140.8 | 0.5 |
| $p_{16}$ | 44.4 | 0.5 |
| $p_{18}$ | -61.1 | 0.5 |
| $p_{19}$ | 146.4 | 0.5 |
| $p_{20}$ | 180.0 | 0.5 |
| $p_{21}$ | 0.0 | 0.5 |
| $p_{22}$ | -107.0 | 0.5 |
| $u_{17}$ | 7.6 | 0.6 |
| $u_{20}$ | 8.4 | 0.7 |
| $u_{106}$ | 6.9 | 0.8 |
| $u_{39}$ | 6.9 | 0.8 |
| $u_{54}$ | 7.0 | 0.8 |
| $u_{105}$ | 7.8 | 0.9 |
| $u_{120}$ | 10.9 | 1.0 |
| $u_{88}$ | 8.4 | 0.8 |

**Table F**. Bond distances ($r_{h1}$ /pm) and amplitudes of vibration ($u$ /pm) obtained in the GED refinement of *arachno*-6,9-$C_2B_9H_{13}$.

| $u$ | Atom pair | $r_{h1}$ | Amplitude |
|---|---|---|---|
| $u_1$ | B(1)-B(2) | 171.5(5) | 7.3(tied to $u_{17}$) |
| $u_2$ | B(1)-B(3) | 179.9(5) | 7.1(tied to $u_{20}$) |
| $u_4$ | B(1)-B(5) | 177.4(5) | 7.4(tied to $u_{20}$) |
| $u_6$ | B(1)-H(11) | 121.6(3) | 8.1(fixed) |
| $u_8$ | B(2)-B(5) | 178.9(8) | 7.0(tied to $u_{20}$) |
| $u_{11}$ | B(2)-H(12) | 121.63 () | 8.1(fixed) |
| $u_{17}$ | B(4)-C(9) | 171.2(13) | 7.6(4) |
| $u_{20}$ | B(5)-C(6) | 179.9(8) | 8.4(2) |
| $u_{21}$ | B(5)-H(15) | 121.6(3) | 8.1(fixed) |
| $u_{22}$ | B(5)-H(23) | 135.3(3) | 10.2(fixed) |
| $u_{24}$ | C(6)-H(16) | 111.8(3) | 7.3(fixed) |
| $u_{25}$ | C(6)-H(21) | 111.8(3) | 7.4(fixed) |
| $u_{30}$ | B(8)-H(24) | 130.1(14) | 10.2(fixed) |
| $u_{37}$ | B(1)...B(7) | 291.2(6) | 6.8(tied to $u_{54}$) |
| $u_{39}$ | B(1)...C(9) | 284.2(11) | 6.9(5) |
| $u_{40}$ | B(1)...H(12) | 260.5(5) | 11.5(fixed) |
| $u_{41}$ | B(1)...H(13) | 262.5(7) | 12.2(fixed) |
| $u_{43}$ | B(1)...H(15) | 260.1(7) | 12.5(fixed) |
| $u_{44}$ | B(1)...H(16) | 371.6(10) | 11.2(fixed) |
| $u_{45}$ | B(1)...H(17) | 396.9(7) | 11.4(fixed) |
| $u_{49}$ | B(1)...H(21) | 338.9(18) | 13.8(fixed) |
| $u_{51}$ | B(1)...H(23) | 245.7(12) | 10.8(fixed) |
| $u_{52}$ | B(1)...H(24) | 351.2(13) | 12.8(fixed) |
| $u_{53}$ | B(2)...B(4) | 274.4(10) | 6.5(tied to $u_{39}$) |
| $u_{54}$ | B(2)...B(8) | 287.7(10) | 7.0(4) |
| $u_{57}$ | B(2)...H(11) | 255.7(10) | 12.0(fixed) |
| $u_{59}$ | B(2)...H(14) | 385.5(10) | 10.7(fixed) |
| $u_{60}$ | B(2)...H(15) | 263.9(7) | 12.3(fixed) |
| $u_{61}$ | B(2)...H(16) | 233.5(13) | 11.6(fixed) |
| $u_{63}$ | B(2)...H(18) | 394.3(8) | 11.5(fixed) |
| $u_{64}$ | B(2)...H(19) | 445.8(11) | 10.7(fixed) |
| $u_{66}$ | B(2)...H(21) | 266.2(13) | 11.1(fixed) |
| $u_{67}$ | B(2)...H(22) | 350.4(15) | 16.9(fixed) |
| $u_{68}$ | B(2)...H(23) | 288.3(12) | 12.4(fixed) |
| $u_{88}$ | B(4)...C(6) | 338.4(10) | 8.4(6) |
| $u_{101}$ | B(4)...H(23) | 284.7(15) | 12.4(fixed) |
| $u_{102}$ | B(4)...H(24) | 284.7(15) | 12.4(fixed) |
| $u_{103}$ | B(5)...B(7) | 296.3(11) | 6.8(tied to $u_{105}$) |
| $u_{104}$ | B(5)...B(8) | 349.3(8) | 7.8(tied to $u_{88}$) |
| $u_{105}$ | B(5)...C(9) | 299.9(5) | 7.8(5) |
| $u_{106}$ | B(5)...B(10) | 185.2(16) | 6.9(7) |
| $u_{107}$ | B(5)...H(11) | 260.8(9) | 12.3(fixed) |
| $u_{108}$ | B(5)...H(12) | 257.2(9) | 12.5(fixed) |
| $u_{109}$ | B(5)...H(13) | 396.8(8) | 11.4(fixed) |

| | | | |
|---|---|---|---|
| $u_{110}$ | B(5)...H(14) | 395.6(11) | 11.5(fixed) |
| $u_{111}$ | B(5)...H(16) | 250.0(11) | 12.1(fixed) |
| $u_{112}$ | B(5)...H(17) | 403.3(12) | 11.4(fixed) |
| $u_{113}$ | B(5)...H(18) | 469.6(8) | 11.0(fixed) |
| $u_{114}$ | B(5)...H(19) | 399.8(7) | 11.6(fixed) |
| $u_{115}$ | B(5)...H(20) | 269.3(16) | 12.6(fixed) |
| $u_{116}$ | B(5)...H(21) | 227.8(14) | 12.8(fixed) |
| $u_{117}$ | B(5)...H(22) | 294.9(13) | 16.8(fixed) |
| $u_{118}$ | B(5)...H(24) | 349.3(11) | 14.7(fixed) |
| $u_{120}$ | C(6)...C(9) | 310.7(18) | 10.9(9) |
| $u_{122}$ | C(6)...H(11) | 390.0(13) | 11.4(fixed) |
| $u_{123}$ | C(6)...H(12) | 242.8(16) | 11.6(fixed) |
| $u_{125}$ | C(6)...H(14) | 459.0(11) | 11.3(fixed) |
| $u_{126}$ | C(6)...H(15) | 265.2(11) | 12.1(fixed) |
| $u_{128}$ | C(6)...H(18) | 409.4(6) | 11.9(fixed) |
| $u_{129}$ | C(6)...H(19) | 419.2(20) | 13.7(fixed) |
| $u_{131}$ | C(6)...H(22) | 266.6()25 | 19.3(fixed) |
| $u_{132}$ | C(6)...H(23) | 237.2(14) | 13.0(fixed) |
| $u_{172}$ | C(9)...H(23) | 232.2(10) | 13.0(fixed) |
| $u_{186}$ | H(11)...H(12) | 303.3(11) | 18.7(fixed) |
| $u_{187}$ | H(11)...H(13) | 301.5(18) | 19.4(fixed) |
| $u_{189}$ | H(11)...H(15) | 299.7(14) | 19.7(fixed) |
| $u_{190}$ | H(11)...H(16) | 463.4(12) | 15.8(fixed) |
| $u_{191}$ | H(11)...H(17) | 490.7(10) | 15.7(fixed) |
| $u_{195}$ | H(11)...H(21) | 453.2(19) | 15.6(fixed) |
| $u_{197}$ | H(11)...H(23) | 335.1(14) | 14.6(fixed) |
| $u_{198}$ | H(11)...H(24) | 467.1(13) | 14.7(fixed) |
| $u_{200}$ | H(12)...H(14) | 488.4(13) | 14.4(fixed) |
| $u_{201}$ | H(12)...H(15) | 298.2(12) | 19.5(fixed) |
| $u_{202}$ | H(12)...H(16) | 252.5(21) | 18.5(fixed) |
| $u_{204}$ | H(12)...H(18) | 491.8(14) | 15.4(fixed) |
| $u_{205}$ | H(12)...H(19) | 566.4(12) | 13.1(fixed) |
| $u_{207}$ | H(12)...H(21) | 351.6(16) | 13.5(fixed) |
| $u_{208}$ | H(12)...H(22) | 465.0(16) | 19.0(fixed) |
| $u_{209}$ | H(12)...H(23) | 384.6(11) | 15.2(fixed) |
| $u_{230}$ | H(14)...H(23) | 379.8(16) | 15.2(fixed) |
| $u_{232}$ | H(15)...H(16) | 294.6(15) | 18.6(fixed) |
| $u_{233}$ | H(15)...H(17) | 499.8(16) | 15.3(fixed) |
| $u_{234}$ | H(15)...H(18) | 589.8(8) | 13.3(fixed) |
| $u_{235}$ | H(15)...H(19) | 501.6(9) | 14.9(fixed) |
| $u_{236}$ | H(15)...H(20) | 312.9(23) | 19.2(fixed) |
| $u_{237}$ | H(15)...H(21) | 314.4(16) | 17.4(fixed) |
| $u_{238}$ | H(15)...H(22) | 397.9(13) | 18.9(fixed) |
| $u_{239}$ | H(15)...H(23) | 202.6(10) | 14.2(fixed) |
| $u_{240}$ | H(15)...H(24) | 464.9(12) | 16.7(fixed) |
| $u_{243}$ | H(16)...H(19) | 525.8(22) | 16.3(fixed) |
| $u_{245}$ | H(16)...H(21) | 181.5(9) | 11.8(fixed) |
| $u_{246}$ | H(16)...H(22) | 363.9(28) | 21.6(fixed) |

| | | | |
|---|---|---|---|
| $u_{247}$ | H(16)...H(23) | 320.0(17) | 15.2(fixed) |
| $u_{260}$ | H(18)...H(23) | 462.4(12) | 16.7(fixed) |
| $u_{261}$ | H(18)...H(24) | 196.7(17) | 14.2(fixed) |
| $u_{265}$ | H(19)...H(23) | 313.7(11) | 15.2(fixed) |
| $u_{271}$ | H(21)...H(22) | 189.5(33) | 23.8(fixed) |
| $u_{272}$ | H(21)...H(23) | 217.5(16) | 19.2(fixed) |
| $u_{274}$ | H(22)...H(23) | 214.3(11) | 19.2(fixed) |
| $u_{276}$ | H(23)...H(24) | 350.4(18) | 21.3(fixed) |

**Table G.** Calculated ($r_e$) structure of *nido*-7,8-$C_2B_9H_{13}$ (pm).

| Geometric Parameter | Level of theory / Basis set | | | | | | |
|---|---|---|---|---|---|---|---|
| | HF | | B3LYP | | MP2 | | |
| | 3-21G* | 6-31G* | 6-31G* | 6-311G* | 6-31G* | 6-311G* | 6-311+G* |
| B(1)-B(2) | 177.8 | 177.3 | 176.7 | 176.6 | 176.4 | 177.2 | 177.2 |
| B(1)-B(3) | 183.0 | 182.4 | 181.1 | 181.0 | 180.0 | 180.8 | 180.8 |
| B(1)-B(5) | 178.3 | 177.6 | 176.8 | 176.7 | 176.3 | 177.2 | 177.2 |
| B(2)-B(3) | 178.4 | 176.8 | 176.2 | 176.2 | 175.5 | 176.3 | 176.3 |
| B(2)-B(6) | 177.8 | 176.6 | 176.7 | 176.7 | 176.9 | 177.8 | 177.8 |
| B(2)-C(7) | 175.5 | 171.1 | 170.5 | 170.5 | 169.3 | 170.2 | 170.2 |
| B(2)-B(11) | 181.7 | 179.0 | 178.0 | 177.9 | 177.2 | 178.1 | 178.1 |
| B(5)-B(6) | 181.1 | 179.6 | 179.1 | 179.1 | 178.6 | 179.5 | 179.5 |
| B(5)-B(9) | 185.5 | 184.5 | 181.8 | 181.9 | 179.7 | 180.4 | 180.4 |
| B(5)-B(10) | 188.8 | 187.6 | 184.5 | 184.5 | 183.3 | 184.0 | 184.0 |
| C(7)-C(8) | 153.9 | 153.1 | 153.5 | 153.3 | 152.6 | 152.8 | 152.8 |
| C(7)-B(11) | 164.1 | 165.0 | 166.0 | 165.7 | 166.7 | 166.9 | 166.9 |
| B(9)-B(10) | 192.9 | 192.4 | 189.6 | 189.5 | 186.8 | 187.2 | 187.2 |
| Energy[a] | -303.6826 | -305.4211 | -307.7727 | -307.8135 | -306.5532 | -306.6469 | -306.6506 |

[a] absolute energy in Hartrees.

# Appendix E

**Figure 1.** Molecular framework for $Ph_2BX$ (X = F, Cl, Br and I).

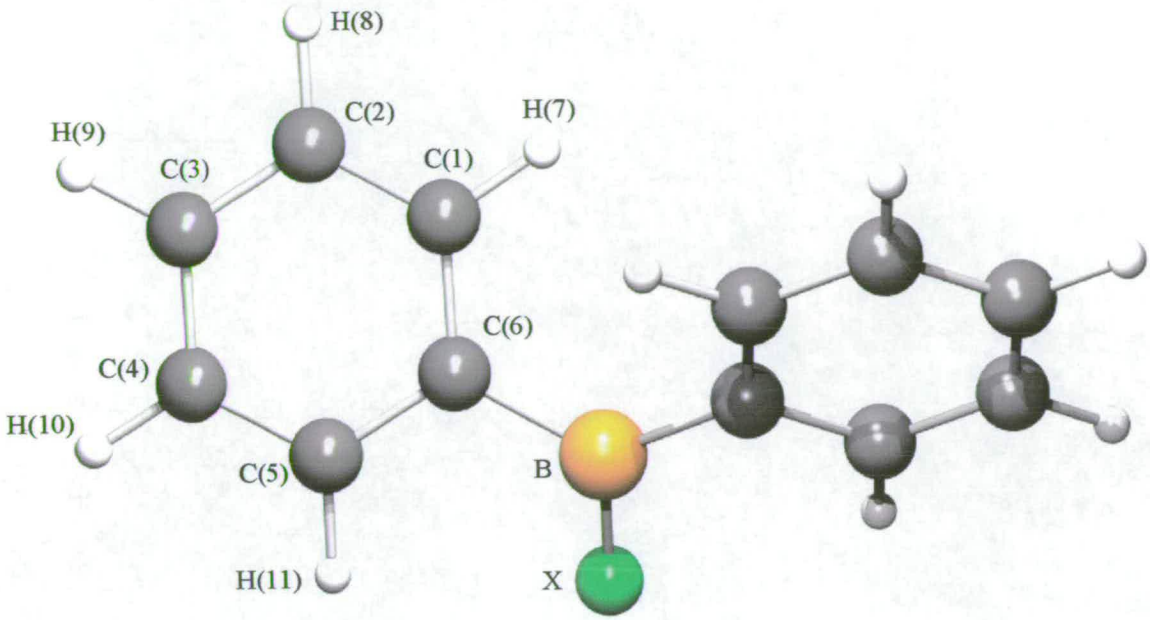


**Figure 2.** Molecular framework for $Me_2BX$ (X = F, Cl, Br and I).

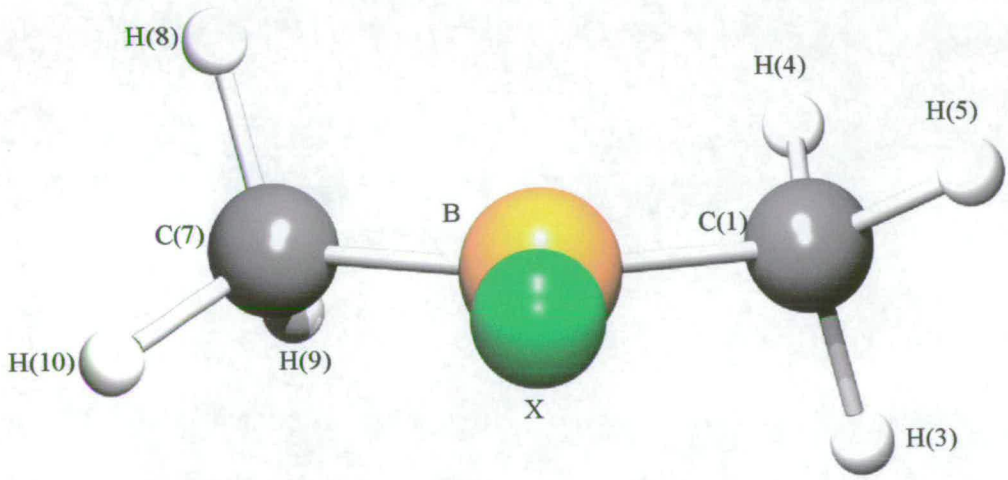

**Table A**. Calculated ($r_e$) geometric parameters for $Ph_2BF$ (Distances in pm, angles in °).

| Geometric Parameter | Level/ Basis set | | | | | | | | |
|---|---|---|---|---|---|---|---|---|---|
| | HF | | | B3LYP | | | MP2 | | |
| | 6-31G* | 6-311G* | 6-311++G* | 6-31G* | 6-311G* | 6-311++G* | 6-31G* | 6-311G* | 6-311++G* |
| ϕ(B-C) | 23.0 | 22.4 | 22.8 | 21.9 | 21.4 | 22.1 | 24.1 | 23.8 | 26.1 |
| C(1)-H(7) | 107.5 | 107.5 | 107.5 | 108.7 | 108.5 | 108.5 | 108.8 | 108.8 | 108.8 |
| C(2)-H(8) | 107.5 | 107.5 | 107.5 | 108.7 | 108.6 | 108.6 | 108.8 | 108.7 | 108.8 |
| C(3)-H(9) | 107.6 | 107.6 | 107.6 | 108.7 | 108.6 | 108.6 | 108.8 | 108.7 | 108.8 |
| C(1)-C(6) | 139.8 | 139.7 | 139.8 | 141.0 | 140.8 | 140.8 | 140.9 | 141.1 | 141.2 |
| C(1)-C(2) | 138.4 | 138.4 | 138.5 | 139.4 | 139.1 | 139.2 | 139.5 | 139.8 | 139.9 |
| C(2)-C(3) | 138.6 | 138.5 | 138.6 | 139.7 | 139.4 | 139.4 | 139.7 | 139.9 | 140.1 |
| B-C | 156.7 | 156.6 | 156.6 | 155.9 | 155.7 | 155.7 | 155.6 | 155.8 | 155.8 |
| B-F | 133.4 | 133.4 | 133.5 | 134.9 | 135.2 | 135.6 | 135.4 | 134.6 | 135.0 |
| C-B-C | 127.8 | 128.0 | 128.0 | 127.7 | 128.1 | 128.0 | 125.9 | 125.5 | 125.3 |
| C(5)-C(6)-B/ | 119.2 | 119.1 | 119.2 | 119.2 | 119.3 | 119.5 | 119.6 | 119.9 | 120.0 |
| C(1)-C(6)-B | 123.0 | 123.1 | 123.0 | 123.2 | 123.1 | 122.9 | 122.2 | 122.0 | 121.7 |
| C(1)-C(6)-C(5) | 117.8 | 117.8 | 117.8 | 117.6 | 117.6 | 117.6 | 118.1 | 118.1 | 118.3 |
| C(2)-C(1)-C(6) | 121.3 | 121.3 | 121.3 | 121.4 | 121.4 | 121.3 | 121.1 | 121.0 | 120.9 |
| C(3)-C(2)-C(1) | 119.8 | 119.8 | 119.8 | 119.8 | 119.9 | 119.9 | 119.9 | 119.9 | 119.9 |
| C(2)-C(3)-C(4) | 120.0 | 120.0 | 120.0 | 120.0 | 119.9 | 119.9 | 120.0 | 119.9 | 120.0 |
| C(6)-C(5)-H(11)/ | 119.3 | 119.3 | 119.4 | 119.0 | 119.1 | 119.2 | 119.2 | 119.3 | 119.4 |
| C(6)-C(1)-H(7) | 119.8 | 119.9 | 119.9 | 119.5 | 119.7 | 119.7 | 119.6 | 119.7 | 119.7 |
| C(4)-C(5)-H(11)/ | 119.4 | 119.3 | 119.3 | 119.6 | 119.5 | 119.5 | 119.7 | 119.7 | 119.7 |
| C(2)-C(1)-H(7) | 119.0 | 118.9 | 118.8 | 119.2 | 119.1 | 119.0 | 119.4 | 119.4 | 119.4 |
| C(1)-C(2)-H(8) | 120.1 | 120.1 | 120.1 | 120.1 | 120.1 | 120.1 | 120.1 | 120.1 | 120.1 |
| C(3)-C(2)-H(8) | 120.1 | 120.1 | 120.1 | 120.0 | 120.0 | 120.0 | 120.0 | 120.0 | 120.0 |
| C(2)-C(3)-H(9) | 120.0 | 120.0 | 120.0 | 120.0 | 120.0 | 120.0 | 120.0 | 120.0 | 120.0 |

**Table B**. Calculated ($r_e$) geometric parameters for $Ph_2BCl$ (Distances in pm, angles in °).

| Geometric Parameter | Level/ Basis set | | | | | | | | |
|---|---|---|---|---|---|---|---|---|---|
| | HF | | | B3LYP | | | MP2 | | |
| | 6-31G* | 6-311G* | 6-311++G* | 6-31G* | 6-311G* | 6-311++G* | 6-31G* | 6-311G* | 6-311++G* |
| ϕ(B-C) | 28.5 | 28.4 | 28.8 | 26.7 | 27.2 | 27.5 | 28.6 | 28.1 | 29.7 |
| C(1)-H(7) | 107.4 | 107.4 | 107.4 | 108.6 | 108.5 | 108.5 | 108.8 | 108.7 | 108.8 |
| C(2)-H(8) | 107.5 | 107.5 | 107.5 | 108.7 | 108.5 | 108.6 | 108.8 | 108.7 | 108.8 |
| C(3)-H(9) | 107.6 | 107.6 | 107.6 | 108.7 | 108.6 | 108.6 | 108.8 | 108.7 | 108.8 |
| C(1)-C(6) | 140.0 | 139.9 | 139.9 | 141.1 | 140.9 | 140.9 | 141.0 | 141.2 | 141.3 |
| C(1)-C(2) | 138.4 | 138.3 | 138.4 | 139.3 | 139.1 | 139.2 | 139.5 | 139.7 | 139.8 |
| C(2)-C(3) | 138.6 | 138.5 | 138.6 | 139.7 | 139.4 | 139.4 | 139.7 | 139.9 | 140.0 |
| B-C | 156.5 | 156.4 | 156.5 | 155.6 | 155.4 | 155.5 | 155.3 | 155.4 | 155.5 |
| B-Cl | 179.5 | 179.8 | 179.7 | 179.9 | 179.8 | 179.7 | 177.0 | 176.9 | 177.0 |
| C-B-C | 124.9 | 125.1 | 125.0 | 125.2 | 125.2 | 125.1 | 123.2 | 123.2 | 122.9 |
| C(5)-C(6)-B/ | 121.9 | 121.9 | 121.8 | 122.0 | 122.1 | 122.0 | 122.0 | 122.0 | 121.9 |
| C(1)-C(6)-B | 120.5 | 120.6 | 120.6 | 120.7 | 120.6 | 120.6 | 120.1 | 120.1 | 120.1 |
| C(1)-C(6)-C(5) | 117.6 | 117.5 | 117.6 | 117.3 | 117.3 | 117.4 | 117.9 | 117.9 | 118.0 |
| C(2)-C(1)-C(6) | 121.3 | 121.3 | 121.3 | 121.4 | 121.4 | 121.4 | 121.1 | 121.0 | 121.0 |
| C(3)-C(2)-C(1) | 119.9 | 119.9 | 119.9 | 120.0 | 120.0 | 120.0 | 120.0 | 120.1 | 120.1 |
| C(2)-C(3)-C(4) | 120.0 | 120.0 | 119.9 | 119.9 | 119.8 | 119.8 | 119.9 | 119.9 | 119.9 |
| C(6)-C(1)-H(7) | 119.6 | 119.6 | 119.7 | 119.3 | 119.4 | 119.4 | 119.4 | 119.5 | 119.5 |
| C(2)-C(1)-H(7) | 119.0 | 118.9 | 118.9 | 119.3 | 119.1 | 119.2 | 119.5 | 119.4 | 119.5 |
| C(1)-C(2)-H(8) | 120.0 | 120.0 | 120.0 | 120.0 | 119.9 | 119.9 | 120.0 | 120.0 | 120.0 |
| C(3)-C(2)-H(8) | 120.1 | 120.1 | 120.1 | 120.0 | 120.0 | 120.0 | 120.0 | 120.0 | 120.0 |
| C(2)-C(3)-H(9) | 120.0 | 120.0 | 120.0 | 120.1 | 120.1 | 120.1 | 120.1 | 120.1 | 120.1 |

**Table C**. Calculated ($r_e$) geometric parameters for $Ph_2BBr$ (Distances in pm, angles in °).

| Geometric Parameter | Level/ Basis set | | | | | | | | |
|---|---|---|---|---|---|---|---|---|---|
| | HF | | | B3LYP | | | MP2 | | |
| | 6-31G* | 6-311G* | 6-311++G* | 6-31G* | 6-311G* | 6-311++G* | 6-31G* | 6-311G* | 6-311++G* |
| ϕ(B-C) | 27.5 | 29.7 | 30.2 | 25.6 | 28.3 | 28.8 | 27.1 | 28.8 | 30.5 |
| C(1)-H(7) | 107.4 | 107.4 | 107.4 | 108.6 | 108.4 | 108.5 | 108.7 | 108.7 | 108.8 |
| C(2)-H(8) | 107.5 | 107.5 | 107.5 | 108.7 | 108.5 | 108.5 | 108.8 | 108.7 | 108.8 |
| C(3)-H(9) | 107.6 | 107.6 | 107.6 | 108.7 | 108.6 | 108.6 | 108.8 | 108.7 | 108.8 |
| C(1)-C(6) | 140.0 | 139.9 | 139.9 | 141.2 | 141.0 | 141.0 | 141.1 | 141.4 | 141.4 |
| C(1)-C(2) | 138.4 | 138.3 | 138.4 | 139.3 | 139.1 | 139.1 | 139.4 | 139.5 | 139.8 |
| C(2)-C(3) | 138.6 | 138.5 | 138.6 | 139.7 | 139.4 | 139.5 | 139.7 | 139.9 | 140.1 |
| B-C | 156.3 | 156.3 | 156.4 | 155.4 | 155.3 | 155.3 | 155.0 | 155.3 | 155.3 |
| B-Br | 195.4 | 196.9 | 196.8 | 195.1 | 196.7 | 196.6 | 193.6 | 193.7 | 193.7 |
| C-B-C | 125.5 | 124.9 | 124.8 | 125.9 | 125.1 | 124.9 | 124.4 | 123.1 | 122.8 |
| C(5)-C(6)-B/ | 122.1 | 122.5 | 122.5 | 122.1 | 122.7 | 122.7 | 122.2 | 122.6 | 122.6 |
| C(1)-C(6)-B | 120.4 | 120.0 | 120.0 | 120.6 | 120.0 | 120.0 | 119.9 | 119.5 | 119.4 |
| C(1)-C(6)-C(5) | 117.5 | 117.5 | 117.5 | 117.3 | 117.3 | 117.3 | 117.9 | 117.9 | 118.0 |
| C(2)-C(1)-C(6) | 121.3 | 121.3 | 121.3 | 121.5 | 121.4 | 121.4 | 121.1 | 121.0 | 121.0 |
| C(3)-C(2)-C(1) | 119.9 | 120.9 | 119.9 | 120.0 | 120.0 | 120.0 | 120.1 | 120.1 | 120.1 |
| C(2)-C(3)-C(4) | 120.0 | 119.9 | 119.9 | 119.8 | 119.8 | 119.8 | 119.9 | 119.8 | 119.9 |
| C(6)-C(1)-H(7) | 119.6 | 119.7 | 119.7 | 119.3 | 119.4 | 119.4 | 119.4 | 119.5 | 119.5 |
| C(2)-C(1)-H(7) | 119.1 | 119.1 | 119.1 | 119.4 | 119.2 | 119.1 | 119.6 | 119.5 | 119.5 |
| C(1)-C(2)-H(8) | 120.0 | 119.9 | 119.9 | 119.9 | 119.9 | 119.9 | 119.9 | 119.9 | 119.9 |
| C(3)-C(2)-H(8) | 120.1 | 120.1 | 120.1 | 120.1 | 120.0 | 120.0 | 120.0 | 120.0 | 120.0 |
| C(2)-C(3)-H(9) | 120.0 | 120.0 | 120.0 | 120.1 | 120.1 | 120.1 | 120.0 | 120.1 | 120.1 |

**Table D**. Calculated ($r_e$) geometric parameters for $Ph_2BI$ (Distances in pm, angles in °).

| Geometric Parameter | Level/ Basis set | | | | | | | | |
|---|---|---|---|---|---|---|---|---|---|
| | HF | | | B3LYP | | | MP2 | | |
| | 6-31G*[a] | 6-311G*[b] | 6-311++G*[c] | 6-31G*[a] | 6-311G*[b] | 6-311++G*[c] | 6-31G*[a] | 6-311G*[b] | 6-311++G*[c] |
| ϕ(B-C) | 31.5 | 31.8 | 32.3 | 29.6 | 30.2 | 30.7 | 30.3 | 30.6 | 32.0 |
| C(1)-H(7) | 107.4 | 107.4 | 107.4 | 108.6 | 108.4 | 108.4 | 108.8 | 108.7 | 108.8 |
| C(2)-H(8) | 107.5 | 107.5 | 107.5 | 108.7 | 108.5 | 108.5 | 108.8 | 108.7 | 108.8 |
| C(3)-H(9) | 107.5 | 107.6 | 107.6 | 108.7 | 108.6 | 108.6 | 108.8 | 108.7 | 108.8 |
| C(1)-C(6) | 140.0 | 139.9 | 139.9 | 141.4 | 141.1 | 141.1 | 141.4 | 141.5 | 141.5 |
| C(1)-C(2) | 138.4 | 138.3 | 138.4 | 139.3 | 139.1 | 139.1 | 139.5 | 139.7 | 139.8 |
| C(2)-C(3) | 138.6 | 138.5 | 138.6 | 139.7 | 139.4 | 139.5 | 139.9 | 139.9 | 140.1 |
| B-C | 156.0 | 156.2 | 156.2 | 155.1 | 155.2 | 155.2 | 155.0 | 155.4 | 155.2 |
| B-I | 221.4 | 219.5 | 219.6 | 219.9 | 218.6 | 218.6 | 217.3 | 213.7 | 213.7 |
| C-B-C | 124.7 | 124.3 | 124.2 | 124.9 | 124.5 | 124.4 | 122.8 | 121.8 | 121.9 |
| C(5)-C(6)-B/ | 123.4 | 123.3 | 123.3 | 123.5 | 123.5 | 123.5 | 123.6 | 123.6 | 123.4 |
| C(1)-C(6)-B | 119.1 | 119.2 | 119.2 | 119.2 | 119.3 | 119.3 | 118.7 | 118.7 | 118.7 |
| C(1)-C(6)-C(5) | 117.5 | 117.5 | 117.5 | 117.2 | 117.2 | 117.2 | 117.7 | 117.7 | 117.9 |
| C(2)-C(1)-C(6) | 121.3 | 121.3 | 121.3 | 121.5 | 121.5 | 121.4 | 121.1 | 121.1 | 121.0 |
| C(3)-C(2)-C(1) | 119.9 | 119.9 | 119.9 | 120.0 | 120.0 | 120.0 | 120.10 | 120.10 | 120.1 |
| C(2)-C(3)-C(4) | 120.0 | 119.9 | 119.9 | 119.8 | 119.8 | 119.8 | 119.8 | 119.8 | 119.8 |
| C(6)-C(1)-H(7) | 119.7 | 119.7 | 119.8 | 119..3 | 119.4 | 119.5 | 119.4 | 119.5 | 119.6 |
| C(2)-C(1)-H(7) | 119.0 | 118.9 | 118.9 | 119.2 | 119.1 | 119.1 | 119.4 | 119.4 | 119.4 |
| C(1)-C(2)-H(8) | 119.9 | 119.9 | 119.9 | 119.9 | 119.9 | 119.9 | 119.9 | 119. 9 | 119.9 |
| C(3)-C(2)-H(8) | 120.1 | 120.1 | 120.1 | 120.1 | 120.0 | 120.0 | 120.0 | 120.0 | 120.0 |
| C(2)-C(3)-H(9) | 120.0 | 120.0/ | 120.0 | 120.1 | 120.1 | 120.1 | 120.1 | 120.1 | 120.1 |

[a] 6-31G* on B, C, H atoms and lanl2dz on I atoms.

[b] 6-311G* on B, C, H atoms and lanl2dz on I atoms.

[c] 6-311++G* on B, C, H atoms and lanl2dz on I atoms.

**Table E**. Calculated ($r_e$) geometric parameters for $Me_2BF$ (Distances in pm, angles in °).

| Geometric Parameter | Level/ Basis set | | | | | | | | |
|---|---|---|---|---|---|---|---|---|---|
| | HF | | | B3LYP | | | MP2 | | |
| | 6-31G* | 6-311G* | 6-311+G* | 6-31G* | 6-311G* | 6-311++G* | 6-31G* | 6-311G* | 6-311++G* |
| *r*BF | 132.9 | 132.9 | 133.3 | 134.2 | 134.5 | 135.0 | 135.0 | 134.3 | 135.0 |
| *r*BC | 157.9 | 157.3 | 157.3 | 157.3 | 156.6 | 156.5 | 157.1 | 157.0 | 156.8 |
| *r*CH | 108.6 | 108.5 | 108.5 | 109.5 | 109.3 | 109.3 | 109.2 | 109.1 | 109.2 |
| | 108.6 | 108.5 | 108.5 | 109.6 | 109.4 | 109.4 | 109.3 | 109.2 | 109.2 |
| | 109.1 | 109.1 | 109.1 | 110.2 | 110.0 | 110.0 | 109.8 | 109.8 | 109.9 |
| ∠FBC | 117.6 | 117.7 | 117.3 | 117.6 | 117.6 | 117.2 | 117.9 | 118.0 | 117.4 |
| ∠CBC | 124.8 | 124.7 | 125.4 | 124.7 | 124.8 | 125.7 | 124.3 | 124.0 | 125.2 |
| ∠BCH(3) | 108.7 | 108.4 | 108.3 | 108.5 | 108.4 | 108.4 | 108.6 | 108.1 | 107.9 |
| ∠BCH(4) | 112.9 | 112.9 | 113.1 | 112.9 | 113.1 | 113.3 | 112.2 | 112.3 | 112.9 |
| ∠BCH(5) | 112.4 | 112.8 | 112.7 | 112.9 | 113.2 | 113.3 | 112.6 | 113.1 | 112.8 |
| ϕH(3)CBF | 90.7 | 92.3 | 90.0 | 92.5 | 93.5 | 91.1 | 97.0 | 97.6 | 91.1 |
| ϕH(9)CBF | -151.4 | -150.1 | -152.2 | -150.1 | -149.4 | -151.6 | -145.7 | -145.6 | -151.6 |

**Table F.** Calculated ($r_e$) geometric parameters for $Me_2BCl$ (Distances in pm, angles in °).

| Geometric Parameter | Level/ Basis set | | | | | | | | |
|---|---|---|---|---|---|---|---|---|---|
| | HF | | | B3LYP | | | MP2 | | |
| | 6-31G* | 6-311G* | 6-311+G* | 6-31G* | 6-311G* | 6-311++G* | 6-31G* | 6-311G* | 6-311++G* |
| *r*BCl | 178.9 | 179.3 | 179.4 | 179.2 | 179.2 | 179.2 | 176.8 | 176.9 | 177.0 |
| *r*BC | 157.5 | 157.0 | 157.0 | 156.8 | 156.2 | 156.2 | 156.7 | 156.6 | 156.6 |
| *r*CH | 108.4 | 108.3 | 108.4 | 109.2 | 109.2 | 109.2 | 109.2 | 109.1 | 109.1 |
| | 108.6 | 108.6 | 108.6 | 109.4 | 109.4 | 109.4 | 109.4 | 109.3 | 109.4 |
| | 109.2 | 109.2 | 109.2 | 110.2 | 110.1 | 110.1 | 109.9 | 109.9 | 110.0 |
| ∠ClBC | 118.0 | 117.9 | 117.9 | 117.9 | 117.9 | 117.9 | 118.4 | 118.5 | 118.3 |
| ∠CBC | 124.0 | 124.2 | 124.2 | 124.2 | 124.2 | 124.3 | 123.2 | 123.1 | 123.3 |
| ∠BCH(3) | 107.8 | 107.5 | 107.6 | 107.6 | 107.6 | 107.7 | 107.6 | 107.1 | 107.2 |
| ∠BCH(4) | 112.3 | 112.5 | 112.5 | 112.5 | 112.8 | 112.8 | 112.0 | 112.1 | 112.3 |
| ∠BCH(5) | 113.6 | 113.7 | 113.8 | 113.9 | 114.2 | 114.2 | 113.7 | 114.1 | 114.0 |
| ϕH(3)CBCl | 88.1 | 88.5 | 88.1 | 89.2 | 89.7 | 89.3 | 92.1 | 94.1 | 93.0 |
| ϕH(9)CBCl | -154.7 | -154.5 | -154.9 | -154.1 | -153.7 | -154.1 | -151.2 | -149.7 | -150.7 |

**Table G**. Calculated ($r_e$) geometric parameters for $Me_2BBr$ (Distances in pm, angles in °).

| Geometric Parameter | Level/Basis set | | | | | | | | |
|---|---|---|---|---|---|---|---|---|---|
| | HF | | | B3LYP | | | MP2 | | |
| | 6-31G* | 6-311G* | 6-311+G* | 6-31G* | 6-311G* | 6-311++G* | 6-31G* | 6-311G* | 6-311++G* |
| *r*BBr | 194.7 | 196.4 | 196.5 | 194.3 | 195.9 | 196.0 | 193.4 | 193.7 | 193.9 |
| *r*BC | 157.3 | 156.9 | 156.9 | 156.7 | 156.1 | 156.0 | 156.5 | 156.5 | 156.5 |
| *r*CH | 108.3 | 108.3 | 108.3 | 109.4 | 109.2 | 109.2 | 109.1 | 109.1 | 109.1 |
| | 108.7 | 108.6 | 108.6 | 109.7 | 109.5 | 109.5 | 109.4 | 109.4 | 109.4 |
| | 109.2 | 109.2 | 109.2 | 110.2 | 110.1 | 110.1 | 109.9 | 110.0 | 110.0 |
| ∠BrBC | 118.1 | 117.8 | 117.6 | 118.0 | 117.8 | 117.8 | 118.2 | 118.3 | 118.3 |
| ∠CBC | 123.9 | 124.4 | 124.5 | 124.0 | 124.4 | 124.5 | 123.5 | 123.4 | 123.5 |
| ∠BCH(3) | 107.6 | 107.4 | 107.4 | 107.6 | 107.5 | 107.5 | 107.4 | 106.9 | 107.0 |
| ∠BCH(4) | 112.1 | 112.3 | 112.3 | 112.2 | 112.6 | 112.6 | 111.7 | 112.0 | 112.1 |
| ∠BCH(5) | 113.8 | 114.0 | 114.0 | 114.3 | 114.6 | 114.6 | 113.8 | 114.3 | 114.4 |
| ϕH(3)CBBr | 91.2 | 87.5 | 87.2 | 93.9 | 89.9 | 89.7 | 93.5 | 92.3 | 93.1 |
| ϕH(9)CBBr | -151.9 | -155.6 | -155.9 | -149.9 | -153.8 | -154.0 | -150.0 | -151.6 | -150.9 |

**Table H**. Calculated ($r_e$) geometric parameters for $Me_2BI$ (Distances in pm, angles in °).

| Geometric Parameter | Level/Basis set | | | | | | | | |
|---|---|---|---|---|---|---|---|---|---|
| | HF | | | B3LYP | | | MP2 | | |
| | 6-31G*[a] | 6-311G*[b] | 6-311+G*[c] | 6-31G*[a] | 6-311G*[b] | 6-311++G*[d] | 6-31G*[a] | 6-311G*[b] | 6-311++G*[d] |
| *r*BI | 220.3 | 219.0 | 219.1 | 218.8 | 217.8 | 218.0 | 216.7 | 213.9 | 214.1 |
| *r*BC | 157.0 | 156.7 | 156.7 | 156.4 | 156.0 | 155.9 | 156.5 | 156.6 | 156.5 |
| *r*CH | 108.3 | 108.3 | 108.3 | 109.4 | 109.1 | 109.1 | 109.1 | 109.0 | 109.0 |
| | 108.7 | 108.6 | 108.6 | 109.8 | 109.5 | 109.6 | 109.5 | 109.4 | 109.5 |
| | 109.2 | 109.2 | 109.2 | 110.3 | 110.1 | 110.1 | 110.0 | 110.0 | 110.1 |
| ∠IBC | 117.5 | 117.7 | 117.7 | 117.7 | 117.9 | 117.8 | 118.5 | 118.9 | 118.7 |
| ∠CBC | 125.0 | 124.7 | 124.7 | 124.7 | 124.3 | 124.4 | 123.0 | 122.3 | 122.5 |
| ∠BCH(3) | 107.5 | 107.3 | 107.3 | 107.2 | 107.3 | 107.4 | 106.8 | 106.5 | 106.6 |
| ∠BCH(4) | 111.9 | 112.1 | 112.1 | 112.1 | 112.4 | 112.4 | 111.5 | 111.8 | 111.8 |
| ∠BCH(5) | 114.1 | 114.3 | 114.4 | 114.7 | 114.9 | 115.0 | 114.8 | 115.0 | 115.2 |
| ϕH(3)CBI | 85.0 | 85.8 | 86.4 | 88.8 | 88.8 | 89.1 | 95.6 | 94.4 | 95.2 |
| ϕH(9)CBI | -157.9 | -157.3 | -156.8 | -155.2 | -155.0 | -154.8 | -148.5 | -150.0 | -149.2 |

[a] 6-31G* on B, C, H atoms and lanl2dz on I atoms.
[b] 6-311G* on B, C, H atoms and lanl2dz on I atoms.
[c] 6-311+G* on B, C, H atoms and lanl2dz on I atoms.
[d] 6-311++G* on B, C, H atoms and lanl2dz on I atoms.

# Appendix F

Courses and Conferences attended

## Courses Attended

- Unix 1, 2000.
- Unix 2, 2000.
- Introduction to demonstrating and tutoring, 2000.
- Safety Programme: risk assessment, reactive hazards and safe waste disposal, 2000.
- Introduction to Programming, 2001.
- Introduction to HTML – Publishing on the web, 2001.
- Introduction to FORTRAN, 2001.
- BCA/ICG Intensive Course in Crystallography, Durham, 2001.
- *CiC* Introduction to Crystallography, 2001.
- HTML, Forms and Scripts, 2002.
- University of Edinburgh Inorganic Section Meetings, 2000-2003.

## Conferences Attended

9th European Symposium on Molecular Structure, 2001
Blaubeuren, Germany.
Poster presentation: "Amazing Asymmetry in $B_8F_{12}$! The Structure Determination of $B_8F_{12}$ by X-ray Crystallography & Gas-phase Electron Diffraction."

Universities of Scotland Inorganic Club (USIC), 2001
University of St. Andrews, U.K.
Poster presentation as previous.

19th Austin Symposium on Molecular Structure, 2002
Austin, U.S.A.
Poster presentation: "$B_8F_{12}$ – How Low Does It Go?"

USIC, 2002

University of Edinburgh, U.K.

Poster presentation: "The Higher Boron Fluorides $B_8F_{12}$ and $B_{10}F_{12}$ – A Structural Study."

Exploring Modern Computational Chemistry, 2002

University of Nottingham, U.K.

$10^{th}$ European Symposium on Molecular Structure, 2003

St. Petersburg, Russia.

Poster presentation "The Butterfly Life Cycle Described by Boron Halides".

USIC, 2003

University of Strathclyde, U.K.

Poster presentation as previous.

# Appendix G

Publications

*The Structures of Borane Carbonyl Compounds $B_4X_6CO$ (X = F, Cl, Br and I) by Gas-phase Electron Diffraction and Ab Initio Calculations*, Iain D. Mackie, Sarah L. Hinchley, Heather E. Robertson, David W. H. Rankin, Jennifer A. J. Pardoe and Peter L. Timms, *J. Chem. Soc., Dalton Trans.*, 2002, 4162.

*The Surprising Structures of $B_8F_{12}$ and $B_{10}F_{12}$*, Jennifer A. J. Pardoe, Nicholas C. Norman, Peter L. Timms, Simon Parsons, Iain Mackie, Colin R. Pulham and David W. H. Rankin, *Angew. Chem. Int. Ed.*, 2003, **42**, 571.

*The Structures of $B_8X_{12}$ (X = F, Cl, Br and I) by Gas-phase Electron Diffraction and Ab Initio Calculations*, Iain D. Mackie, Sarah L. Hinchley, Simon Parsons, David W. H. Rankin, Jennifer A. J. Pardoe and Peter L. Timms, *manuscript in preparation.*

*The Structures of $B_8X_8H_4$ and $B_8X_4H_8$ (X = F, Cl, Br and I) by Ab Initio Calculations*, Iain D. Mackie and David W. H. Rankin, *manuscript in preparation.*

*The Structures of $B_{10}X_{12}$, $B_{10}X_8H_4$ and $B_{10}X_4H_8$ (X = F, Cl, Br and I) by Ab Initio Calculations*, Iain D. Mackie and David W. H. Rankin, *manuscript in preparation.*

*Gas-phase Electron Diffraction Studies on two 11-vertex dicarboranes, closo-2,3-$C_2B_9H_{11}$ and nido-2,9-$C_2B_9H_{13}$*, Iain D. Mackie, Heather E. Robertson, David W. H. Rankin, John M. Malget and Mark A. Fox, *manuscript in preparation.*

*The Structure of Arachno-6,9-$C_2B_8H_{14}$ by Gas-phase Electron Diffraction and Ab Initio Calculations*, Iain D. Mackie, Konstantin Borisenko, Heather E. Robertson, Sarah L. Hinchley, David W. H. Rankin, Drahomír Hynk and Josef Holub, *manuscript in preparation.*